

30720



National Library of Canada

Bibliothèque nationale du Canada

CANADIAN THESES ON MICROFICHE

THÈSES CANADIENNES SUR MICROFICHE

NAME OF AUTHOR/NOM DE L'AUTEUR DOUGLAS JOHNSON

TITLE OF THESIS/TITRE DE LA THÈSE PHYSICAL AND CHEMICAL STUDIES ON
PYRIMIDINE PURINE DNA

UNIVERSITY/UNIVERSITÉ ALBERTA

DEGREE FOR WHICH THESIS WAS PRESENTED/
GRADE POUR LEQUEL CETTE THÈSE FUT PRÉSENTÉE P.H.D.

YEAR THIS DEGREE CONFERRED/ANNÉE D'OBTENTION DE CE DEGRÉ 1976

NAME OF SUPERVISOR/NOM DU DIRECTEUR DE THÈSE DR. A. R. MORGAN

Permission is hereby granted to the NATIONAL LIBRARY OF CANADA to microfilm this thesis and to lend or sell copies of the film.

L'autorisation est, par la présente, accordée à la BIBLIOTHÈQUE NATIONALE DU CANADA de microfilmer cette thèse et de prêter ou de vendre des exemplaires du film.

The author reserves other publication rights, and neither the thesis nor extensive extracts from it may be printed or otherwise reproduced without the author's written permission.

L'auteur se réserve les autres droits de publication; ni la thèse ni de longs extraits de celle-ci ne doivent être imprimés ou autrement reproduits sans l'autorisation écrite de l'auteur.

DATED/DATE SEPT. 13, 1976 SIGNED/SIGNÉ Douglas Johnson

PERMANENT ADDRESS/RÉSIDENCE FIXE Box 11, 6th Street
RR #12 Hemworth
Ontario N0H 1P0

INFORMATION TO USERS

THIS DISSERTATION HAS BEEN
MICROFILMED EXACTLY AS RECEIVED

This copy was produced from a microfiche copy of the original document. The quality of the copy is heavily dependent upon the quality of the original thesis submitted for microfilming. Every effort has been made to ensure the highest quality of reproduction possible.

PLEASE NOTE: Some pages may have indistinct print. Filmed as received.

Canadian Theses Division
Cataloguing Branch
National Library of Canada
Ottawa, Canada K1A 0N4

AVIS AUX USAGERS

LA THESE A ETE MICROFILMEE
TELLE QUE NOUS L'AVONS RECUE

Cette copie a été faite à partir d'une microfiche du document original. La qualité de la copie dépend grandement de la qualité de la thèse soumise pour le microfilmage. Nous avons tout fait pour assurer une qualité supérieure de reproduction.

NOTA BENE: La qualité d'impression de certaines pages peut laisser à désirer. Microfilmée telle que nous l'avons reçue.

Division des thèses canadiennes
Direction du catalogage
Bibliothèque nationale du Canada
Ottawa, Canada K1A 0N4

THE UNIVERSITY OF ALBERTA

PHYSICAL AND CHEMICAL STUDIES ON PYRIMIDINE-PURINE

DNA

by

© DOUGLAS A. JOHNSON

A THESIS

SUBMITTED TO THE FACULTY OF GRADUATE STUDIES AND RESEARCH

IN PARTIAL FULFILLMENT OF THE REQUIREMENTS FOR THE DEGREE

OF DOCTOR OF PHILOSOPHY

DEPARTMENT OF BIOCHEMISTRY

EDMONTON, ALBERTA

FALL, 1976

THE UNIVERSITY OF ALBERTA
FACULTY OF GRADUATE STUDIES AND RESEARCH

The undersigned certify that they have read, and
recommend to the Faculty of Graduate Studies and Research,
for acceptance, a thesis entitled

PHYSICAL AND CHEMICAL STUDIES ON PYRIMIDINE-PURINE DNA

submitted by DOUGLAS ALLAN JOHNSON

in partial fulfilment of the requirements for the degree of
Doctor of Philosophy in Biochemistry.

A. R. Morgan.....

Supervisor

Robert K. Littland.....

Kenneth L. Ray.....

R. B. Smilie.....

Barbara.....

John T. Spencer.....

External Examiner

Date *August 30, 1976*

ABSTRACT

Pyrimidine-purine DNAs of repeating sequence which contain G-C base pairs undergo a reversible strand rearrangement in solutions of moderate ionic strength when the pH is lowered to less than 6. This transformation has been studied by both physical and chemical approaches which, along with model building studies, lead to the hypothesis that this new structure is a tetraplex with base tetrads containing both Watson Crick and Hoogsteen hydrogen bonds. These studies extend the range of possible rearrangements which have been previously observed for a variety of pyrimidine-purine DNAs.

Many of the reagents and synthetic DNAs used during the course of these experiments are interesting in their own right and some of their properties and reactions have been further investigated. Ethanedial (glyoxal) has been shown to be a useful probe of polynucleate structure. Also this reagent has been used in a number of preparative procedures involving pyrimidine-purine DNAs. The replication of a pyrimidine-purine DNA with a random base order has been studied and compared to the pattern of synthesis with a pyrimidine-purine DNA with a repeating base sequence. The results of these experiments support the proposal that pyrimidine-purine DNAs with a repeating sequence replicate via a slippage mechanism.

Also included in this thesis are three appendices describing work either done in collaboration with other researchers or work not immediately relevant to the main body of the thesis. Appendix 1 describes the application of fluorescence techniques to the study of the reactions of alkylating and cross-linking reagents with DNA.

Appendix 2 describes an enzymatic method for the conversion of adenosine 5'-monophosphate analogues to their respective 5'-triphosphates and Appendix 3 describes the isolation and characterization of a new terminal deoxynucleotidyl transferase from calf thymus.

ACKNOWLEDGEMENTS

Research is a collective effort and this thesis represents the exertions of many individuals. These include David Pulleyblank, Vern Paetkau, Bill Lown, Chris Bleackley, Doug Scraba, Asher Beglieter, Malcom MacCoss, Suree Narindrasorasak, Mike Burrington, Jo-Ann Forsythe, Terry Elgert, Morris Aarbo, Vic Ledsham, Cathy Hicks, Roger Bradley, Kim Oikawa and my many other friends in Edmonton.

Special thanks are due to Ms Peggy Finster who typed the majority of this thesis and Jackie Dorsey who typed much of the Appendices.

I wish to express my thanks and gratitude to Dick Morgan for his leadership throughout the course of this work.

This work was made possible by a Studentship from the Medical Research Council of Canada and a Dissertation Fellowship from the University of Alberta.

TABLE OF CONTENTS

	PAGE
ABSTRACT	iv
ACKNOWLEDGEMENTS :	vi
LIST OF FIGURES.	ix
LIST OF TABLES	xii
CHAPTER	
I. INTRODUCTION	1
II. MODEL BUILDING	27
III. MATERIALS AND METHODS	38
Ultraviolet Spectroscopy	39
Ultracentrifugation	39
Electrophoresis	40
Natural and Synthetic DNAs	40
Ethidium Fluorescence Assays	44
Radioactive Counting	46
Multiplex Studies	46
Reaction of Chemicals With DNAs	48
Replication of $d(TC)_n \cdot d(GA)_n$ in the Presence of Base Analogues	55
Synthesis of the Random $Py_n \cdot Pu_n$ DNA $d(T,C)_n \cdot d(G,A)_n$	59
Reactions with Glyoxal	60
IV. FORMATION OF $Py_n \cdot Pu_n$ MULTIPLEXES	63
V. THE REPLICATION OF $Py_n \cdot Pu_n$ DNAs	97

TABLE OF CONTENTS (Continued)

CHAPTER	PAGE
VI. GLYOXAL AS A PROBE OF NUCLEIC ACID STRUCTURE	105
Denaturation Mapping of λ DNA	115
Cross-linking of DNA by Glyoxal	120
The Separation of $d(AT)_n$ from $Py_n \cdot Pu_n$ DNAs	124
The Separation of the Strands of $d(TC)_n \cdot d(GA)_n$	126
VII. DISCUSSION	130
BIBLIOGRAPHY	133
APPENDIX 1: STUDIES RELATED TO ANTITUMOR ANTIBIOTICS	141
Part V. Reactions of Mitomycin C with DNA	
Examined by Ethidium Fluorescence Assay	142
Part VI. Correlation of Covalent Cross-linking	
of DNA by Bifunctional Aziridinoquinones with	
Their Antineoplastic Activity	158
Effects of Alkylation of Dimethyl Sulfate,	
Nitrogen Mustard and Mitomycin C on DNA	
Structure as Studied by the Ethidium Binding	
Assay	180
APPENDIX 2. THE ENZYMIC SYNTHESIS OF ATP ANALOGUES	197
APPENDIX 3. THE ISOLATION OF A HIGH MOLECULAR WEIGHT TERMINAL	
DEOXYNUCLEOTIDYL TRANSFERASE FROM CALF THYMUS	203

LIST OF TABLES

Table	Description	Page
1	Parameters of Classical DNA and RNA Structures Derived From Fibre Diffraction Studies	7
2	Structure of Synthetic DNAs Determined By X-Ray Fibre Diffraction Studies	10
3	Physical Properties of the $Py_n \cdot Pu_n$ DNAs Used in These Studies	42
4	Analysis of Products of Reaction of $d(TC)_n \cdot d(GA)_n$ With Dimethyl Sulfate at pH 7.0	53
5	Formation of the $d(TC)_n \cdot d(GA)_n$ Multiplex Monitored By Buoyant Density In Cs_2SO_4 at pH 5.0	68
6	Summary of the Physical Properties of the $Py_n \cdot Pu_n$ Multiplexes	73
7	Chemical Reagents as Probes of $d(TC)_n \cdot d(GA)_n$ Multiplex Structure	86
8	Separation of $d(AT)_n$ from $Py_n \cdot Pu_n$ DNAs	95

LIST OF FIGURES

Figure		Page
1	Ribofuranose Sugar Conformations	8
2	Circular Dichroism Spectrum of $d(T)_n \cdot d(A)_n$	14
3	Base Pair Hydrogen Bonding Schemes	29
4	Proposed Hydrogen Bonding for the Triplex $d(TC)_n \cdot d(GA)_n \cdot d(TC^+)_n$	31
5	Proposed Hydrogen Bonding for the Triplex $d(TC)_n \cdot d(GA)_n \cdot d(GA^+)_n$	32
6	Possible Hydrogen Bonding for the Triplex $d(TC)_n \cdot d(GA)_n \cdot d(AG)_n$	33
7	Tetrad Hydrogen Bonding of McGavin (1971)	36
8	Possible Tetrad Hydrogen Bonding Involving Hoogsteen Hydrogen Bonds	37
9	Plots of T_M and ρ Cs_2SO_4 Versus Mole Fraction G+C For Synthetic $Py_n \cdot Pu_n$ DNAs	43
10	Reaction Vessel For the Titration of $d(TC)_n \cdot d(GA)_n$	49
11	Standard Curve For The Reaction of Dimethyl Sulfate With $d(TC)_n \cdot d(GA)_n$	51
12	Structures of Purine Deoxynucleoside Analogues	56
13	Structures of Some AMP Analogues	56
14	Polyribopurine Synthesis With ATP Analogues	58
15	Rearrangement of $Py_n \cdot Pu_n$ DNAs Monitored by the Ethidium Fluorescence Assay	64
16	Rearrangement of $d(TC)_n \cdot d(GA)_n$ Monitored by Analytical Cs_2SO_4 Equilibrium Centrifugation	67
17	Absorbance-Temperature Transitions of Rearranged $d(TC)_n \cdot d(GA)_n$	70
18	Absorbance of Rearranging $d(TC)_n \cdot d(GA)_n$	75
19a	Circular Dichroism Spectra of $d(TG)_n \cdot d(CA)_n$	76

LIST OF FIGURES (Continued)

Figure		Page
19b	Circular Dichroism Spectra of $d(TC)_n \cdot d(GA)_n$	77
20	Absorbance of $d(TC)_n \cdot d(GA)_n$ Multiplex at Various Temperatures	78
21	Preparative Cs_2SO_4 Density Gradients of Rearranged Double-labelled $Py_n \cdot Pu_n$ DNAs at pH 5.0	80
22	Concentration Dependence of $d(TC)_n \cdot d(GA)_n$ Rearrangement	83
23	Reactions of Dimethyl Sulfate with $d(TC)_n \cdot d(GA)_n$	87
24	Titration of Rearranging $d(TC)_n \cdot d(GA)_n$	90
25	Replication of $d(TC)_n \cdot d(GA)_n$ in the Presence of 7-MedGTP	93
26	Interaction of $d(TC)_n$ and $d(GA)_n$ With $d(TC)_n \cdot d(GA)_n$ at pH 5.0	95
27	<u>In Vitro</u> DNA Synthesis With <u>E. Coli</u> DNA Polymerase I	98
28a	DNA Replication By a Strand Displacement Mechanism	99
28b	DNA Replication By a Slippage Mechanism	99
29	RNA Primed DNA Synthesis With <u>E. coli</u> DNA Polymerase I	101
30	Replication of $d(T,C)_n \cdot d(G,A)_n$ at $41^\circ C$.	102
31	Possible Conformations of Glyoxal-guanosine Adduct	106
32	Reaction of <u>E. coli</u> DNA With Glyoxal As Measured By The Reduction in T_M	107
33	Denaturation of λ DNA as Measured by the Fluorescence Assay	109
34	Reaction of Glyoxal With PM2 CCC DNA	110
35	Histograms of Partially Denatured λ DNA	116
36	Electron Micrograph of a Representative λ DNA Molecule at 30.5% Loss of Fluorescence	117

LIST OF FIGURES (Continued)

Figure		Page
37	Histograms of Partially Denatured λ DNA	118
38	Cross-linking of λ DNA With Glyoxal	122
39	Cross-linking of PM2 DNA With Glyoxal	123
40	Separation of $d(TC)_n$ and $d(GA)_n$ By The Glóxal/ Borate Method	128
41	Schematic Representation of DNA Folding	132

ABBREVIATIONS

a, c, g, t	the four common bases
A, C, G, T	nucleosides
dAMP, dCMP, dGMP, dTMP	deoxynucleoside 5'-monophosphate
(d)NTP	(deoxy)nucleoside 5'-triphosphate
dBrU	5-bromodeoxyuridine
$d(TC)_n \cdot d(GA)_n$	a duplex DNA polymer with alternating thymidylate and cytidylate residues in one strand and alternating adenylate and guanylate residues in the complementary strand
$d(TC)_n \cdot d(GA)_n \cdot r(UC^+)_n$	the above DNA with the alternating ribopolymer $r(UC^+)_n$ hydrogen bonded to the purine strand via Hoogsteen hydrogen bonds
CCC DNA	covalently closed circular DNA (also RFI)
OC DNA	open circular DNA (also RFII)
CLC DNA	covalently linked complementary DNA
DTT	dithiothreitol
DMS	dimethyl sulfate
SDS	sodium dodecyl sulfate
SSC	standard saline citrate (0.015M sodium citrate 0.15M NaCl, pH 7.0)
EB	ethidium bromide
E_p^{260}	extinction coefficient at 260 nanometers expressed in terms of (moles phosphate/litre) ⁻¹

T_M

the temperature at the midpoint of the helix to coil transition during the thermal denaturation of a polymer.

$d(T,C)_n \cdot d(G,A)_n$

a duplex DNA with pyrimidines in one strand and purines in the complementary strand. The base order in each strand is random. The synthesis of this polymer is described in this thesis.

S

sedimentation coefficient

CHAPTER I INTRODUCTION

The conformation and function of DNA is determined by its sequence and interaction with its environment. The structure of DNA which codes for genetic information seems largely conservative, varying little regardless of the source or specific base order. However, various other regions possessing base compositions and/or sequences deviating widely from the average may be expected to have anomalous conformations when compared to bulk DNA.

This possibility exists for sequences in the lac control region (Dickson et al., 1975) which contains repeats of $\text{pdC}(\text{pdT})_3\text{pdA}$, a block of AT rich DNA sandwiched between two blocks of GC rich DNA and potential palindromes (Gierer, 1966) or cruciform structures; features which may lead to a unique structure (Chan and Wells, 1974). Because of recent advances in DNA sequencing technology (Salser, 1974) many other examples similar to these can be gleaned from the literature. For example, the rightward promoter/operator sequence of λ DNA contains alternating blocks with high AT and GC content, has a repeating sequence of $\text{d}(\text{pdT})_3\text{pdA}$ and a centre of two-fold symmetry (Pirotta, 1975; Walz and Pirotta, 1975) and similar features are also found for the promoter regions of fd phage DNA (Sugimoto et al., 1975) and SV40 DNA (Dhar et al., 1974). The sites recognized by restriction endonucleases exhibit two-fold symmetry (Salser, 1974). Pyrimidine tracts of various lengths have been found in phage DNAs (Mushynski and Spencer, 1970) and Szybalski and coworkers have shown that a wide variety of phage and bacterial DNAs contain sites capable of binding $r(\text{U})_n$ and $r(\text{G})_n$ which are presumably mostly $\text{d}(\text{A})_n$ and $\text{d}(\text{C})_n$ (Kubinski et al., 1966; Opara-

Kubinska et al., 1964). DNA from eukaryotic cells contains long stretches of $\text{Py}_n \cdot \text{Pu}_n$ DNA (Birnboim and Straus, 1975) which in *D. melanogaster* are tightly clustered, forming a cryptic satellite (Sederoff et al., 1975). Sequence analysis reveals a very simple repeat, $(\text{ApGpApApG})_n$, analogous to simple synthetic DNAs. And on a larger scale eukaryotic DNA forms discrete satellite bands in CsCl density gradients indicative of a base composition different from the bulk DNA. These satellite DNAs have simple repeating sequences and in some cases at least are $\text{Py}_n \cdot \text{Pu}_n$ in character (Sederoff et al., 1975).

It is not known how the local DNA conformation would be affected by the presence of any of these features. However, the classical approach to this problem has been to construct synthetic defined DNAs of repeating sequences in order to amplify the parameter of interest, and study their various properties by chemical, physical and enzymatic means. These approaches have emphasized not only the effects of base composition on the physical and chemical parameters of interest, but also differences between $\text{Py}_n \cdot \text{Pu}_n$ DNAs and synthetic DNAs with pyrimidines and purines in both strands which resemble natural DNA in their properties. Thus, a more concrete basis for speculation concerning roles that $\text{Py}_n \cdot \text{Pu}_n$ DNAs may possess in vivo and various transformations which they may undergo can be provided.

Numerous researchers have used a wide range of systems to investigate these differences, including the following means:

- i) various drugs bind differentially to DNAs of different base composition. In 0.1M NaCl netropsin binds specifically to AT or IC base pairs but not GC base pairs in duplex DNA (Wartell et al., 1974); actinomycin D binds to duplex DNA at GC base pairs (Sobell,

1973), and $\text{Py}_n \cdot \text{Pu}_n$ DNAs bind less of the drug than their corresponding isomers with pyrimidines and purines in the same strand (which also bind the drug more tightly) (Wells and Larsen, 1970).

ii) cross-linking agents that react with a specific base require that base in both polynucleate strands and thus may not cross-link $\text{Py}_n \cdot \text{Pu}_n$ DNAs. For example, mitomycin C is thought to cross-link DNA by adduct formation with deoxyguanosine residues (possibly the 6-keto position, Tomasz et al., 1974) and would not be expected to cross-link $\text{d}(\text{TC})_n \cdot \text{d}(\text{GA})_n$. Similarly, base specific reagents would exhibit different product distribution between strands. For

example, dimethyl sulfate (Singer, 1975) methylates the 7-position of g and the 3-position of a in a ratio of 6:1. For a natural DNA these products would be distributed amongst both strands; however, a $\text{Py}_n \cdot \text{Pu}_n$ DNA would have all the methylated species in one strand.

iii) certain histone fractions have been reported to have differential affinities towards AT rich DNA (for the lysine-rich histones, Ohba, 1966) and GC rich DNA (for the arginine rich histones, Clark and Felsenfeld, 1972).

iv) Riggs et al., (1972) have investigated the binding of the lac repressor to twenty synthetic DNAs and demonstrated a preference for $\text{d}(\text{AT})_n$ compared to $\text{d}(\text{GC})_n$.

v) replication in vitro of synthetic DNAs with E. coli DNA polymerase I is different for $\text{Py}_n \cdot \text{Pu}_n$ DNAs compared to natural DNAs (see Results) or synthetic DNAs with pyrimidines and purines in both strands.

vi) in vitro transcription studies with E. coli RNA polymerase in the presence of all the necessary triphosphates demonstrate that

the rate of transcription of the $d(Py)_n$ strand of a $Py_n \cdot Pu_n$ DNA is greater than the $d(Pu)_n$ strand unlike the approximately equivalent rates for the isomeric DNA with pyrimidines and purines in both strands. This has been observed for $d(C)_n \cdot d(G)_n$ (Szybalski et al., 1969) as well as $d(TC)_n \cdot d(GA)_n$ and $d(TTC)_n \cdot d(GAA)_n$ (Morgan, 1970).
 vii) various nucleases degrade $Py_n \cdot Pu_n$ DNAs and their isomers with pyrimidines and purines in the same strand at different rates. An example is micrococcal nuclease (Szybalski et al., 1969) which degrades $d(AT)_n$ faster than $d(A)_n \cdot d(T)_n$.

However, the three most important approaches have been direct physical and chemical studies, X-ray crystallography and studies on rearrangements that only $Py_n \cdot Pu_n$ DNAs seem to undergo.

Wells et al., (1970)* have studied three homopolymer pairs, five repeating dinucleotide DNAs and four repeating trinucleotide DNAs in order to investigate the effect of base composition and sequence on melting transitions, buoyant density and circular dichroism spectra.

These results can be summarized as follows:

- i) the extinction coefficient of the $Py_n \cdot Pu_n$ DNA is always lower compared to its sequence isomer or natural DNA with the same base composition;
- ii) the melting temperature of a $Py_n \cdot Pu_n$ DNA in the presence of monovalent cations is lower than its sequence isomer and the difference between the two diminishes as the sequence complexity increases. They concluded that as the repeat size increased (eg. from a repeating dimer to a repeating trimer) the $Py_n \cdot Pu_n$ polymer's melting behaviour became more like that of a natural DNA, suppressing the anomolous effects of the asymmetric pyrimidine and purine

- distribution. Note that $d(T)_n \cdot d(A)_n$ is an apparent exception with a T_M greater than $d(AT)_n$ and also that addition of a divalent cation causes the T_M of $d(TC)_n \cdot d(GA)_n$ to increase to above that of $d(TG)_n \cdot d(CA)_n$ (unpublished observation of author);
- iii) the DNA with the higher T_M has the lower density in Cs_2SO_4 ;
- iv) natural DNA has a T_M which increases $\sim 18^\circ C/10$ fold increase in the ionic strength (as calculated from linear plots of T_M versus \log_{10} salt concentration). For synthetic DNAs this value depends on the length of the sequence repeat. For a 10 fold increase in salt concentration the T_M increases by $\sim 18^\circ C$ for DNAs with only two nucleotides (eg. $d(T)_n \cdot d(A)_n$, $d(AT)_n$, $d(C)_n \cdot d(I)_n$ and $d(IC)_n$), by $\sim 13^\circ C$ for DNAs with repeating dinucleotides (eg. $d(TC)_n \cdot d(GA)_n$ and $d(TG)_n \cdot d(CA)_n$) and by $\sim 12^\circ C$ for DNAs with repeating trinucleotides (eg. $d(TTC)_n \cdot d(GAA)_n$, $d(TTG)_n \cdot d(CAA)_n$, $d(TAC)_n \cdot d(GTA)_n$ and $d(ATC)_n \cdot d(GAT)_n$). The results of Morgan *et al.*, 1974 for $d(TCC)_n \cdot d(GGA)_n$ suggest a value of $\sim 18^\circ C$ which is anomolous.
- v) attempts were made to establish relationships between T_M and ρ $CsCl$ and mole fraction G+C and ρ Cs_2SO_4 . Trends could be inferred but values differed from the graphs determined for natural DNAs (in fact, the best fit would be for the average value of a $Py_n \cdot Pu_n$ DNA and its sequence isomers);
- vi) the CD spectra of each polymer is unique (discussed later).
- These results emphasize the differences between $Py_n \cdot Pu_n$ DNAs as a class distinct from natural DNAs or their base isomers with pyrimidines and purines on both strands.

Perhaps the most definitive technique for structural investigation is X-ray crystallography; however, polynucleates have not been crystall-

ized (except tRNA) and what information we have is derived from fibre diffraction and model building studies (for a "discussion" of the validity of this approach see articles by Donohue and by Arnott, Wilkins, Crick, Marvin and Hamilton, *Science* 167, 1693-1702, 1970. Recently published structures of ApU (Seeman et al., 1976) and GpC (Rosenberg et al., 1976) show that they both form interstrand Watson-Crick type hydrogen bonds with coordinates similar to those assumed for residues in polymer models, thus supporting the validity of this approach). Arnott has termed this approach the linked-atom least-squares method (Arnott, 1970) in which a least-squares refinement is used to fit models to the observed diffraction data (in contrast to protein crystal structure determination in which a model is derived from the data and then refined). Originally, these models are assigned values (i.e. bond lengths and torsion angles) determined from surveys of crystal structures of nucleosides and nucleotides.

Fibre diffraction of natural DNAs revealed that more than one crystalline structure can form depending upon the experimental conditions (especially the relative humidity and salt/DNA phosphate ratio). These include the so-called A, B, C, and D forms each of which could contain many structures with minor variations (Table 1). Recent work by Arnott et al. (1974a) and Arnott and Selsing (1974b) provides a basis for classifying these into two families "A" and "B" although each member has its own unique geometry. The "A" family is characterized by a C_3 endo sugar conformation (Figure 1) and base pairs displaced forward from the helix axis (usually $>3 \text{ \AA}$ (Arnott et al., 1974b)) and with positive base tilts (although the rather large value of 20° for the classical A RNA structure is not always reached). The "B" family has a C_3 exo

	A DNA	B DNA	C DNA	D DNA	A RNA	A' RNA
Conditions:						
relative humidity	<92%	>92%	<66%	d(AT) _n or d(ATT) _n d(AAT) _n under conditions similar to A DNA	low	
ionic strength	no excess salt	excess salt	"Li DNA"		low	>20% salt
pitch (Å)	28.15	34	31	24.3	--	--
fold (base pairs/turn)	11	10	~9.3	8	11	12
rise (Å)	2.56	3.4	3.33	3.03	2.81	3.01
tilt (degrees)	20.2	-5.9	-6	-16	+20	--
twist (degrees)	-112	-2.1	5	--	--	--
sugar conforma- tion	C ₃ endo	C ₃ exo	C ₃ exo	C ₃ exo	C ₃ endo	C ₃ endo
displacement (Å)	4.72	0	-2	-1.8	4.3	4.7

TABLE 1 Parameters of Classical DNA and RNA Structures
Derived From Fibre Diffraction Data

Data for this table are taken from Arnott(1970) and Arnott and
Selsing(1974a)

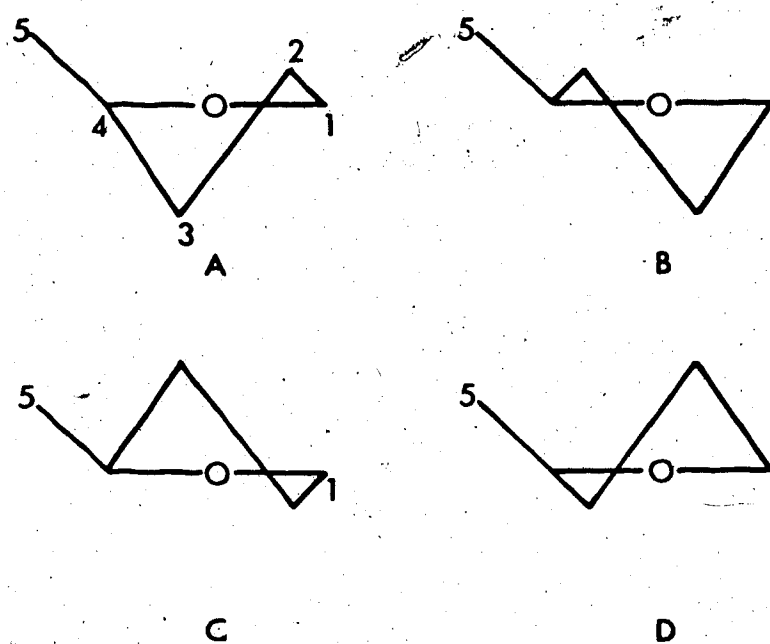


Figure 1 Ribofuranose Sugar Conformations

- A 3' exo
- B 2' exo
- C 3' endo
- D 2' endo

sugar conformation (Figure 1), base pairs straddling (classical B type DNA) or behind the helix axis (C type or D type) and smaller base tilts. The main distinguishing feature is the sugar conformation. Also the number of residues/turn of helix is greater for A type structure resulting in smaller rotations/residue (B form $\sim 36^\circ$ - 45° , A form $\sim 30^\circ$ - 33°). Generally, the A form is more stable at low relative humidity and little or no excess salt; raising the humidity or increasing the counterion concentration results in a B structure being formed. Both A and B families consist of right handed duplex DNA with Watson-Crick hydrogen bonding.

Structures of synthetic DNAs fall into these two categories (Table 2). Although each individual structure is unique there are some interesting generalizations. DNAs with 100% A+T content prefer a B conformation ($d(T)_n \cdot d(A)_n$, $d(AT)_n$, $d(ATT)_n \cdot d(AAT)_n$). Lowering the relative humidity does not cause a change to an A form as is the case with natural DNAs (although $d(AT)_n$ may form an unstable A form (Arnott, et al., 1974b)) but to the new D form which is part of the B family but has a pitch of $\sim 24 \text{ \AA}$, 8 base pairs/turn, and a small negative displacement. This effect, which causes a 11.8% shortening of the duplex from the B form may be important for sequences in vivo with high AT contents, presuming that this change can be mimicked. Also the D form is packed more closely in the unit cell than the B form (and both more tightly than the A form) which could be important for in vivo DNA packaging and DNA condensation. Arnott has also speculated that the presence of AT clusters may help destabilize neighbouring A structures (Selsing et al., 1975) possibly affecting transcription since RNA-DNA hybrids exist in A forms.

Synthetic DNA	Sugar Conformation ¹	Family	Reference
$d(ATT)_n \cdot d(AAT)_n$	C_3 exo	"B"	Selsing <u>et al.</u> , (1975)
$d(AT)_n \cdot d(AT)_n$	C_3 exo	"B"	Arnott <u>et al.</u> , (1974a)
$d(GC)_n \cdot d(GC)_n$	C_3 exo	"B"	Arnott <u>et al.</u> , (1974a)
$d(IC)_n \cdot d(IC)_n$	C_3 exo	"B"	Arnott <u>et al.</u> , (1974a)
$d(T)_n \cdot d(A)_n$	C_3 exo	"B"	Arnott and Selsing, (1974a)
$d(TG)_n \cdot d(CA)_n$? ²	"B" (?)	Langridge (1969)
$d(I)_n \cdot d(C)_n$?	"B" (?)	Langridge (1969)
$d(TC)_n \cdot d(GA)_n$?	"A" (?)	Langridge (1969)
$d(C)_n \cdot d(G)_n$	C_3 endo	"A"	Arnott and Selsing, (1974b)
$d(T)_n \cdot d(A)_n \cdot d(T)_n$	C_3 endo	"A"	Arnott and Selsing, (1974a)

TABLE 2 Structure of Synthetic DNAs Determined By X-Ray Fibre Diffraction Studies

1. for an explanation of the terms see text.
2. either unknown or tentative assignment.

Although DNAs with pyrimidines and purines in the same strand are in the B family, $\text{Py}_n \cdot \text{Pu}_n$ DNAs may not be. Arnott and Selsing (1974a) reported that while $\text{d(T)}_n \cdot \text{d(A)}_n$ exists in a B type structure, $\text{d(C)}_n \cdot \text{d(G)}_n$ preferred an A like structure (Arnott and Selsing, 1974b). Although no data was presented Langridge (1969) reported that while $\text{d(C)}_n \cdot \text{d(I)}_n$ and $\text{d(TG)}_n \cdot \text{d(CA)}_n$ gave diffraction patterns similar to B DNA, $\text{d(TC)}_n \cdot \text{d(GA)}_n$ gives an anomalous pattern similar to $\text{d(C)}_n \cdot \text{d(G)}_n$ (which is A like) when fibres were drawn from solutions known to favour formation of the B form. The hypothesis that $\text{d(TC)}_n \cdot \text{d(GA)}_n$ exists in an A like conformation is tentative but should be investigated further. However, since $\text{Py}_n \cdot \text{Pu}_n$ DNA has been implicated in the initiation of transcription (Szybalski et al., 1966) the existence of these DNA clusters in A conformations could facilitate this process, as has been proposed for $\text{d(C)}_n \cdot \text{d(G)}_n$ tracts (Arnott and Selsing, 1974b).

$\text{d(T)}_n \cdot \text{d(A)}_n$ can be converted to an A conformation by the addition of a third strand (d(T)_n) to form the triplex $\text{d(T)}_n \cdot \text{d(A)}_n \cdot \text{d(T)}_n$, probably due to the enlarged size of the major groove in A conformations (Arnott and Selsing, 1974a) into which this strand must fit. The overall diameter of the polymer is only marginally increased (similar structures were reported for $\text{r(U)}_n \cdot \text{r(A)}_n \cdot \text{r(U)}_n$, and $\text{r(U)}_n \cdot \text{d(A)}_n \cdot \text{r(U)}_n$, Arnott and Bond, 1973). This observation suggests that transcription could be initiated by the addition of a third strand to form a triplex and facilitate a B to A transition (Arnott et al., 1974a) although in view of the reduced transcription rate in vitro of triplexes compared to the corresponding duplex (Morgan, 1970; Murray and Morgan, 1973) this would apply only to neighbouring AT rich regions and thus result from an indirect interaction.

The relation of these structures to the structure in solution is not known. Tunis-Schneider and Maestre(1970) have obtained circular dichroism spectra of E. coli and calf thymus DNAs in thin films under conditions (salt concentration and relative humidity) where either A or B forms are normally present. The A form spectrum exhibits a positive peak centred at about 260 nm, a minimum at 210 nm with a variable trough at 280-300nm, this variability suggestive of a family of structures. B DNA is characterized by a broad maximum at 270-280nm, a minimum at 240-250nm (of amplitude approximately equal to the amplitude of the maximum) and another maximum at about 220nm. In solution (0.1M NaCl) the spectrum is almost identical to the B spectrum recorded for the unoriented film. Also the A spectrum is similar to that recorded for double-stranded RNA which exists only in the A conformation (Arnott and Bond, 1973). It was concluded that natural DNAs in solution are in a B form and RNAs in an A form. Wide angle X-ray scattering studies of calf thymus DNA in gels and solution (Bram, 1971) at moderate ionic strength (0.05 - 0.15M monovalent cation) supports this conclusion. When the spherically averaged scattering curve for various models was fitted to the experimental data the A form was obviously at variance with the results. The best fit was a modified B form with the pitch increased to 37 Å and the rotation/residue reduced by 8.4% (this structure or a similar one persists in nucleohistone). Infrared spectroscopy of natural DNAs has been used to empirically assign conformations (Pilet and Brahm, 1972). At neutral pH, with a sodium chloride concentration of 3-4% and a relative humidity estimated by the absorption at 3400 cm^{-1} (-O-H stretching) a plot of relative humidity against dichroic ratio (antisymmetric/symmetric stretching vibration of the

phosphate group) showed a reversible transition centred at $\sim 85\%$ relative humidity assigned to the B form (RH $> 85\%$) and A form (RH $< 85\%$). The spectrum of the latter form was similar to that reported for RNA. These authors also investigated the effect of base composition on the B to A transition, concluding that at a G+C content $< 30\%$ the A form should not be observed as was inferred later from studies on fibre diffraction for AT rich DNAs. These investigations support the existence for A and B forms in solution for natural DNAs. The correlations for synthetic DNAs have been less well investigated and since $\text{Py}_n \cdot \text{Pu}_n$ DNAs can undergo many rearrangements in solution at varying ionic strengths and pHs, in some cases the species under investigation is in doubt (eg. see Arnott, 1975). Using the generalized features described for the A and B forms of natural DNAs then almost all of the synthetic polymers investigated by Wells *et al.* (1970) would be in B like conformations (including $\text{d(T)}_n \cdot \text{d(A)}_n$, d(AT)_n , $\text{d(C)}_n \cdot \text{d(G)}_n$, d(GC)_n , $\text{d(TG)}_n \cdot \text{d(CA)}_n$, $\text{d(TC)}_n \cdot \text{d(GA)}_n$, $\text{d(ATC)}_n \cdot \text{d(GAT)}_n$, $\text{d(TAC)}_n \cdot \text{d(GTA)}_n$, $\text{d(TTG)}_n \cdot \text{d(CAA)}_n$, $\text{d(C)}_n \cdot \text{d(I)}_n$). The spectrum of d(GC)_n has its maximum at 272.5nm characteristic of B conformations but the shorter wavelength region resembles the A pattern while d(IC)_n has a unique inverted B spectrum (all spectra were obtained for samples in 1mM potassium phosphate pH 7.5, 10mM NaCl, 0.1mM EDTA except d(GC)_n which was run at pH 7.3, conditions which result in B conformations for natural DNAs). However, this is somewhat arbitrary in that the spectra of homopolymeric DNA and $\text{Py}_n \cdot \text{Pu}_n$ DNA differ from the classical B spectrum (as does d(GC)_n mentioned above). Figure 13 of Wells *et al.* (1970) (Figure 2) of the CD spectrum of $\text{d(T)}_n \cdot \text{d(A)}_n$ illustrates the complexity of these types of spectra, which makes a simple B or A assignment difficult. Although

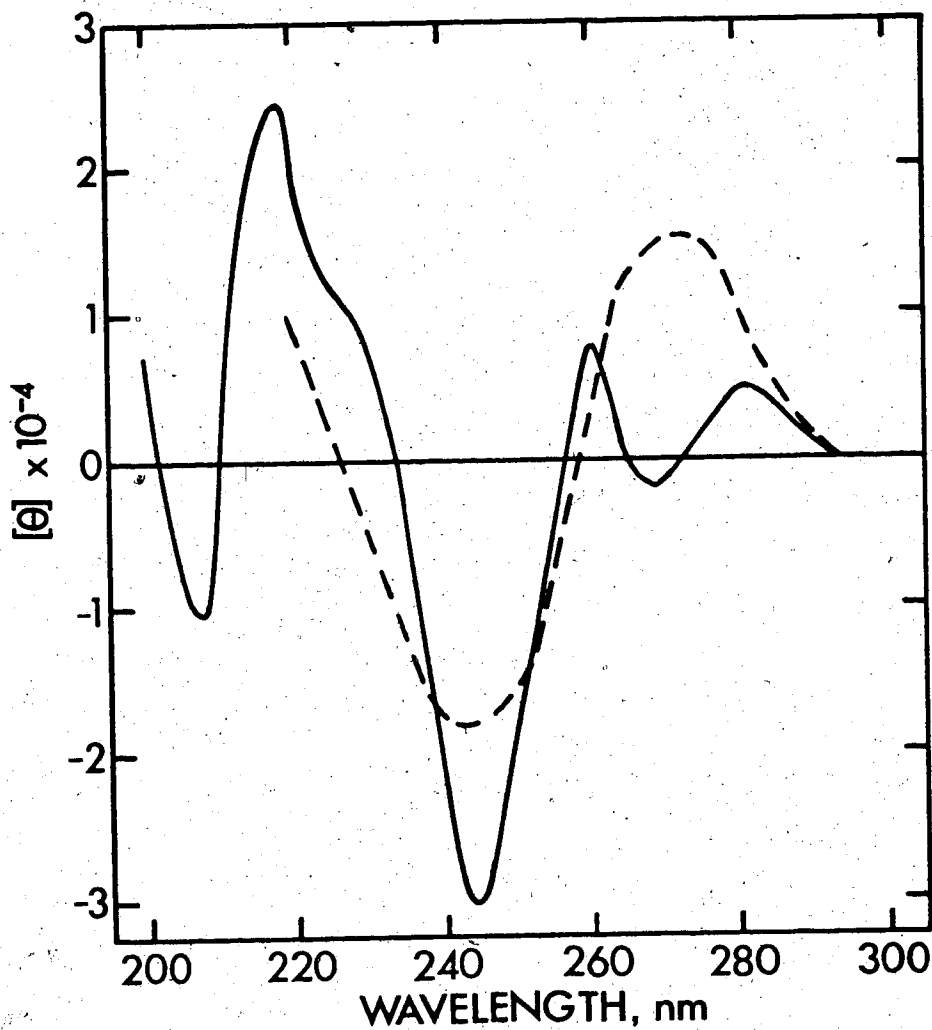


Figure 2 Circular Dichroism Spectrum of $d(T)_n \cdot d(A)_n$

Reproduction of the CD spectrum of $d(T)_n \cdot d(A)_n$ (Figure 13 of Wells et al., 1970) with a typical B spectrum (dashed line) superimposed.

the spectrum of $d(IC)_n$ differs dramatically from the rest (Mitsui et al., 1970) results from fibre diffraction suggest it is in a B like conformation (Arnott et al., 1974a). Also the inclusion of $d(C)_n \cdot d(G)_n$ in the B family is tenuous. Firstly the spectrum (Wells et al., 1970) has a maximum at 290nm which Gray and Bollum (1974) interpret as a contribution of $d(C)_n \cdot d(C^+)_n$ from excess $d(C)_n$ assumed present in the preparation. Secondly, the position of the largest maximum is at 260nm which is more reasonably interpreted as derived from an A structure (although the shorter wavelength region resembles the B spectrum). Finally, fibre diffraction studies (Arnott and Selsing, 1974b) show that $d(C)_n \cdot d(G)_n$, at 75% relative humidity, is in an A conformation. Raising the relative humidity to >90% does not result in the usually observed (for natural DNAs) A to B transition suggesting an A like conformation may exist at higher relative humidity and in solution. A further complication arises from attempts to calculate CD spectra using model compounds as standards (Arnott, 1975). These studies show that for the range of synthetic DNAs and satellite DNAs of known sequence considered, the relationship between the calculated and observed spectra was very good. Included in this group was $d(C)_n \cdot d(G)_n$, ($d(T)_n \cdot d(A)_n$ was an exception) implying a similar structure as the rest of the polymers some of which are known to be in B like conformations. However, these results were based on two assumptions both of which may not be entirely correct. Firstly, $d(C)_n \cdot d(G)_n$ was used as one standard to determine $\Theta[dC \cdot dG \text{ base pair} \equiv \text{the characteristic molar ellipticity of such a pair embedded in an infinite polymer } d(C)_n \cdot d(G)_n]$ which was used in the remaining calculations. Hence, the inclusion of $d(C)_n \cdot d(G)_n$ in the same structural family as the remaining polymers represents a circular

argument. Secondly, the similar value θ [dT·dA base pair] was derived from the spectrum of the block copolymer $d(C_{15}A_{15}) \cdot d(T_{15}G_{15})$ (Burd and Wells, 1975) although it has been shown by a variety of physical techniques that the presence of the GC base pairs affects the structure of the AT base pairs (Burd and Wells, 1975; Burd et al., 1975a and b). I have dwelt on the possible structure of $d(C)_n \cdot d(G)_n$ in solution since it may be uniquely A like and also since the only fibre diffraction study of $d(TC)_n \cdot d(GA)_n$ (Langridge, 1969) suggests the two structures are similar and different from B DNA (under conditions where normally B DNA is detected, although these are not specified). It must be concluded that the structures of any of the synthetic $Py_n \cdot Pu_n$ or homopolymer DNAs in solution are not known although polymers such as $d(AT)_n$, $d(IC)_n$ or $d(GC)_n$ at high relative humidity (and presumably in solution) are probably in B conformations (Arnott et al., 1974a), as are synthetic DNAs with pyrimidines and purines in both strands (Langridge, 1969).

The nature of CD interpretations negates exact predictions about structure. However, physical studies of synthetic DNAs emphasize their unique character (as judged by X-ray fibre analysis and CD spectra) and provides a firmer basis for the hypothesis that sequences along DNA may have differing conformations depending upon the base composition and distribution.

Perhaps the most interesting property of synthetic polymers is their ability to undergo strand rearrangements and in addition, form multistranded structures (many of which involve Hoogsteen hydrogen bonding (Figure 3) such that usually only $Py_n \cdot Pu_n$ DNAs will form these structures). Much of the literature describes these features for RNA polymers as these were generally available before the correspond-

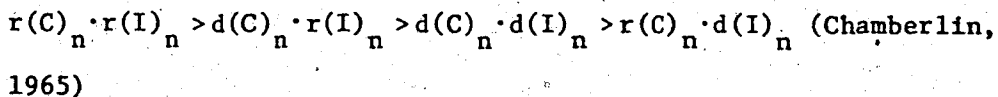
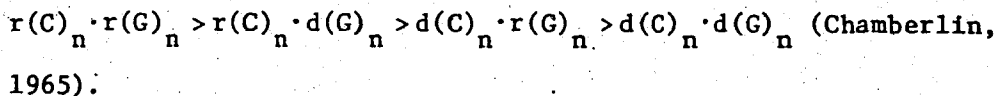
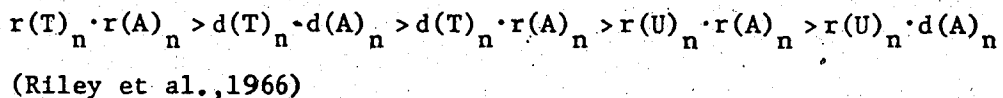
ing DNA polymers but many, if not all, of the structures can be formed with DNA polymers as well as oligomers and even purine nucleotides (probably due to their greater propensity to stack in solution using the pyrimidine polymer as "template"). Characterization of these complexes usually involves ultraviolet spectroscopy, CD studies, buoyant density studies, determination of the melting temperatures and most importantly the determination of the complex stoichiometry by the method of continuous variation (Job, 1928).

A displacement reaction can be represented by equation (1)

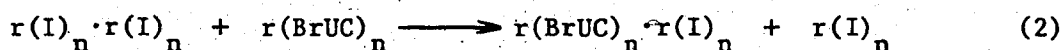


in which the more energetically favourable AC complex is formed at the expense of the AB complex with the liberation of free B. If B subsequently self associated then this association could provide an additional free energy favourable to the displacement. For polymer complexes such as AB the possible displacement induced by addition of a third strand can be judged from a knowledge of the relative stabilities of the complexes (if this rearrangement is carried out under kinetically favourable conditions).

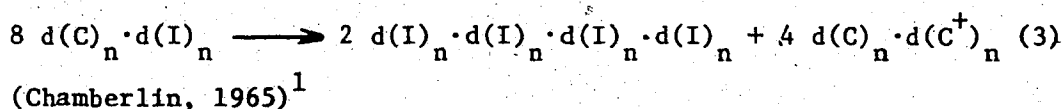
Examples of these stability series are:



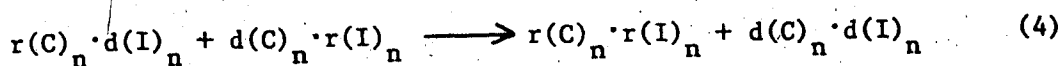
There seems no obvious rationale for the relative stabilities in these series. Thus addition of, for example, $r(C)_n$ to $d(C)_n \cdot r(G)_n$ would result in the formation of $r(C)_n \cdot r(G)_n$ and $d(C)_n$ providing the conditions did not favour additional structural rearrangements to three stranded structures. These relationships presume the polymers to be of comparable chain lengths. If the added strand is shorter than the strand to be displaced then incomplete displacement is observed (Haas *et al.*, 1976) and presumably nucleotides may not be able to displace a polymer even though the binary complex would readily be formed if a polymer was added. Polymers with modified bases would probably follow the same scheme viz. if the T_M of the complex formed is greater, displacement will occur (2) (Michelson *et al.*, 1967).



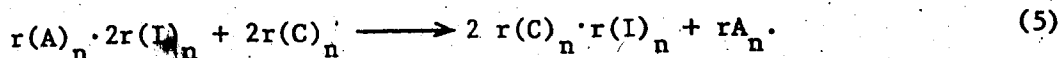
There is no evidence concerning similar relationships for polymers other than homopolymers although under favourable conditions (namely those used for transcription with RNA polymerase) the hybrid $r(\text{UC})_n \cdot d(\text{GA})_n$ is formed at the expense of $d(\text{TC})_n \cdot d(\text{GA})_n$. (Murray, 1972). More complicated rearrangements have been observed (3), (4), (5), with different polymer systems (the more stable complex is always formed)



¹Chamberlin proposed that $r(I)_n \cdot r(I)_n \cdot r(I)_n$ would be formed based on a previous (Rich, 1958) fibre diffraction study. The results of Arnott *et al.* (1974b) suggest that $r(I)_n \cdot r(I)_n \cdot r(I)_n \cdot r(I)_n$ is the proper structure and the equation has been modified to accommodate this observation.

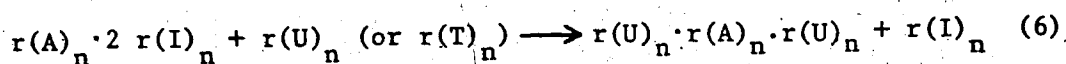


(Michelson et al., 1967)

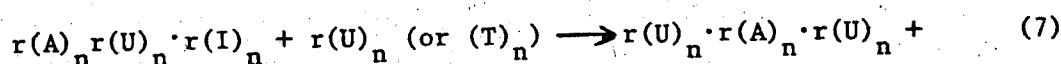


(Michelson et al., 1967)

(from reaction (4) it may be additionally inferred that for the IC series hybrid polymers are less stable). Triplexes may also be susceptible to displacement reactions (6), (7),

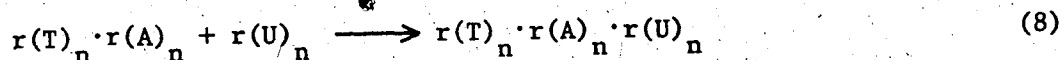


(De Clercq et al., 1975)

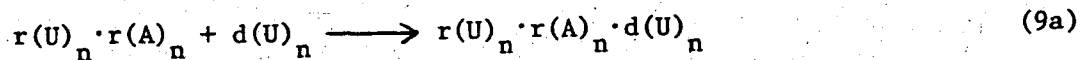
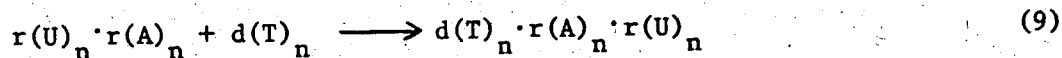
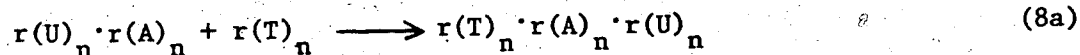


$r(I)_n$ (De Clercq et al., 1975)

and it is interesting that the formation of triplexes may also be accompanied by displacement to form the most stable Watson-Crick duplex (8) and (8)a, (9) and (9a) (Torrence et al., 1976).

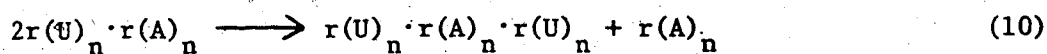


while



$Py_n \cdot Pu_n$ DNAs can form three stranded structures by the addition of a third strand, in the major groove, via Hoogsteen hydrogen bonding to the purine base (these structures are also discussed in the section on Model Building). Hoogsteen hydrogen bonding has been demonstrated from

fibre diffraction studies on $r(U)_n \cdot r(A)_n \cdot r(U)_n$ (Arnott and Bond, 1973), $d(T)_n \cdot d(A)_n \cdot d(T)_n$ (Arnott and Selsing, 1974a) and from infrared spectra of $r(C)_n \cdot d(G)_n \cdot r(C^+)_n$ (Hattori et al., 1976). It may be inferred from these studies that all triplexes of the class $Py_n \cdot Pu_n \cdot Py_n$ exhibit Watson-Crick and Hoogsteen hydrogen bonding. The range of triplexes reported for homopolymers is large and includes $r(C)_n \cdot r(G)_n \cdot r(G)_n$ (Chamberlin, 1965), $r(C)_n \cdot r(G)_n \cdot r(C^+)_n$ (Hattori et al., 1976; Thiele and Guschlbauer, 1971), $r(C)_n \cdot d(G)_n \cdot r(C^+)_n$ (Haas et al., 1976), $r(C)_n \cdot d(G)_n \cdot r(C^+)_n$ (Haas et al., 1976), $r(U)_n \cdot r(A)_n \cdot r(U)_n$ (Riley et al., 1966), $d(T)_n \cdot r(A)_n \cdot r(U)_n$ (Torrence et al., 1976), $d(T)_n \cdot r(A)_n \cdot d(T)_n$ (Riley et al., 1966), $d(T)_n \cdot d(A)_n \cdot d(T)_n$ (Riley et al., 1966), $r(U)_n \cdot d(A)_n \cdot r(U)_n$ (Riley et al., 1966), $r(T)_n \cdot r(A)_n \cdot r(T)_n$ (Howard et al., 1971), $d(C)_n \cdot d(I)_n \cdot d(I)_n$ (Chamberlin, 1965) and $r(C)_n \cdot d(I)_n \cdot d(I)_n$ (Chamberlin, 1965). Additionally, many of these triplexes can be formed by disproportionation of the duplex under appropriate conditions (high ionic strength or increased temperature) in a manner analogous to equation (10).



(Stevens and Felsenfeld, 1964).

Similar reactions have been reported for $r(T)_n \cdot r(A)_n$ (Howard et al., 1971) and $r(C)_n \cdot r(G)_n$ at acid pH (Thiele and Guschlbauer, 1971). Under the proper conditions these may also be expected with the corresponding deoxy polymers.

In view of the number of possible complexes that may be present when two homopolymers are mixed, extreme care must be taken in controlling the annealing conditions and in characterizing the products. The report by Stevens and Felsenfeld (1964) on the disproportionation of $r(U)_n \cdot r(A)_n$

is especially informative. They have shown that the formation of $r(U)_n \cdot r(A)_n \cdot r(U)_n$ from a mixture of $r(A)_n + 2r(U)_n$ is accompanied by hypochroism at 280nm but the formation of $r(U)_n \cdot r(A)_n$ from $r(A)_n + r(U)_n$ is not. The melting profile of $r(U)_n \cdot r(A)_n$ when conditions favour disproportionation, shows a monophasic shift at 67.2°C at 260nm (reflecting only the $r(U)_n \cdot r(A)_n \cdot r(U)_n$ melting) while at 280nm there is a biphasic profile with a hypochromic shift at 49.5°C (reflecting disproportionation) and the normal triplex melting at 67.5°C . Hence, rearrangements may be observed only under certain strict conditions and only when observing carefully chosen experimental parameters.

Triplex formation has also been reported for $d(TC)_n \cdot d(GA)_n \cdot r(UC^+)_n$ (Morgan and Wells, 1968) at pHs as high as 7.3. The complex was characterized by buoyant density studies, optical density-temperature profiles, ultraviolet spectral properties and by a continuous variation study. In common with $d(T)_n \cdot d(A)_n \cdot r(U)_n$ inhibition of transcription by E. coli RNA polymerase was observed. By analogy to the homopolymer triplexes the $r(UC^+)$ strand adopts Hoogsteen hydrogen bonding. Model building studies of $d(TC)_n \cdot d(GA)_n \cdot r(UC^+)_n$ in which the third strand has reverse Hoogsteen hydrogen bonding demonstrated that the triads formed were non-isomorphous and not to be expected (Figure 3). The formation of a triplex by $d(TC)_n \cdot d(GA)_n$, in which only Hoogsteen hydrogen bonding is expected, aids in the decision between choosing Hoogsteen or reverse Hoogsteen bonding for all triplexes since models of homopolymer triplexes can be made with either type of hydrogen bonding.

Many other multistrand structures have been postulated but few have been characterized. One exception is the structure of $4r(I)_n$

(Arnott et al., 1974a), and by extension $4r(G)_n$. Each member of the four stranded structure is hydrogen bonded to the adjoining bases by Hoogsteen hydrogen bonds (for $4r(I)_n$ these are $N-1$ to $0-6$ and for $4r(G)_n$ $N-1$ to $0-6$ and $N7$ to $2-NH_2$). Structures have also been proposed for $r(A)_n$, $d(A)_n$, $r(C)_n$ and $d(C)_n$ at acid pH where homopolymer duplexes are formed (Arnott, 1971). $Py_n \cdot Pu_n$ DNAs are more likely to form ordered multi-stranded structures due to their ability to form Hoogsteen hydrogen bonds as well as Watson-Crick hydrogen bonds. For example, both $d(T)_n \cdot d(A)_n$ and $d(C)_n \cdot d(G)_n$ at neutral pH form complexes of unknown structure depending upon the rate of cooling after a heat step and in the presence of metal ions or salts (A.R. Morgan, personal communication; D. Johnson, unpublished results). Also $d(C)_n \cdot d(G)_n$ and $d(C)_n \cdot d(I)_n$ can vary in buoyant density in Cs_2SO_4 (Wells et al., 1970) by as much as 96mg/cc even though the preparations were well characterized and, for $d(C)_n \cdot d(I)_n$ care was taken to ensure an equimolar ratio of $d(I)_n$ and $d(C)_n$. And Wells et al. (1970) also have described anomalous densities in Cs_2SO_4 at neutral pH for $d(TC)_n \cdot d(GA)_n$ preparations although these had equivalent buoyant densities in $CsCl$, identical CD spectra, and the same T_M in either 0.05M or 0.2M salt (all were authentic $d(TC)_n \cdot d(GA)_n$ as judged by nearest neighbour frequency, transcription studies and a variety of physical techniques). If either of the two preparations was heated to $90^\circ C$ in 10mM NaCl, 0.1mM EDTA pH 7.4 and slowly cooled a species with the buoyant density expected for $d(TC)_n \cdot d(GA)_n$ was obtained. However, rapid cooling resulted in the formation of a new species with a higher buoyant density. It was postulated that in the presence of metal ions or in solutions of high ionic strength, with or without heating, these DNAs can be trapped in metastable states and/

or multistranded complexes.

The sum total of these physical studies emphasizes the uniqueness of DNAs with repeating sequences, especially $\text{Py}_n \cdot \text{Pu}_n$ DNAs, and that many possible structures and complexes can be formed by each polymer (for a discussion of some of these in more detail see the section on Model Building). It is appropriate to discuss their possible roles in vivo and to assess the possibilities of isolating such structures (to this date, only two base triads have been confirmed in a polynucleate, the tRNA_{phe} structure (Ladner et al., 1975)). A major problem in isolating such structures may be the different conditions under which each is stable. An obvious example is any structure involving a Hoogsteen GC^+ base pair (although proteins or other species may stabilize a protonated c at neutral pH in vivo, the isolated polynucleate may require a lower pH). Other examples are the triplex $\text{r}(\text{U})_n \cdot \text{r}(\text{A})_n \cdot \text{r}(\text{U})_n$ which in the presence of ethidium bromide loses the Hoogsteen $\text{r}(\text{U})_n$ strand (Waring, 1974) although $\text{d}(\text{T})_n \cdot \text{d}(\text{A})_n \cdot \text{r}(\text{U})_n$ and $\text{d}(\text{T})_n \cdot \text{d}(\text{A})_n \cdot \text{d}(\text{T})_n$ are unaffected (N. Murray, unpublished; D. Johnson, unpublished) and $\text{r}(\text{T})_n \cdot \text{r}(\text{A})_n \cdot \text{r}(\text{T})_n$ which is selectively destabilized in the presence of tetraethylammonium ion (Howard et al., 1971), losing the Hoogsteen strand. SDS, which is used in many purification procedures, disrupts the triplex $\text{d}(\text{T})_n \cdot \text{d}(\text{A})_n \cdot \text{r}(\text{U})_n$ when Mg^{++} is present as the counterion (D. Johnson, unpublished) probably by competing with the triplex for Mg^{++} . The $\text{r}(\text{U})_n$ strand of this triplex is also sensitive to pancreatic RNase (Murray and Morgan, 1973), although less sensitive than free $\text{r}(\text{U})_n$, such that the presence of RNase in the isolation procedure could destroy the triplex. Most of the triplexes previously mentioned are stabilized by divalent metal ions or high ionic strength. However,

just as certain duplex DNAs are destabilized by increasing the ionic strength viz. $r(A)_n \cdot r(A^+)_n$ (Michelson et al., 1967) and $r(C)_n \cdot r(C^+)_n$ (Michelson et al., 1967), some triplexes may also be disrupted by these conditions as is the triplex $r(I)_n \cdot r(A)_n \cdot r(I)_n$ (Morgan and Wells, 1968). In the first two cases, the stabilization due to reduced phosphate-phosphate repulsion does not compensate for the weakened electrostatic attraction although in triplexes the phosphate repulsion would be more significant an effect and any electrostatic force relatively less important. Since these triplexes are stable under different conditions then a priori arguments would be needed to fix the choice of isolation conditions.

The stability of a putative triplex would depend strongly on the chain length of the polymers involved (in vitro studies utilize polymers of 6-10S). If a model predicted that a triplex was involved in a control or regulatory mechanism at a fine level, then this triplex would probably be difficult to isolate because of its perhaps transient nature and also probable short chain length, since most pyrimidine tracts that have been isolated are of short chain length. Sederoff et al. (1975) have isolated polypyrimidines 750 residues long which, if they formed triplexes, would be quite stable. There is an additional technical problem in that these triplexes may represent only a small percentage of the total polynucleotide present. A useful tool in the isolation of triplexes may be antibodies (Stollar and Raso, 1974) which can distinguish between triplexes and duplex synthetic homopolymers.

Postulated roles for $Py_n \cdot Pu_n$ DNAs have centred on various direct interactions. The only indirect interaction postulated (Arnott et al. 1974b) involves the possible effect of the B to A transition found

when $d(T)_n \cdot d(A)_n$ forms a triplex $d(T)_n \cdot d(A)_n \cdot d(T)_n$ on the transcription rate of immediately adjacent sequence (discussed earlier). These functions include the formation of triplexes as potential control elements in gene regulation and chromosome structure (Britten and Davidson, 1969; Crick, 1971); a triplex has been proposed to explain the compact structure of the E. coli folded chromosome (Pettijohn and Hecht, 1973); pyrimidine clusters in DNA have been implicated as initiation and termination signals for RNA polymerase (Szybalski et al., 1969). T_7 DNA is asymmetrically transcribed in vivo and in vitro (Summers and Szybalski, 1968) and the transcribed strand contains all the pyrimidine clusters as measured by $r(G)_n$ binding (> 99% of T_7 and T_3 mRNA synthesized in vivo hybridizes to the $r(G)_n$ binding strand); $d(T)_n \cdot d(A)_n$ clusters proximal to the origin of replication in E. coli may have a function in the initiation of DNA replication (Baril and Kubinski, 1975); studies on the poly $r(G)_n$ bindings sites in λ DNA led to correlations (Champoux and Hogness, 1971) between these sites and intercistronic regions of λ polycistronic mRNA implying a possible function in regulating the size of a particular mRNA from a single promoter (perhaps as an anti-terminator locus after the first cistron); $Py_n \cdot Pu_n$ sequences may be metastable intermediates in protein DNA interactions, directing a particular protein to a neighbouring sequence (this hypothesis may explain the rapid kinetics of protein DNA interactions when both the DNA sequence and protein concentrations are low. A primary interaction with DNA that has a unique conformation would result in an increased association rate for the protein); sequence analysis of both Drosophila (Gall and Atherton, 1974) and mouse (Biro et al., 1975) satellite DNAs show that these can be classified into

families of repeating sequences differing only by a single base change. Although not $Py_n \cdot Pu_n$ it may be important that none of these substitutions leads to the formation of $Py_n \cdot Pu_n$ DNA suggesting a distinct role for this type of DNA. In addition the results of this thesis suggest other possible roles for $Py_n \cdot Pu_n$ DNA which will be discussed later. Although none of these postulates have been proven, physical studies have provided a solid base for many of the predictions some of which may yet be found in the wide diversity of nature.

More sophisticated questions about the properties of any sequence can be posed as more sophisticated model systems can be constructed. Recent work on chemically defined block polymers eg. $d(C_{20}A_{10}) \cdot d(T_{10}G_{20})$ (Burd et al., 1975a; Burd et al., 1975b) has shown that each region exerts an effect on the structure and stability of the other region providing a rationale for "regulation" at proximal sites both in the presence and absence of other regulators (in the model system the probes netropsin (binds to AT region) and actinomycin D (binds to GC region) raised the melting temperature of the entire complex - no hysteresis was observed - and protected both regions against nuclease digestion). New approaches with chemically defined DNAs, such as this one and the possible inclusion of defined sequences into natural DNAs using restriction endonucleases, will be useful in approaching many of the problems concerning the effects of base sequence and allow physical and chemical tests of many of the above models.

The purpose of this thesis is to define and characterize a new class of polymer structures, "multiplexes", which are formed reversibly by $Py_n \cdot Pu_n$ DNAs (except $d(T)_n \cdot d(A)_n$) of repeating sequence.

CHAPTER II MODEL BUILDING

Various models can be postulated to explain the properties of the multiplex. These include the invocation of a conformational change only, the formation of a Hoogsteen-type duplex or related structures, the rearrangement to triplexes and finally the construction of tetraplexes (ordered four-stranded structures). Although other higher-ordered complexes may be possible, these are considered the most likely to involve specific hydrogen bonds between the pyrimidine and purine bases. Various types of hydrogen bonding schemes which might stabilize these structures and various experimental approaches which may differentiate between these models are considered.

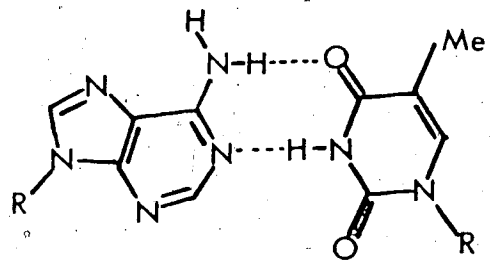
Single crystal analysis of the interactions of purine and pyrimidine bases and their derivatives, reveals a wide range of possible hydrogen bonding patterns in which almost every possible donor and acceptor can participate (Vogt and Rich, 1970). However, ordered multistranded structures cannot accommodate all of these possible arrangements for two reasons. Firstly, many of the less energetically favourable interactions are found only when a more favourable site for interaction is chemically modified, which is not the case for these synthetic polymers. The converse is also true for one obvious example. The purine N-9 position and the pyrimidine N-3 are "blocked" due to the formation of the glycosidic bond and unavailable for hydrogen-bond formation. Secondly, the structures formed must be isomorphous, i.e. residues must be related by symmetry operations. (An example will be given in the discussion of the triplex models). These restrictions limit the range of models which can be postulated for the multiplex.

For the purposes of this discussion the bases are assumed to be in the anti conformation (χ (the angle between N-(pyrimidine C2 or purine C4) and sugar C1-C2) $\sim 90^\circ$ (Arnott, 1970)) as has been found for all ordered duplex or triplex structures characterized to this time. A possible duplex structure involving $r(8\text{BrA})_n$ with the base in the syn conformation ($\chi \sim 300^\circ$ (Arnott, 1970)) has been reported (Howard et al., 1974) but conclusive evidence in favour of a duplex structure has not been presented.

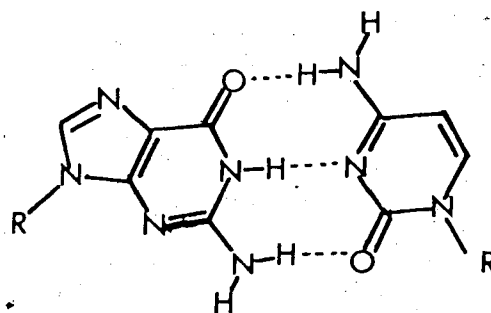
Watson-Crick hydrogen bonding (Crick and Watson, 1954; Arnott, 1970) makes use of the purine 1, 2 and 6-positions and the pyrimidine 2, 3 and 4-positions to form specific AT and GC base pairs (Figure 3). The formation of these hydrogen bonds reduces the accessibility of these sites to various chemical reagents (eg. formaldehyde, Grossman, 1968; glyoxal, this thesis and Litt, 1969; alkylating agents, Singer, 1975) but in a B type helix the purine 3 and 7-positions are available, in the minor and major grooves respectively, to both chemicals (Singer, 1975) and possibly various proteins (Seeman et al., 1976) and polyamines (Suwalsky et al., 1969). In contrast, Hoogsteen hydrogen bonding (Hoogsteen, 1959; Arnott, 1970) shown in Figure 3 , involves the purine 6 and 7-positions and the pyrimidine 3 and 4-positions in base pairing. Note that these positions are now blocked and that the purine 1, 2 and 3-positions are available to various probes. Hence, the reactions of site-specific chemical reagents may be useful in determining which positions are involved in multiplex stability. Also a Hoogsteen GC base pair requires protonation of the cytosine N-3 which may be detectable experimentally. Although no DNA duplex with Hoogsteen hydrogen bonding has been observed, models can be constructed

Figure 3 Base Pair Hydrogen Bonding Schemes

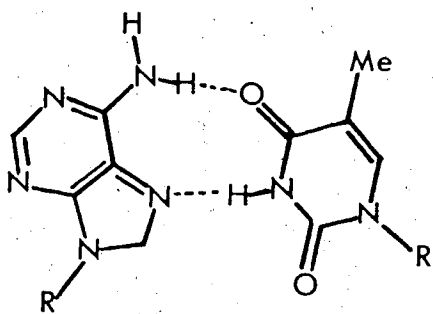
- A AT base pair with Watson-Crick hydrogen bonding
- B GC base pair with Watson-Crick hydrogen bonding
- C AT base pair with Hoogsteen hydrogen bonding
- D GC base pair with Hoogsteen hydrogen bonding
- E AT base pair with reverse Hoogsteen hydrogen bonding
- F GC base pair with reverse Hoogsteen hydrogen bonding



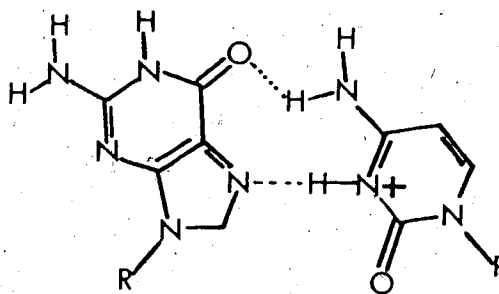
A.



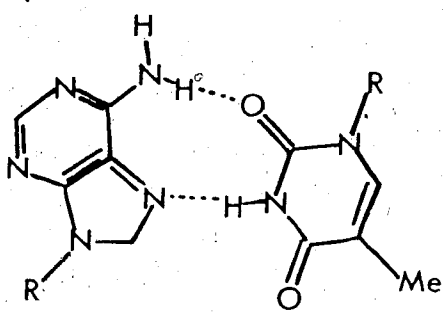
B.



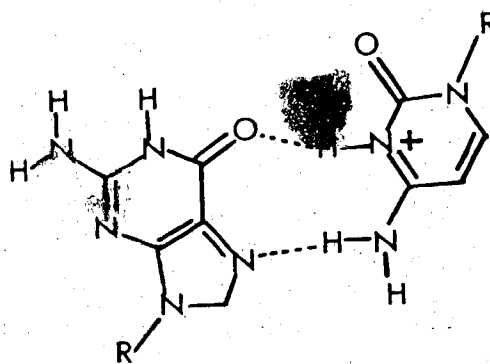
C.



D.



E.



F.

which have isomorphous base pairs and a related type of hydrogen bonding has been observed for the poly rA helix at acid pH (Rich et al., 1961).

Hoogsteen hydrogen bonding has been observed in triplexes such as $r(U)_n \cdot r(A)_n \cdot r(U)_n$ (and by analogy $d(T)_n \cdot d(A)_n \cdot r(U)_n$ and $d(T)_n \cdot d(A)_n \cdot d(T)_n$) in which the $r(U)_n$ strand winds in the major groove of the Watson-Crick $r(A)_n \cdot r(U)_n$ duplex forming specific hydrogen bonds between adenine and uracil residues (Arnott and Bond, 1973). The Hoogsteen strand is of the same polarity (if the bases are anti as defined earlier) as the Watson-Crick purine strand and antiparallel with respect to the Watson-Crick pyrimidine strand. Since there is also evidence in favour of the triplex $d(TC)_n \cdot d(GA)_n \cdot r(UC^+)_n$ (Morgan and Wells, 1968) by analogy the all DNA triplex shown in Figure 4, $d(TC)_n \cdot d(GA)_n \cdot d(TC^+)_n$, could be expected. The isomorphous pyrimidine-purine-pyrimidine base triads TAT and CGC^+ are stabilized by both Watson-Crick and Hoogsteen hydrogen bonds and the Hoogsteen cytosine is protonated at N-3. If the keto base t is replaced by g and a^+ substituted for the amino base c^+ the isomorphous pyrimidine-purine-purine triads TAG and CGA^+ can be formed (Figure 5), again utilizing both Watson-Crick and Hoogsteen hydrogen bonding and involving a protonated base, in this case the N-1 of adenine. To digress, these figures can also be used to illustrate the meaning of isomorphous. If the triads TAT and TAG are superimposed upon each other (as in a repeating polymer) then the position of the Hoogsteen glycosidic bond (N_1 of T and N_9 of G) changes sufficiently between residues that an ordered structure is not possible and these triads are non-isomorphous. For similar reasons $d(TG)_n \cdot d(CA)_n$ cannot form triplexes as the available purine 6- and 7-positions alternate from strand to strand along the length of the duplex. This may be the

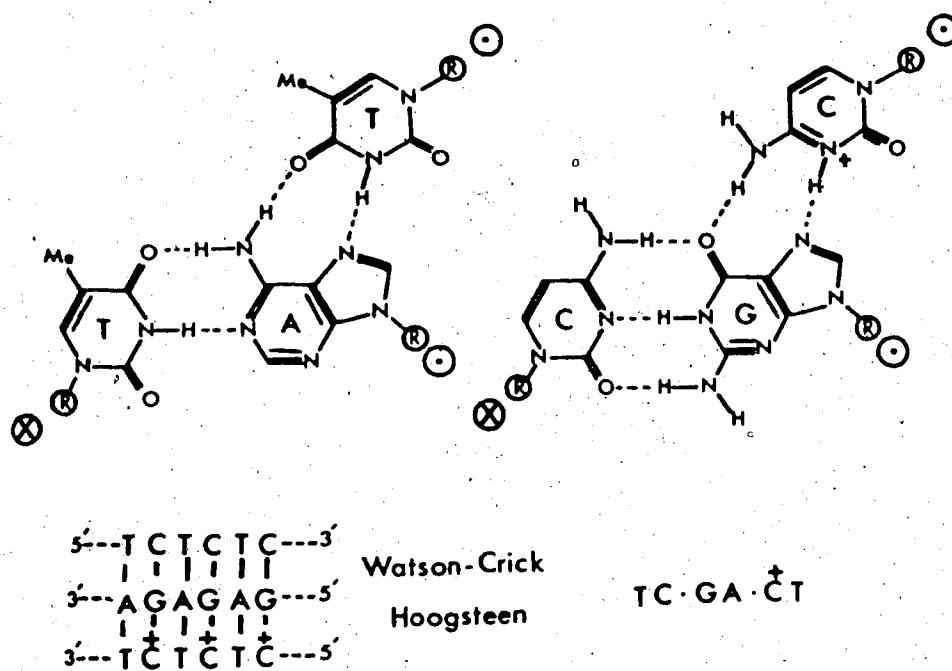
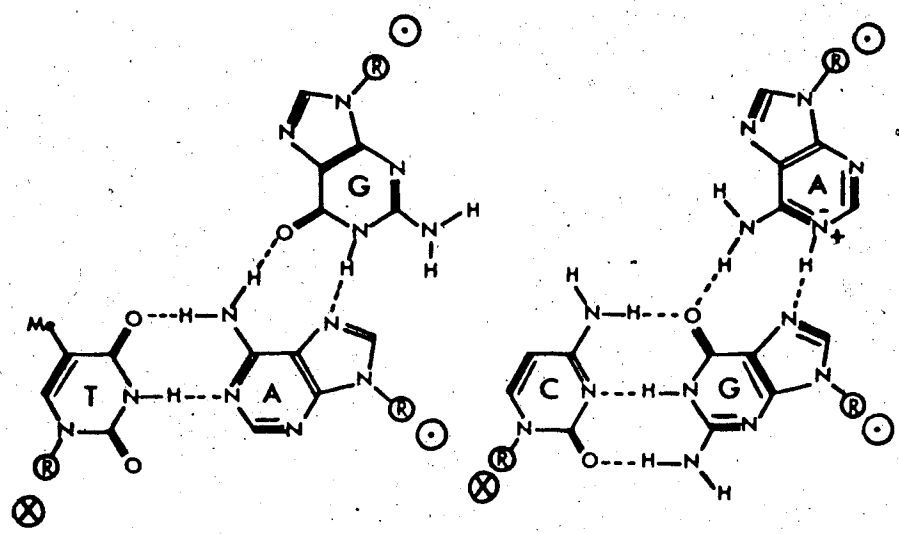


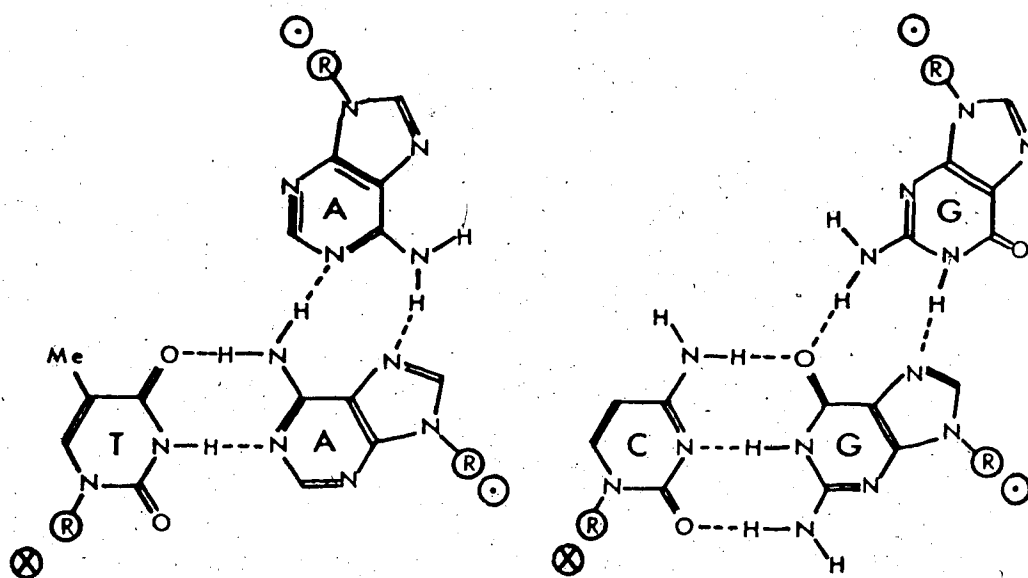
Figure 4 Proposed Hydrogen Bonding for the Triplex
 $d(\text{TC})_n \cdot d(\text{GA})_n \cdot d(\text{TC}^{\oplus})_n$



5'---TCTCTC---3'
 | | | | |
 3'---AGAGAG---5' Watson-Crick
 | | | | |
 3'---GAGAGA---5' "Hoogsteen"

TC · GA · GA⁺

Figure 5. Proposed Hydrogen Bonding for the Triplex $d(TC)_n \cdot d(GA)_n \cdot d(GA^+)_n$



Not Strictly Isomorphous TC·GA·AG

Figure 6 Possible Hydrogen Bonding for the Triplex
 $d(TC)_n \cdot d(GA)_n \cdot d(AG)_n$

reason why $d(TG)_n \cdot d(CA)_n$ does not form a multiplex. Figure 6 describes the pyrimidine-purine-purine triads TAA and CCG which are also stabilized by Watson-Crick and Hoogsteen hydrogen bonds but involve no protonated bases. These are not strictly isomorphous and would not be expected in ordered polymer structures although similar triads are involved in stabilizing tRNA structure (Quigley *et al.*, 1975; Ladner *et al.*, 1975) i.e. $U_{12}A_{23}A_9$ and $C_{13}G_{22}^{7Me}G_{46}$.

The final variety of model considered is an ordered structure of base tetrads called a tetraplex. McGavin (1971) has constructed models of the base tetrads $\begin{matrix} AT \\ TA \end{matrix}$ and $\begin{matrix} GC \\ CG \end{matrix}$ (Figure 7) which are stabilized by Watson-Crick hydrogen bonds plus the additional hydrogen bonds formed when the two duplexes are brought together. Additionally tetrads involving both Watson-Crick and Hoogsteen hydrogen bonds can be constructed (Figure 8). Both types of tetrads can be formed with C.P.K. models and the tetrads of each are isomorphous with each other but not with the tetrads of the other type. One obvious difference between them is the involvement of a protonated base (N3 of cytosine) in Hoogsteen hydrogen bonding. Another is more subtle.

Although the tetraplex described by McGavin can in theory be formed by moving the two duplexes together into the proper position additional limitations are imposed on the formation of the tetraplex with Hoogsteen hydrogen bonding since the second pyrimidine strand is parallel to the purine strand of the Watson-Crick duplex. Either of two processes are possible. One would involve disruption of the original duplex perhaps involving a process akin to branch migration with a single polypyrimidine strand first forming a Hoogsteen triplex with subsequent incorporation of a polypurine strand from the same or

a different molecule into the tetraplex in the proper orientation. This second purine strand may be either parallel or antiparallel to the Hoogsteen pyrimidine strand. In an alternate process two duplexes would approach each other in an orientation such that the pyrimidine strand destined to form the Hoogsteen hydrogen bonds has the proper polarity (parallel to the Watson-Crick purine strand) with subsequent rotation of the bases breaking the Watson-Crick duplex to form the structure shown in Figure 8. In this case, the second purine strand remains antiparallel to the Hoogsteen pyrimidine strand. Both types of rearrangement imply that sites not normally available to chemical modification in either the duplex or multiplex may become transiently exposed during the rearrangement.

Both tetraplex and triplex models predict a multiplex which is rather inert to chemical reagents although in theory the purine N-3 is available. There is one additional point to be made. X-ray fibre analysis of the triplex $r(U)_n \cdot r(A)_n \cdot r(U)_n$ (Arnott and Bond, 1973) has shown its diameter to be only slightly increased from that of the duplex $r(A)_n \cdot r(U)_n$ (minimum effective diameter is 24.6 \AA compared to 23.2 \AA for A' RNA helix). Also, the diameter of the tetraplex model constructed by McGavin is the same as that of the parent duplex. For these reasons, it would seem impossible to be able to infer the number of strands in the multiplex by careful analysis of electron micrographs, regardless of technical problems associated with the spreading, staining, and shadowing of the sample.

Figure 7 Tetrad Hydrogen Bonding of McGavin (1971)

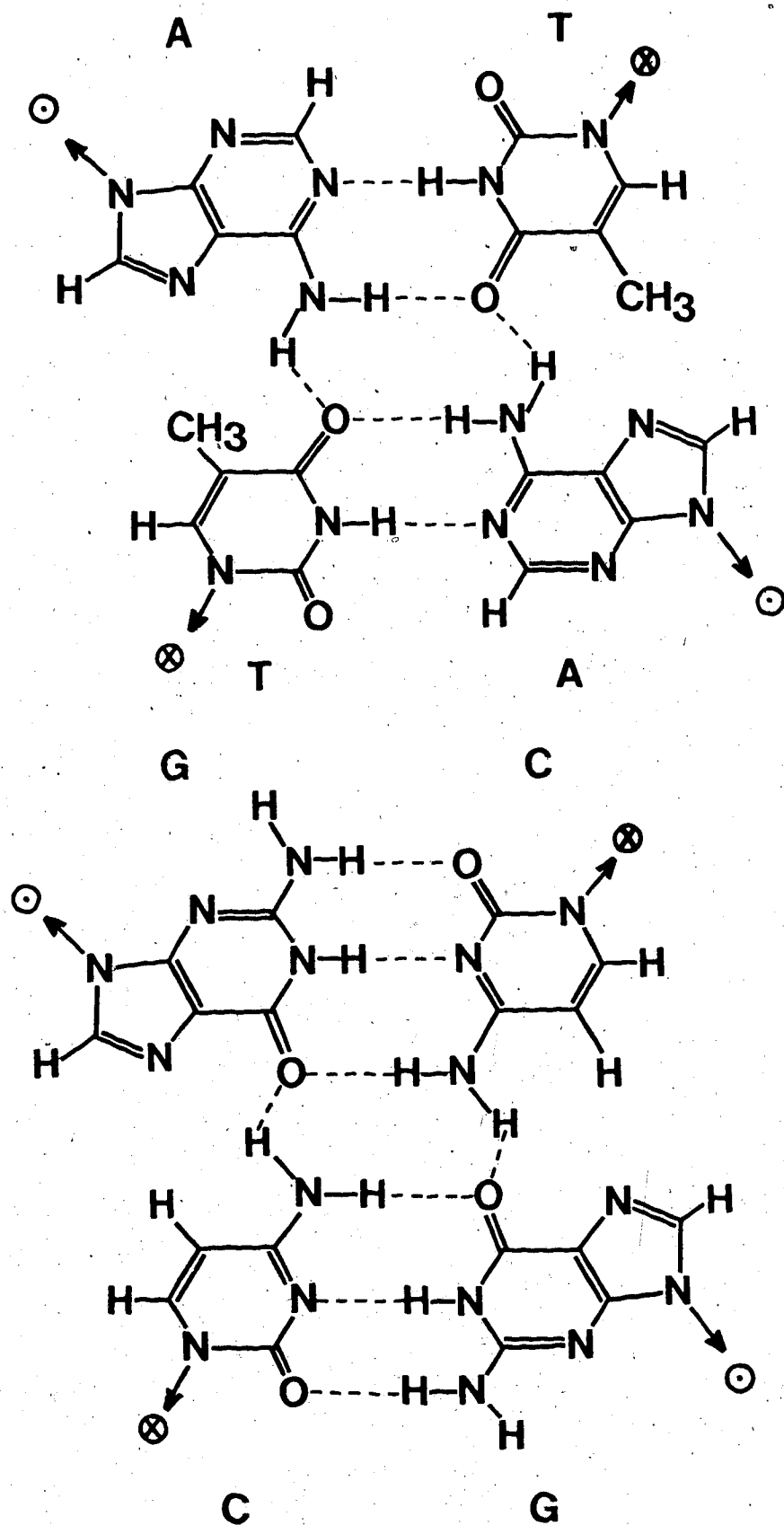
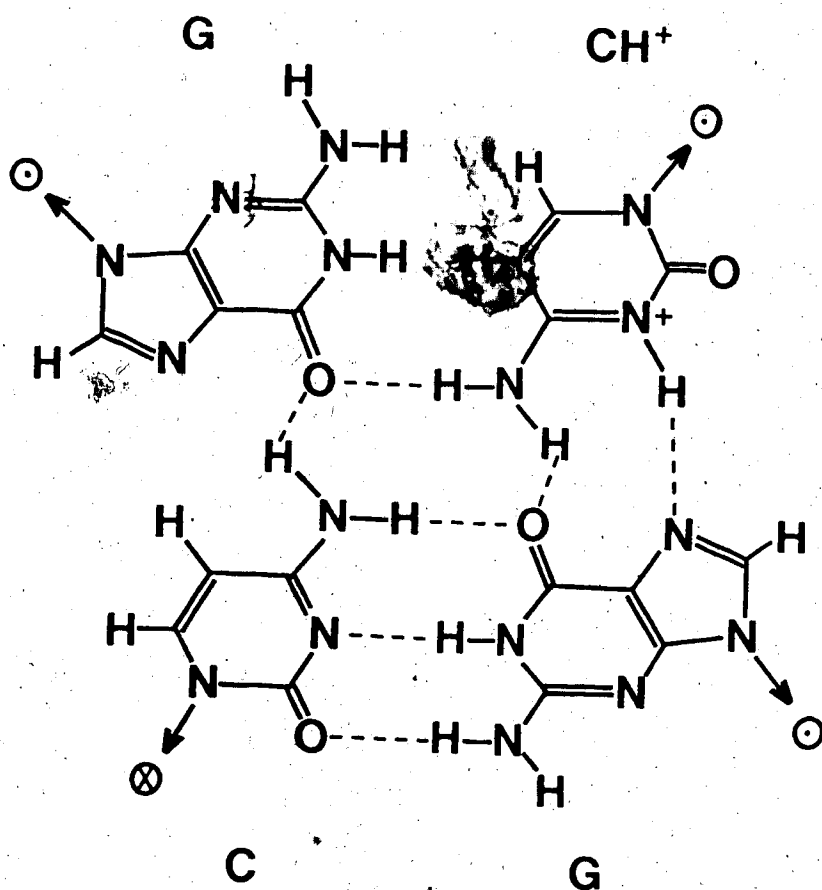
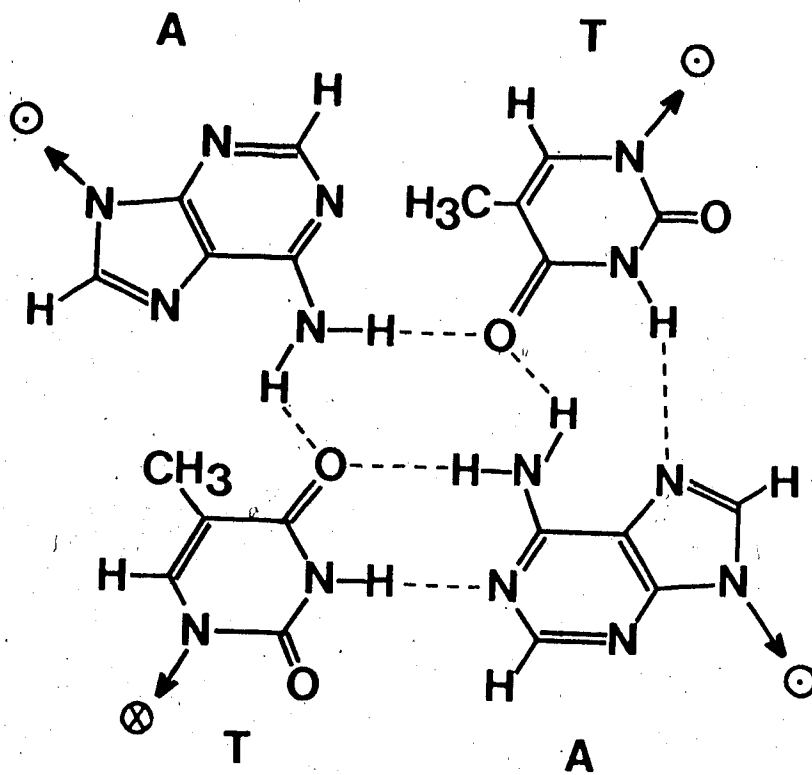


Figure 8 Possible Tetrad Hydrogen Bonding Involving Hoogsteen Hydrogen Bonds



CHAPTER III MATERIALS AND METHODS

Chemicals and enzymes

Most chemicals used in these studies were reagent grade and are freely available. One exception is Tris base, which was either from Schwarz/Mann (enzyme grade) or was purified by passage over Norit to remove uv absorbing material. Unlabelled dNTPs were obtained from P-L Biochemicals and ^3H or ^{14}C dNTPs or NTPs from Schwarz/Mann. CsCl was purchased from Pierce Chemical Co. and Cs_2SO_4 from Kerr-McGee Chemical Corporation. Ethidium bromide was from Sigma, spermine from Nutritional Biochemical, glyoxal (~40% aqueous solution) from Fisher and formaldehyde from Fisher. Unlabelled dimethylsulfate was obtained from Aldrich and ^3H DMS from Amersham/Searle. Norit-A was from Fisher.

Nucleases were purchased from Worthington Biochemical Corporation. The DIII fraction used in the DNA synthetic reactions is a byproduct of the E. coli RNA polymerase purification procedure of Paetkau and Coy (1972). Before use it was treated as described by Morgan et al. (1974).

Sephadex gels were purchased from Pharmacia, agarose gels from Bio-Rad Labs, Hydroxylapatite (Bio-Gel HT) from Bio-Rad Labs and DEAE cellulose and phosphocellulose from Whatman.

RNA polymerase was isolated from E. coli (Burgess, 1969) and was a gift of P. D'Obrenan. Various E. coli DNA polymerase preparations were used to synthesize the repeating DNAs. No differences in specificity were observed between the various enzymes. Polymerase prepared by the method of Jovin et al. (1969) was a gift of M.G. Burrington. T. Elgert isolated the polymerase prepared by the method of Heijneker et al. (1973).

Ultraviolet Spectroscopy

All measurements were performed on a Gilford model 2400 spectrophotometer equipped with an insulated cell compartment and a recorder.

Absorbance-temperature transitions were measured at $\lambda = 260\text{nm}$ on samples ($0.5-1.0 A_{260}$), dialyzed against the appropriate solvent, in 10mm light path length (0.5ml capacity) quartz cuvettes. The samples were purged with helium and tightly sealed. The temperature of the cell compartment was regulated by a Haake constant temperature circulator filled with ethylene glycol/H₂O and monitored by a thermocouple. Transitions were recorded automatically and were reproducible to $\pm 1.0^\circ\text{C}$ when the temperature was raised 1 degree C/2-3 minutes. These values were not corrected for thermal expansion of the solution or cuvette.

Ultraviolet absorbance spectra were determined manually at ambient temperature or after melting at the given temperature.

Ultracentrifugation

Analytical CsCl or Cs₂SO₄ density gradient centrifugation was carried out on a Beckman Model E ultracentrifuge equipped with uv optics and for later studies with an electronic scanner. Centrifugation was at 48,000 rpm (CsCl runs) or 44,000 rpm (Cs₂SO₄ runs) for at least 20 hours at 25°C. The DNA buoyant density was calculated using the isoconcentration method (Vinograd, 1963) in which case the initial density was determined from the refractive index measured on an Abbe refractometer or, more routinely, by including a DNA of known density. Values of β were from Chervenka(1969) for CsCl and from Morgan and Wells (1968) for Cs₂SO₄.

Sedimentation velocity centrifugation of DNA was carried out using a Vinograd type 1 band forming centrepiece. Usually, centrifugation was at 48,000 rpm with 8 minute photographs for synthetic DNAs, 44,000 for natural DNAs. Solvents used were 0.1M NaCl, 0.9M NaOH for alkaline runs and 10mM Tris HCl pH 8.0, 2.83M CsCl for neutral runs. Corrections for the viscosity and density of the media were from Studier (1965) for alkaline runs and from Gray et al. (1971) for neutral runs. Sedimentation coefficients and molecular weights were calculated according to Studier (1965).

Electrophoresis

SDS polyacrylamide gel electrophoresis was performed as described by Weber and Osborn (1969). Recrystallized acrylamide was not used but the stock solution of 29% (w/v) acrylamide and 1% (w/v) methylenebisacrylamide was purified by stirring with Norit (5 grams per 100 mls solution) and filtering under vacuum through a Millipore filter (Pulleyblank, 1974). Tube gels were run using a Canalco apparatus with a Buchler power supply. Gels were stained 2 hours in 0.2% Coomassie Brilliant Blue in 45% (v/v) MeOH, 10% (v/v) acetic acid and destained with a Canalco destainer using a 7.5% (v/v) acetic acid, 10% (v/v) methanol destaining solution. These were traced with a Gilford Spectrophotometer equipped with a gel scanner at $\lambda = 540\text{nm}$.

Natural and synthetic DNAs

Bacterial DNAs and calf thymus DNA were purchased from Worthington or in some cases isolated by standard techniques (Smith, 1967).

Phage DNAs were extracted from isolated phage using a 3 to 1 mixture of redistilled chloroform and n-butanol. These were then

dialysed against 10mM Tris HCl pH 8.0, 0.1mM EDTA and frozen (-20°C) in the same buffer. T_7 phage was prepared by the method of Summers and Szybalski(1968) and λ phage from heat induced E. coli CSH45 (F^- carrying a λ lysogen with a temperature sensitive repressor). PM2 CCC DNA was isolated by a modification of the method of Salditt et al.(1972).

Synthetic DNAs were synthesized with either chemically synthesized oligomers (eg. see Wells et al., 1970; Morgan et al., 1974) or previously defined polymers as templates. The buoyant densities in Cs_2SO_4 at pH 7.0 and the T_M s in SSC/10 of the $\text{Py}_n \cdot \text{Pu}_n$ DNAs used in this study are given in Table 3 and are in agreement with previously reported values. A plot of T_M (in SSC/10) against mole fraction G+C is a straight line for a mole fraction G+C 0.33 to 1.00 (Figure 9). Extrapolating to 0.00 mole fraction G+C gives a value of 47°C . The $\text{Py}_n \cdot \text{Pu}_n$ DNA $d(\text{T})_n \cdot d(\text{A})_n$ is the only $\text{Py}_n \cdot \text{Pu}_n$ DNA to have a T_M greater than the corresponding DNA with pyrimidines and purines in the same strand when no divalent cation is present. Also, a plot of $\rho \text{Cs}_2\text{SO}_4$ against mole fraction G+C (Figure 9) approximates a straight line, this time with $d(\text{C})_n \cdot d(\text{G})_n$ falling off the line at a $\rho \text{Cs}_2\text{SO}_4$ of 1.467g/cc. Extrapolation of this plot to 1.00 mole fraction G+C predicts a value of 1.443g/cc which is close to that reported for $d(\text{GC})_n$ (1.448g/cc) by Wells et al.(1974). These relationships (T_M and $\rho \text{Cs}_2\text{SO}_4$) are presented to emphasize the differences of $\text{Py}_n \cdot \text{Pu}_n$ DNAs, especially of extreme base compositions, when compared to natural DNAs. Also, they were useful in predicting approximate base compositions for unknown $\text{Py}_n \cdot \text{Pu}_n$ DNAs such as those synthesized from L cell pyrimidine tracts using methods described in the section on the replication of $\text{Py}_n \cdot \text{Pu}_n$ DNAs.

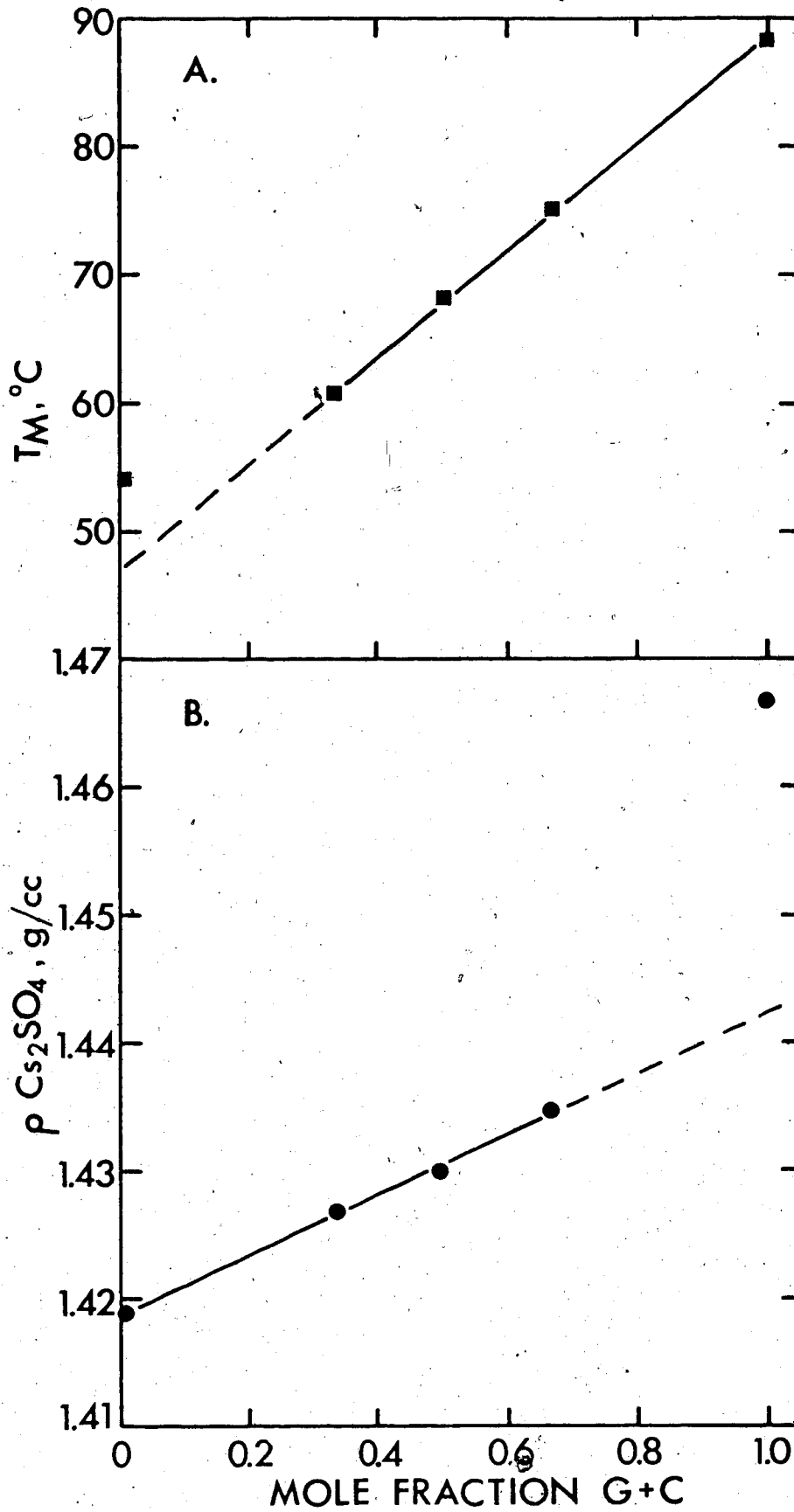
$\text{Py}_n \cdot \text{Pu}_n$ DNA	$\rho \text{ Cs}_2\text{SO}_4$ (g/cc) ¹	T_M (°C) ²
$d(\text{T})_n \cdot d(\text{A})_n$	1.419	54.0
$d(\text{TTC})_n \cdot d(\text{GAA})_n$	1.427	60.5
$d(\text{TC})_n \cdot d(\text{GA})_n$	1.430	68.0
$d(\text{TCC})_n \cdot d(\text{GGA})_n$	1.435	75.0
$d(\text{C})_n \cdot d(\text{G})_n$	1.467	88.0
$d(\text{BrUC})_n \cdot d(\text{GA})_n$	1.481	73.0

TABLE 3 Physical Properties of the $\text{Py}_n \cdot \text{Pu}_n$ DNAs Used In These Studies

1. determined in 10mM potassium phosphate, pH 7.0 with either λ DNA (1.426g/cc) or M_{13} single-stranded DNA (1.4465g/cc) as an internal standard.
2. T_M buffer was SSC/10.

Figure 9 Plots of T_M and ρ Cs_2SO_4 Versus Mole Fraction G+C
For Synthetic $\text{Py}_n \cdot \text{Pu}_n$ DNAs

- A. T_M (SSC/10) plotted as a function of mole fraction G+C (solid line) and extrapolated to 0.0 mole fraction G+C (broken line). Actual values are given in Table 3.
- B. ρ Cs_2SO_4 at pH 7.0 plotted as a function of mole fraction G+C (solid line) and extrapolated to 1.0 mole fraction G+C (broken line). Actual values are given in Table 3.



Synthetic DNAs were replicated in reaction mixtures containing 0.05M potassium phosphate pH 7.5, $MgCl_2$ in excess over total deoxy 5'-triphosphate by 5-10mM, 2mM each dNTP (for $d(TC)_n \cdot d(GA)_n$), DIII fraction diluted 1/100, 10 μ g/ml tRNA to inhibit endonuclease I activity in the DIII fraction, 50pg/ml DNase I (which provides primers to stimulate the reaction but at this level does not degrade the product), 10-25 μ g/ml template and 10-20 μ g/ml purified DNA polymerase. For a template such as $d(TTC)_n \cdot d(GAA)_n$, dGTP and dCTP were present at 1mM each and dTTP and dATP at 2mM each. Incubation was at 37°C and synthesis was monitored using the neutral ethidium fluorescence assay with known standards. If a contaminating side reaction ($d(AT)_n$ synthesis) was detected by a return of after heat fluorescence, then the reaction was immediately terminated. In any event, synthesis was terminated after 4-6 hrs by the addition of 0.1% SDS, 20mM EDTA (final concentrations) and heating for 10 minutes at 55°C. The product DNA was isolated by chromatography over Agarose 15M, in 10mM Tris HCl pH 8.0, 0.1mM EDTA, (from which it was excluded), concentrated, dialysed against the same buffer and stored in the same buffer at -20°C. These procedures are described by Morgan *et al.* (1974). The synthesized DNAs were characterized by uv absorption, fluorescence in EB solutions, buoyant density and melting temperature. Their molecular weights ranged from $3-5 \times 10^5$ daltons.

Ethidium Fluorescence Assays

Many of the assays used in this work have been described by Morgan and Paetkau (1972) or Morgan and Pulleyblank (1974). Only a brief summary is included here. For a description of the properties of the ethidium-DNA complex see LePecq and Paoletti (1967).

When ethidium intercalates into duplex structures a 50-fold fluorescence enhancement is observed which is dependent on the integrity of the duplex structure. Most synthetic DNAs, when heat denatured (usually 2 minutes at 95°C) under low ionic strength conditions at about neutral pH, do not reanneal and show a complete loss of fluorescence. Self-complementary polymers such as $d(AT)_n$ or covalently linked complementary structures show a return of fluorescence, after the heat step, proportional to the amount of duplex reformed, a property which can be used to differentiate the two classes. Duplex DNA, heat denatured at neutral pH, gives a 50% return of fluorescence due to the formation of intramolecular duplex regions. These can be selectively destabilized with respect to native DNA by raising the pH and thus when natural DNAs are measured an alkaline ethidium buffer is used.

The neutral ethidium mixture contains 5mM Tris HCl pH 8.0, 0.5mM EDTA and 0.5 μ g/ml ethidium bromide while the alkaline ethidium mixture contains 20mM potassium phosphate pH 11.7, 0.4mM EDTA, 0.5 μ g/ml ethidium bromide. Both assay systems are sensitive (0.5 - 1.0 μ g DNA/assay point) and since normally a 1/200 dilution of sample into the ethidium mixture occurs, interference by any compound in the reaction mixture is usually negligible.

Any ligand which modifies (usually reduces) the binding of ethidium can be assayed with this system (see especially Appendix I for the reactions of chemical reagents with DNA). The use of CCC DNA as a substrate for various enzymes in combination with the ethidium assay is described in Morgan and Pulleyblank(1974), Appendix I and where necessary in the text.

All measurements were made on a Turner Spectrofluorometer, model

430, with 525nm the excitation wavelength and emission at 600nm, at 25°C. Machine fluctuation was monitored by the use of a DNA standard.

Radioactive Counting

Samples were pipetted onto prewashed (0.1M Na pyrophosphate) Whatman 3MM paper discs and washed 3 x 10 minutes with ice-cold 5% (w/v) trichloroacetic acid and 1 x 5 minutes with ethanol. These were then dried and counted in a toluene based scintillation fluid (4g Omnifluor (New England Nuclear)/litre toluene) to determine TCA precipitable or acid precipitable counts. Samples which contained water and salts were counted in Aquasol (New England Nuclear).

Multiplex Studies

Rearrangement of $Py_n \cdot Pu_n$ DNAs to form multiplexes was normally monitored by the use of modified ethidium fluorescence assays which varied depending upon the specific requirements of the experiment but all included buffers at low pHs. LePecq and Paoletti(1967) have shown that the enhanced ethidium fluorescence is observed at any pH value where duplex DNA is stable which includes pH 4.0, the lowest value used in these experiments. Since divalent metal ions (Mg^{++} usually although Zn^{++} can substitute) or monovalent cations (usually 100 - 1000mM) are needed for the rearrangement and are essential to the stability of the multiplex, one or the other is included in the ethidium assay buffer. If the concentration of ethidium in the buffer used for rearrangement is $>2\mu g/ml$ no loss of fluorescence is observed presumably due to stabilization of the initial duplex. The inclusion of salts or metal ions in the ethidium buffer diminishes the fluor-

escence per mole nucleotide. Although the neutral ethidium assay requires only 0.5 - 1.0 μ g of DNA per reading, inclusion of salts necessitates the addition of larger amounts of DNA.

Preparative Cs_2SO_4 buoyant density gradients of rearranged material were performed as follows: the appropriate double-labelled polymer (labelled with ^3H dAMP and ^{14}C dTMP, counted with narrow channels to reduce ^{14}C spillover into the ^3H channel) was incubated at λ_{260} in 1 ml of 0.1M Na acetate pH 5.0, 0.1mM EDTA, 0.5M NaCl for up to 4 days at room temperature. Then solid Cs_2SO_4 was added to 45% saturation and the volume increased to 5ml with a final Na acetate concentration of 0.05M. Two 100 μ l samples were pipetted onto filter paper discs, washed and counted. The remaining material was centrifuged in a 50Ti rotor, at 20°C, at 35,000 rpm for 60 - 70 hrs on a Beckman L2-65B. Gradients were fractionated with the aid of a peristaltic pump (LKB) directly onto filter paper discs, washed and counted as described.

EB/ Cs_2SO_4 gradients were run on a Beckman Model E analytical ultracentrifuge. Ethidium concentrations were calculated using the extinction coefficients of Gray et al. (1971).

Circular dichroism measurements of $d(\text{TG})_n \cdot d(\text{CA})_n$ and rearranging $d(\text{TC})_n \cdot d(\text{GA})_n$ were recorded on a Cary 60 Spectropolarimeter equipped with model 6001 circular dichroism accessory and thermostated cell (25°C). Data treatment was according to Wells et al. (1970). For $d(\text{TG})_n \cdot d(\text{CA})_n$ an extinction coefficient of 6.5×10^3 at 260nm was used and E_p^{260} for $d(\text{TC})_n \cdot d(\text{GA})_n$ was 5.7×10^3 (Morgan and Wells, 1968). Solutions were filtered through a Millipore filter (HAWP 02500, 0.45 μ) before use.

Titration of rearranging $d(TC)_n \cdot d(GA)_n$ with 0.0113 M HCl (prepared, stored and standardized with NaOH as described in Skoog and West) was performed on 10ml aliquots of $d(TC)_n \cdot d(GA)_n$ ($\sim 0.5mM$ solutions) dialysed (3 x 2 litres, overnight each) against 0.5M NaCl, 1.0 μ M EDTA pH 7.4. Solutions were purged 10 minutes with N_2 before titration and over the period of titration (3 - 4 hours) N_2 was constantly bubbled through the solution as shown in Figure 10. HCl was delivered via an 'Alga' Micrometer All-glass Syringe (Wellcome Reagents Ltd.) which was calibrated by weight. Experiments were performed using a Radiometer 26 pH meter, Titrator II and Titrigraph SBR 2c connected to a Radiometer GK2302C electrode by titrating from neutrality to pH 4.5 with the aid of the pH stat accessory over a long time period. The electrode was standardized immediately before the initiation of titration and checked immediately afterwards. Appreciable drift was not observed. The solution was constantly mixed with a magnetic stirring bar. Data are presented as volume HCl versus time since $d(TC)_n \cdot d(GA)_n$ undergoes rearrangement over a long time period. Controls (buffer alone or buffer with calf thymus DNA) were titrated to correct for the amount of acid necessary to titrate from pH \sim 7.0 to 4.5 in the absence of reaction and also the small amount of acid taken up over the time course of the experiment.

Reaction of Chemicals with DNAs

Formaldehyde, glyoxal and dimethylsulfate were reacted with both $d(TC)_n \cdot d(GA)_n$ at pH 7 - 7.5 and the corresponding multiplex at pH \sim 5.0, with the extent of reaction monitored by a variety of means.

Reaction of $d(TC)_n \cdot d(GA)_n$ with dimethyl sulfate at pH 7.0 was in

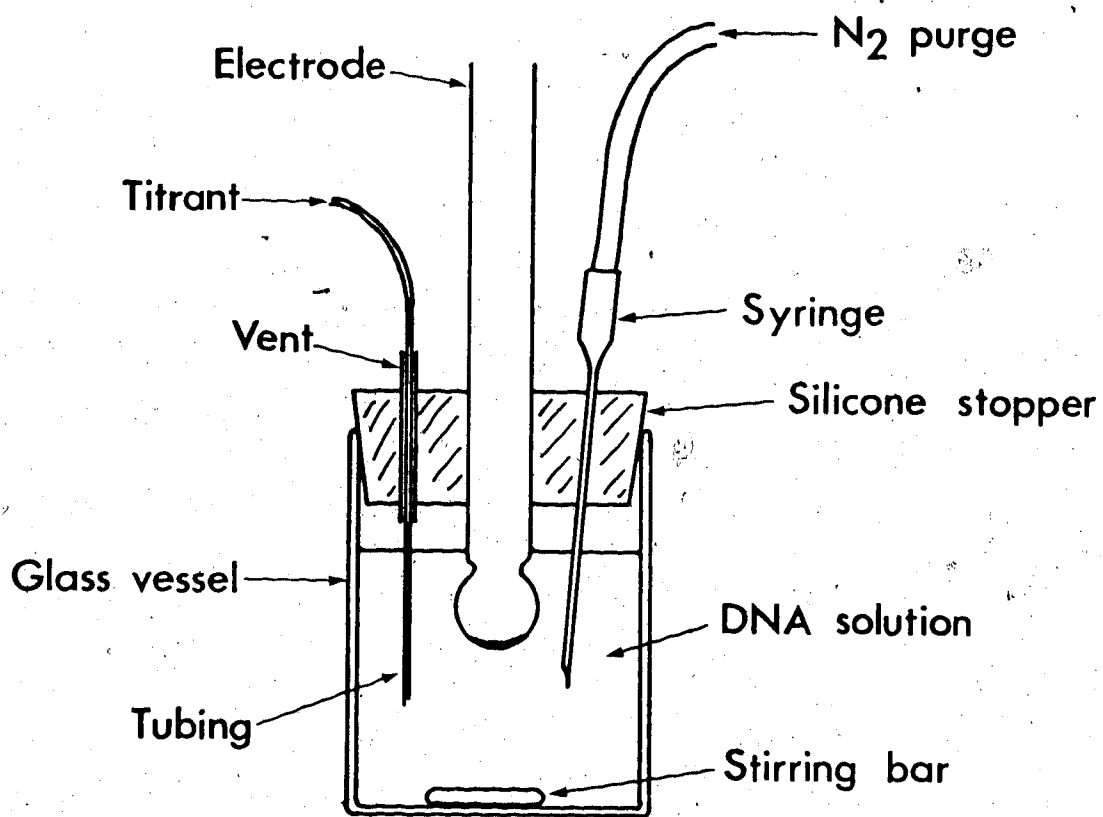


Figure 10 Reaction Vessel For the Titration of $d(TC)_n \cdot d(GA)_n$

a solution containing $\sim 1 A_{260} d(TC)_n \cdot d(GA)_n$, 0.2M Na cacodylate pH 7.0 (Uhlenhopp and Krasna, 1971) and 0 - 0.1M dimethyl sulfate at 37°C for one hour. The extent of reaction (i.e. total bases modified) was determined by passing reaction mixtures of $d(TC)_n \cdot d(GA)_n$ that had been reacted with 3H DMS plus increasing concentrations of unlabelled DMS (specific activity determined by isotope dilution) through a Pasteur pipette-sized Agarose 15M 200-400 mesh column equilibrated with 0.2M Na cacodylate pH 7.0. The excluded material (all the TCA precipitable counts) was counted in Aquasol (New England Nuclear). The standard curve obtained is shown in Figure 11 and is similar to that obtained by Uhlenhopp and Krasna for calf thymus DNA (also for λ DNA, determined by a different method, Hansen Hsiung personal communication). To determine the distribution of 3H -methylated products, markers were added, reaction mixtures were made 1.0 N in HCl and depurinated by heating 10 minutes at 95°C in a sealed tube. The mixture was spotted on cellulose thin layer plates (Eastman #13255) with known markers and developed with butanol/concentrated ammonium hydroxide/water: 86/5/14 (v/v). Preliminary experiments with labelled $d(TC)_n \cdot d(GA)_n$ DNA (either in a or g) showed that the only major products were 7-Meg, 7-Mea and 3-Mea. Standards of these were obtained from P-L Biochemicals (7-Meg) and Vega-Fox Biochemicals (3-Mea, 7-Mea; also 1-Mea, 1-Meg, 3-Meg). In this solvent system, relative to 7-Meg which migrated slowly, 7-Mea and 3-Mea had a R_{7-Meg} of 3.3 and 5.8 respectively. At all concentrations of DMS up to 0.1M the relative proportion of methylated products was $\sim 85.5\%$ 7-Meg, $\sim 7.5\%$ 7-Mea and $\sim 7\%$ 3-Mea (12.2/1.1/1). The usually observed ratio of 7-Meg/3-Mea is $\sim 6/1$ (Uhlenhopp and Krasna, 1971) with 7-Mea not usually quantitated. The reasons for this difference have

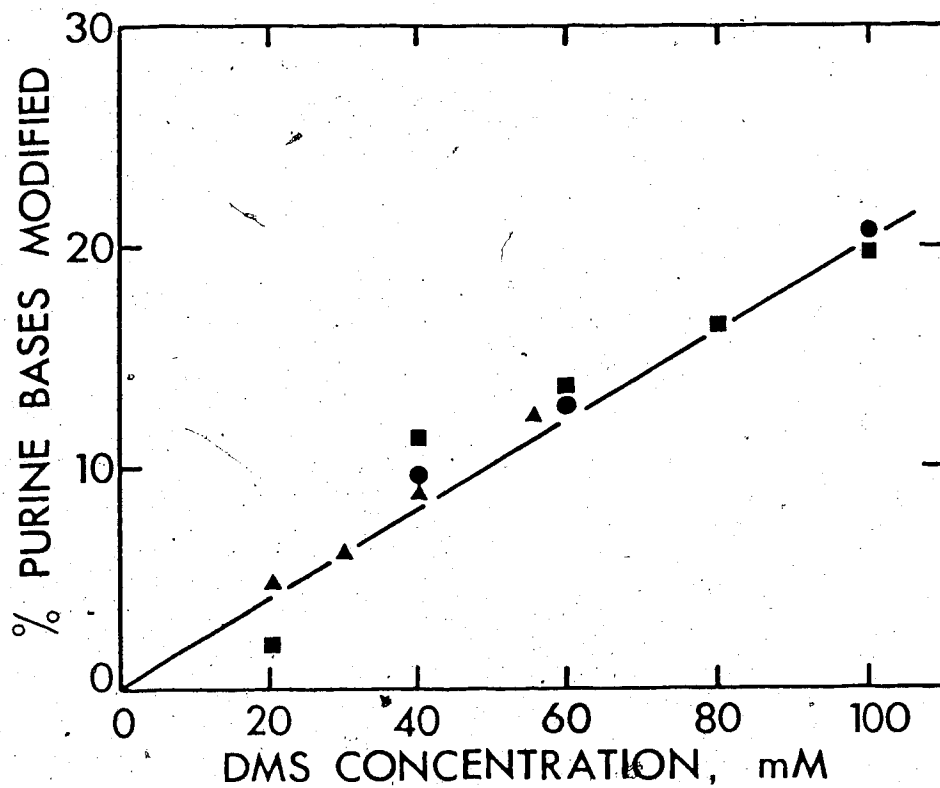


Figure 11 Standard Curve For The Reaction of Dimethyl Sulfate
With $d(TC)_n \cdot d(GA)_n$

Reaction conditions are given in Materials and Methods.
The different symbols refer to independent determinations.

not been systematically investigated but may be related to the structure of these DNAs. Methylation of RNA with DMS also leads to the formation of 7-Mea and 3-Mea ($\sim 3:1$) with 7-Meg accounting for $\sim 80\%$ of the methylated bases (Singer, 1975). Although the methylation of DNA is "qualitatively similar" (Singer, 1975) to the methylation of RNA the ratio of 7-Mea/3-Mea is $\sim 1:4$ in the few cases where they have both been quantitated. We have found a ratio closer to 1:1 which may reflect differences in the structure of $\text{Py}_n \cdot \text{Pu}_n$ DNAs which should be investigated for a series of these DNAs with different base compositions. As discussed in the Introduction $\text{d}(\text{TC})_n \cdot \text{d}(\text{GA})_n$ may have an "A" like structure which would explain this discrepancy. In any event, regardless of the value one assumes for the ratio 7-Mea/3-Mea the preponderance of 7-Meg is the most important consideration. Combination of these data with the results from calculations of the total bases modified reveals that for an average $\text{Py}_n \cdot \text{Pu}_n$ DNA of 500,000 daltons (~ 750 base pairs), as expected, mostly 7-Meg is modified (up to 34.5% of g is 7-Meg at a 0.1M DMS concentration (Table 4)).

The effect of methylation on the ability of $\text{d}(\text{TC})_n \cdot \text{d}(\text{GA})_n$ to form a multiplex was determined by fluorescence loss and shift in buoyant density when the pH was lowered. The most highly methylated sample of $\text{d}(\text{TC})_n \cdot \text{d}(\text{GA})_n$ [^3H dGMP] showed no loss of TCA precipitable counts after the 1.5 hr incubation time used to form the multiplex at 37°C and pH 5.5. This was taken as evidence that no large amount of depurination had occurred. Reaction of unlabelled DMS with the $\text{d}(\text{TC})_n \cdot \text{d}(\text{GA})_n$ multiplex was estimated by the resulting reduction in melting temperature (Uhlenhopp and Krasna, 1971). Mixtures of the

[DMS] mM	% Purines Methylated	Distribution of Main Methylated Products*				
		g	7-Meg	a	7-Mea	3-Mea
0	0	375	0	375	0	0
20	2.6	358	17	373	1.5	1.5
40	10.6	317	68	363	6	6
60	13.2	290	85	361	7	7
80	16.4	270	105	357	9	9
100	20.2	245	130	353	11	11

TABLE 4 Analysis of Products of Reaction of $d(TC)_n \cdot d(GA)_n$
With Dimethyl Sulfate at pH 7.0

*Calculated for an "average" $d(TC)_n \cdot d(GA)_n$ of 750 base pairs
(5×10^5 daltons).

$d(TC)_n \cdot d(GA)_n$ multiplex at $0.5 A_{260}$ and a natural or synthetic DNA which does not form a multiplex (used as an internal control) were reacted at $37^\circ C$ for 1 hour with varying concentrations of DMS in 0.2M Na cacodylate pH 5.5 and then dialysed overnight at $4^\circ C$ against 5mM Na acetate pH 5.0, 25mM NaCl. T_M s were determined as described before. In this buffer system, the $d(TC)_n \cdot d(GA)_n$ multiplex had a T_M of $86.5^\circ C$, $d(TTG)_n \cdot d(CAA)_n$ (gift of V. Paetkau) melted at $65.3^\circ C$ and C. perfringens DNA at $64.3^\circ C$.

Formaldehyde (boiled $95^\circ C$ for 10 minutes before use) and glyoxal reactions were monitored spectrophotometrically at $\lambda = 275nm$ and from the A_{280}/A_{250} ratio respectively. For both reagents, the reactions with deoxynucleoside 5'-monophosphates and single-stranded and double-stranded polymers were investigated as controls (Grossman, 1968; Broude and Budowsky, 1971). Conditions for the reaction with duplex DNA were 10mM potassium phosphate pH 7.5, 1mM EDTA, $1 A_{260} d(TC)_n \cdot d(GA)_n$ 3% (w/v) formaldehyde (or 0.1M glyoxal) at $95^\circ C$ for 5 minutes then 2 hours at $37^\circ C$. One half the sample was incubated in 50mM Na acetate pH 5.0, 0.25M NaCl, (conditions in which $d(TC)_n$ and $d(GA)_n$ reanneal to form a multiplex), the other half dialysed versus 50mM Tris HCl pH 9.5 at $4^\circ C$ to remove any adduct and then checked for the ability to form the multiplex. Glyoxal addition was freely reversible giving a product, after pH 5.0 incubation, with a T_M of $91.5^\circ C$ and a buoyant density of 1.471g/cc. Interpretation of the reaction with formaldehyde is more difficult since the adduct is not completely stable at pH 5.0 as is the case with glyoxal. However, as judged by hyperchromicity, the dialysed sample was 63% multiplex (T_M $91.5^\circ C$) and the undialysed sample was 28% "multiplex" with a T_M of $86^\circ C$. Reaction of formaldehyde

with the $d(TC)_n \cdot d(GA)_n$ multiplex was carried out in 50mM Na acetate pH 5.0, 0.1mM EDTA and 0.2M NaCl, 3% (w/v) formaldehyde at 23°C, (under these conditions the reaction with mononucleotides is ~70% complete in 1 hour as judged by the change in A_{275} while $d(T)_n \cdot d(A)_n$ shows no reaction.) Glyoxal reaction conditions were 1 A_{260} $d(TC)_n \cdot d(GA)_n$ multiplex, 10mM Na acetate pH 5.0, 0.1mM EDTA, 50mM glyoxal, 0.2M NaCl at 30°C (under these conditions the reaction with 5' pdG is complete in 25 hours, the reaction with d(G,A) complete in 80 - 90 hours (both calculated from absorption spectra) and the reaction with E. coli DNA after 8 days results in a decrease in T_M of 10.5°C).

Replication of $d(TC)_n \cdot d(GA)_n$ in the Presence of Base Analogues

7-MedGTP was prepared by the direct methylation of dGTP in a reaction mixture containing 0.5M Na cacodylate pH 7.0, 50mM dGTP and 250mM dimethylsulphate at 23°C for 1 hour followed by separation on DEAE cellulose (HCO_3^-) with a gradient 0 - 0.5M in triethylammonium bicarbonate pH 7.7 (Smith and Khorana, 1963). 7-MedGTP was characterized by its uv absorption spectra at alkaline and neutral pHs, its electrophoretic mobility in 50mM potassium phosphate pH 7.5 and by its chromatographic behaviour on polyethylene imine plates with 1.0M KCl as solvent (both indicative of net charge corresponding to a diphosphate) and the chromatographic properties of the nucleoside after bacterial alkaline phosphatase hydrolysis (corresponding to 7MedG when run on paper with $(NH_4)_2SO_4/H_2O/2$ -propanol (79/19/2(v/v)) as solvent). Replication of $d(TC)_n \cdot d(GA)_n$ was carried out (see page 44, this thesis) with varying concentrations of 7-MedGTP except that ^{14}C dCTP (2110cpm/nmole), dTTP and dATP were at a concentration of 1mM each (in the presence or absence of 1mM dGTP)

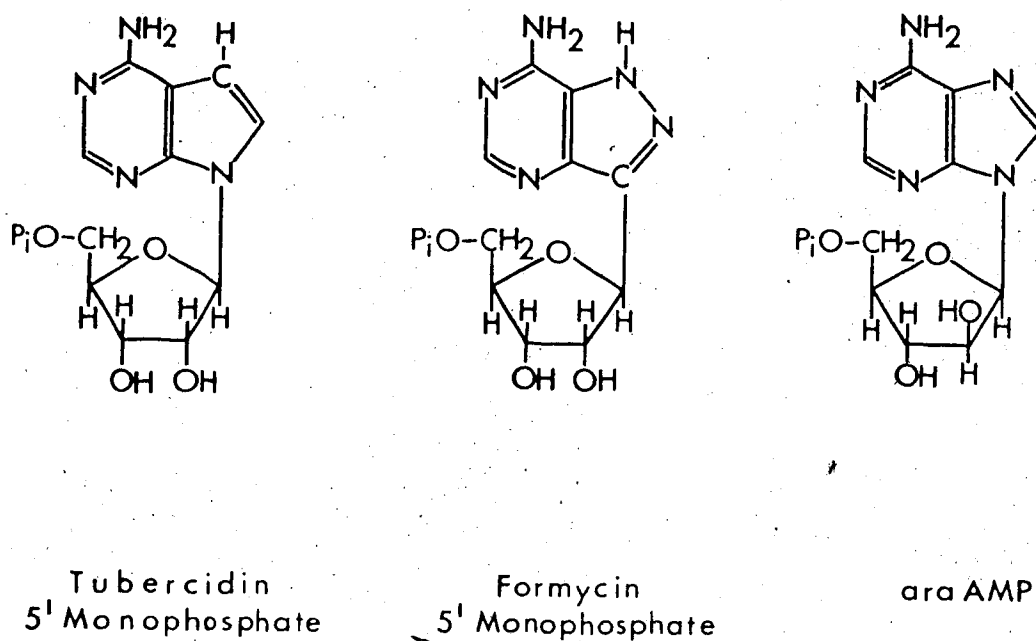


Figure 13 Structures of Some AMP Analogues

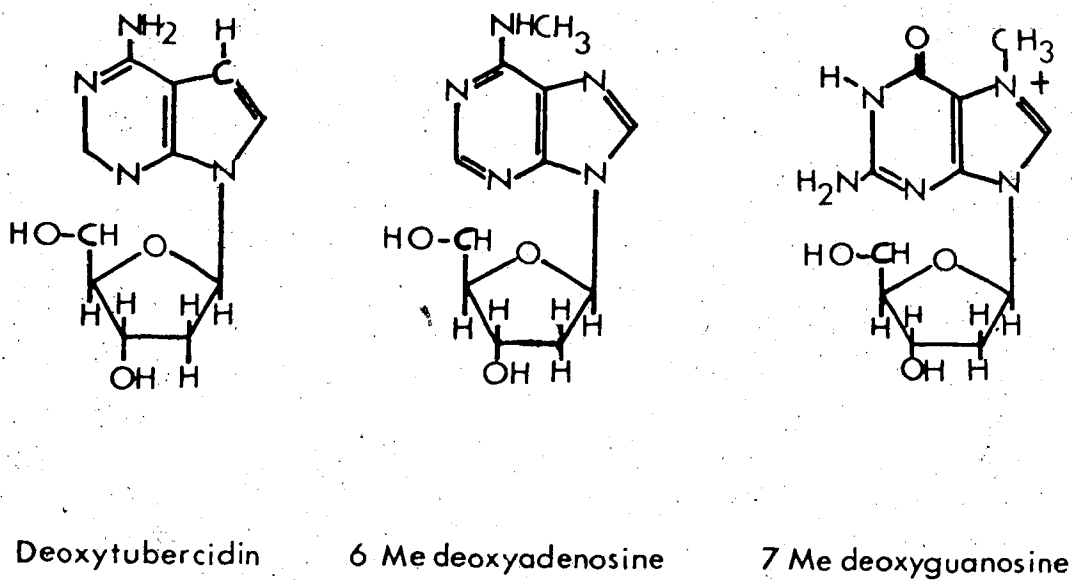


Figure 12 Structures of Purine Deoxynucleoside Analogues

Deoxytubercidin was a gift of W. Muhs of the Chemistry Department, University of Alberta. It was converted to the triphosphate (Figure 12) by a combination of chemical and enzymatic reactions as described in Appendix 2. 6-MedATP (Figure 12) was prepared from dAMP by the method of Griffen and Reese (1962). Methylated 1-MedAMP was converted to 6-MedAMP by titration to pH 11 with ammonium hydroxide and incubation overnight at 45°C and isolated by chromatography over a Bio-Rad Ag 1x2 (formate) with a linear gradient 0 - 1.0M in formic acid. The isolated product had the spectral characteristics ($\lambda_{\text{max}}^{0.1N \text{ HCl}} = 267\text{nm}$) and chromatographic properties expected for 6-MedAMP. Conversion to the triphosphate was achieved by enzymatic means. Replication of $d(\text{TC})_n \cdot d(\text{GA})_n$ was attempted using a coupled enzyme system containing 0.05M potassium phosphate pH 7.2, 0.025M MgCl_2 , 0.01M phosphoenolpyruvate, 2mM each dTTP, dCTP, dGTP, 0.5 A_{260} $d(\text{TC})_n \cdot d(\text{GA})_n$, DNase I, DIII and tRNA as before, 5mM deoxynucleoside 5'-monophosphate (dAMP, dTuMP or 6-MedAMP), 130 $\mu\text{g/ml}$ phosphoenolpyruvate synthetase and 10 $\mu\text{g/ml}$ *E. coli* DNA polymerase I. Under these conditions, at 37°C, 30 fold net synthesis is observed with dAMP as the adenine substrate after 5 hours.

Reaction conditions for the synthesis of the DNA-RNA hybrids were 0.05M Tris HCl pH 8.0, 0.01M MgCl_2 , 0.4 A_{260}^S $d(\text{TC})_n$, 0.25mM rATP (or analogue), 0.25mM ^{14}C rGTP (2320 cpm/nmole) and 250 $\mu\text{g/ml}$ RNA polymerase. Analogues were gifts of M. MacCoss of the Chemistry Department (TuMP, FMP) or synthesized by the method of Griffen and Reese (1963) (6-MeAMP). These were converted to the triphosphate enzymatically as described in Appendix 2. The hybrids synthesized with ATP, TuTP, or formycin 5'-triphosphate (Figure 13) all yielded less fluorescence per nmole DNA than $d(\text{TC})_n \cdot d(\text{GA})_n$ in the neutral ethidium assay. If $d(\text{TC})_n \cdot d(\text{GA})_n$ is

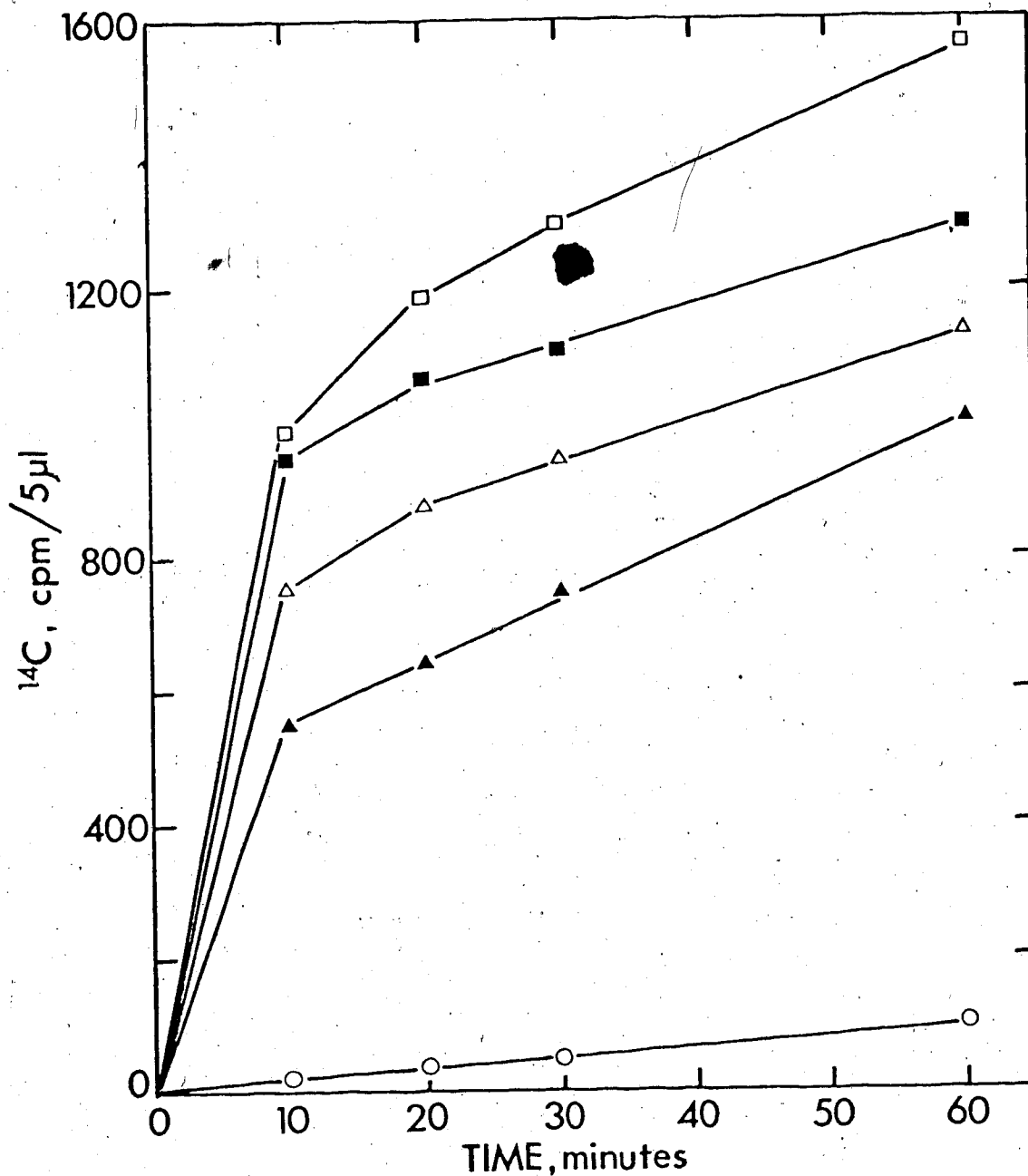


Figure 14 Polyribopurine Synthesis With ATP Analogues

$d(TC)_n \cdot d(A)_n$ was used as a template for *E. coli* RNA polymerase catalysed polyribopurine synthesis. Various ATP analogues were tested for their ability to substitute for ATP.

- | | | |
|----------|------------------------------|-----------|
| □ ATP | △ Tubercidin 5'-Triphosphate | ○ ara ATP |
| ■ 6MeATP | ▲ Formycin 5'-Triphosphate | |

substituted for d(TC) as template at a concentration of $1 A_{260}$ then these analogues, and others can be incorporated into polyribopurine (Figure 14).

Synthesis of the Random $Py_n \cdot Pu_n$ DNA $d(T,C)_n \cdot d(G,A)_n$

Random $d(G,A)_n$ was synthesized in a reaction mixture (10 ml) containing 40mM K cacodylate pH 7.0, 10mM $MgCl_2$, 1mM DTT, 2mM dATP, 2mM dGTP, $0.1 A_{260}^{pT}_{4-5}$ and 0.1mg/ml TDT1 (Bollum's enzyme) (6800U/mg) (Appendix III). After incubation for 4 hours at $37^\circ C$ the reaction mixture was chromatographed on a Sephadex G-100 column equilibrated with 0.5M NH_4HCO_3 pH 8.5, 6.0M urea (Stanley, 1967) and developed with the same solvent. The product $d(G,A)_n$ was excluded, implying a chain length > 100 (Stanley, 1967). This excluded material was dialyzed vs 10mM NaOH, then 1mM NaOH and adjusted to pH 8.0 by the addition of 1.0M Tris HCl to 10mM. Total OD_{260} recovered was 3.85:

In order to synthesize the complementary strand, $d(G,A)_n$ was incubated with E. coli RNA polymerase in a reaction mixture (1 ml) containing 50mM Tris HCl pH 7.5, 10mM $MgCl_2$, 1mM DTT, $0.97 A_{260} d(G,A)_n$, $0.28mM^{14}C$ CTP (2250 cpm/nmole), 0.24mM UTP and 0.11 mg/ml RNA polymerase (Burgess, 1969) for 3 hours at $37^\circ C$ to provide a primer and then 3H dTTP (1220 cpm/nmole) and dCTP to $\sim 0.5mM$ were added along with 30 μg E. coli DNA polymerase (1.94 mg/ml, 1800 dAT units/mg (Jovin et al, 1969)). Incubation was continued for 7 hours at $37^\circ C$ and then extended for 3 hours with an additional 10 μg of DNA polymerase. The product $d(T,C)_n \cdot d(G,A)_n$, after incubation with 20mM EDTA, 0.1% SDS 10 minutes at $55^\circ C$, was isolated on a Sephadex G-100 column developed with 10mM Tris HCl pH 8.0, 0.1mM EDTA. $0.66 OD_{260}$ were recovered ($\sim 50\%$).

The excluded material was ~70% double-stranded as judged by the incorporation of ^3H dTMP into TCA precipitable material and 65% double-stranded as judged by hyperchromicity when "melted" in 1/10 SSC. (T_M ~65.5°C equivalent to a G+C content of 42% (data of Wells et al., 1970 and of author)). The A_{260}/A_{280} ratio was 1.719 and maximal absorbance was at 254nm. No after heat fluorescence was observed.

Identical conditions were used when net synthesis was measured either at 37°C or 41°C with all four deoxynucleoside triphosphates at a concentration of ~ 0.5mM. Synthesis was monitored by the neutral ethidium fluorescence assay, as well as incorporation of radioactivity into TCA precipitable counts.

Reactions with Glyoxal

The standard conditions for the reaction of glyoxal with polymers were 10mM potassium phosphate pH 7.5, 1.0mM EDTA, 50% (v/v) EtOH (spectral grade), ~ 0.1M glyoxal (Fisher ~ 40% aqueous solution) and DNA (usually 1 A_{260}). Modifications are noted in the figure legends. The extent of reaction was monitored by removal of aliquots into the alkaline ethidium mixture (for natural DNAs) or neutral ethidium mixture (for synthetic polymers).

Denaturation maps were prepared from micrographs of partially denatured λ DNA spread by the formamide method of Davis et al. (1971) which were traced onto Albanene tracing paper using a Nikon Shadowgraph 6C, measured with a KE map measure and presented as according to Inman (1967).

Under the denaturation conditions the loss of fluorescence is related to, but greater than, the extent of denaturation visualized in the electron micrographs, perhaps due to reannealing of the partially

denatured DNA as the sample is processed (Inman, 1967).

Irradiation of crosslinked PM2 DNA was performed as described in Denniss and Morgan (1976) in the alkaline ethidium solution.

When $Py_n \cdot Pu_n$ DNAs were derivatized for the removal of $d(AT)_n$ the conditions were modified as follows: the DNA was incubated for 5 minutes at $95^\circ C$ in the absence of ethanol (which is no longer necessary to aid denaturation) and then for an additional 2 hours at $37^\circ C$ to ensure derivatization. Hydroxyapatite separation was performed by the batch procedure of Paetkau and Langman (1975). Since both ethanol and glyoxal were found to interfere with the separation the ethanol was omitted and glyoxal in the reaction mixture was reduced to 5mM. During the absorption step in 50mM potassium phosphate pH 6.8 buffer a further 1/4 dilution was effected. Although Langman and Paetkau observed that 0.16M potassium phosphate removes single-stranded DNA selectively, it was found that $d(AT)_n$ elutes at a phosphate concentration as low as 0.14M. Therefore, only the material eluting between 0.05M and 0.12M potassium phosphate was combined. Dederivatization was accomplished by titrating this fraction to pH 12 with KOH and heating for 10 minutes at $95^\circ C$, followed by dialysis vs 1mM NaOH.

For the separation of $d(TC)_n$ and $d(GA)_n$ the reaction conditions were 10mM potassium phosphate pH 7.5, 1mM EDTA, $\sim 0.1M$ glyoxal and $d(TC)_n \cdot d(GA)_n$ ($\sim 1 A_{260}$). Derivatization was performed by heating 10 minutes at $95^\circ C$, then 2 hrs at $37^\circ C$, after which an equal volume of 50mM Tris borate pH 8.3 was added and the sample adsorbed to a DEAE cellulose column equilibrated in the same buffer. The column was developed first with a gradient of NaCl (0M - 2.0M) in Tris borate, then with 0.5M NaCl, 0.1M NaOH. Glyoxal was removed as described for the

$d(AT)_n$ separation and fractions were dialyzed vs 1mM NaOH. Occasionally the isolated strands were contaminated with the complementary strand at a level of 2% - 5%, perhaps due to incomplete strand separation. This double-stranded material can be removed by the hydroxyapatite procedure described previously.

When the polymer $d(TC)_n(^3HC) \cdot d(GA)_n(^{14}CA)$ was subjected to either strand separation or removal of added $d(AT)_n$ by these procedures and losses of radioactivity monitored, the greatest losses occurred in steps involving dialysis and these were subsequently limited to as few as possible. However, losses of single-stranded material during dialysis remains a problem, perhaps due to losses of material through the dialysis membrane as glyoxal treatment reduces the molecular weight of these polymers. Also, during the hydroxyapatite step losses of $\sim 10\% - 15\%$ occur because $d(AT)_n$ elutes at a lower $[P_1]$ than expected for a normal double-stranded polymer, and thus the single-stranded material that would be contaminated with $d(AT)_n$ must be discarded. DEAE cellulose chromatography of $d(TC)_n$ and $d(GA)_n$ results in a loss of material on the column which is not removable by 5M NaCl or 1mM NaOH and leads to poor recovery.

CHAPTER IV FORMATION OF $Py_n \cdot Pu_n$ MULTIPLEXES

$Py_n \cdot Pu_n$ DNAs which contain repeating sequences and G-C base pairs undergo a reversible strand rearrangement in solutions of moderate ionic strength when the pH is lowered to <6 . The formation of these structures which we have named multiplexes results in a number of changes in the physical and chemical properties of these $Py_n \cdot Pu_n$ DNAs, alterations which can be useful both in characterizing these structures and monitoring the extent of rearrangement.

As rearrangement proceeds the fluorescence due to intercalated ethidium decreases as shown in Figure 15 for $d(TC)_n \cdot d(GA)_n$ incubated under a variety of conditions. This fluorescence loss is dependent on the presence of monovalent or divalent cations (here 0.1M NaCl or 1mM $MgCl_2$) and the rate of fluorescence loss increases as the concentration of these ligands is increased. After extended incubation, the residual fluorescence is 5% - 15% of the original fluorescence perhaps indicative of an equilibrium between $d(TC)_n \cdot d(GA)_n$ which binds ethidium and exhibits fluorescent properties and multiplex which does neither. This residual fluorescence and amount of residual

duplex is lowered by decreasing the buffer pH or increasing the incubation temperature. Analysis of analytical Cs_2SO_4 density gradients shows that in the presence of ethidium there is a small buoyant density decrease compared to the value without ethidium present noted for the $d(TC)_n \cdot d(GA)_n$ multiplex (~ 10 mg/cc) while the buoyant density of λ DNA, which does not form a multiplex, decreases by ~ 66 mg/cc. The ratio of these two values (0.15) approximates the residual fluorescence of the $d(TC)_n \cdot d(GA)_n$ multiplex suggesting that the loss of fluorescence is due to ethidium exclusion. The $Py_n \cdot Pu_n$ DNAs $d(TTC)_n \cdot$

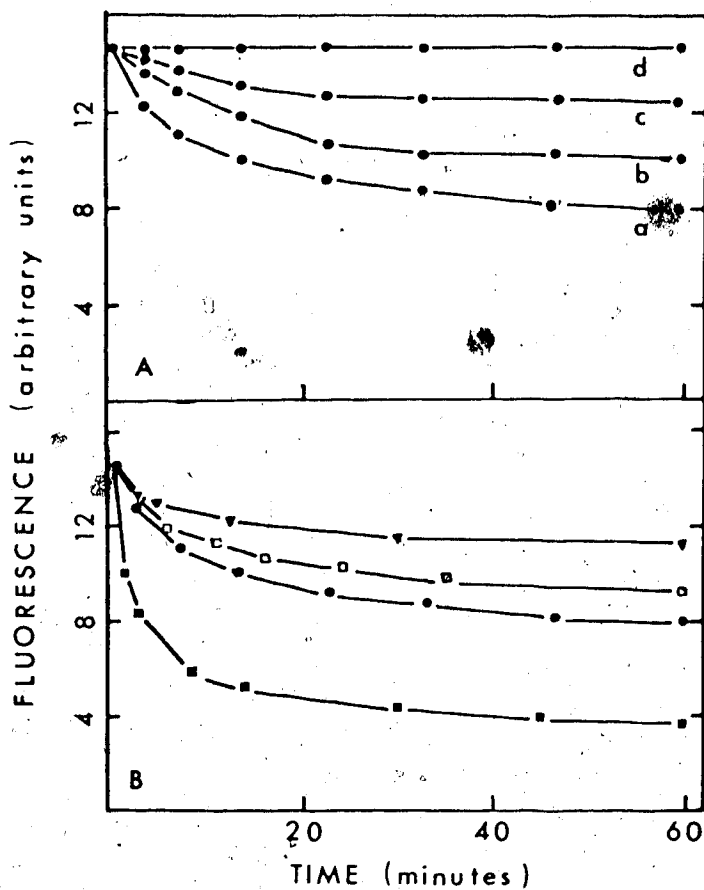


Figure 15 Rearrangement of $\text{Py}_n \cdot \text{Pu}_n$ DNAs Monitored by the Ethidium Fluorescence Assay

- A. Requirements for the rearrangement of $\text{d}(\text{TC})_n \cdot \text{d}(\text{GA})_n$ ($6.5 \mu\text{g}/\text{ml}$)
- 5mM Na acetate pH 5.0, 2mM MgCl_2
 - 5mM Na acetate pH 5.0, 1mM MgCl_2
 - 5mM Na acetate pH 5.0, 0.1M NaCl
 - 5mM Na acetate pH 5.0, 0.5mM EDTA

- B. Rearrangement of various polymers in 5mM Na acetate pH 5.0, 2mM MgCl_2

● $\text{d}(\text{TC})_n \cdot \text{d}(\text{GA})_n$ ■ $\text{d}(\text{C})_n \cdot \text{d}(\text{G})_n$ □ $\text{d}(\text{TTC})_n \cdot \text{d}(\text{GAA})_n$
 ▼ $\text{d}(\text{TCC})_n \cdot \text{d}(\text{GGA})_n$

In addition all incubation mixtures contained ethidium bromide at a concentration of $0.5 \mu\text{g}/\text{ml}$.

Rearrangements were carried out at room temperature.

$d(\text{GAA})_n$, $d(\text{TC})_n \cdot d(\text{GA})_n$, $d(\text{TCC})_n \cdot d(\text{GGA})_n$ and $d(\text{C})_n \cdot d(\text{G})_n$ all exhibit this fluorescence loss at low pH but $d(\text{T})_n \cdot d(\text{A})_n$ does not suggesting that G-C base pairs are in some way necessary (Figure 15b). Natural DNAs and synthetic DNAs with pyrimidines and purines in both strands (eg. $d(\text{TG})_n \cdot d(\text{GA})_n$ or $d(\text{TTG})_n \cdot d(\text{CAA})_n$) do not form multiplexes.

The presence of ethidium slows the rate of fluorescence loss. At concentrations $> 2\mu\text{g/ml}$ ethidium bromide no rearrangement is observed (as monitored by fluorescence loss). Therefore, although this technique is useful in practical terms, the rearrangement is affected by the presence of ethidium.

Other $\text{Py}_n \cdot \text{Pu}_n$ DNAs were investigated for the ability to form multiplexes. A DNA isolated from E. coli (gift of M. Coulter) was judged $\text{Py}_n \cdot \text{Pu}_n$ both by its mode of replication (no CLC DNA synthesis observed, see section on the replication of $\text{Py}_n \cdot \text{Pu}_n$ DNAs) and by characterization with transcriptional assays using E. coli RNA polymerase (the incorporation of labelled rGMP into TCA precipitable material was dependent upon the presence of rATP and the incorporation of labelled rAMP upon rGMP but neither reaction was dependent upon the presence of rUTP or rCTP). It had a buoyant density in Cs_2SO_4 at pH 7.0 of 1.424g/cc and a T_M in SSC/10 of 68°C suggesting a G+C content of 50%. When incubated at pH 5.0 both the fluorescence loss and a buoyant density shift (discussed later) indicative of multiplex formation were observed. The random $\text{Py}_n \cdot \text{Pu}_n$ DNA $d(\text{T,C})_n \cdot d(\text{G,A})_n$ synthesized for the $\text{Py}_n \cdot \text{Pu}_n$ replication studies did not show rearrangement, pointing out the need for a repeating sequence. Finally, L cell pyrimidine tracts (gift of H.C. Birnboim) were repaired and replicated by the same techniques described for the random $\text{Py}_n \cdot \text{Pu}_n$ DNA.

From the pattern of synthesis and analysis of the products it was concluded that one or possibly a small number of sequences were selectively amplified, a different set for each reaction mixture. When these were tested for fluorescence loss, some of the preparations exhibited the expected loss of fluorescence but one did not. These results indicate that the source of the $Py_n \cdot Pu_n$ DNA is unimportant and that the ability of the DNA to form a multiplex is an inherent property related to the type of sequence. The exception mentioned had a T_M in SSC/10 of $54^\circ C$ and a buoyant density in Cs_2SO_4 at pH 7 of 1.421g/cc consistent with it being an A-T rich DNA. Thus a certain mole fraction of G-C base pairs may be necessary for rearrangement. Since synthetic polymers with repeating sequences of four or larger replicate very poorly the in vitro synthesis of defined DNAs with G+C contents < 20% necessary to test this hypothesis may not be possible. Another more feasible approach would lie in the analysis of $Py_n \cdot Pu_n$ satellite DNAs which have been sequenced (Sederoff et al., 1976).

Multiplex formation also results in buoyant density increases of 30-50mg/cc in Cs_2SO_4 at pH 5.0. As observed for $d(TC)_n \cdot d(GA)_n$ this shift occurs in two stages (Figure 16 and Table 5). There is initially an increase of 5mg/cc. As the length of incubation increases the buoyant density gradually decreases to a final value of 1.469g/cc after 8-10 days at room temperature with no further changes observed upon increasing the time of incubation or upon storage at $-20^\circ C$. Returning the pH to neutrality results in a rapid reversal to material with a buoyant density of authentic $d(TC)_n \cdot d(GA)_n$ emphasizing the reversible nature of the rearrangement. The successive decrease in buoyant density is accompanied by a sharpening of the observed peak which may

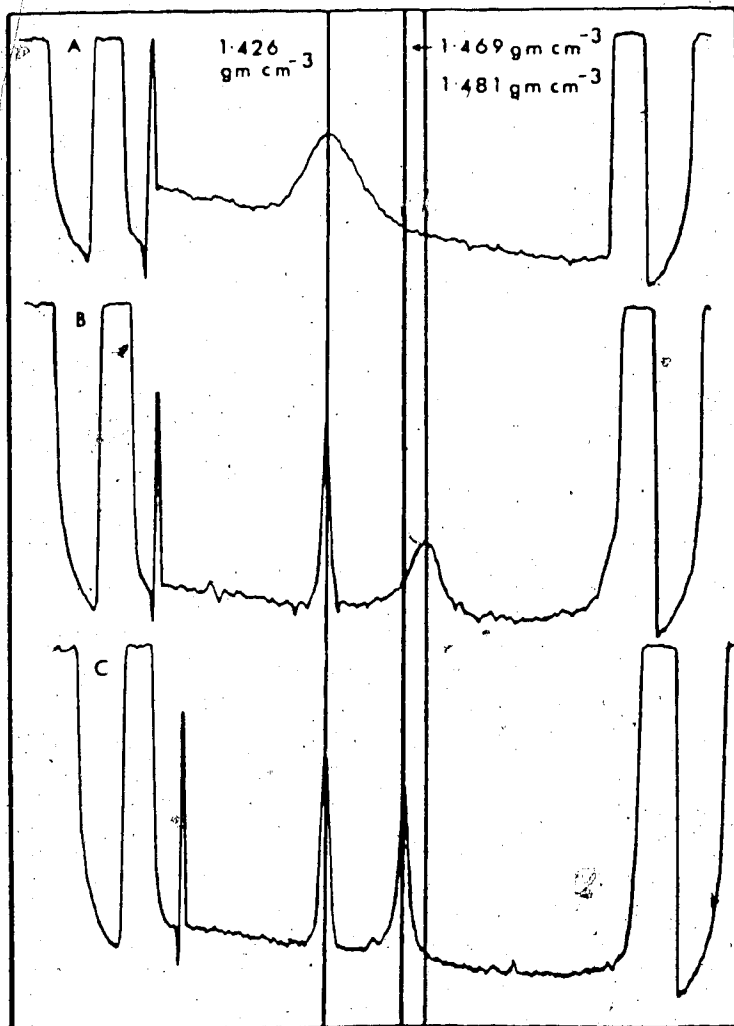


Figure 16 Rearrangement of $d(TC)_n \cdot d(GA)_n$ Monitored by Analytical Cs_2SO_4 Equilibrium Centrifugation

Samples were centrifuged to equilibrium (20 hours) after incubation under various conditions. Tracings B and C also include λ DNA as a density marker (density=1.426 g/cc)

- A. $d(TC)_n \cdot d(GA)_n$ at neutral pH
- B. $d(TC)_n \cdot d(GA)_n$ incubated for 1 hour at $24^\circ C$ in 0.5M NaCl
50mM Na acetate pH 5.0
- C. $d(TC)_n \cdot d(GA)_n$ incubated as in B for 10 days.

Incubation Time (hours)	ρ Cs_2SO_4 (g/cc)	Band width
0	1.481	broad
6	1.476	moderate
30	1.473	moderate
54	1.471	sharp
78	1.471	sharp
240	1.469	sharp

TABLE 5

Formation of the $(\text{GA})_n$ Multiplex Monitored
By Buoyant Density in Cs_2SO_4 at pH 5.0

The incubation conditions were as described for Figure 16.

indicate an increase in molecular weight due to aggregation. Sedimentation velocity studies in 1.0M NaCl, 50mM Na acetate pH 5.0 of rearranging $d(TC)_n \cdot d(GA)_n$ suggest aggregation after 3 days incubation at room temperature under the above conditions. However, this behaviour, which could be predicted by any of the models, is not necessary to the stability of any of the proposed structures.

The melting profile of the $d(TC)_n \cdot d(GA)_n$ multiplex at pH 5.0 is shown in Figure 17a. Although a moderately high salt concentration is required for multiplex formation, once formed it is stable in 50mM NaCl (at pH 5.0 in 50mM NaCl no fluorescence increase with time is observed). If the concentration of NaCl is lowered to 25mM then a gradual return of fluorescence (interpreted as a return to duplex structure) is observed. Two hyperchromic shifts accounting for all the expected increase in absorbance are observed. The first, centred at $48.5^\circ C$ with a 6%-8% hyperchromicity, represents residual $d(TC)_n \cdot d(GA)_n$ duplex regions which are responsible for the ethidium binding and fluorescent properties of the multiplex. These can be eliminated in either of two ways without affecting the buoyant density or T_M of the multiplex. Formaldehyde reacts selectively with these regions at $55^\circ C$ to yield a product that exhibits no ethidium fluorescence and no hyperchromicity when the temperature is raised to $80^\circ C$, although the T_M of the multiplex is unaffected. Reaction of formaldehyde with $d(TC)_n \cdot d(GA)_n$ results in material with a buoyant density of 1.45g/cc and a decrease in the multiplex buoyant density may have been expected. However, since the hydroxymethyl adduct is not stable, it may have been removed during the time necessary for the centrifugation step (20 hours), with reannealing of the (formerly derivatized) $d(TC)_n$

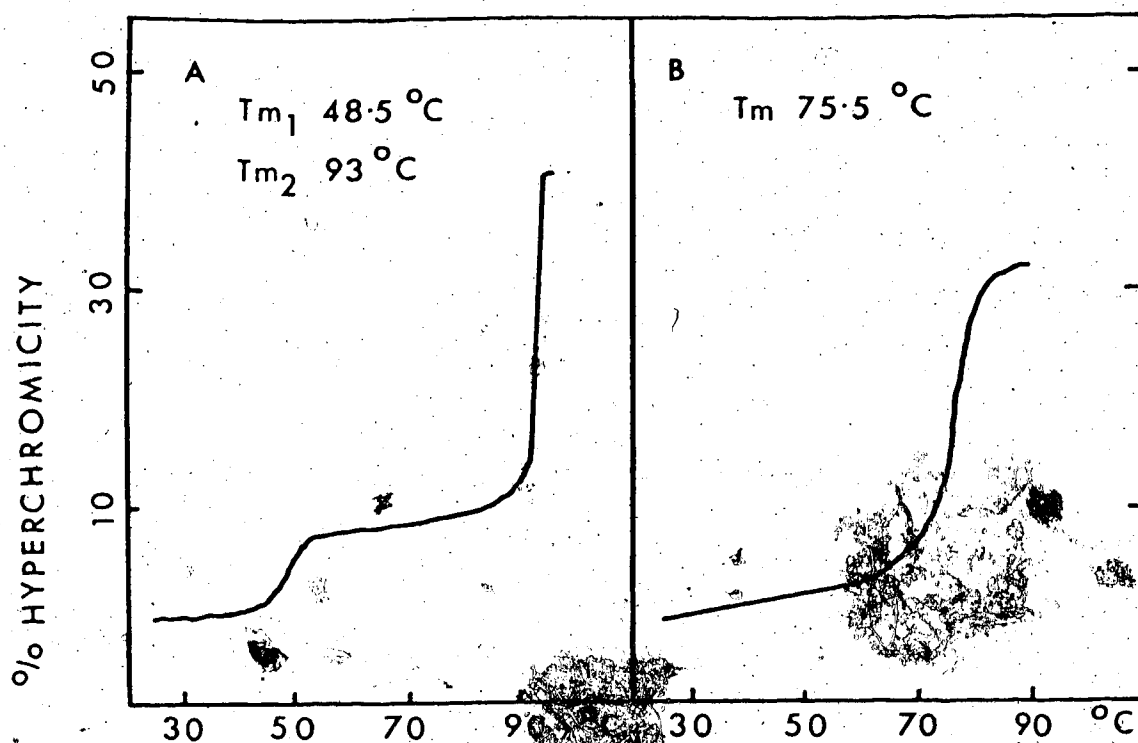


Figure 17 Absorbance-Temperature Transitions of Rearranged $d(TC)_n \cdot d(GA)_n$

- Rearranged $d(TC)_n \cdot d(GA)_n$ was dialysed into 10mM Na acetate pH 5.0, 50mM NaCl, 0.1mM EDTA and the absorbance-temperature transition recorded.
- A sample of rearranged $d(TC)_n \cdot d(GA)_n$ prepared as in A was adjusted to pH 7.6 with 1.0M Tris HCl pH 8.0 and the absorbance-temperature transition recorded.

and $d(GA)_n$ directly to multiplex such that very little material was actually derivatized when the density was measured. Secondly use can be made of the observation that $d(TC)_n$ and $d(GA)_n$ (or $d(TC)_n \cdot d(GA)_n$ heat denatured at neutral pH) when annealed at pH 5.0 directly form the multiplex. This multiplex has all the properties of the normally rearranged $d(TC)_n \cdot d(GA)_n$ multiplex but shows no ethidium fluorescence and no hyperchromicity when the temperature is raised to 75°C (this observation supports the contention that the multiplex does not bind ethidium). The second hyperchromic shift (30% - 35% increase in absorbance) centred at 93°C represents the melting of the multiplex. Several conclusions can be drawn. This melting temperature is $\sim 17^\circ\text{C}$ higher than the corresponding value for $d(TC)_n \cdot d(GA)_n$ at the same ionic strength but at neutral pH suggesting a much more stable structure than the initial duplex and providing a rationale for the rearrangement (assuming that the base stacking and other hydrophobic interactions which contribute to the stability of $d(TC)_n \cdot d(GA)_n$ and its multiplex are about equal then one can calculate, using the van 't Hoff relationship, that the multiplex is more stable by ~ 15 kcal/mol "basepair", a very favourable ΔH° for the rearrangement). The narrowness of the transition suggests a highly cooperative melting phenomenon. When Tris HCl pH 8.0 is added to the multiplex to raise the pH to ~ 7.6 (Figure 17b) a broader melting profile with a T_M of 75.5°C , identical to the T_M of authentic $d(TC)_n \cdot d(GA)_n$ under these conditions, is observed again emphasizing the reversible nature of multiplex formation. Lastly, the ratio of hyperchromicity (at the T_M of 48.5°C)/hyperchromicity (T_M of 93°C) + hyperchromicity (T_M of 48.5°C) is as expected from the residual ethidium fluorescence and ethidium binding studies (~ 0.18).

Table 6 summarizes the properties of all the $\text{Py}_n \cdot \text{Pu}_n$ multiplexes which have been studied in detail (the T_M of the $\text{d(C)}_n \cdot \text{d(G)}_n$ multiplex was expected to be $> 100^\circ\text{C}$ and not determined). All form ordered structures, as indicated by banding on Cs_2SO_4 and melting profiles, which revert back to duplex DNA when the pH is raised to neutrality. The increase in buoyant density ranges from 31mg/cc (for $\text{d(TTC)}_n \cdot \text{d(GAA)}_n$) to 59mg/cc (for $\text{d(TCC)}_n \cdot \text{d(GGA)}_n$) (compare with Table 3) and the corresponding increase in T_M is $15^\circ\text{C} - 19^\circ\text{C}$. A comparison of $\text{d(TTC)}_n \cdot \text{d(GAA)}_n$, $\text{d(TC)}_n \cdot \text{d(GA)}_n \cdot \text{d(TCC)}_n \cdot \text{d(GGA)}_n$ and $\text{d(C)}_n \cdot \text{d(G)}_n$ with their respective multiplexes shows the same relative order for these properties in both structures i.e. the polymer with the higher T_M at pH 7.0 forms a multiplex with a higher T_M at pH 5.0, although there is no hard and fast rule as to the extent to which either the T_M or buoyant density will increase when forming the multiplex. These similarities in properties strongly suggest that a common structural organization may be responsible for the stability of these multiplexes. The increase in T_M upon multiplex formation suggests a structure more stable than the corresponding duplex. Theoretical calculations by Pullman *et al.* (1967) demonstrate that the formation of the triad C.G.C^+ which involves a Hoogsteen base pair containing a protonated hydrogen bond (Figure 4) is accompanied by a very large interaction energy (-47.86 kcal/mole) when compared to duplex interactions (-10 to -12 kcal/mole) or the triad U. A. U. (-11.63 kcal/mole). These calculations are for the interaction in vacuo and although the absolute values are probably in error for interactions in solution, these relative values may still be expected and could be important in rationalizing the stability of the multiplex.

$\text{Py}_n \cdot \text{Pu}_n$ Multiplex	$\rho \text{ Cs}_2\text{SO}_4$ (g/cc) ¹	T_M (°C) ²
$d(\text{TTC})_n \cdot d(\text{GAA})_n$	1.458	82.5
$d(\text{TC})_n \cdot d(\text{GA})_n$	1.469	93.0
$d(\text{TCC})_n \cdot d(\text{GGA})_n$	1.494	96.0
$d(\text{C})_n \cdot d(\text{G})_n$	1.513	ND ³
$d(\text{BrUC})_n \cdot d(\text{GA})_n$	1.519	99.0

TABLE 6 Summary of the Physical Properties of the $\text{Py}_n \cdot \text{Pu}_n$ Multiplexes

1. determined in Na acetate buffer pH 5.0 with either λ DNA (1.426g/cc) or M_{13} single-stranded DNA (1.4465g/cc) as an internal standard.
2. T_M buffer was 10mM Na acetate pH 5.0, 50mM NaCl, 0.1mM EDTA.
3. not determined.

Formation of the $d(TC)_n \cdot d(GA)_n$ multiplex also leads to changes in the ultraviolet absorption spectrum (Figure 18) and the circular dichroism spectrum (Figure 19). The discussion of these is strictly qualitative. When $d(TC)_n \cdot d(GA)_n$ is rearranged at pH 5.0 the extinction coefficient increases at both short and long wavelengths with an isosbestic point in the vicinity of 250nm. The CD spectrum has an isosbestic point at ~ 257.5 nm. Although the spectrum of the $d(TG)_n \cdot d(CA)_n$ control is very similar at pH 8.0 and 5.0, with only a small decrease in ellipticity at 240nm, the spectrum of $d(TC)_n \cdot d(GA)_n$ changes from one quantitatively similar to that observed by Wells et al. (1970) with decreases in molar ellipticity at both 280nm, which now exposes a minimum at ~ 302.5 nm with a cross-over at ~ 297.5 nm, and at shorter wavelengths such that a local minimum is observed at 244nm and a local maximum at 232nm before the ellipticity drops rapidly at wavelengths < 230 nm. Tunis-Schneider and Maestre (1970) have correlated changes in the CD patterns of unoriented gels with a B to A transition which leads to decreases in ellipticity at long and short wavelengths. It is tempting to speculate that this observation may also apply to the formation of the multiplex structure since X-ray fibre analysis of duplex DNA compared to the corresponding triplex eg $d(T)_n \cdot d(A)_n$, $d(T)_n \cdot d(A)_n \cdot d(T)_n$ (Arnott and Selsing, 1974) shows a change in sugar conformation from C_3 exo to C_3 endo, usually associated with a B to A transition, upon binding on the Hoogsteen $d(T)_n$ strand. Hoogsteen hydrogen bonding then may be involved in the multiplex structure. When the $d(TC)_n \cdot d(GA)_n$ multiplex is "melted", then at 60°C the spectrum shows hyperchromicity only at intermediate wavelengths (240nm - 280nm) and at 96°C hyperchromicity is observed at wavelengths less than ~ 290 nm and hypochromicity at wavelengths > 290 nm. This hypochromicity may be interpreted as disaggregation of the multiplex, a

Figure 18 Absorbance of Rearranging $d(TC)_n \cdot d(GA)_n$

$d(TC)_n \cdot d(GA)_n$ was allowed to rearrange in 0.05M Na acetate pH 5.0, 0.5M NaCl and the absorbance profile measured at different times.

Incubation was at 23°C.

- ▲ 0 hours, at pH 8.0
- 3 hours, at pH 5.0
- 40 hours, at pH 5.0
- △ 88 hours, at pH 5.0

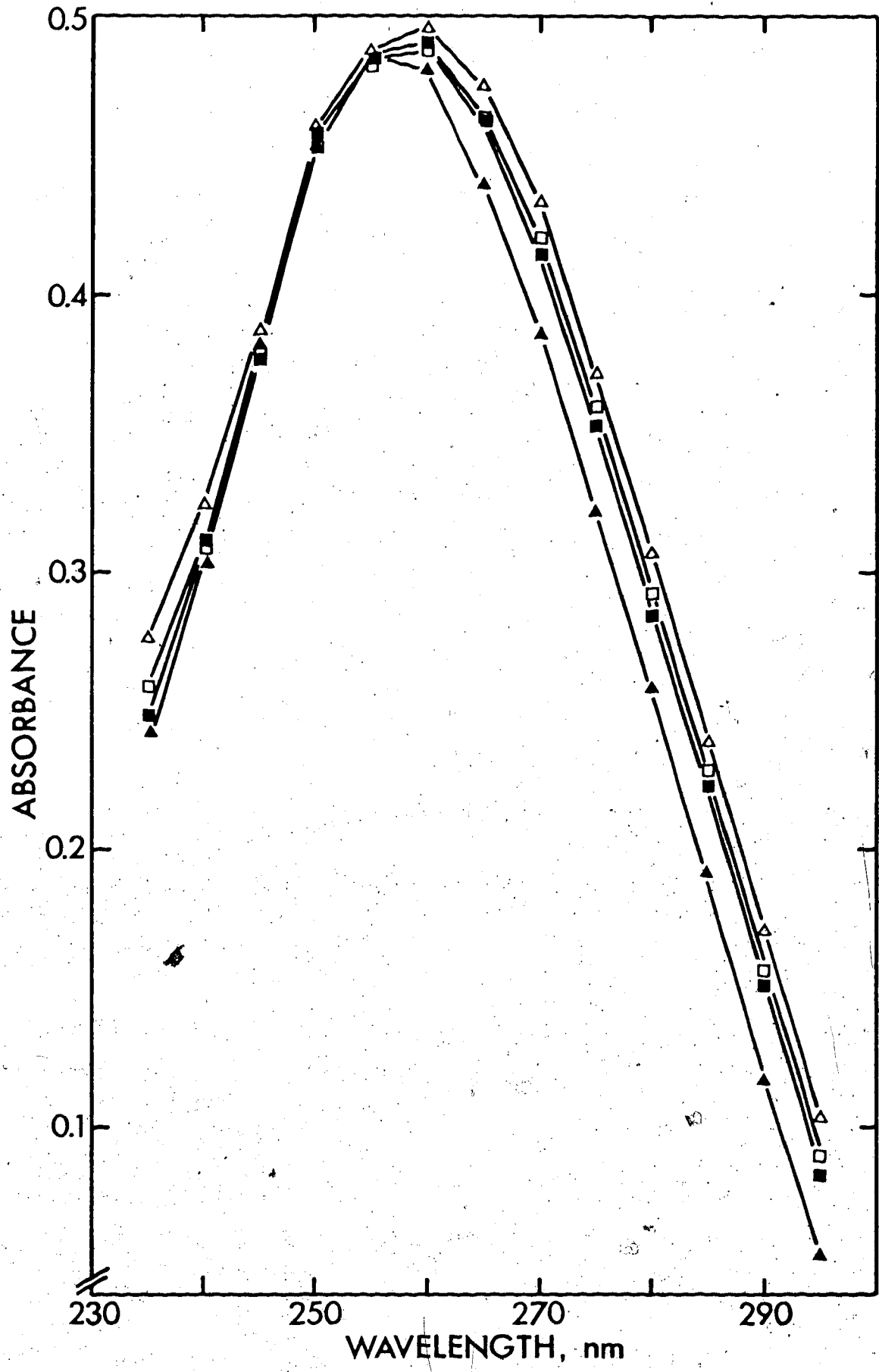


Figure 19a Circular Dichroism Spectra of $d(TG)_n \cdot d(CA)_n$

Spectra were compiled as described in Materials and Methods for $d(TG)_n \cdot d(CA)_n$ at pH 8.0 (dashed line) and at pH 5.0 (solid line). Values of $[\theta]$ are in degrees $\text{cm}^{-1} \text{molar}^{-1}$.

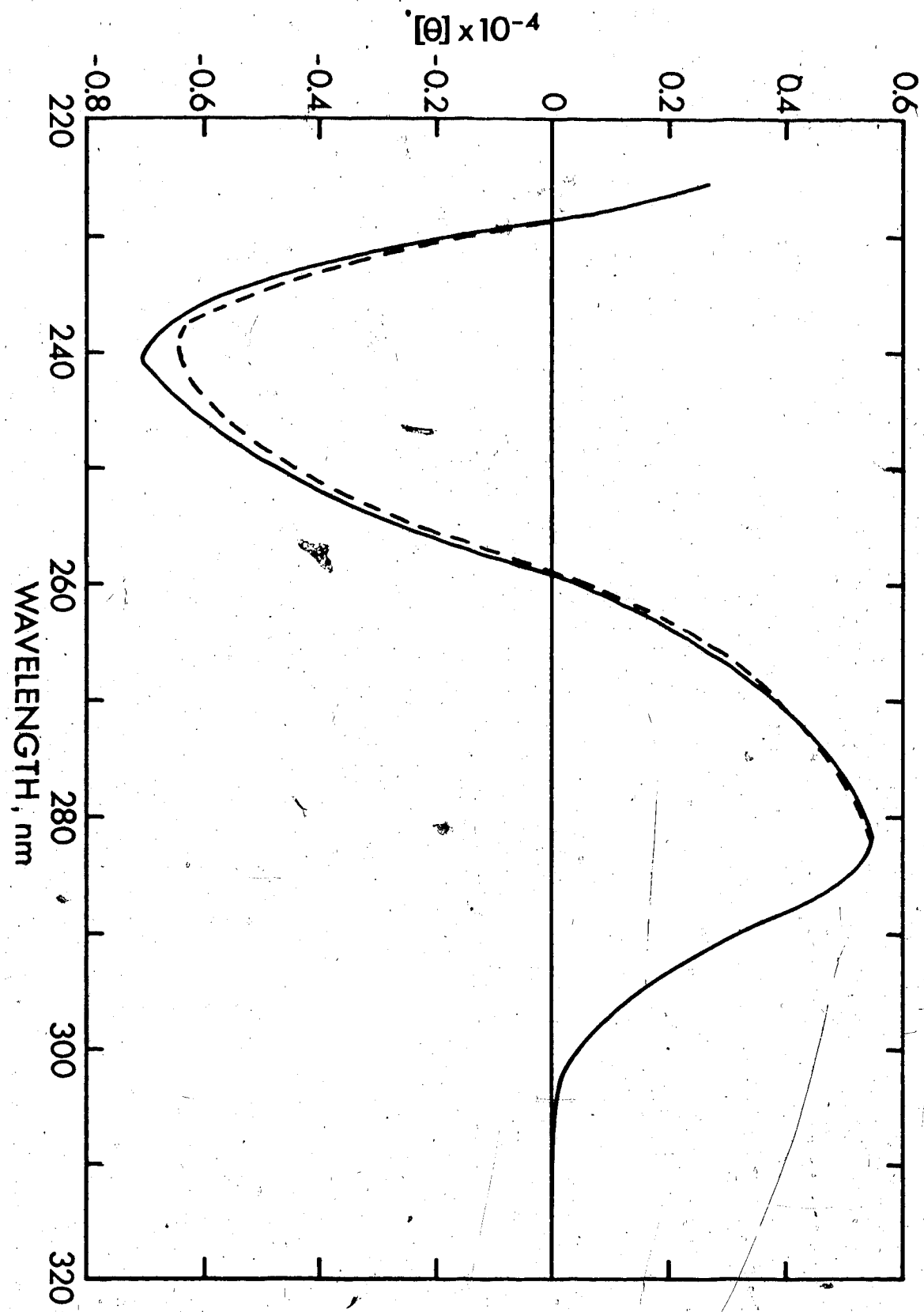


Figure 19b Circular Dichroism Spectra of $d(\text{TC})_n \cdot d(\text{GA})_n$

Spectra were compiled as in Materials and Methods for $d(\text{TC})_n \cdot d(\text{GA})_n$ at pH 8.0 (dashed line) and at pH 5.0 after incubation for 6 days at room temperature. Values for $[\theta]$ as before.

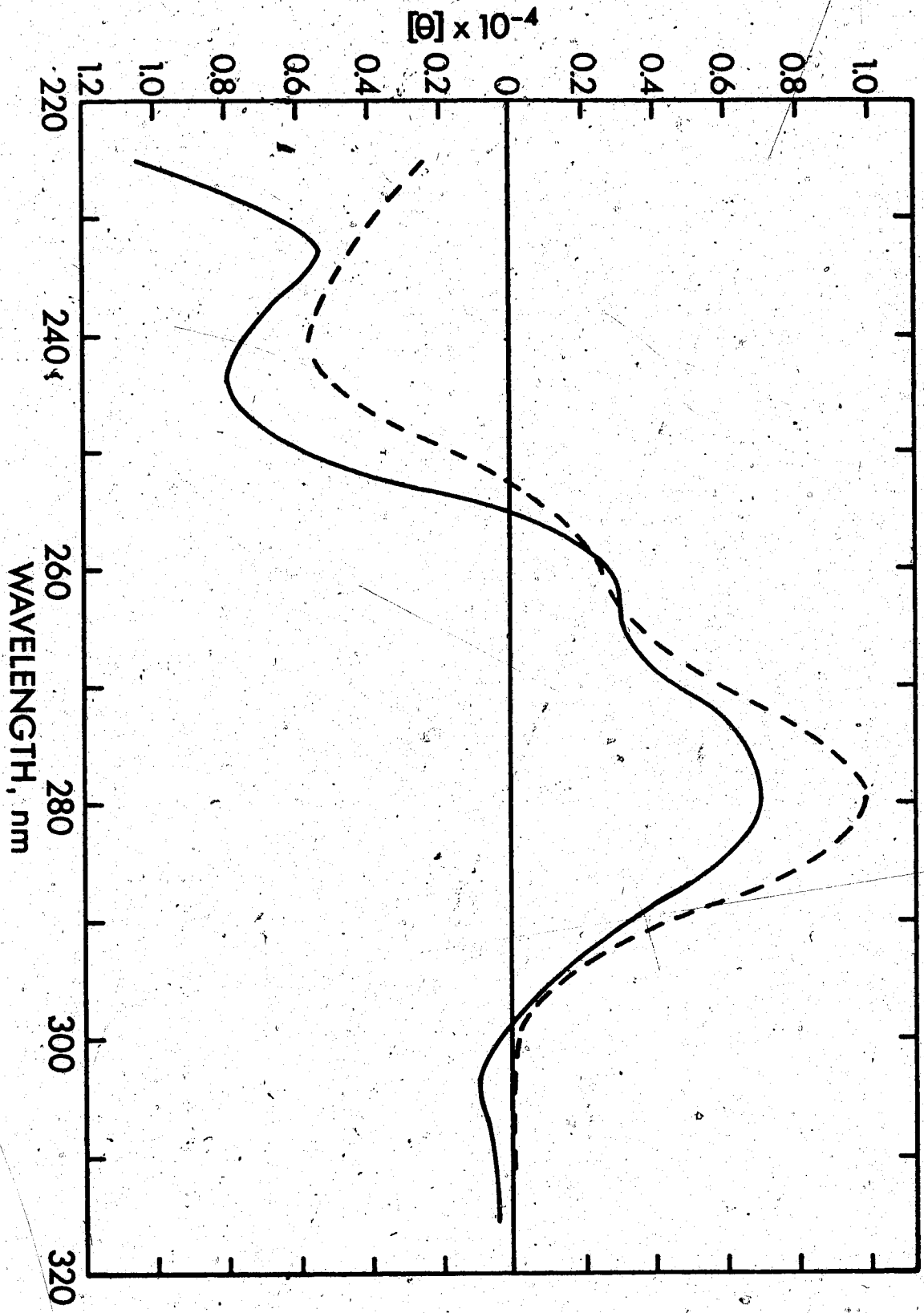




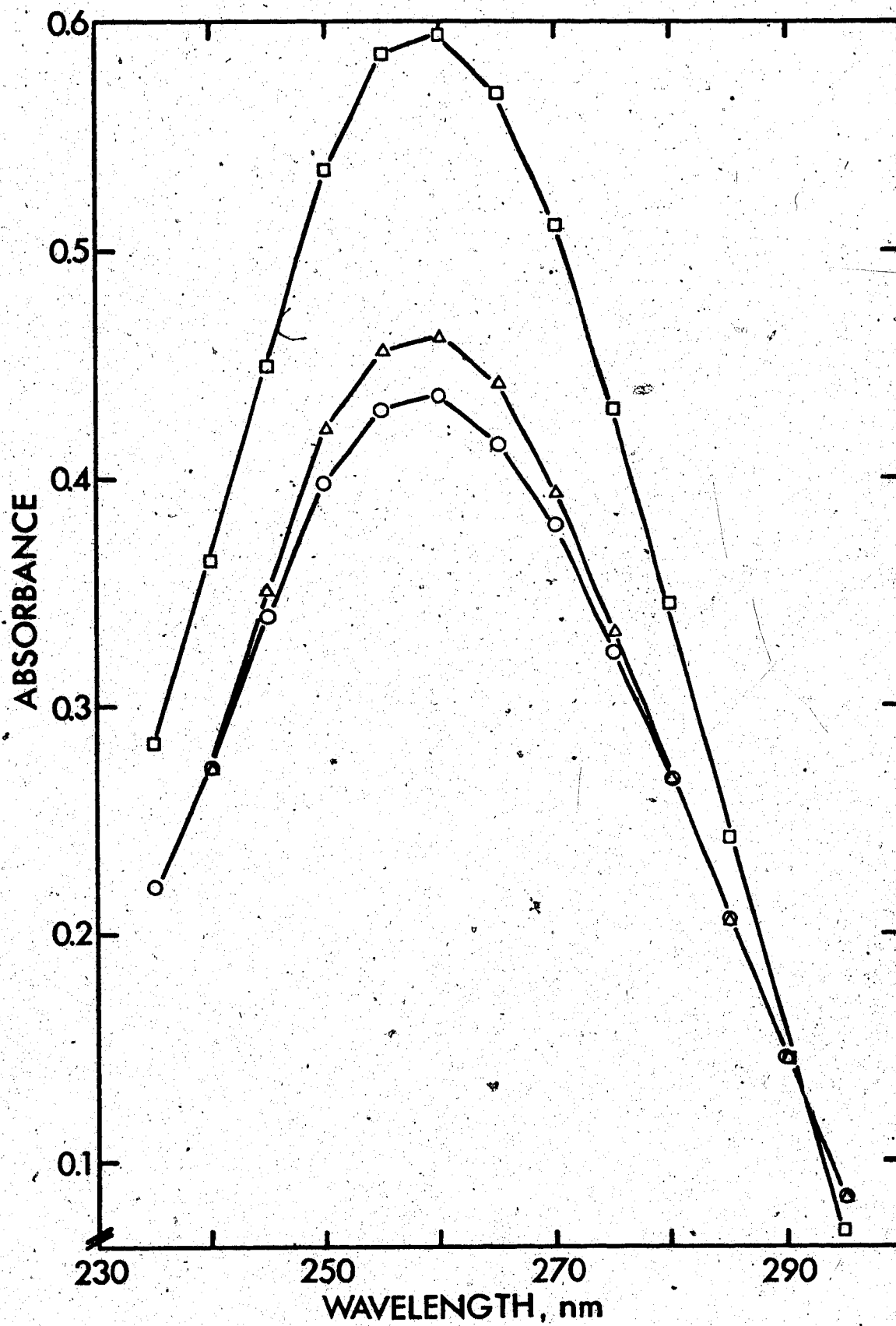
Figure 20 Absorbance of $d(TC)_n \cdot d(GA)_n$ Multiplex at Various Temperatures

The $d(TC)_n \cdot d(GA)_n$ multiplex was melted in 0.05M NaCl, 0.01M Na acetate pH 5.0, 0.1mM EDTA and the absorbance measured as a function of temperature.

○ 23°C

△ 60°C

□ 96°C



reversal of the change observed for multiplex formation (Figure 20).

Multiplexes of double-labelled $\text{Py}_n \cdot \text{Pu}_n$ DNAs ($^3\text{HdAMP}$ and $^{14}\text{CdTMP}$) were centrifuged to equilibrium in Cs_2SO_4 at pH 5.0 to test the hypothesis that a triplex was formed accompanied by the liberation of single-stranded material. In this case the ratio of pyrimidine strands to purine strands ($^{14}\text{C}/\text{H}^3$) in the triplex would change from the ratio at pH 8. Since single-stranded material would not be expected to form a sharp band on Cs_2SO_4 , "smearing" across the gradient, its presence may be detected as an increase in ^{14}C or ^3H counts (depending on the type of triplex) outside of the main peak. However, the results observed for $\text{d}(\text{TC})_n \cdot \text{d}(\text{GA})_n$, $\text{d}(\text{TTC})_n \cdot \text{d}(\text{GAA})_n$ and $\text{d}(\text{TCC})_n \cdot \text{d}(\text{GAA})_n$ (Figure 21) suggest that all the material originally present at pH 8 is present in the complex at pH 5.0 in the same ratio of pyrimidine strands to purine strands eliminating this model. It also may be proposed that two triplexes with very similar buoyant densities are formed perhaps linked by the residual $\text{d}(\text{TC})_n \cdot \text{d}(\text{GA})_n$ regions, in which case the ratio of $^{14}\text{C}/\text{H}^3$ should abruptly reverse when traversing the peak fractions especially after treatment with formaldehyde to eliminate the residual $\text{d}(\text{TC})_n \cdot \text{d}(\text{GA})_n$. When the double-labelled $\text{d}(\text{TC})_n \cdot \text{d}(\text{GA})_n$ multiplex was reacted with formaldehyde at 55°C (eliminating the first hyperchromic shift in the melting profile and reducing the molecular weight as judged by the band width in Cs_2SO_4 density gradients) and centrifuged to equilibrium in Cs_2SO_4 at pH 5.0 again only one peak of material with a constant ratio of $^{14}\text{C}/\text{H}^3$ across the band, equivalent to the ratio at pH 8.0, is observed contrary to the predictions of the triplex model (recovery of 62%).

Rearrangement to more than one type of triplex which could then aggregate together (repeating polymers can readily aggregate due to

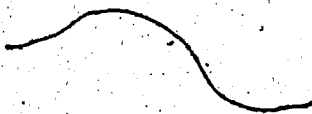
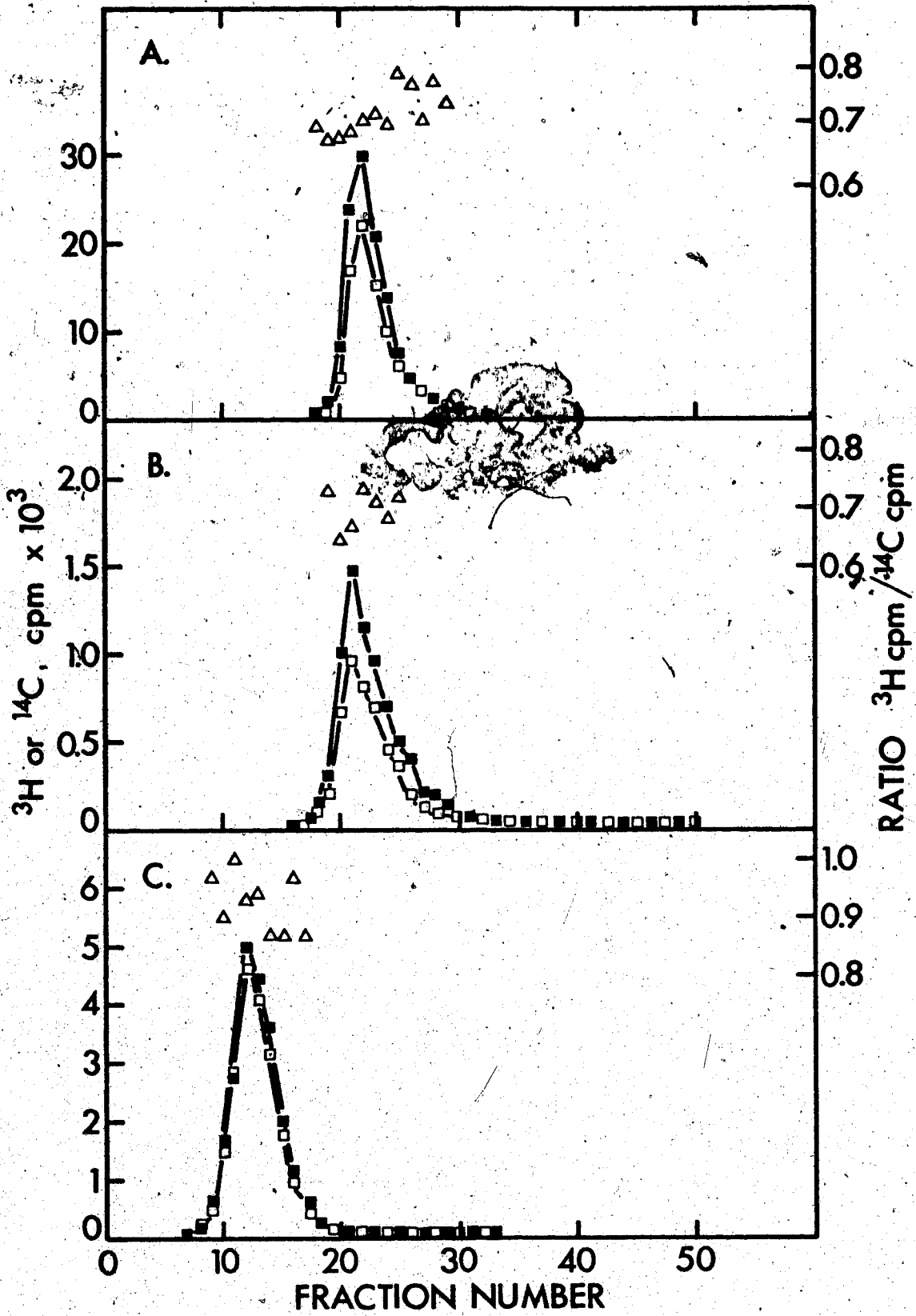


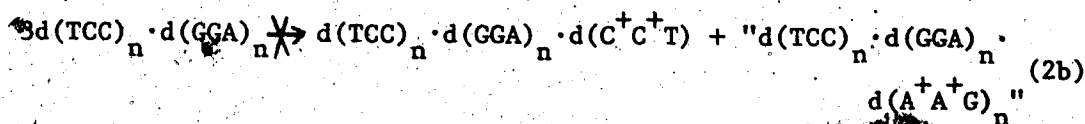
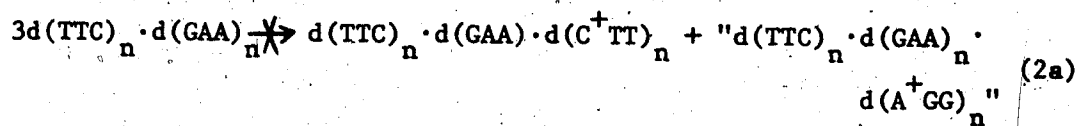
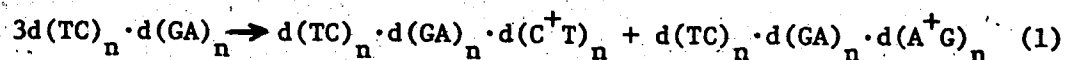
Figure 21 Preparative Cs_2SO_4 Density Gradients of Rearranged
Double-labelled $\text{Py}_n \cdot \text{Pu}_n$ DNAs at pH 5.0

Experiments were carried out as described in Materials and Methods
(□) ^3H cpm in dAMP, (●) ^{14}C cpm in dTMP, (▲) ratio ^3H cpm/ ^{14}C cpm

- A. d(TC)_n · d(GA)_n Recovery of radioactivity was 82% and the ^3H cpm/ ^{14}C cpm ratio at pH 8.0 was 0.69.
- B. d(TTC)_n · d(GAA)_n Recovery of radioactivity was 89% and the ^3H cpm/ ^{14}C cpm ratio at pH 8.0 was 0.75.
- C. d(TCC)_n · d(GGA)_n Recovery of radioactivity was 60% and the ^3H cpm/ ^{14}C cpm ratio at pH 8.0 was 0.88.



their ability to slip forming single-strand complementary ("sticky") ends is thought unlikely for two reasons. $d(TC)_n \cdot d(GA)_n$ could rearrange (1) to form two triplexes $Py_n \cdot Pu_n \cdot Py_n$ and $Py_n \cdot Pu_n \cdot Pu_n$ since the requirement that $A = G$, necessary for the formation of the $Py_n \cdot Pu_n \cdot Pu_n$ triplex, is fulfilled.



The repeating trimers (2a, 2b) cannot form $Py_n \cdot Pu_n$ triplexes of the same type, but only triplexes with the triads TAA and CGG which are not isomorphous (and also do not require protonation of one of the bases). If a common structure is basic to all of these multiplexes, since two triplexes cannot be constructed for the repeating trimers, by inference the triplex model is not plausible. Secondly, it seems unlikely that for the range of polymers which form multiplexes with G+C contents of 33% to 100% both triplex species derived from each polymer would have similar buoyant densities and melting temperatures. Aggregation of the two triplexes may lead to one peak on Cs_2SO_4 but separate melting shifts should be observable. If reaction with formaldehyde at $55^\circ C$ or $93^\circ C$ is used to reduce the molecular weight of the multiplex, still only one hyperchromic shift and one peak in Cs_2SO_4 is observed.

Three independent lines of evidence belie the hypothesis that

multiplex formation results from a simple conformational change of these $Py_n \cdot Pu_n$ DNAs. Random $d(T,C)_n \cdot d(G,A)_n$ which would be expected to undergo conformational changes does not form a multiplex (also emphasizing the need for a repeating sequence). Secondly, the rearrangement is concentration dependent (Figure 22) suggesting an interaction between at least two species. Lastly, $d(TC)_n \cdot d(GA)_n$ and $d(BrUC)_n \cdot d(GA)_n$ (a density labelled analogue of $d(TC)_n \cdot d(GA)_n$ with $dBrUMP$ residues replacing $dTMP$) rearranged together form a third species. The $d(TC)_n \cdot d(GA)_n$ multiplex has a T_M of $93^\circ C$ and a buoyant density in Cs_2SO_4 of $1.469g/cc$. The corresponding values for the $d(BrUC)_n \cdot d(GA)_n$ multiplex are $99^\circ C$ and $1.519g/cc$ (Table 6). When rearranged separately and then mixed together two peaks are observed in Cs_2SO_4 gradients and two hyperchromic shifts at high temperature are seen as expected if there was no interaction of the final products. However, when transformed together only one peak at a density of $1.493g/cc$ in Cs_2SO_4 gradients (which is almost equidistant from the value of the individual multiplexes) is observed and from the melting profile three hyperchromic shifts of approximately equal magnitude are observed at $93^\circ C$ ($d(TC)_n \cdot d(GA)_n$ multiplex), $99^\circ C$ ($d(BrUC)_n \cdot d(GA)_n$ multiplex) and at $95.5^\circ C$. This later shift is presumably due to the interaction of $d(TC)_n \cdot d(GA)_n$ and $d(BrUC)_n \cdot d(GA)_n$ and again is approximately equidistant from the values of the individual multiplexes. Therefore, while confirming an interaction between the two polymers, contrary to the results expected for a conformational change, these data also suggest the interaction may be 1:1.

The reactions of various site specific chemical reagents with

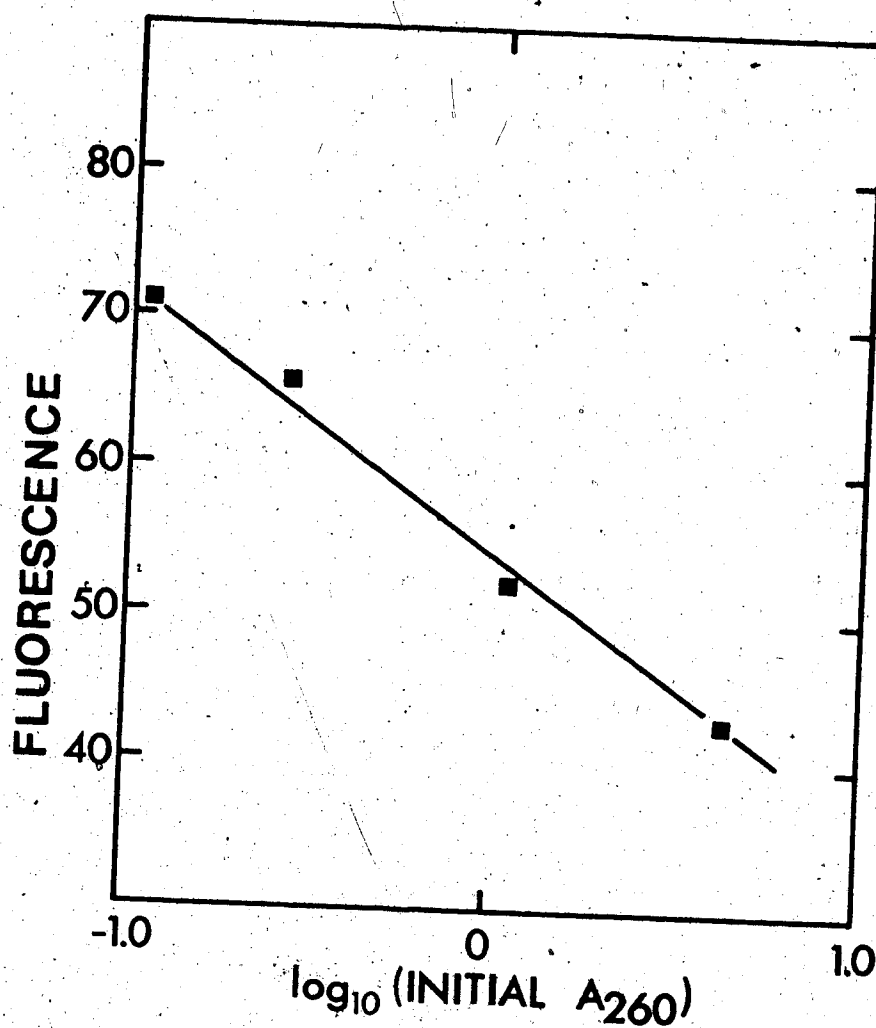


Figure 22 Concentration Dependence of $d(\text{TC})_n \cdot d(\text{GA})_n$ Rearrangement

$d(\text{TC})_n \cdot d(\text{GA})_n$ was allowed to rearrange at room temperature overnight at various concentrations in 50mM Na acetate pH 5.0, 200mM NaCl. The incubation mixtures were adjusted to 50mM Na acetate pH 5.0, 200mM NaCl, 0.5 $\mu\text{g}/\text{ml}$ ethidium bromide and the fluorescence reading taken.

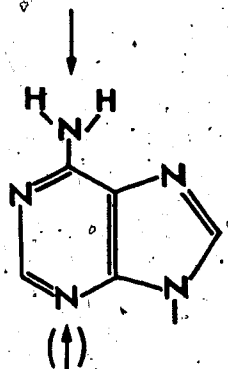
$d(TC)_n \cdot d(GA)_n$ and with the corresponding multiplex were investigated with the following rationale: if a particular site is important for the formation of the multiplex then by blocking that site at neutral pH rearrangement to the multiplex should be inhibited or abolished depending on the extent of modification. Conversely once the multiplex is formed that site should be less accessible to chemical reagents especially if involved in hydrogen bonding. Chemicals that were used as probes included formaldehyde (Grossman, 1968), glyoxal (Broude and Budowsky, 1971) and dimethyl sulfate (Singer, 1975). Formaldehyde reacts with free amino groups reversibly forming an hydroxymethyl compound. Glyoxal also reacts with amino groups but the only stable adduct formed is with guanine due to subsequent cyclization after reaction at the 1-position (the structure of this adduct is discussed in the section concerning the reactions of glyoxal) and this adduct decomposes at alkaline pH's with the recovery of guanine. The relative stability of the adducts formed with nucleosides (Broude and Budowsky, 1971) has been confirmed for polymers by use of fluorescence assays. The polymers dA_n , rA_n and rC_n when reacted with glyoxal at pH 7.5 and dialysed at pH 5.0 form the expected duplex DNAs, as measured by fluorescence at pH 5.0, when annealed with the complementary strand dT_n , rU_n and rI_n respectively confirming the reversible nature of the reaction with a or c. The guanine adduct is stable under these conditions. Dimethyl sulfate reacts with purine bases and to a limited extent with the phosphate backbone (Singer, 1975), compared to other alkylating agents. The extent of phosphodiester hydrolysis is low. The products are 7-Meg, 7-Mea and 3-Mea in a ratio of 12:1:1 (the literature value for the ratio of 7-Meg to 3-Mea is 6-7:1, see Materials and Methods).

Results of these modification experiments (Table 7) suggests that the 6-amino of a and the 1-, 7- and 2-amino positions of g are important to the multiplex structure. Neither glyoxal nor formaldehyde react with duplex DNA at neutral pH nor with the multiplex at pH 5.0 as measured by ultra-violet absorption, buoyant density in Cs_2SO_4 and melting temperature. After 1 hour at 23°C in the presence of 3% formaldehyde there were no spectral changes and the buoyant density of the multiplex was 1.468g/cc (under these conditions the reaction with dAMP is 70% complete, as judged by the change in A_{275}). After four days at 30°C in the presence of 50mM glyoxal, the T_M of the multiplex was 92°C and material incubated for one month at 23°C had a buoyant density of 1.468g/cc (both formaldehyde and glyoxal treated $d(\text{TC})_n \cdot d(\text{GA})_n$, when completely derivatized show a broad band in Cs_2SO_4 centred at 1.45g/cc). These experiments rule out the possibility of a Hoogsteen duplex especially since reaction with the 2-amino and 1-position (of g) would have been observed (note that Hoogsteen hydrogen bonding could be involved in a larger complex which also included Watson-Crick hydrogen bonding). Denatured $d(\text{TC})_n \cdot d(\text{GA})_n$ reannealed at pH 5.0 directly forms a multiplex. If either glyoxal or formaldehyde is reacted with denatured $d(\text{TC})_n \cdot d(\text{GA})_n$ inhibition of multiplex formation is observed. However, decomposition of these adducts by dialysis at pH 9.5 allows reformation of the original duplex at neutral pH or the multiplex at pH 5.0 (monitored by fluorescence, buoyant density and melting temperature).

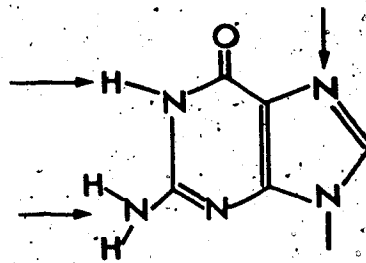
The extent of reaction of dimethyl sulfate with the multiplex as measured by the decrease in T_M (Uhlenhopp and Krasna, 1971) is less than for duplex DNA (Figure 23a). At a dimethyl sulfate concentration of 100 mM the decrease in T_M for duplex DNA is 6°C and

REAGENT	ABILITY OF DERIVATIZED $d(TC)_n \cdot d(GA)_n$ TO FORM MULTIPLEX	REACTION WITH MULTIPLEX AT pH 5.0
Formaldehyde	No	No
Glyoxal	No	No
Dimethyl Sulfate	No	Low

SITES IMPLICATED IN MULTIPLEX FORMATION



A



G

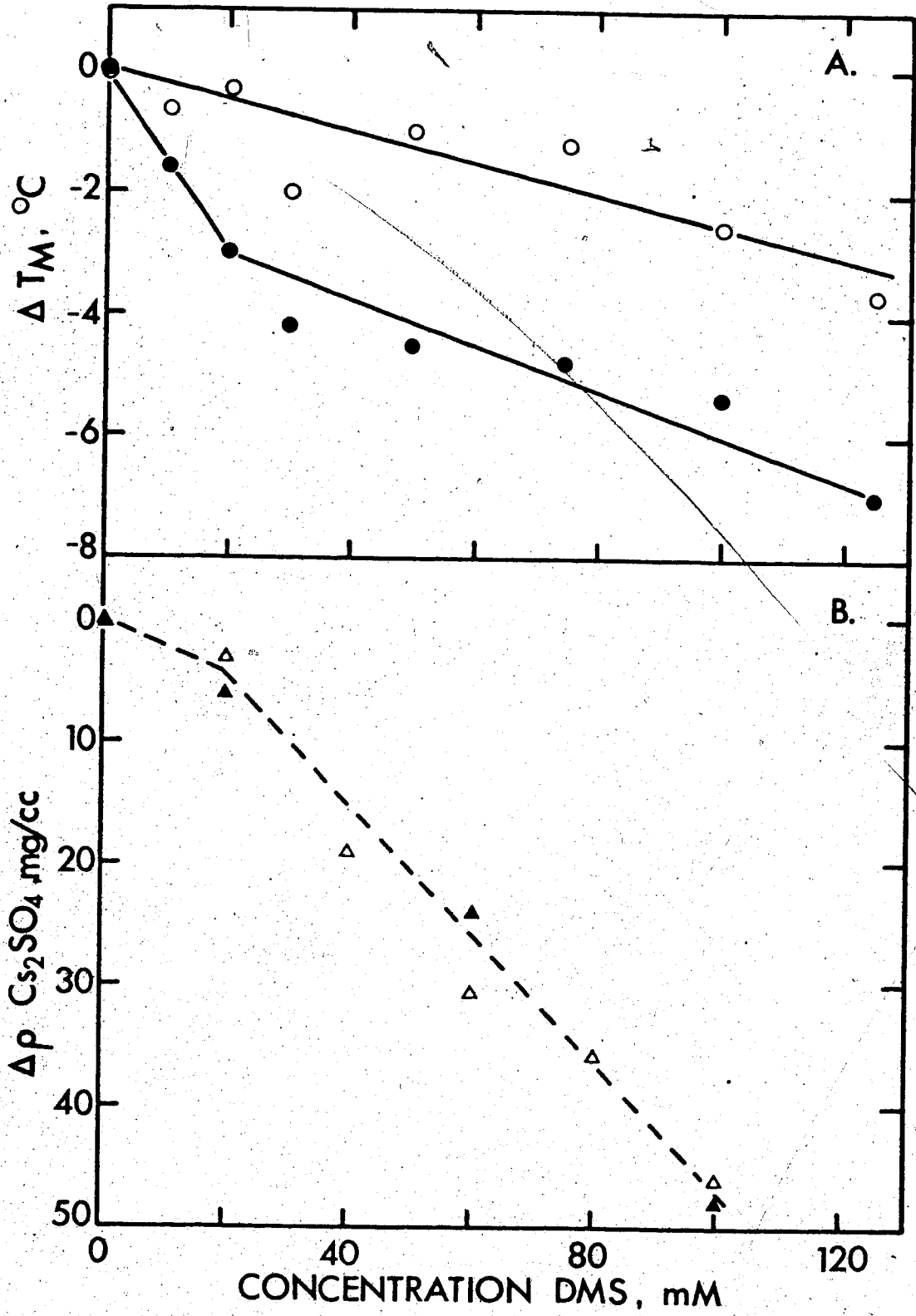
TABLE 7

Chemical Reagents as Probes of the $d(TC)_n \cdot d(GA)_n$
Multiplex Structure

Details given in Materials and Methods and in text.

Figure 23 Reactions of Dimethyl Sulfate with $d(TC)_n \cdot d(GA)_n$

- A. Effect of DMS on the T_M of the $d(TC)_n \cdot d(GA)_n$ multiplex (○) and control duplex DNA (●). For experimental, see Materials and Methods.
- B. Inhibition of multiplex formation by reaction with DMS as measured by the decrease in buoyant density shift. For experimental details, see Materials and Methods.



the decrease for the $d(TC)_n \cdot d(GA)_n$ multiplex is $2.6C^0$. This suggests that the 7-position of the purine bases (the major site of methylation) is not as accessible as in duplex DNA and that these sites (especially the 7-position of g) are involved in the stability of the multiplex structure. (It is perhaps a coincidence that, judged by the reduction in T_M , one half as many sites are available in the multiplex (i.e., the 7-position of g) as predicted for one of the tetraplex models (Figure 8)). Methylation of $d(TC)_n \cdot d(GA)_n$ at neutral pH reduces its ability to rearrange as measured by the inhibition of the buoyant density shift that accompanies rearrangement and by a decreased fluorescence loss. Reaction with 100mM DMS is sufficient to stop multiplex formation (Figure 23b). It has been shown that methylation of the pyrimidine 5-position leads to various changes in the buoyant density (in CsCl or Cs_2SO_4) depending on the polymer (Gill et al., 1974); however, this methylation increases the T_M (stabilizes the duplex) contrary to the effect of methylation at the 7-position which decreases the T_M . The distribution of purine bases for an average $d(TC)_n \cdot d(GA)_n$ of 750 base pairs methylated with 100mM DMS (as calculated from Table 4) is 246 g, 130 7-Meg, 354 a, 11 7-Mea and 11 3-Mea. It is obvious that more than one methylation is necessary to stop multiplex formation but the preponderance of modified g residues suggests the 7-position is necessary for multiplex formation (implying Hoogsteen hydrogen bonding) and perhaps also the 3-position of a. If one accepts the premise that a common structural element exists for all the multiplexes then the observation that $d(C)_n \cdot d(G)_n$ forms such a structure reduces the possibility that methylation at the 3-position interferes with multiplex formation. Also recent experiments

with methylated $d(C)_n \cdot d(G)$ confirm that the methylated polymer rearranges at a much reduced rate.

Many of the experiments described suggest that protonation of one of the bases may be involved in the multiplex structure. This hypothesis was tested by direct titration of rearranging $d(TC)_n \cdot d(GA)_n$ to pH 4.5 (in order to increase the rate of rearrangement) compared to standard duplex DNA titrated to pH 4.5 under the same conditions (Figure 24). Clearly protons are being taken up to the extent of one mole of acid per 7.6-9.1 moles nucleotide. The titrated material was characterized as usual and judged > 97% multiplex by fluorescence. These results are in good agreement with the value predicted for a tetraplex with Hoogsteen hydrogen bonds (Figure 8) which predicts a value of 8:1, although they do not fix the site of protonation which one can only infer to be the 3-position of c from model building studies.

The tetraplex structure with Hoogsteen hydrogen bonds is the most reasonable model, sufficient to explain the properties of the multiplex. It satisfactorily rationalizes the need for the low pH, the increased stability of the multiplex (due to the formation of a protonated hydrogen bond) and the necessity for G-C base pairs, and the relative inertness towards chemical reagents. Also the inclusion of Hoogsteen hydrogen bonding into the structure explains the observation that only $Py_n \cdot Pu_n$ DNAs form multiplexes. Inspection of models does not lead to any obvious reason why $d(T)_n \cdot d(A)_n$ cannot form a tetraplex and there is some preliminary evidence that such a structure may be formed at neutral pH in Cs_2SO_4 gradients (A.R. Morgan, personal communication).

Although incubation at low pH is used in these experiments to form

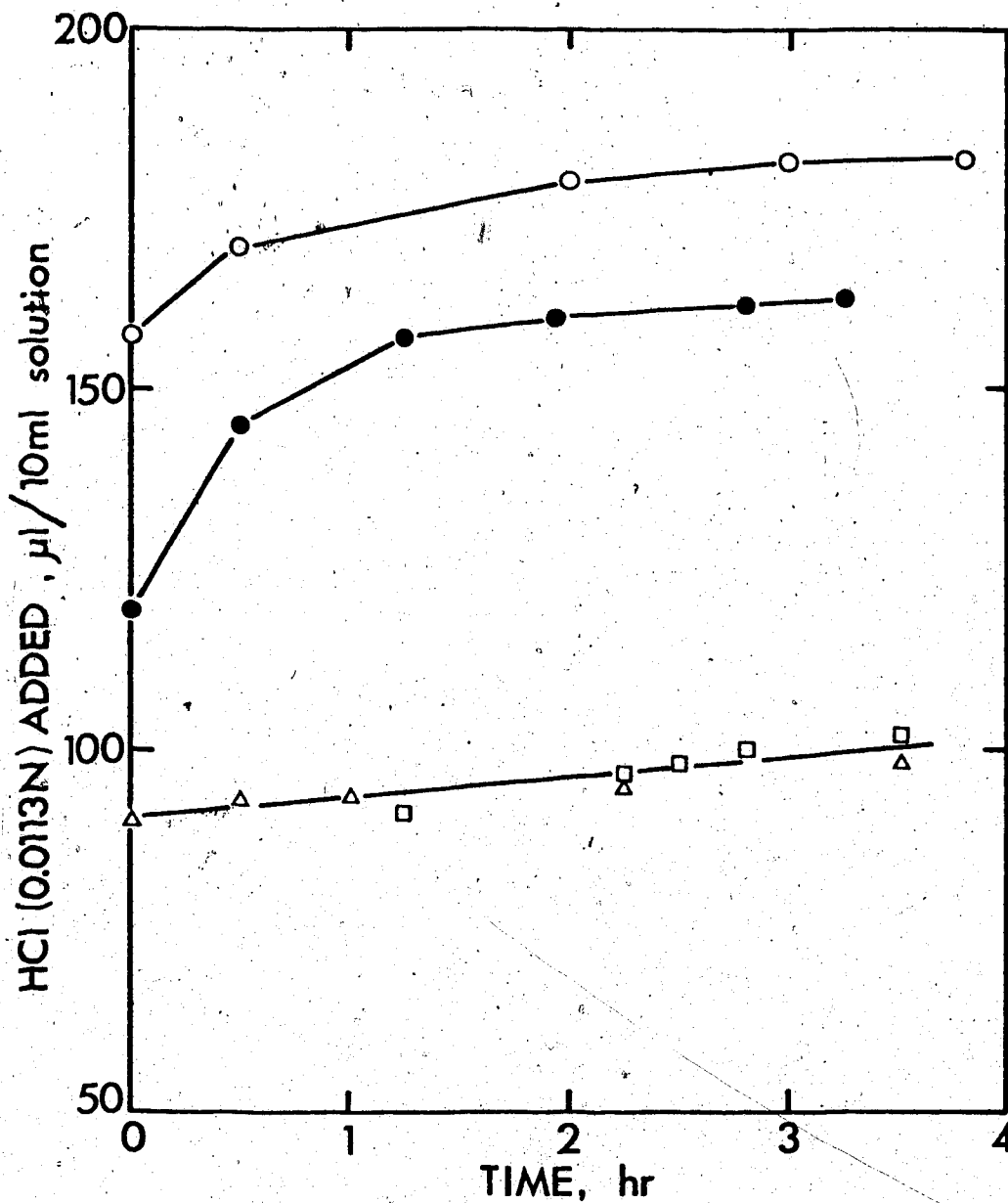


Figure 24 Titration of Rearranging $d(TC)_n \cdot d(GA)_n$

Aliquots of 0.0113N HCl were added to $d(TC)_n \cdot d(GA)_n$ in 0.5M NaCl, 1.0 μ M EDTA pH 7.4 until rearrangement was complete using the apparatus previously described in Materials and Methods.

- △ Control, buffer with calf thymus DNA at 6.7 A_{260}
- Control, buffer alone
- Titration #1, 0.69 mM DNA
- Titration #2, 0.61 mM DNA

these putative tetráplexes it may be possible, especially since they are more stable than the corresponding duplexes, to form them at neutral pH under different conditions or in the presence of a particular protein. In this regard there is evidence that the triplex $d(TC)_n \cdot d(GA)_n \cdot r(C^+U)_n$ can indeed be formed at neutral pH (Morgan and Wells, 1968) well above the pKa normally associated with the protonation of c.

One approach to understanding the structural basis for the multiplex is to insert bases, which have been modified to eliminate certain hydrogen bonding sites, into these polymers and observe their effect on multiplex formation. RNA·DNA hybrids analogous to $d(TC)_n \cdot r(GA)_n$ were synthesized using tubercidin 5'-triphosphate and 6-Methyladenosine 5'-triphosphate (Figure 13) as precursors replacing rATP. However $d(TC)_n \cdot r(GA)_n$ did not show the fluorescence loss associated with multiplex formation. The reason why an RNA·DNA hybrid does not form a multiplex is obscure. Arnott has shown these to be (in fibres) in A conformations (Arnott *et al.*, 1973) but $d(C)_n \cdot d(G)_n$ which forms a multiplex also has an A structure (Arnott and Selsing, 1974b). Therefore, the inability of these hybrids to form multiplexes may be related to the close packing expected for the structure which may be disrupted by the presence of the hydroxyl moiety at the 2'-position. The deoxyribose 5'-triphosphate analogues corresponding to the above ribose analogues were then synthesized and substituted for dATP in the synthesis of $d(TC)_n \cdot d(GA)_n$. In addition, 7-MedGTP was synthesized and substituted for dGTP in a similar reaction. The use of these analogues would test the effect on multiplex formation of modifying the 7-position of g, the 7-position of a and the 6-amino position of adenine.

None of these analogues were incorporated into DNA when $d(TC)_n \cdot d(GA)_n$ was used as template and in contrast to previous reports (Novogradsky *et al.*, 1966) we were unable to replicate $d(AT)_n$ using 6-MedATP as a substrate. In addition 7-MedGTP inhibited the synthesis of $d(TC)_n \cdot d(GA)_n$ in the presence of 1mM dGTP (Figure 25) as measured both by fluorescence and incorporation of radioactivity into acid insoluble counts (the polymers synthesized in the presence of 7-MedGTP and dGTP contained <1 residue of 7-MedGMP per 500,000 daltons of DNA). Work in this area is still in progress.

As judged by its melting behaviour, the $d(TC)_n \cdot d(GA)_n$ multiplex binds spermine. With the addition of 10 μ M spermine·HCl to 10mM Na acetate pH 5.0, 50mM NaCl, 0.1mM EDTA the T_M is raised from 93°C (Table 6) to 97.5°C and decreasing the ionic strength increases the T_M as expected from the interaction of spermine with duplex DNA. Spermine is thought to bind to DNA phosphates in the minor groove (Suwalsky *et al.*, 1969) and although the multiplex structure may not contain major and minor grooves per se there is a conformation with the proper geometry for spermine binding.

If $d(TC)_n \cdot d(GA)_n$ is incubated at pH 5.0 in the presence of 1% formaldehyde the multiplex formed has a buoyant density of 1.463g/cc, lower than the normal 1.469. This decrease is expected if formaldehyde reacted with the polymer although no reaction with the multiplex or duplex is observed under identical conditions. Thus amino groups may be transiently exposed during rearrangement as predicted for the tetraplex involving Hoogsteen hydrogen bonding (as well as a number of other models). Glyoxal substituted for formaldehyde at a concentration of 0.1M does not affect the buoyant density although this may

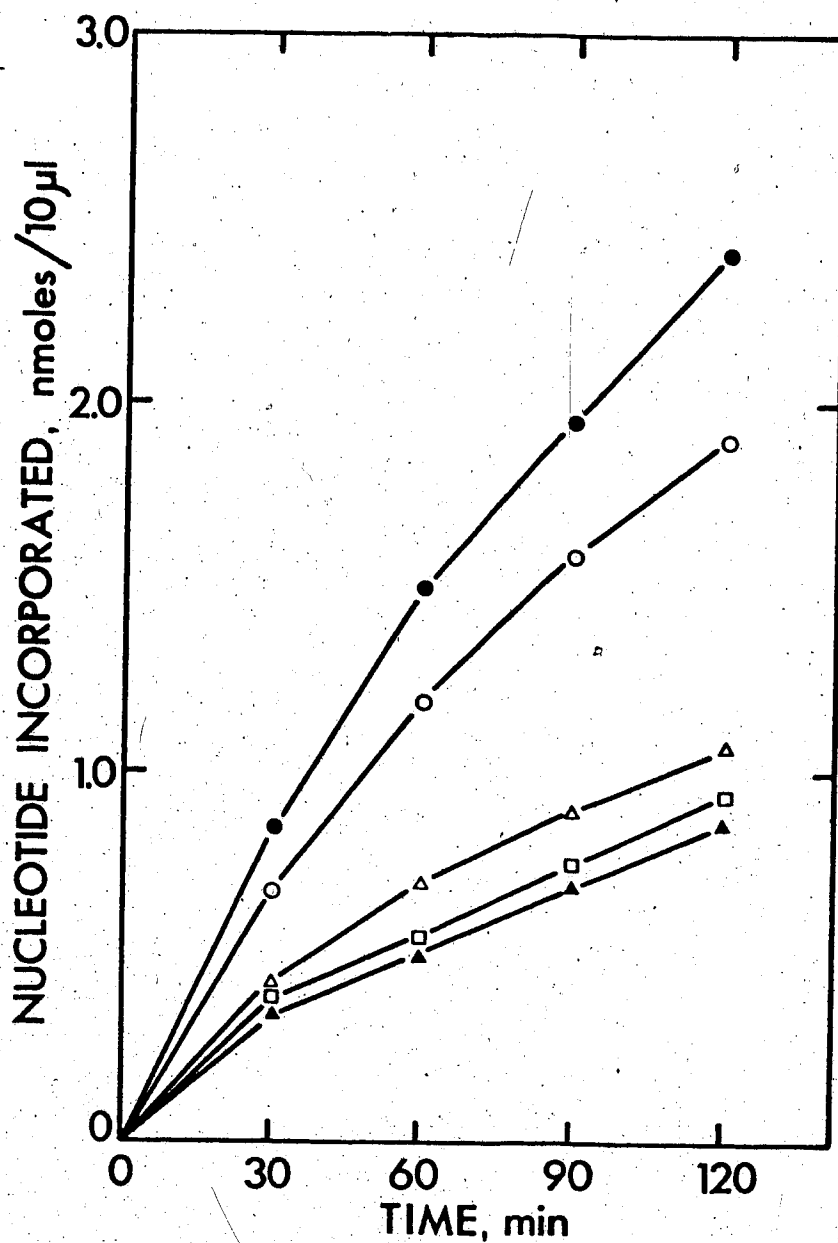


Figure 25 Replication of $d(TC)_n \cdot d(GA)_n$ in the Presence of 7-MedGTP

Conditions were as described in Materials and Methods with 1mM dGTP and 7-MedGTP at concentrations of 0mM (●), 0.5mM (○), 1.1mM (△), 1.6mM (□), and 2.1mM (▲).

be related to kinetic phenomena, the rate constant of the reaction with guanosine at pH 5.0 is $< 1 \times 10^2 \text{ min}^{-1}$ (Broude and Budowsky, 1971) while the rate constants for the reaction of formaldehyde with dAMP, dGMP, and dCMP are in the range $1-4 \times 10^2 \text{ min}^{-1}$ (Grossman, 1968) or to a steric effect due to the larger size of glyoxal compared to formaldehyde.

The interaction of $d(\text{TC})_n \cdot d(\text{GA})_n$ with $d(\text{TC})_n$ or $d(\text{GA})_n$ was studied fluorometrically (Figure 26) with the hope of isolating triplexes which could possibly be intermediates in multiplex formation. Both $d(\text{TC})_n$ and $d(\text{GA})_n$ interact with $d(\text{TC})_n \cdot d(\text{GA})_n$ at pH 5.0 as measured by the increase in fluorescence of intercalated ethidium, but not at pH 8.0 at the same ionic strength. The fluorescence increments are 9.0% - 22.0% (after 6 minutes incubation) and 2.0% - 5.5% (after 2 minutes), for $d(\text{TC})_n$ and $d(\text{GA})_n$ respectively. In both cases (at longer times) there is the fluorescence loss associated with multiplex formation. The reasons for the difference in the fluorescence increase could reflect either intrinsic differences in the fluorescence/mole nucleotide between the two putative triplexes or kinetic differences in their association rates especially since polypurines form more ordered structures than polypyrimidines (Felsenfeld and Miles, 1967) which could inhibit $\text{Py}_n \cdot \text{Pu}_n \cdot \text{Pu}_n$ triplex formation. The addition of either of these single-strand polynucleates retards, but does not stop, multiplex formation implying that the multiplex is the more stable structure. It is interesting that in the studies on the triplex $d(\text{TC})_n \cdot d(\text{GA})_n \cdot r(\text{C}^+\text{U})_n$ Morgan and Wells did not observe any rearrangement to a structure reassembling the multiplex at pH's as low as 5.0 (A.R. Morgan, personal communication). It seems unlikely, in view of

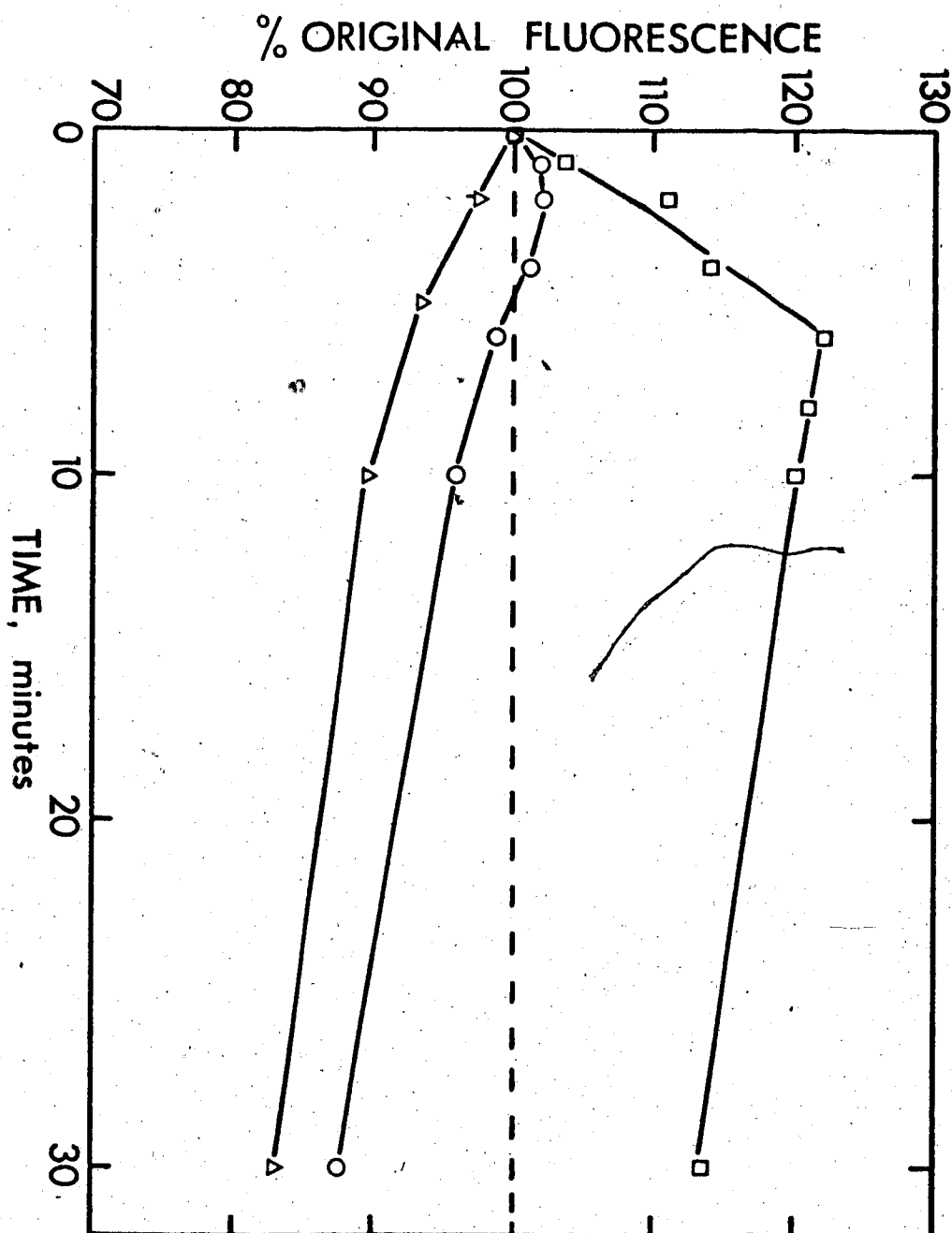


Figure 26 Interaction of $d(TC)_n$ and $d(GA)_n$ With $d(TC)_n$
 $d(GA)_n$ at pH 5.0

- △ Rearrangement of $d(TC)_n \cdot d(GA)_n$ ($\sim 0.042 A_{260}$) in 10mM Na acetate
 pH 5.0, 200mM NaCl, 0.5 μ g/ml ethidium bromide.
- As above plus $d(GA)_n$ (0.014 A_{260})
- As for $d(TC)_n \cdot d(GA)_n$ plus $d(TC)_n$ (0.013 A_{260})

the great stability of the multiplex, that this lack of rearrangement is due simply to a difference in the incubation mixtures but may be related to the difficulty in packaging the 2'-hydroxyl of the ribose moiety into such a compact structure as proposed in the discussion concerning the RNA·DNA hybrids. Research into this area should be pursued further not only with the hope of isolating putative intermediates in multiplex formation by varying the incubation conditions but also in order to study the relative stabilities of the three types of polymers (multiplex, $d(TC)_n \cdot d(GA)_n \cdot r(C^+U)_n$ and " $d(TC)_n \cdot d(GA)_n \cdot d(C^+T)_n$ " and " $d(TC)_n \cdot d(GA)_n \cdot d(A^+G)_n$ ").

An X-ray fibre diffraction study would yield the most definitive identification of the multiplex structure (McGavin has calculated the expected intensities for the tetraplex model which he has proposed (McGavin, 1971)). This is the approach now under investigation.

CHAPTER V THE REPLICATION OF $\text{Py}_n \cdot \text{Pu}_n$ DNAs

Modes of DNA synthesis have been studied in vitro using E. coli DNA polymerase I (Kornberg's enzyme) and a variety of DNA templates (Schildkraut, 1964; Paetkau, 1969). When the in vitro synthesis of $\text{Py}_n \cdot \text{Pu}_n$ DNAs is compared to the synthesis of a natural DNA such as E. coli DNA or a synthetic DNA with pyrimidines and purines in both strands, such as $\text{d}(\text{TG})_n \cdot \text{d}(\text{CA})_n$, differences are immediately apparent. These different patterns of synthesis are most easily illustrated using the fluorescence assay as shown in Figure 27.

All the newly synthesized DNA is 100% CLC when E. coli DNA is used as template; only the input DNA shows no return of fluorescence after the heat step (Figure 27a). In contrast, during the synthesis of $\text{d}(\text{TC})_n \cdot \text{d}(\text{GA})_n$ (Figure 27b) CLC DNA formation is never observed (even if the temperature is raised). When $\text{d}(\text{TG})_n \cdot \text{d}(\text{CA})_n$ is used as the template intermediate values of CLC DNA synthesis are observed, in this case 25% CLC DNA after 5 hrs. (Figure 27c). This suggests a mode of synthesis intermediate between E. coli DNA and $\text{d}(\text{TC})_n \cdot \text{d}(\text{GA})_n$ or a combination of the two modes.

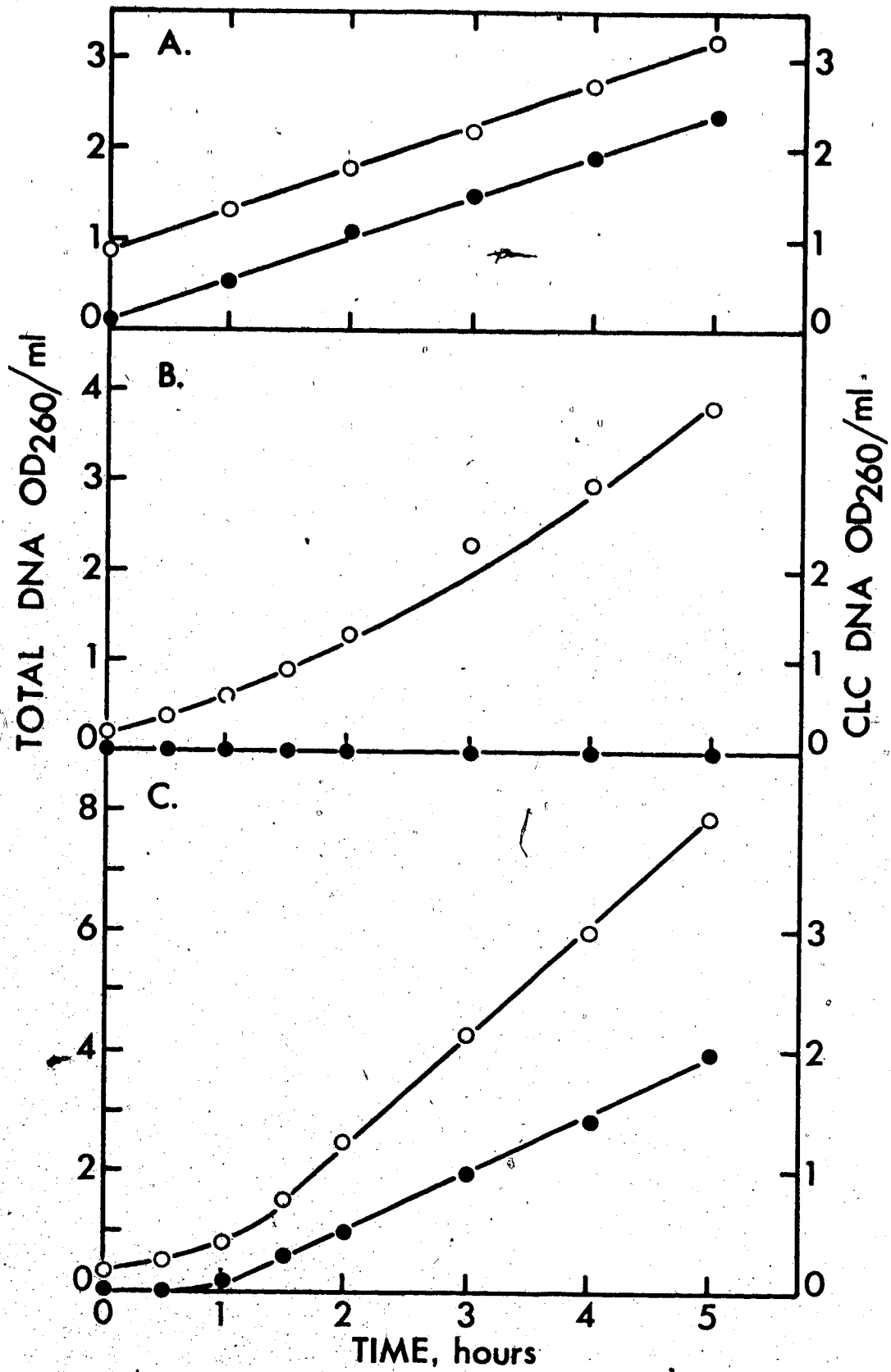
Two different mechanisms illustrated in Figure 28 have been postulated to explain the observed types of synthesis. Strand switching mechanisms (Figure 28a) propose that synthesis directed by a template strand displaces the complementary strand (Kornberg, 1974) until at some stage the polymerase "switches" strands and now begins to copy the complementary strand. All the newly synthesized DNA becomes CLC, renaturing spontaneously after the heat denaturation step of the fluorescence assay. This mode of replication is thought to occur with natural DNAs as templates in vitro and perhaps also in vivo (Guild, 1968)

Figure 27 In Vitro DNA Synthesis With E. Coli DNA Polymerase I

DNA synthesis was measured by use of the ethidium bromide assay mixtures at pH 8.0 (panels B. and C.) or pH 11.7 (panel A.). CLC DNA synthesis was estimated from the fluorescence after the heat step. The input templates were E. Coli DNA (A.), $d(TC)_n \cdot d(GA)_n$ (B.), and $d(TG)_n \cdot d(CA)_n$ (C.). These figures are the work of Dr. A. R. Morgan.

○ Total DNA

● CLC DNA



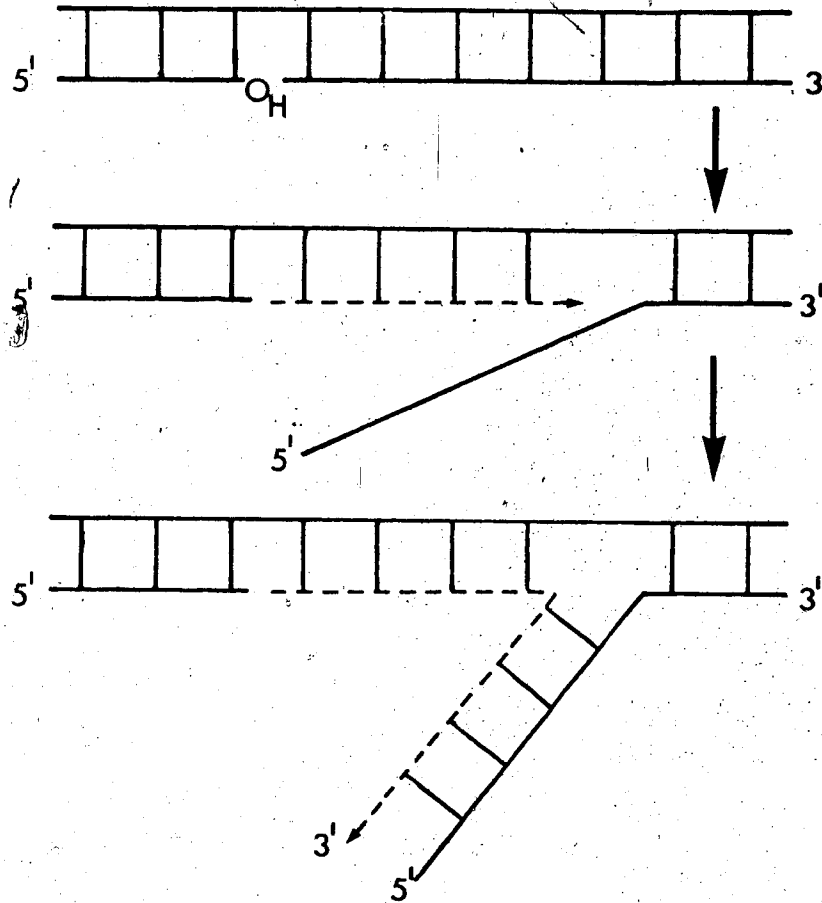


Figure 28a DNA Replication By a Strand Displacement Mechanism

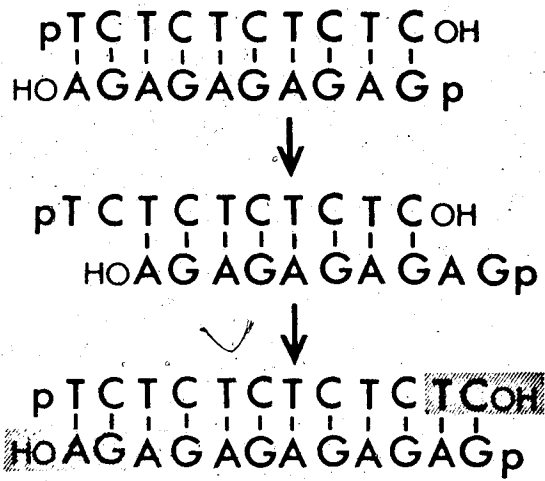


Figure 28b DNA Replication By a Slippage Mechanism

and requires pyrimidines and purines in both strands. Slippage mechanisms (Kornberg, 1974) require repeating sequences so that the DNA strands can slide with respect to each other and synthesis occurs at the ends of the molecule via a repair-type reaction (Figure 28b). At all times the complementary strands are separable by denaturation (no CLC DNA observed). This type of mechanism has been postulated to explain the replication of $\text{Py}_n \cdot \text{Pu}_n$ DNAs. If $d(\text{TC})_n \cdot d(\text{CA})_n$ is used as a template then its mode of synthesis may be a combination of "slippage" and "strand switching" or some other mechanism.

"Slippage" as the mechanism for $\text{Py}_n \cdot \text{Pu}_n$ DNA synthesis was tested by constructing a $\text{Py}_n \cdot \text{Pu}_n$ DNA with a random base order which could not slip and would, therefore, not be expected to show the same pattern of synthesis as observed for $d(\text{TC})_n \cdot d(\text{GA})_n$ if "slippage" is important. This duplex DNA was synthesized as described in Materials and Methods p59 with $d(\text{G,A})_n$ as template, added primer and dTTP and dCTP. After repair of the random $d(\text{T,C})_n$ strand with random $d(\text{G,A})$ as template to give $d(\text{G,A})_n \cdot d(\text{T,C})_n$ no synthesis was detectable, either by the incorporation of radioactivity into acid precipitable counts or by the fluorescence assay. As shown in Figure 29, the extent of $d(\text{T,C})_n$ synthesis is 60% - 80% of the input $d(\text{G,A})_n$. In contrast, when alternating $d(\text{GA})_n$, which would give rise to $d(\text{TC})_n \cdot d(\text{GA})_n$, was used as template a large net synthesis (up to 45 fold after 4 hours) was observed. Thus, a repeating sequence is necessary for $\text{Py}_n \cdot \text{Pu}_n$ DNA synthesis under these conditions as predicted by a slippage model.

This type of system, i.e., the use of an RNA primer for DNA synthesis, could also serve as a model system for DNA replication since synthesis is accompanied by degradation of the RNA primer, presumably by the polymerase's RNase H activity. Also, this methodology has been

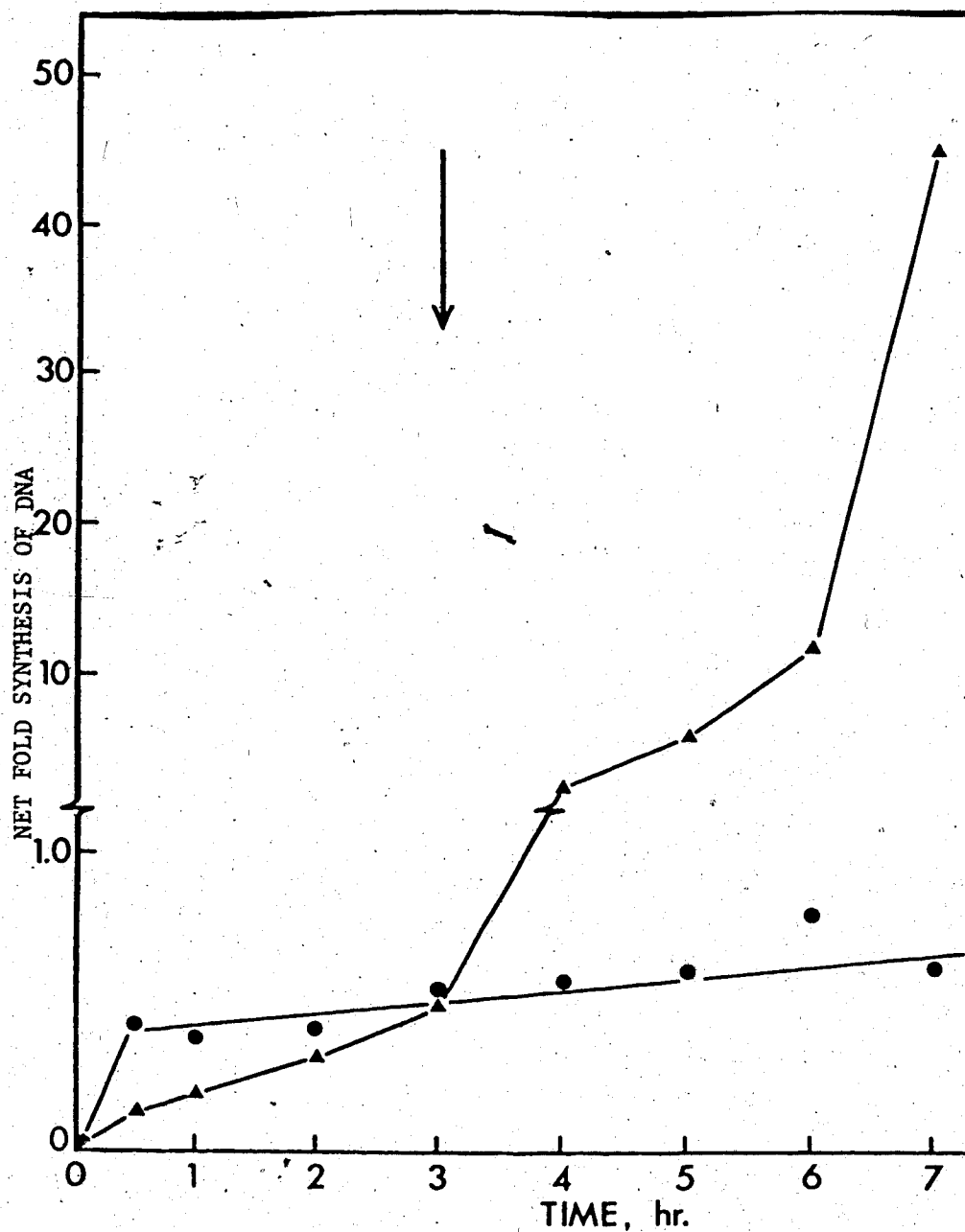


Figure 29 RNA Primed DNA Synthesis With *E. coli* DNA Polymerase I

DNA synthesis was measured using RNA primed d(GA) (▲) or d(G,A) (●) as template (see Materials and Methods). After an initial phase of repair synthesis, all four deoxytriphosphates were added (arrow) along with additional DNA polymerase. Note the change in the ordinate scale.

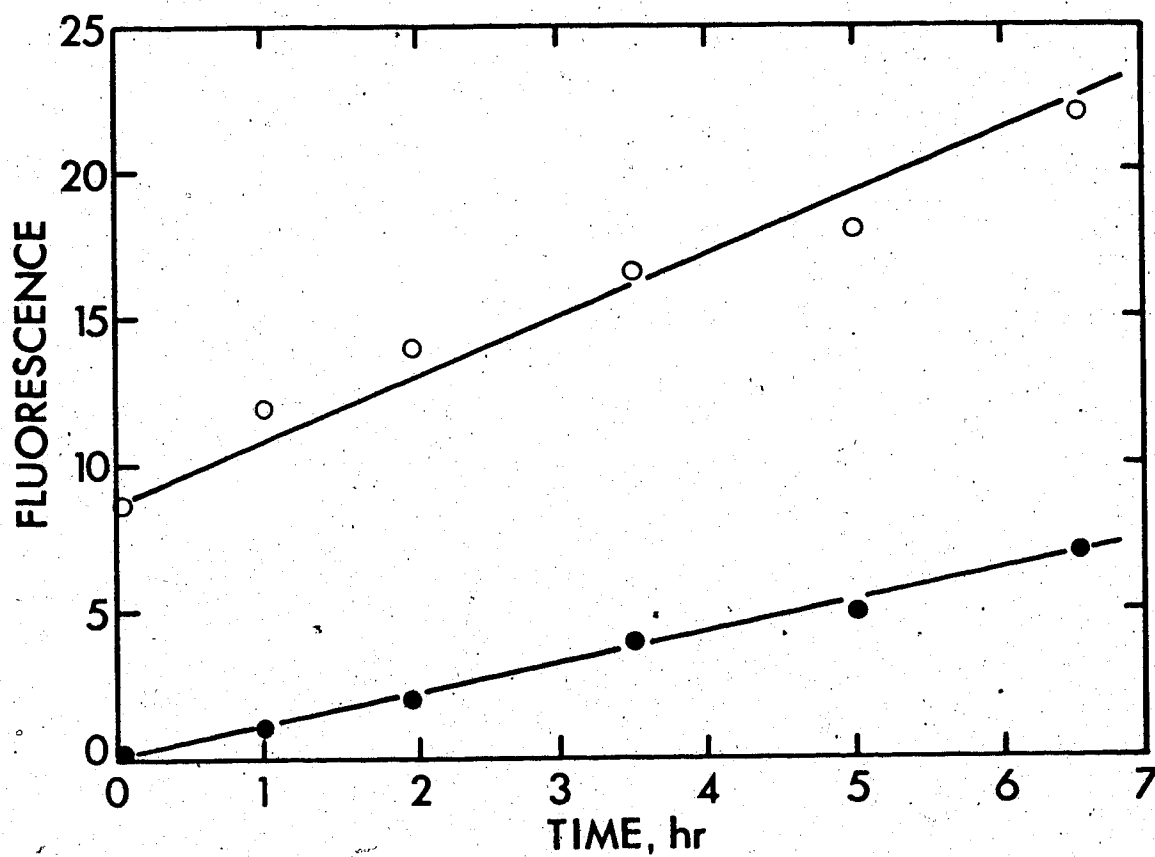


Figure 30 Replication of $d(T,C)_n \cdot d(G,A)_n$ at 41°C

Conditions for replication are given in Materials and Methods. Synthesis was monitored by the removal of aliquots into the neutral ethidium assay mixture.

○ before heat values

● after heat values

utilized to repair and then replicate $\text{Py}_n \cdot \text{Pu}_n$ DNAs starting from pyrimidine tracts isolated from L cell DNA (Birnboim and Straus, 1975).

Although duplex $d(\text{T,C})_n \cdot d(\text{G,A})_n$ is not replicated at 37°C net synthesis is observed when the temperature is raised. Figure 30 shows the pattern of synthesis at 41°C, as studied by the fluorescence assay, to be similar to that observed with $d(\text{TG})_n \cdot d(\text{CA})_n$ as template. Compared to the rate of synthesis with either $d(\text{TG})_n \cdot d(\text{CA})_n$ or $d(\text{TC}) \cdot d(\text{GA})$ as template, this rate is slow; however, after 6.5 hrs 3 fold net synthesis is observed with 32% CLC DNA formed. Therefore, CLC DNA can be synthesized with $\text{Py}_n \cdot \text{Pu}_n$ DNAs as templates if they are unable to slip and it is not necessary for both strands to contain pyrimidines and purines as earlier surmised.

A possible rationale for this data may be as follows: DNAs that are synthesized via a slippage mechanism do not give rise to CLC sequences. If an impediment to slippage such as a random base sequence is introduced, then net synthesis is dependent upon strand separation which allows the polymerase to switch strands with the subsequent formation of CLC sequences. In the presence of Mg^{++} , the T_M of $d(\text{TG})_n \cdot d(\text{CA})_n$ is less than the melting temperature of $d(\text{TC})_n \cdot d(\text{GA})_n$ (the T_M s are 87.5°C and 94°C respectively 2mM Tris HCl, pH 7.7, 2mM MgCl_2 , 0.2 mM EDTA) and would be expected to undergo strand separation more readily than $d(\text{TC})_n \cdot d(\text{GA})_n$. Since the replication of $d(\text{TG})_n \cdot d(\text{CA})_n$ does not give rise to 100% CLC DNA slippage or some other mechanism not leading to CLC DNA formation must also occur. The synthesis of $d(\text{T,C})_n \cdot d(\text{G,A})_n$ is similar to $d(\text{TG})_n \cdot d(\text{CA})_n$. Since natural DNAs give rise to 100% CLC sequences, then $d(\text{T,C})_n \cdot d(\text{G,A})_n$ may contain some repeating sequences such that the product is not also 100% CLC.

This simple model implies a "competition" between slippage and strand displacement modes of synthesis based on the requirement for strand separation before synthesis. However, other modes of synthesis leading to CLC DNA formation can be accommodated. One of these (Morgan, 1970) predicts that the branched, single-stranded DNA expected in the initial stages of a strand displacement mechanism should not be found.

CHAPTER VI. GLYOXAL AS A PROBE OF NUCLEIC ACID STRUCTURE

The use of glyoxal (ethanedial) as a potential probe of nucleic acid structure has been widely investigated (Shapiro and Hachman, 1966; Broude and Budowsky, 1971). Its advantages include a relative specificity for guanine residues, reactivity over a wide range of pH values and ionic strength conditions, and reversibility of adduct formation by simply raising the pH. Broude and Budowsky (1971) have shown that this reagent could be especially useful in the pH range 5 - 7. The rate of decomposition of the guanine adduct is negligible and products formed with adenine or cytidine amino groups are unstable in this pH range. The structure of the adduct formed with guanine is in doubt. A five-membered ring is formed but the hydroxyls may be positioned either cis or trans (Figure 31). Shapiro et al. (1969) have interpreted the lack of coupling between protons 1 and 2, when the NMR spectrum was determined in D₂O, as evidence in favour of a trans conformation. However, the ultraviolet spectral values reported for the glyoxal-guanine adduct differed from those reported by Shapiro and Hachman (1966) for the glyoxal-guanosine adduct which is not unexpected, but Shapiro and Hachman (1966) do not report an infrared absorption for the hydroxyl protons which should be prominent and the adduct he describes seems less stable at pH 5.0 than expected from the later work of Broude and Budowsky (1971). In contrast, the increased stability of this adduct in the presence of borate buffers at slightly alkaline pH's (Litt, 1969) would argue in favour of a cis conformation (Khym, 1967). Although the data presented here favours the cis conformation, the results do not depend strictly on either of the two possible structures being correct.

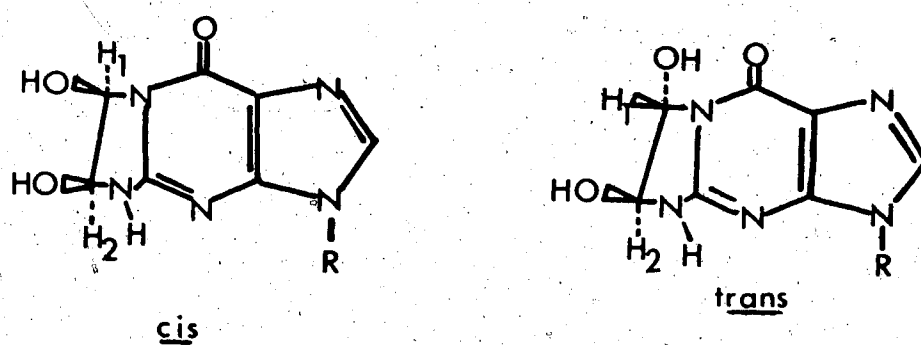


Figure 31 Possible Conformations of Glyoxal-guanosine Adduct

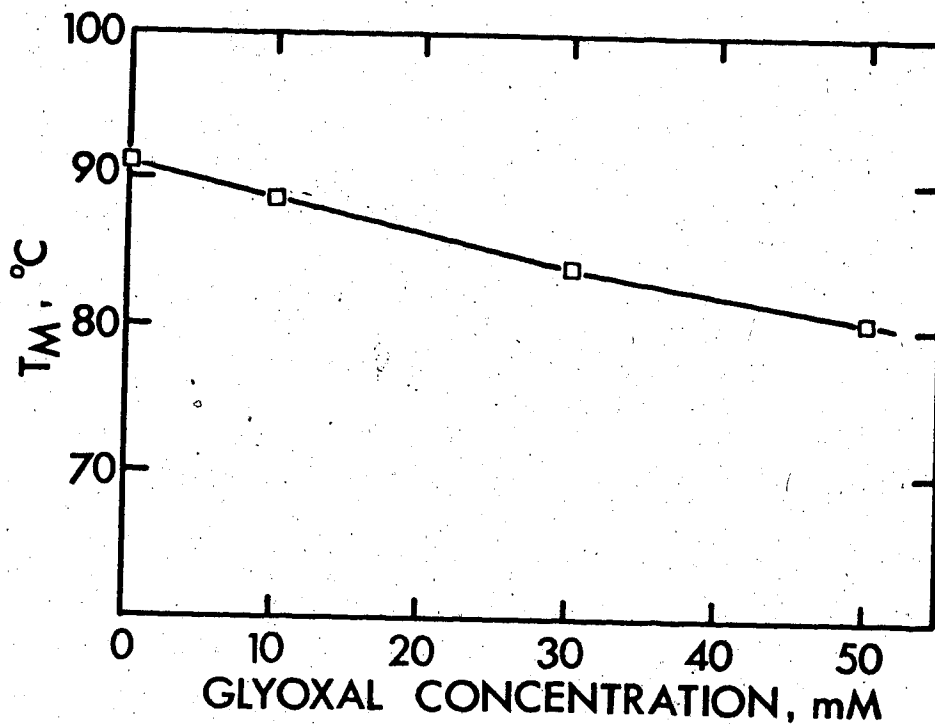


Figure 32 Reaction of *E. coli* DNA With Glyoxal As Measured By The Reduction in T_M

E. coli DNA at $1 A_{260}$ was incubated for 8 days at room temperature with increasing concentrations of glyoxal in 10mM Na acetate pH 5.0, 0.1mM EDTA, 0.2M NaCl. After dialysis against the same buffer to remove excess glyoxal the temperature-absorbance shift was measured.

During the investigation of the $d(\text{TC})_n \cdot d(\text{GA})_n$ multiplex structure, in which glyoxal was used as a probe, some of the reactions of glyoxal with various polymers were studied and techniques developed which may be of general interest.

The reaction of glyoxal with bases, nucleosides or nucleotides can be easily monitored spectrophotometrically (Broude and Budowsky, 1971) since adduct formation causes pronounced shifts in the observed spectra. Reaction with duplex DNA changes a large number of the physical properties of the DNA, such as sedimentation coefficient, buoyant density or melting temperature (see Figure 32) which can be useful in monitoring the extent of reaction. However, the most convenient and sensitive assay method presently available is the ethidium assay described in Materials and Methods. The reaction of glyoxal with λ DNA under a wide variety of conditions is shown in Figure 33 and with PM2 CCC DNA in Figure 34, both measured by the alkaline ethidium assay method.

The reaction with λ DNA points out a number of interesting comparisons. As the temperature is raised from 52°C (Line e) through 55°C (Line a) to 60°C (Line d) the rate of reaction increases, as would be expected. Under these conditions λ DNA is partially denatured but would renature immediately upon addition to the alkaline ethidium mixture. Reaction with glyoxal prevents this renaturation by blocking hydrogen bond formation resulting in the observed fluorescence loss. The increased rate of fluorescence loss as the temperature is raised probably results from both an increased reaction rate for glyoxal addition and the increased rate and extent of local denaturation. Increasing the ionic strength from 0 to 50mM added KCl does not

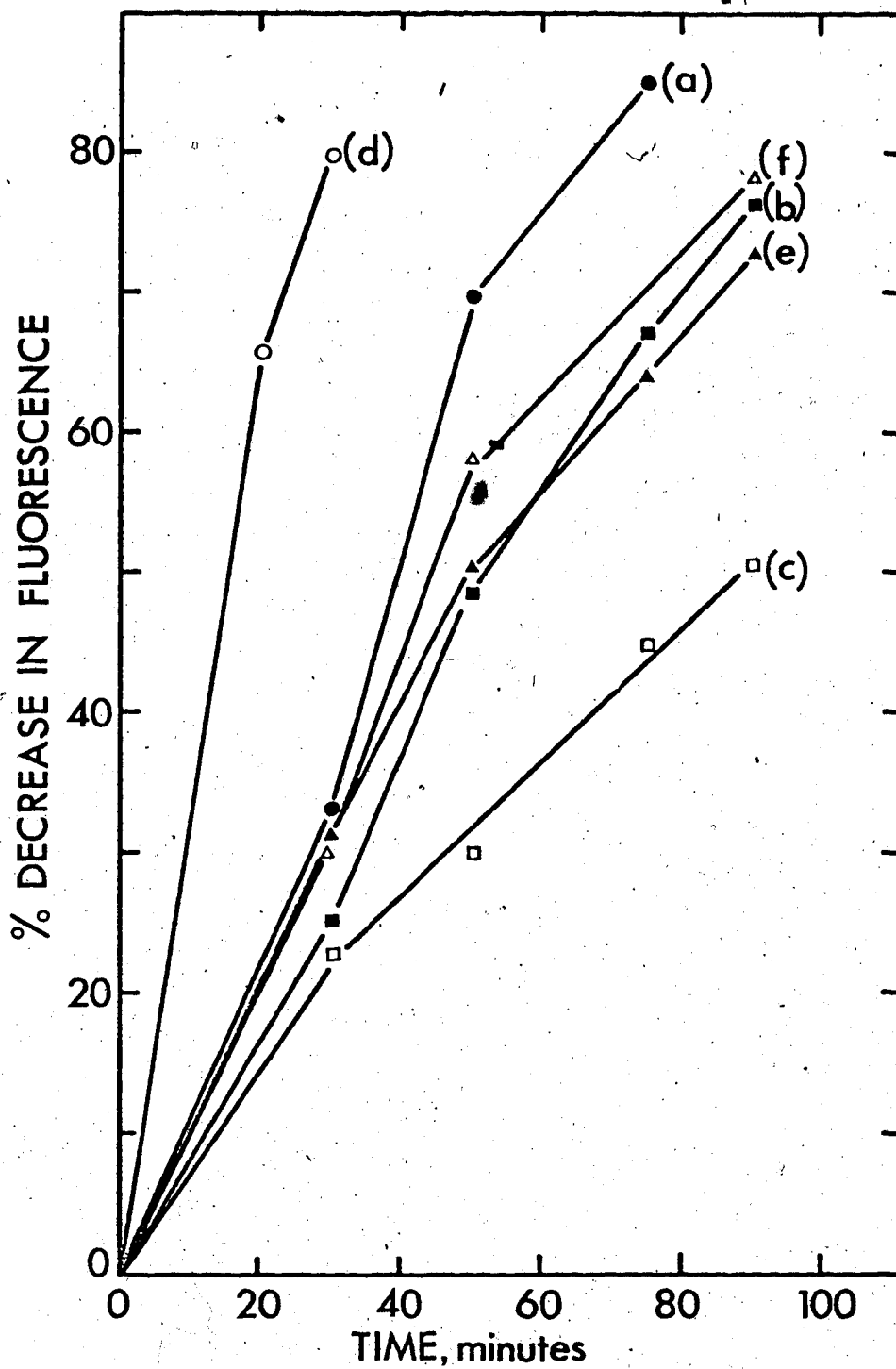


Figure 33 Denaturation of λ DNA as Measured by the Fluorescence Assay
 (a) standard conditions pH 7.5, 55°C. All other experiments as (a) except for the following changes: (b) pH 7.0, (c) pH 6.5, (d) 60°C, (e) 52°C, (f) 52°C plus 50 mM KCl.

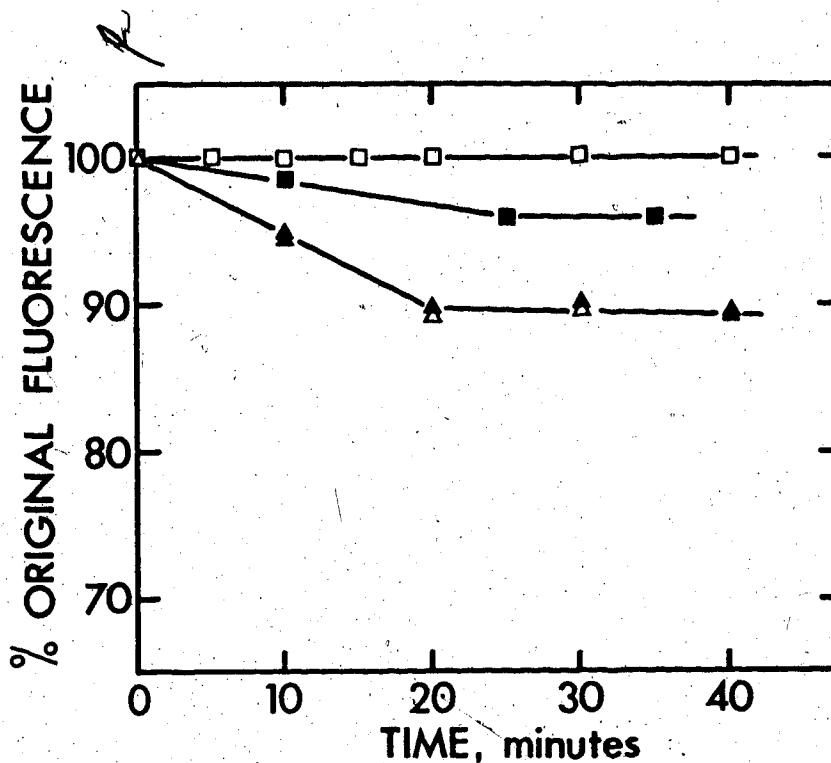


Figure 34 Reaction of Glyoxal With PM2 CCC DNA

The reaction conditions were 10mM potassium phosphate pH 7.5, 1mM EDTA, 50% (v/v) ethanol, ~0.1M glyoxal, 0.9 A₂₆₀ PM2 CCC DNA.

At timed intervals aliquots were removed into the alkaline ethidium mixture and the fluorescence measured.

- △ Reaction at 45°C
- ▲ Reaction at 37°C
- Reaction at 37°C without ethanol
- Reaction at 45°C, after heat

drastically affect the rate of denaturation (Lines e,f). If the pH of the reaction mixture is lowered from 7.5 (Line a) to 6.5 (Lines b,c) the rate of denaturation decreases. The reaction of glyoxal with guanosine is also pH dependent and independent of ionic strength (Broude and Budowsky, 1971). At temperatures less than 45°C denaturation is not observed, although reaction with glyoxal does occur (see section on cross-linking). The reaction of λ DNA with glyoxal has been used in conjunction with the fluorescence assay to develop a new method of DNA denaturation mapping which is discussed in a later section.

In contrast, the reaction with PM2 CCC DNA at 37°C or 45°C, when monitored by the fluorescence assay, shows an initially rapid reaction with cessation of fluorescence loss after about 20 minutes. The omission of the denaturant ethanol from the reaction mixture reduces the extent of fluorescence loss but does not change the type of kinetics observed. In this respect glyoxal is a reagent that acts in a manner similar to formaldehyde or carbodiimide.

The introduction of superhelical turns into a closed circular DNA causes strain in the molecule which can be partially relieved by unwinding the Watson-Crick duplex. A large negative-free energy ($-\Delta G^{\circ}$) is associated with the reaction of any reagent which further unwinds the primary duplex and further relieves this torsional strain. Hence, the initial rate of reaction of formaldehyde or carbodiimide or glyoxal is rapid. If the duplex is locally denatured to an even greater extent, supertwists will be introduced into the molecule and the reaction rate will fall dramatically due to the $+\Delta G^{\circ}$ associated with the introduction of superhelical turns (Bauer and

Vinograd, 1974). Ethidium also unwinds the duplex (unwinding angle is 26° per intercalated ethidium molecule, Wang, 1974b; Pulleyblank and Morgan, 1975).

Therefore, as the reaction with glyoxal proceeds less ethidium can intercalate and the observed fluorescence decreases. Unwinding by glyoxal (due to reaction with glyoxal and local denaturation) in effect mimics the action of ethidium. Controversy exists as to whether the partially unwound primary duplex contains true single-stranded regions (presumably AT rich). Lebowitz *et al.* interpreted the reaction of low concentrations of formaldehyde or methylmercuric hydroxide with CCC DNA (but not the corresponding OC DNA) as evidence in favour of unpaired regions (Dean and Lebowitz, 1971; Beerman and Lebowitz, 1973). Beerman and Lebowitz further suggested that the increase in sedimentation rate observed during the initial binding of these reagents was due to denaturation of hairpin loops (intrastrand hydrogen bonds) formed in the unpaired (i.e. not normal Watson-Crick duplex) regions which allowed the formation of interstrand hydrogen bonds with a resultant increase in the superhelix density resulting in an increased sedimentation coefficient. However, binding of low levels of ethidium also increased the sedimentation coefficient, an effect interpreted as a stiffening of the molecule (Friefelder, 1971). Wang has disputed Lebowitz's evidence (Wang, 1974a) and the initial binding studies of methylmercuric hydroxide to denatured calf thymus DNA upon which it is based. His model predicts a highly twisted DNA with a few disrupted base pairs (much less than the 4% - 7% of the molecule predicted by Lebowitz) which may be susceptible to chemicals, due to the large $-\Delta G^\circ$ of reaction as discussed above, and also susceptible

to the "single-strand" specific endonucleases which he uses as probes. However, the use of such nucleases as probes can be criticized on the grounds that their substrate range is unknown. Since it is not possible to systematically vary the conformation of DNA from a B form duplex to an extended single-stranded chain, one could argue that there are regions in CCC DNA which are unpaired but still not in a conformation favourable for the endonuclease. An intermediate hypothesis can be proposed based largely on the hydrogen-exchange data of Teitelbaum and Englander (1975a and b) which showed that linear duplex DNA has 0.1% - 1.0% of its bases transiently unpaired (i.e. able to exchange tritium for hydrogen) at any one time. They proposed that this number of nucleotides was not a summation of single bases sticking out into solvent (which is entropically unfavourable and also due to loss of stacking interactions has an unfavourable enthalpy) but most likely is divided into a few large regions, in which most of the stacking interactions are maintained. One can then postulate that the bases in a CCC DNA are not unpaired at all (although base pairing must be different with respect to the angles and distances involved) but that as the superhelix density increases the fraction of bases transiently available to solvent increases as does the fraction of time spent unpaired. The reaction rates with various chemicals would then be increased due to more substrate being available and subsequent reaction would be facilitated due to the large $-\Delta G^{\circ}$ of reaction as proposed by Wang (1974a). The ethidium effect could then be rationalized as a stabilization of the duplex at the expense of the open state which would lead to a stiffening of the molecule. Both this model and the model of Wang predict an increased rate of hydrogen exchange as the

superhelix density increases but for different reasons. The model presented here, however, emphasizes the dynamic properties of DNA molecules in solution.

The reversibility of adduct formation is shown by the constant after heat values when the alkaline ethidium buffer is used (if the adduct was not removed during the heat step the after heat fluorescence should decline paralleling the before heat fluorescence decrease). This reversibility at high pH and the comparison of these results to those of Broude and Budowsky (1971) also suggests that the only site of reaction under these conditions is guanine.

Pulleyblank and Morgan (1975) have determined the sense of naturally occurring superhelices and deduced a value for the unwinding angle of intercalated ethidium from studies on the interaction of N-cyclohexyl-N'- β (4-methylmorpholinium) ethyl carbodiimide with PM2 CCC DNA. The procedure is to relax derivatized PM2 by nicking and then after sealing with ligase to dederivatize the CCC DNA formed. The extent of adduct formation is related to the experimentally determined superhelix density from which a value for the ethidium unwinding angle can be determined. A crucial feature is the need for a reversible reagent. Glyoxal reacts with PM2 CCC DNA with kinetics similar to this carbodiimide and adduct formation is reversible as shown by the fluorescence assay. Therefore, it may prove useful as a substitute for the carbodiimide especially since the adduct formed is neutral. The carbodiimide adduct has a positive charge. The additional assumption, namely that the interaction between this adduct and the phosphate backbone is not ordered in some manner (i.e. the entropically favoured unwound conformation exists) so as to introduce errors into the final

values calculated, must be made. For this purpose radioactive glyoxal (presently not available) would be useful.

Denaturation Mapping of λ DNA

Inman, in 1966, was the first to introduce the technique of partial denaturation mapping in order to provide information concerning DNA structure and function. The usual method of mapping involves fixation of sites along the duplex which have been selectively denatured (AT rich regions) by heat or pH with formaldehyde, followed by visualization of the denatured sites by electron microscopy (Inman and Schnös, 1974).

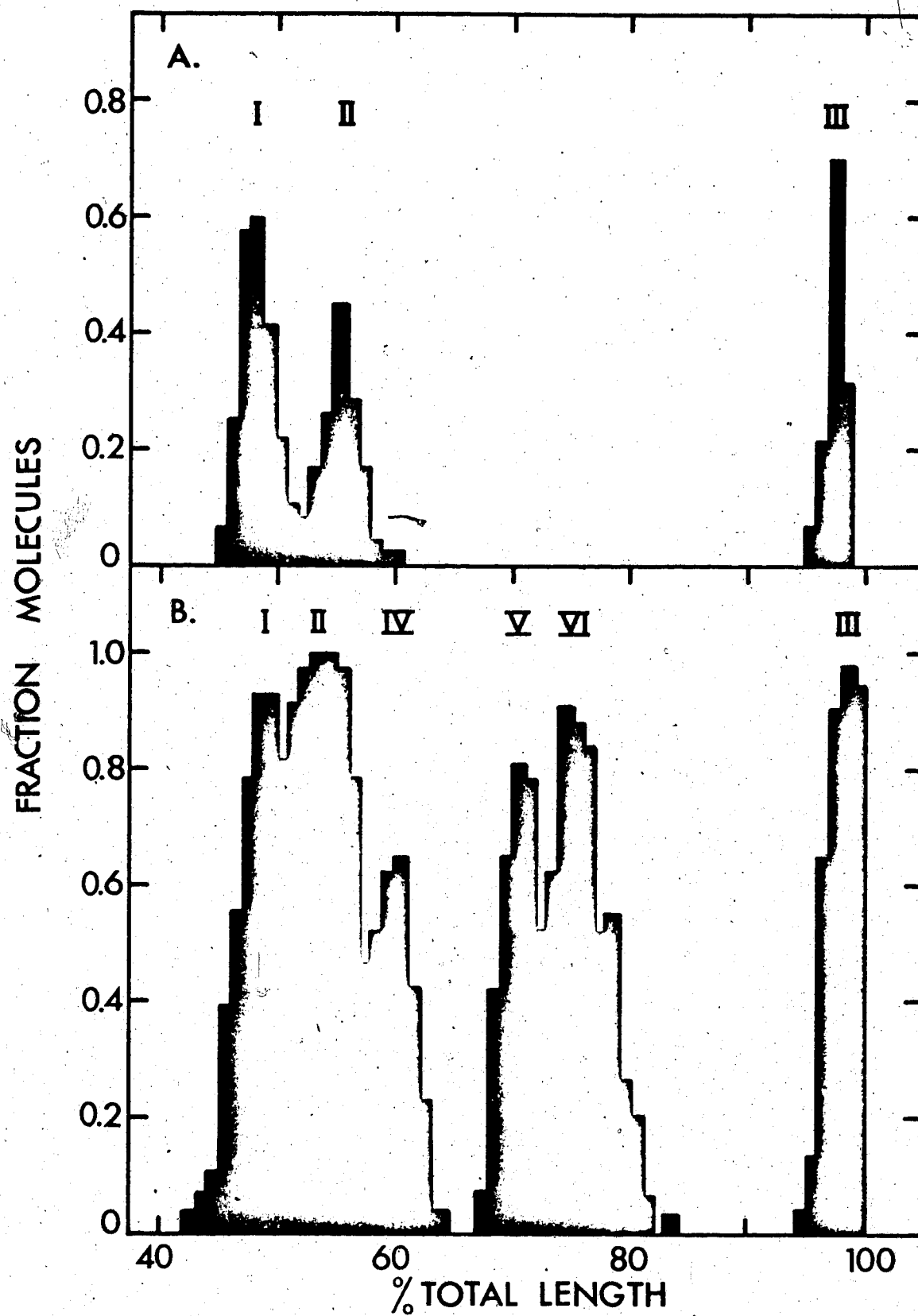
The combination of heat denaturation, fixation with glyoxal and monitoring of the reaction with the ethidium fluorescence assay has been used to produce very good denaturation maps under a wide variety of conditions and also to provide information about the order of the appearance of denatured regions.

Under partial denaturation conditions, glyoxal reacts with deoxyguanosine residues in AT rich regions, preventing renaturation and resulting in a fluorescence loss when the rate of denaturation is measured by the fluorescence assay. As described before for Figure 33, the extent of reaction is pH-dependent, temperature-dependent and independent of the concentration of added KCl up to 0.2M at which concentration DNA precipitation occurs. The main advantage of this technique is that set conditions are not required, only that the reaction proceeds to the same fluorescence loss.

Histograms compiled for λ DNA at 17% loss of fluorescence and 30.5% loss of fluorescence are shown in Figure 35 with a micrograph

Figure 35 Histograms of Partially Denatured λ DNA

Histograms of λ DNA at 17.0% loss of fluorescence (A) and 30.5% loss of fluorescence (B). 41 and 31 molecules respectively were measured.



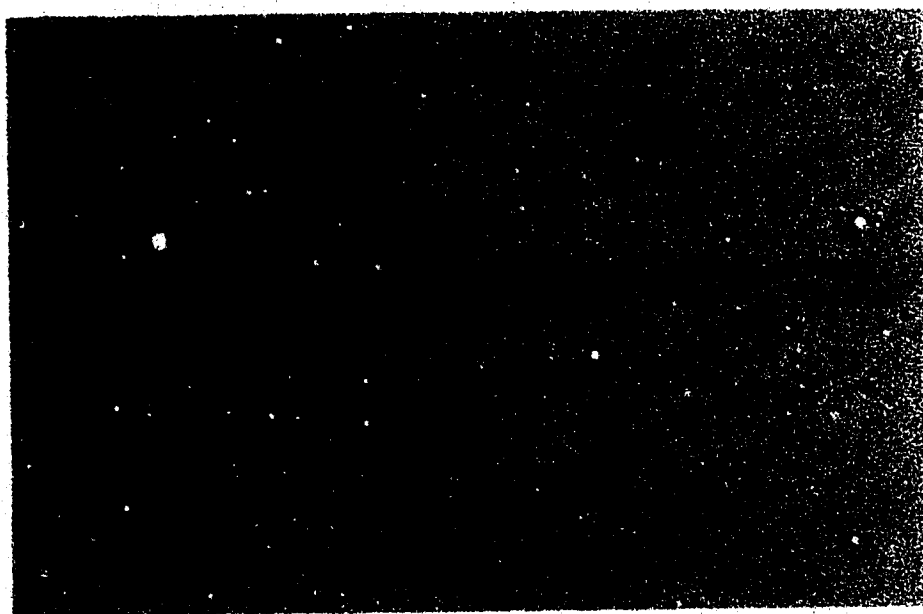


Figure 36 Electron Micrograph of a Representative λ DNA Molecule at 30.5% Loss of Fluorescence


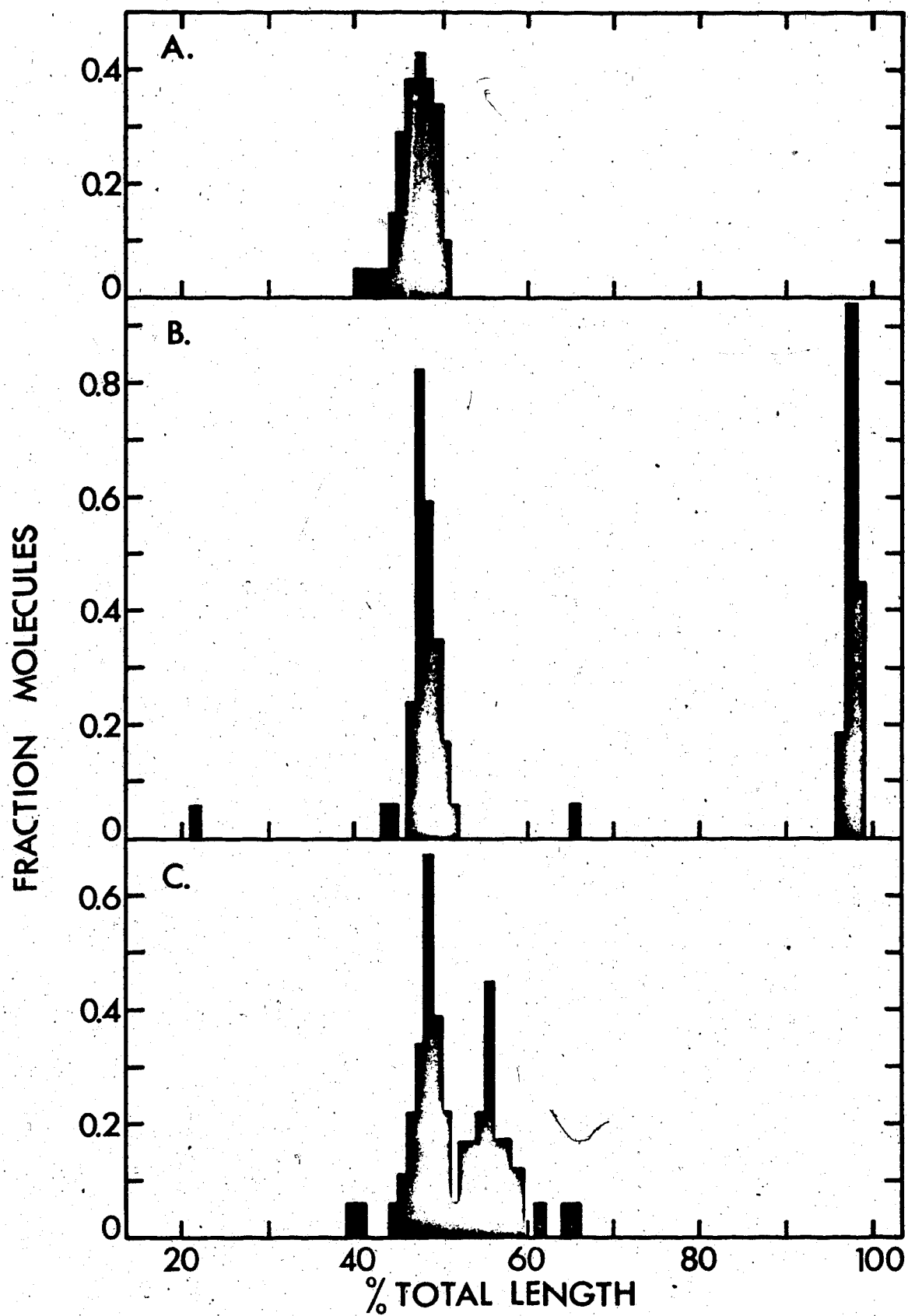


Figure 37 Histograms of Partially Denatured λ DNA

Denaturation was performed as described in Materials and Methods and in text. Histograms were constructed from a preparation of λ DNA with a 15% loss of fluorescence. Only molecules with one or two denaturation loops were mapped. The position of the peak in histogram A. was ascertained from inspection of histograms B. and C. with the assumption that this peak would be observed at a constant position in all three histograms.



of a λ molecule at 30.5% loss of fluorescence shown in Figure 36 . The positions of the peaks correspond exactly to those published before for λ DNA. Schnös and Inman state that "thermal denaturation seems to give rise to a higher background of random denatured sites" when formaldehyde is used (Inman & Schnös, 1974), but this is not observed when glyoxal is used, perhaps due to the relative specificity of the reagent. When two different preparations with the same fluorescence loss are compared, the reproducibility is very good. Peaks II and III of Figure 35 are identically positioned and Peak I has shifted only from the 48.5% to 49.5% length interval. Also, the relative proportions of molecules with bubbles at those positions are similar, which confirms the reproducibility of the fluorescence assay.

It is possible to deduce the order of appearance of the denatured regions by constructing histograms of molecules with only one or two bubbles (Figure 37). If only molecules with one bubble are chosen (Figure 37a), then the first region of denaturation could occur at either Position I or Position II or both. However, histograms of molecules with two bubbles fall into two classes, either I or II together (Figure 37c) or I and III together (Figure 37b). This suggests that Peak I appears first, then II and III with about equal probability and then as denaturation proceeds to 30.5% loss of fluorescence Peaks I and II coalesce, III denatures to the end of the molecule producing a Y branch and Peaks IV, V and VI appear.

The reaction of glyoxal with λ DNA does not produce any gross length distortion, the average length of these molecules being 14.8 μ which is equivalent to the length of renatured λ homoduplexes spread under these conditions (Dr. D.G. Scraba, personal communication).

One note of caution is that glyoxal reacts with ethidium in the assay mixture to produce a fluorescent compound. However, by using a standard concentration of glyoxal (0.1M) the fluorescence mixture becomes 0.05mM in glyoxal and at this concentration and at room temperature the interference is negligible for up to 15 minutes. Formaldehyde reacts within 15 seconds. Since normally the concentration of formaldehyde used is 10%(w/v) (33x the concentration of glyoxal used), this interference makes use of the fluorescence assay difficult.

This technique has two other potential applications. Since the denaturation and glyoxal reaction is performed at neutral pH, it should be possible to partially denature double-stranded RNA molecules for mapping by this technique. Secondly, both single-strand RNA and DNA have ordered secondary structures in benign solution due to intramolecular hydrogen bonding. The fluorescence of these regions can be observed if an ethidium assay mixture containing 5mM Tris HCl pH 8.0, 0.5mM EDTA, 0.5µg/ml ethidium bromide is employed. Heat treatment combined with glyoxal reaction can be used to systematically remove these regions, analogously to denaturation, and this reaction can be monitored with the ethidium assay.

Cross-linking of DNA by Glyoxal

Glyoxal was found to cross-link DNA under conditions similar to those used for denaturation but at lower temperatures such that before heat losses of fluorescence were not observed. Cross-linking was monitored using the alkaline ethidium fluorescence assay (see Materials and Methods for a description of this assay). (Appendix I describes experiments in which the alkylation and cross-linking of mitomycin C

and chemically synthesized analogues of mitomycin C are studied using, in part, this assay system). Figure 38 shows the cross-linking of λ DNA at 45°C. Once introduced, this cross-link is not removable by dialysis against 0.1N NaOH at room temperature, although the glyoxal-guanosine adduct shown in Figure 31 decomposes readily under these conditions. This situation is reminiscent of the reaction of formaldehyde with DNA, in that under conditions in which most of the monoadduct is removed, some remains permanently bound (Grossman, 1968).

PM2 superhelical DNA can also be cross-linked with glyoxal. Since normally PM2 CCC DNA gives 100% return of fluorescence, the introduction of a cross-link must be shown indirectly, by making use of the fact that exposure of DNA in the alkaline ethidium mixture to light causes nicking of the molecule by a free radical mechanism (Dennis and Morgan, 1976). If a supertwisted molecule is nicked, then heat denatured at pH 11.7, the fluorescence falls to 0. However, if cross-linked the introduction of a single nick leaves a nucleus for renaturation and there will be a complete return of fluorescence.

As the length of exposure to light increases, repeated cleavage of the phosphodiester backbone leads to a loss of duplex regions after the heat step, with subsequent loss of fluorescence. As more cross-links are introduced the length of exposure to light necessary to cause cleavages between the cross-links, and loss of the single strands upon heat denaturation, increases. Thus the extent of cross-linking can be related to a decreased rate of after heat loss of fluorescence as increased cross-linking protects against loss of duplex structure. One example is shown in Figure 39 which shows a small but detectable amount of cross-linking.

Figure 38 Cross-linking of λ DNA With Glyoxal

λ DNA at 1 A_{260} was incubated at 45°C with 0.05M glyoxal, as described in Materials and Methods and cross-linking measured using the alkaline ethidium mixture.

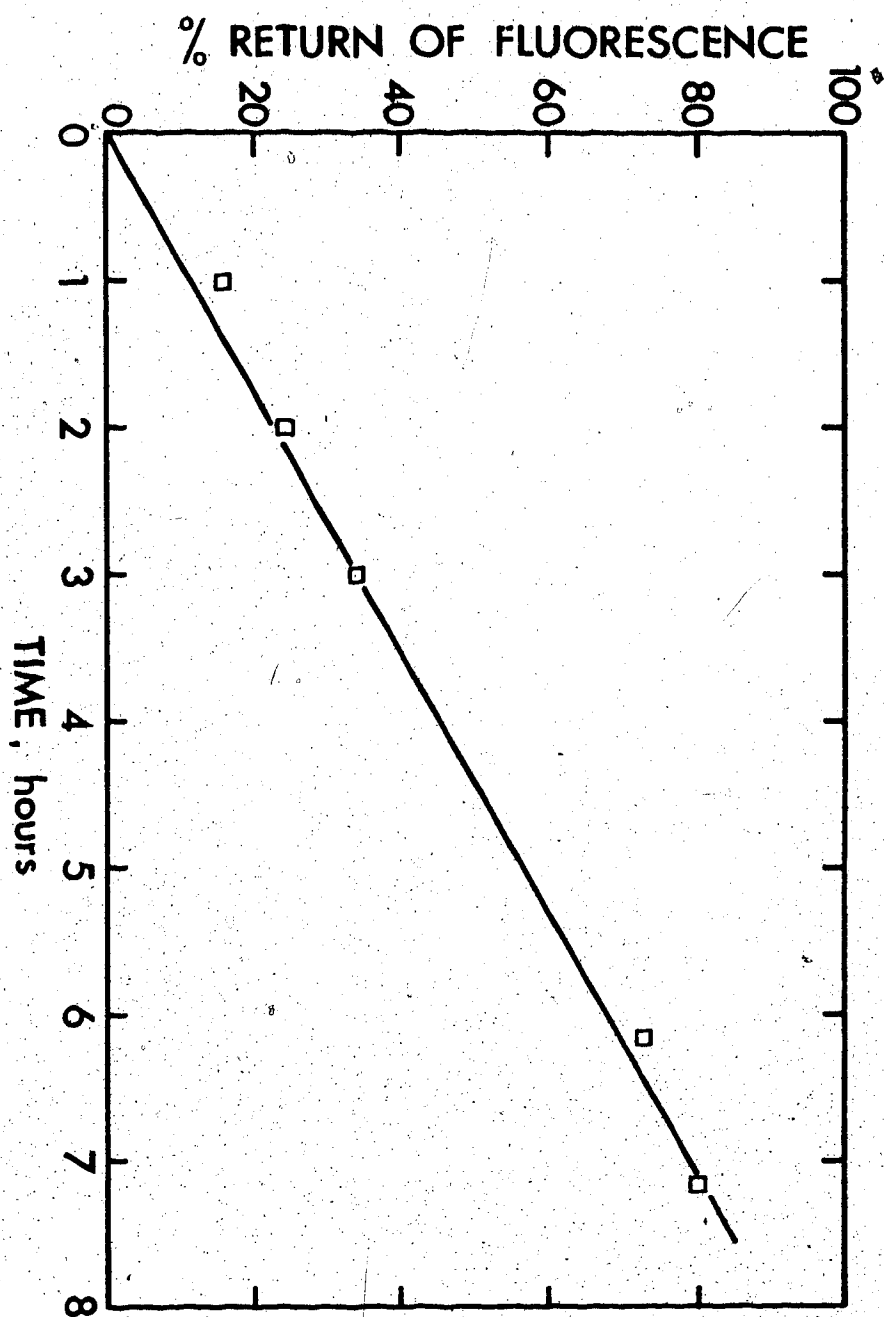


Figure 39 Cross-linking of PM2 DNA With Glyoxal

DNA samples were pipetted into the alkaline ethidium buffer and exposed to light for various times at room temperature. The after heat fluorescence values were read and normalized with the zero time exposure equivalent to 100%.

A. Standard DNAs (o) PM2 CCC DNA

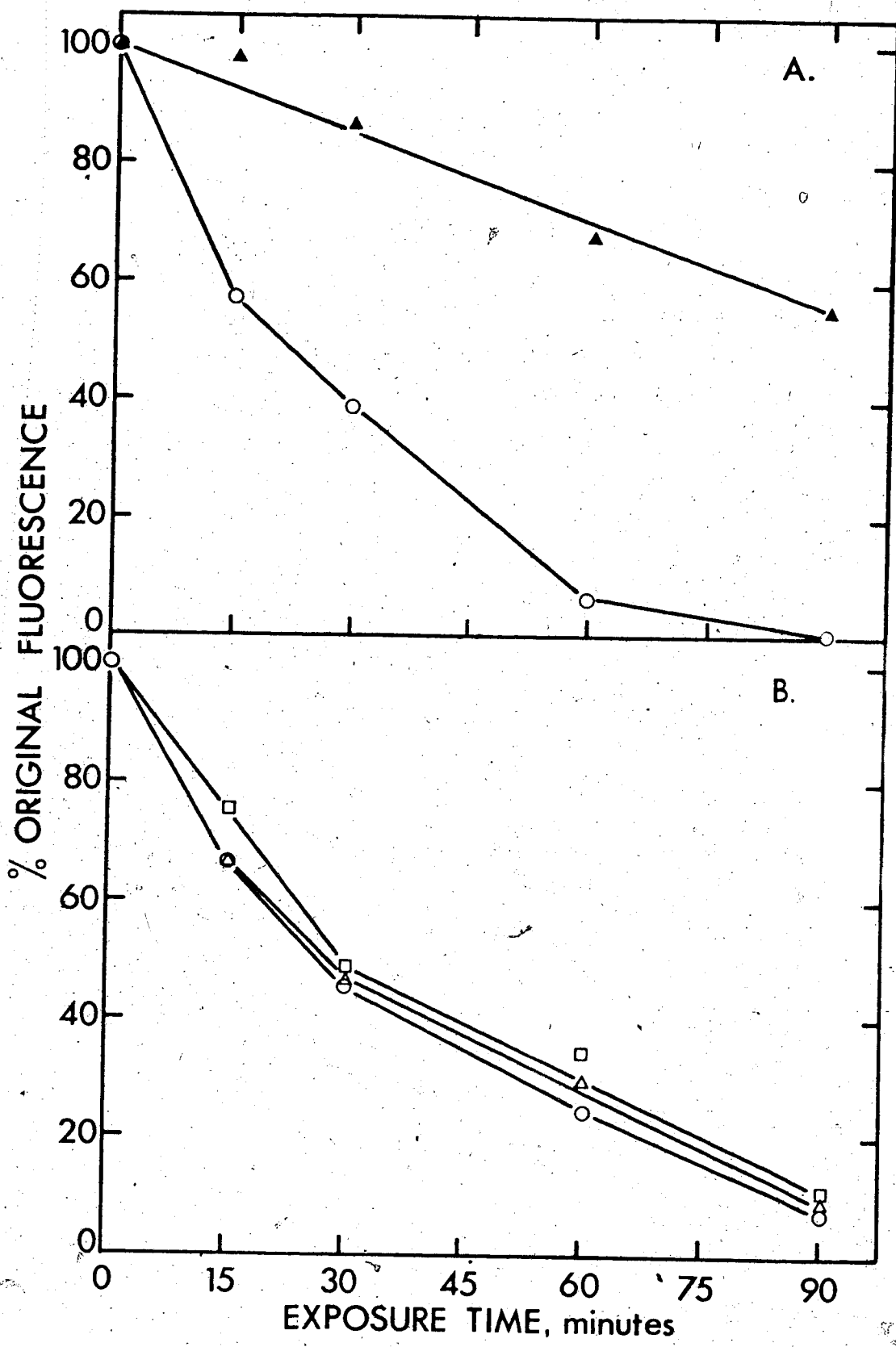
(Δ) λ DNA cross-linked with glyoxal as per Figure 38 to the extent of 33%.

B. PM2 CCC DNA was reacted with 50mM glyoxal at 37°C and aliquots were removed into the alkaline ethidium buffer at various times for exposure to light. Reaction with glyoxal for

(o) 0 minutes

(Δ) 30 minutes

(□) 60 minutes



Although glyoxal can be shown to cross-link DNA, the chemistry of the cross-link has not been investigated. However, these may be analogous to the bis methylene structures found with formaldehyde (Feldman, 1967).

The Separation of $d(AT)_n$ from $Py_n \cdot Pu_n$ DNAs

During the replication of synthetic DNAs with E. coli DNA polymerase I, the alternating copolymer $d(AT)_n$ can arise de novo, sequester the polymerizing system and essentially replace the original template due to its high affinity for DNA polymerase. These DNAs become unusable as further templates due to the $d(AT)_n$ contamination. A technique has been developed which removes this contaminant by combining the properties of glyoxal reaction with hydroxyapatite chromatography:

The rationale for this procedure is as follows: complete reaction of a $Py_n \cdot Pu_n$ DNA and $d(AT)_n$ with glyoxal modifies the a, c and g residues. Since the a and c adducts are unstable, then dilution of the reaction mixture results in renaturation of $d(AT)_n$ but not the $Py_n \cdot Pu_n$ DNA since modification of g residues prevent this renaturation. Hydroxyapatite chromatography is used to separate single-stranded DNA from double-stranded $d(AT)_n$ by a batch-wise procedure. Removal of the glyoxal adduct at pH 12 at a suitable ionic strength allows renaturation of the Py_n and Pu_n strands free of $d(AT)_n$.

Results of separations of $d(AT)_n$ from $d(TC)_n \cdot d(GA)_n$, $d(TTC)_n \cdot d(GAA)_n$ and $d(TCC)_n \cdot d(GGA)_n$ are summarized in Table 8. Recoveries of the $Py_n \cdot Pu_n$ DNA are between 38% and 55%, with the recovery dropping as the G+C content increases, which may reflect difficulties in removing

$\text{Py}_n \cdot \text{Pu}_n$ DNA	% d(AT)_n^1	% Recovery	T_M of Product ²
$\text{d(TC)}_n \cdot \text{d(GA)}_n$	24	46	67.0
$\text{d(TTC)}_n \cdot \text{d(GAA)}_n$	29	56	58.0
$\text{d(TCC)}_n \cdot \text{d(GGA)}_n$	22	38	69.0

TABLE 8 Separation of d(AT)_n From $\text{Py}_n \cdot \text{Pu}_n$ DNAs

1. as determined by the neutral ethidium fluorescence assay.
2. determined in SSC/10.

the glyoxal adduct. No $d(AT)_n$ is present. This can be shown by the fluorescence assay, the lack of a hyperchromic shift at the appropriate temperature when the melting temperature is determined or the lack of $d(AT)_n$ synthesis when the isolated $(Py)_n \cdot (Pu)_n$ DNA is used as a template for DNA polymerase. The recovered polymers show the expected buoyant density shift when incubated at low pH (multiplex formation) but have melting temperatures $1C^{\circ} - 2C^{\circ}$ lower than expected. This may be due to imperfections in the helix if not all the glyoxal was removed (but not enough adduct remaining to interfere with synthesis) or due to the lowered molecular weight of the material after glyoxal treatment. This treatment does lower the sedimentation coefficient of T7 DNA under alkaline conditions and mixes PM2 DNA as shown by the fluorescence assay.

Generally, this procedure has been most useful for the removal of small amounts of $d(AT)_n$ before many-fold replication of the appropriate synthetic DNA.

The Separation of the Strands of $d(TC)_n \cdot d(GA)_n$

The separation of $d(TC)_n$ from $d(GA)_n$ by alkaline buoyant density gradients is not possible since the two strands have similar buoyant densities. In order to obtain purified single strands for physical studies, indirect procedures must be adopted such as the derivitization of one or both strands, separation of the derivitized strands by some physical technique and subsequent dederivatization.

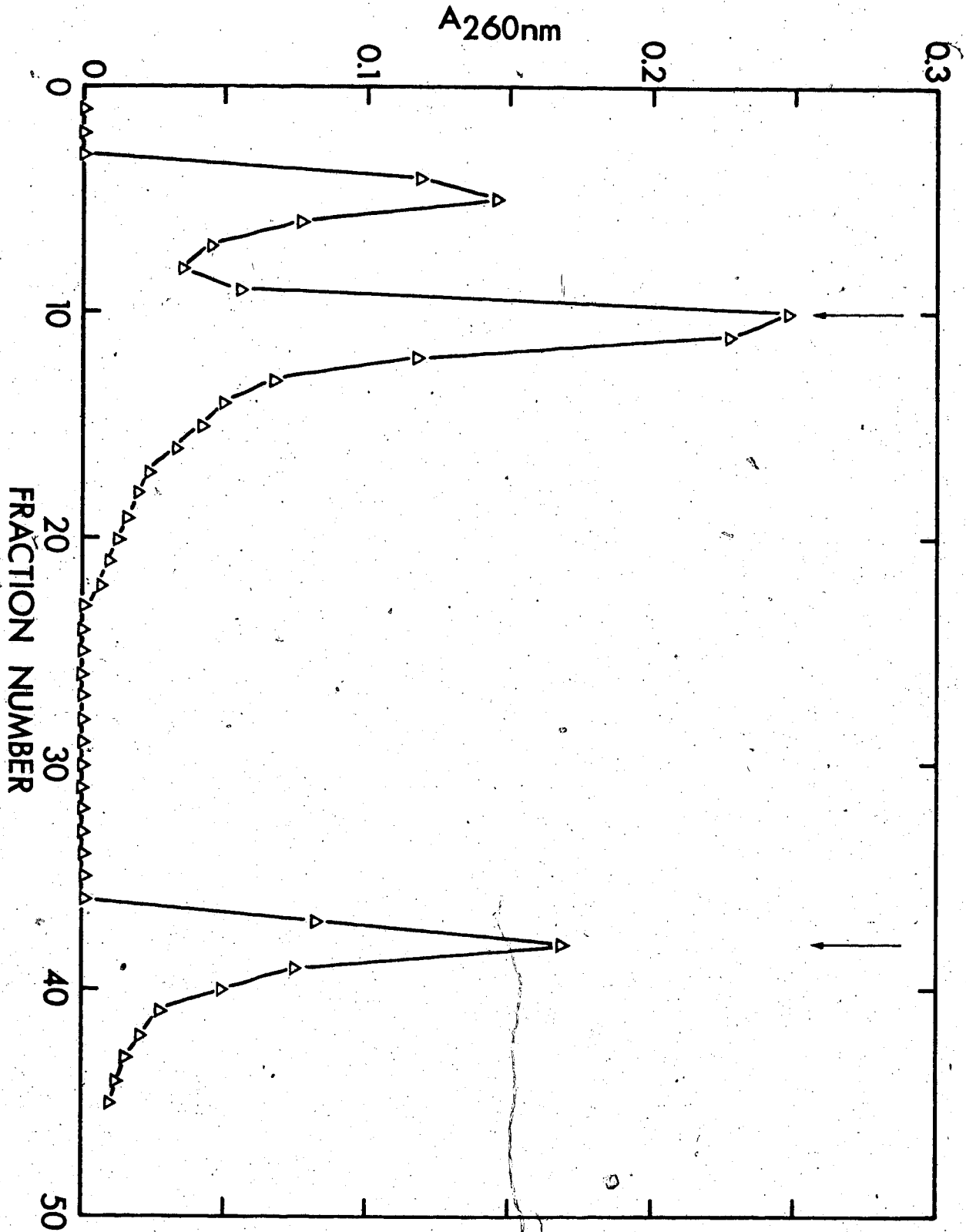
The carbodiimide, N-cyclohexyl-N'- β -(4-methylmorpholinium)ethyl carbodiimide p-toluenesulfonate, has been used in combination with CsCl equilibrium centrifugation to separate $d(TC)_n$ and $d(GA)_n$ (Coulter et al.,

1974). Complete derivatization with glyoxal followed by chromatography on DEAE cellulose in the presence of borate buffer allows the isolation of material that is of lowered molecular weight, and that could not be isolated by any buoyant density technique due to band broadening.

Borate ion binds specifically to cis diols and this binding has been utilized to purify tRNA molecules on borate columns (Schott *et al.*, 1973). Since borate is known to stabilize the glyoxal-guanine adduct (Litt, 1969), we would expect that derivatized $d(GA)_n$ would be retarded by DEAE cellulose to a greater extent than $d(TC)_n$ when chromatographed in the presence of borate buffer due to the increased negative charge. The separation of $d(TC)_n$ and $d(GA)_n$ using this procedure is shown in Figure 40. Peak I is unreacted glyoxal and other reaction byproducts. $d(TC)_n$ is eluted with a NaCl gradient in 50mM Tris borate pH 8.3, being recovered at 0.45M NaCl. The binding of $d(GA)_n$ is so strong that salt concentrations up to 2.0M do not wash off this polymer (as long as the adduct is stable) and $d(GA)_n$ is not recovered until the pH is raised, in this case to pH 9.4 in the presence of 0.5M NaCl. The tight binding of derivatized $d(GA)_n$ to DEAE cellulose in the presence of borate is evidence that favours the presence of a cis diol. The separated strands were identified by spectra, by the ability of $d(TC)_n$ to act as a template for $r(GA)_n$ synthesis with *E. coli* RNA polymerase and by monitoring the separation of 3H and ^{14}C cpm when the polymer $d(TC)_n(^3HC)d(GA)_n(^{14}CA)$ was subjected to this treatment. Recoveries were variable, with the best results being 41% recovery of the dGA strand and 38% recovery of the dTC strand. As occurred with the separation of $d(AT)_n$ from $Py_n \cdot Pu_n$ DNAs dialysis of single-stranded materials resulted in large losses as did irreversible

Figure 40 Separation of $d(TC)_n$ and $d(GA)_n$ By the Glyoxal/Borate Method

Glyoxal derivatized $d(TC)_n \cdot d(GA)_n$ (as in Materials and Methods) was chromatographed over DEAE cellulose in 50mM Tris borate pH 8.3. $d(TC)_n$ (fraction 11) was eluted with a NaCl gradient in Tris borate, at 0.45M NaCl. $d(GA)_n$ (fraction 38) was eluted with 0.5M NaCl, 1mM NaOH at pH 9.4. The first peak is unreacted glyoxal.



absorption of material to the DEAE cellulose column. This method should also be applicable to other $\text{Py}_n \cdot \text{Pu}_n$ DNAs. (See Materials and Methods).

In summary, glyoxal can be a useful reagent for the study of nucleic acid structure and in the preparative procedures described. Its interaction with polymers can be easily monitored by the various fluorescence procedures described and these should be extendable to a wide variety of other chemical reagents. The preparation of radiolabelled glyoxal (preferably ^{14}C since an aldehydic proton would be expected to exchange with solvent) would greatly facilitate quantitation of these reactions and also serve to standardize the fluorescence assay.

CHAPTER VII DISCUSSION

A series of chemical and physical approaches along with model building studies have been used to try to determine the structure of the $\text{Py}_n \cdot \text{Pu}_n$ multiplexes. The most reasonable hypothesis is that these are ordered structures containing base tetrads (tetraplexes).

Two implicit assumptions upon which this work is based are, firstly, that there is a common structural basis for all these rearranged DNAs and, secondly, that only isomorphous structures are involved. In light of the data presented, the first assumption seems quite reasonable. All the repeating $\text{Py}_n \cdot \text{Pu}_n$ DNAs (except $\text{d}(\text{T})_n \cdot \text{d}(\text{A})_n$) show a loss of fluorescence, increase in T_M and increase in buoyant density in Cs_2SO_4 when the pH is lowered and reassume the properties of the original duplex when the pH is subsequently raised to neutrality. The second assumption, while intellectually satisfying, has not been proven necessary for the construction of ordered polymer structure. However, every duplex structure proposed (derived from fibre diffraction studies and from other physical techniques) has incorporated this concept into its model. An interesting case is the structure of poly-2-thiouridylate (Mazumdar *et al.*, 1974) in which the two polymer chains are not equivalent but even in this case all residues in a given chain are isomorphous, as is the basic repeating unit, the base pair.

In order to postulate *in vivo* roles for these structures an additional assumption, that one of the bases (cytosine) can remain protonated at about neutral pH, is necessary. In light of the results of Morgan and Wells (1968) for $\text{d}(\text{TC})_n \cdot \text{d}(\text{GA})_n \cdot \text{r}(\text{UC}^+)_n$ which forms at pH 7.3 this assumption seems reasonable. A restriction on possible

in vivo roles is the requirement that the Watson-Crick purine strand and Hoogsteen pyrimidine strand be parallel, both anti-parallel to the Watson-Crick pyrimidine strand. This would make a role in, for example, recombination unlikely. However, an involvement (permanently or transiently) in DNA folding is possible.

Analysis of $Py_n \cdot Pu_n$ DNAs in *Drosophila* (Sederoff et al., 1975) shows repeats to be spaced at intervals throughout the genome, most likely with polypyrimidines in the same strand. In mouse DNA (H.C. Birnboim, unpublished) these are at intervals of about 2500 base pairs and inverted i.e. polypyrimidines alternate between the two DNA strands. During folding of *Drosophila* DNA a rotation of 180° about the helix axis is necessary to orient the $Py_n \cdot Pu_n$ stretches properly resulting in a U-shaped structure (Figure 41a). However, the folding of mouse DNA would result in a looped structure (Figure 41b). While the reduction in DNA length (packing ratio) for the first case is 2:1 for the second case it is closer to 3:1 (note that this type of folding now defines the polarity of the second purine strand i.e. antiparallel to the Watson-Crick purine strand).

In summary the $Py_n \cdot Pu_n$ DNAs which we have studied (except $d(T)_n \cdot d(A)_n$) form tetraplexes with the bases involved in both Watson-Crick and Hoogsteen hydrogen bonding (Figure 8). Additionally if these structures are formed by the coalescence of two duplexes then the Hoogsteen pyrimidine strand is parallel to the Watson-Crick purine and the second purine strand must be antiparallel to the Watson-Crick purine strand.

The conditions necessary for this rearrangement are a lowered pH and the presence of monovalent or divalent cations (Figure 15). When any of the $Py_n \cdot Pu_n$ DNAs which we have used are incubated under these

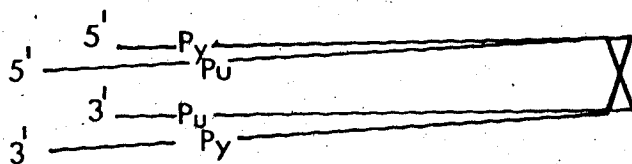
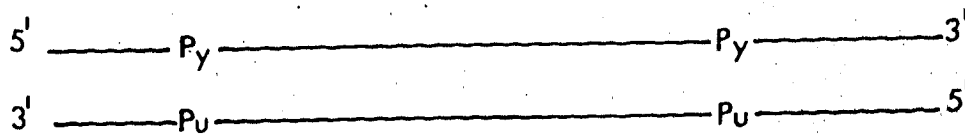
conditions the ability of ethidium bromide to intercalate between the bases is lost (Figure 15), the buoyant density in Cs_2SO_4 increases (Figure 16) and the measured T_M increases dramatically (Figure 17). Experiments with $\text{Py}_n \cdot \text{Pu}_n$ DNAs labelled differentially in the pyrimidine and purine strands (Figure 21) demonstrate that the structure formed contains all the material originally present at neutral pH. Thus a unique structure with physical properties different from the initial duplex is formed. The similarity amongst the changes observed for a variety of these DNAs suggests a common structural basis for all the multiplexes.

In order to investigate the structural basis for the multiplex, we have proposed various models and then tried to differentiate between them experimentally. Using this approach we were able to eliminate models which proposed the formation of Hoogsteen duplexes or the formation of triplexes or a simple conformational change. Essential to these interpretations was observation of the reactions of the site-specific reagents formaldehyde, glyoxal and dimethyl sulfate.

By the process of elimination the tetraplex model is the most likely. Two types of tetraplex are possible (Figures 7 and 8). The crucial feature which differentiates between them is the presence of a protonated cytosine in the tetraplex involving Hoogsteen hydrogen bonding (Figure 8). Protonation to the extent predicted by the model has been confirmed experimentally; however, numerous other observations also suggested that the multiplex was protonated, i.e. the need for the lowered pH, the requirement for G-C base pairs, the fact that only $\text{Py}_n \cdot \text{Pu}_n$ DNAs formed multiplexes.

An X-ray fibre diffraction study is in progress in order to confirm our hypothesis. If validated these structures become the first experimentally characterized tetraplexes.

A.



B.

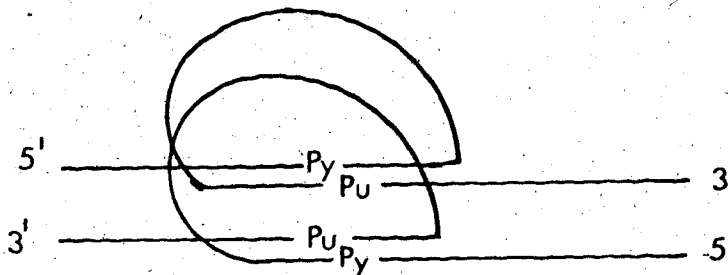
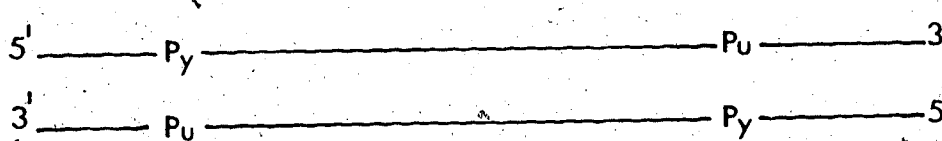


Figure 41 Schematic Representation of DNA Folding

For a discussion of the figures see text. Py and Pu refer to repeating sequences such as the one discussed by Sederoff *et al.*, 1975. A. Drosophila DNA B. Mouse DNA

BIBLIOGRAPHY

- Arnott, S. (1970) in Prog. Biophys. Mol. Biol. 21, 265-319.
- Arnott, S. (1975) Nucl. Acid Res. 2, 1493-1502.
- Arnott, S. and Bond, P.J. (1973) Nat. New Biol. 244, 99-101:
- Arnott, S., Chandrasekaran, R. and Martilla, C. (1974a) Biochem. J. 141, 537-543.
- Arnott, S., Chandrasekaran, R., Hukins, D.W.L., Smith, P.J.C. and Watts, L. (1974b) J. Mol. Biol. 88, 523-533.
- Arnott, S. and Hukins, D.W.L. (1973) *ibid* 81, 93-105.
- Arnott, S., Hukins, D.W.L., Dover, S.D., Fuller, W. and Hodgson, A.R. (1973) *ibid* 81, 107-122.
- Arnott, S. and Selsing, E. (1974a) *ibid* 88, 509-521.
- Arnott, S. and Selsing, E. (1974b) *ibid* 88, 551-552.
- Arnott, S. and Selsing, E. (1975) *ibid* 98, 265-269.
- Baril, B.B. and Kubinski, H. (1975) Nature 255, 252-253.
- Bauer, W. and Vinograd, J. (1974) in Basic Principles in Nucleic Acid Chemistry II, pp. 265-303, Academic Press.
- Beerman, T.A. and Lebowitz, J. (1973) J. Mol. Biol. 79, 451-470.
- Birnboim, H.C. and Straus, N.A. (1975) Can. J. Biochem. 53, 640-643.
- Biro, P.A., Carr-Brown, A., Southern, E.M. and Walker, P.M.B. (1975) J. Mol. Biol. 94, 71-86.
- Bram, S. (1971) *ibid* 58, 277-288.
- Britten, R.J. and Davidson, E.H. (1969) Science 165, 349-357.
- Broude, N.E. and Budowsky, R.I. (1971) Biochem. Biophys. Acta 254, 380-388.
- Burd, J.F., Larsen, J.E. and Wells, R.D. (1975a) J. Biol. Chem. 250, 6002-6007.
- Burd, J.F., Wartell, R.M., Dodgson, J.B. and Wells, R.D. (1975b) *ibid* 250, 5109-5113.

- Burgess, R.R. (1969) *ibid* 244, 6160-6167.
- Chamberlin, M.J. (1965) *Fed. Proc.* 24, 1446-1457.
- Champoux, J.J. and Hogness, D.S. (1972) *J. Mol. Biol.* 71, 383-405.
- Chan, H.W. and Wells, R.D. (1974) *Nature* 252, 205-209.
- Chervenka, C.H. (1969) *A Manual of Methods for the Analytical Ultracentrifuge*, Palo Alto, Calif., Spinco Division, Beckman Instruments, Inc.
- Clark, R.J. and Felsenfeld, G. (1972) *Nat. New Biol.* 240, 226-229.
- Coulter, M., Flintoff, W., Paetkau, V., Pulleyblank, D. and Morgan, A.R. (1974) *Biochem.* 13, 1603-1609.
- Crick, F.H.C. (1971) *Nature* 234, 25-27.
- Crick, F.H.C. and Watson, J.D. (1954) *Proc. Roy. Soc. London, A*, 223, 80-96.
- Davis, R.W., Simon, M. and Davidson, N. (1971) in *Methods In Enzymology* XXI D, 413-428.
- Dean, W.W. and Lebowitz, J. (1971) *Nat. New Biol.* 5, 231-238.
- DeClercq, E., Terrence, P.E. DeSomer, P. and Witkop, B. (1975) *J. Biol. Chem.* 250, 2521-2531.
- Denniss, I. and Morgan, A.R. (1976) *Nucl. Acid Res.* 3, 315-323.
- Dhar, R., Weissman, S.M., Zain, B.S., Dan, J. and Lewis, A.M. (1974) *ibid* 1, 595-613.
- Dickson, R.C., Abelson, J., Barnes, W.M. and Reznikoff, W.F. (1975) *Science* 187, 27-35.
- Feldman, M.J. (1967) *Biochem. Biophys. Acta* 149, 20-33.
- Felsenfeld, G. and Miles, H.T. (1967) *Ann. Rev. Biochem.* 36, 407-448.
- Freifelder, D. (1971) *L. Mol. Biol.* 60, 401-403.
- Gall, J.G. and Atherton, D.D. (1974) *ibid* 85, 633-664.
- Gierer, A. (1966) *Nature* 212, 1480-1481.

- Gill, J.E., Mazrimas, J.A. and Bishop, C.C. (1974) *Biochem. Biophys. Acta* 335, 330-348.
- Gray, D.M. and Bollum, F.J. (1974) *Biopolymers* 13, 2087-2102.
- Gray, H.B. Upholt, W.B. and Vinograd, J. (1971) *J. Mol. Biol.* 62, 1-19.
- Griffen, B.E. and Fese, C.B. (1962) *Biochem. J.* 68, 185-192.
- Grossman, L. (1968) in *Methods In Enzymology XII B*, 467-486.
- Guild, W.R. (1968) *Cold Spr. Harb. Symp. Quant. Biol.* 33, 142-143.
- Haas, B.L., Sarocchi, M. Th. and Guschlbauer, W. (1976) *Nucl. Acid Res.* 3, 1549-1559.
- Hattori, M., Frazier, J. and Miles, H.T. (1976) *Biopolymers* 15, 523-531.
- Heijneker, H.L., Ellens, D.J., Tjeerde, R.H., Glickman, B.W., vanDorp, B. and Pouwels, P.H. (1973) *Molec. gen. Genet.* 124, 83-96.
- Hoogsteen, K. (1959) *Acta Crystallogr.* 12, 822-823.
- Howard, B.H., Frazier, J. and Miles, H.T. (1971) *J. Biol. Chem.* 246, 7073-7086.
- Howard, B.H., Frazier, J. and Miles, H.T. (1974) *ibid* 249, 2987-2990.
- Inman, R. (1966) *J. Mol. Biol.* 18, 464-476.
- Inman, R. (1967) *ibid* 28, 103-116.
- Inman, R. and Schnoss, M. (1974) in *Principles and Techniques of Electron Microscopy*, Vol. 4, pp. 64-86, Van Nostrand Reinhold, New York.
- Job, P. (1928) *Anal. Chim. Acta* 9, 113.
- Jovin, T.J., Englund, P.T. and Bertsch, L.L. (1969) *J. Biol. Chem.* 244, 2996-3007.
- Khym, J.X. (1967) in *Methods In Enzymology XII A*, 93-101.
- Kornberg, A. (1974) *DNA Synthesis*, W.H. Freeman and Co., San Francisco.
- Kubinski, H., Opara-Kubinska, Z. and Szybalski, W. (1966) *J. Mol. Biol.* 20, 313-329.

- Ladner, J.E., Jack, A., Robertus, J.D., Brown, R.S., Rhodes, D., Clark, B.F.C. and Klug, A. (1975) Proc. Nat. Acad. Sci. (USA) 72, 4414-4418.
- Langridge, R. (1969) J. Cell Physiol. 74, Supplement 1, 1-20.
- LePecq, J.B. and Paoletti, C. (1967) J. Mol. Biol. 27, 87-106.
- Litt, M. (1969) Biochem. 8, 3249-3253.
- Mazumdar, S.K., Saenger, W. and Scheit, K.H. (1974) J. Mol. Biol. 85, 213-229.
- McGavin, S. (1971) J. Mol. Biol. 55, 293-298.
- Michelson, A.M., Massoulie, J. and Guschlbauer, W. (1967) in Prog. Nucl. Acid Res. Mol. Biol. 6 83-141.
- Mitsui, Y., Langridge, R., Shortle, B.E., Cantor, C.R., Grant, R.C., Kodamn, M. and Wells, R.D. (1970) Nature 228, 1166-1169.
- Morgan, A.R. (1970) J. Mol. Biol. 52, 441-466.
- Morgan, A.R., Coulter, M., Flintoff, W. and Paetkau, V. (1974) Biochem. 13, 1596-1603.
- Morgan, A.R. and Paetkau, V. (1972) Can. J. Biochem. 50, 210-216.
- Morgan, A.R. and Pulleyblank, D.E. (1974) Biochem. Biophys. Res. Comm. 61, 396-403.
- Morgan, A.R. and Wells, R.D. (1968) J. Mol. Biol. 37, 63-80.
- Murray, N.L. (1972) M. Sc. Thesis, University of Alberta.
- Murray, N.L. and Morgan, A.R. (1973) Can. J. Biochem. 51, 436-449.
- Mushynski, W.E. and Spencer, J.H. (1970) J. Mol. Biol. 52, 107-120.
- Novogrodsky, A., Gefter, M., Maitra, U., Gold, M. and Hurwitz, J. (1966) J. Biol. Chem. 241, 1977-1984.
- Ohba, Y. (1966) Biochem. Biophys. Acta 123, 84-90.
- Opara-Kubinska, Z., Kubinski, H. and Szybalski, W. (1964) Proc. Nat. Acad. Sci. (USA) 52, 923-930.

- Paetkau, V.H. (1969) *Nature* 224, 370-371.
- Paetkau, V. and Coy, G. (1972) *Can. J. Biochem.* 50, 142-150.
- Paetkau, V. and Langman, L. (1975) *Anal. Biochem.* 62, 525-532.
- Pettijohn, D.E. and Hecht, R. (1973) *Cold. Spr. Harb. Symp. Quant. Biol.* 38, 31-41.
- Pilet, J. and Brahms, J. (1972) *Nat. New Biol.* 236, 99-100.
- Pirotta, V. (1975) *Nature* 254, 114-117.
- Pulleyblank, D.E. (1974) Ph.D. Thesis, University of Alberta.
- Pulleyblank, D.E. and Morgan, A.R. (1975) *J. Mol. Biol.* 91, 1-13.
- Pullman, B., Claverie, P. and Caillet, J. (1967) *Proc. Nat. Acad. Sci. (USA)* 57, 1633-1639.
- Quigley, G.J., Wang, A.J.H., Seeman, N.C., Suddath, F.L., Rich, A., Sussman, J.L. and Kim, S.H. (1975) *ibid* 72, 4866-4870.
- Rich, A. (1958) *Biochem. Biophys. Acta* 29, 502-509.
- Rich, A., Davies, D.R., Crick, F.H.C. and Watson, J.D. (1961) *J. Mol. Biol.* 3, 71-86.
- Riggs, A.D., Lin, S. and Wells, R.D. (1972) *Proc. Nat. Acad. Sci. (USA)* 69, 761-764.
- Riley, M., Maling, B. and Chamberlin, M.J. (1966) *J. Mol. Biol.* 20, 359-389.
- Rosenberg, J.M., Seeman, N.C., Day, R.O. and Rich, A. (1976) *ibid* 104, 145-167.
- Salditt, M., Braunstein, S.N., Camerini-Otero, R.D. and Franklin, R.M. (1972) *Virology* 48, 259-262.
- Salser, W.A. (1974) *Ann. Rev. Biochem.* 43, 923-965.
- Schildkraut, C.L., Richardson, C.C. and Kornberg, A. (1964) *J. Mol. Biol.* 9, 24-45.
- Schott, H., Eberhard, R., Schmidt, R., Roychoudhury, R. and Kossel, H. (1973) *Biochem.* 12, 923-928.

- Sederoff, R., Lowenstein, L. and Birnboim, H.C. (1975) *Cell* 5, 183-194.
- Seeman, N.C., Rosenberg, J.M. and Rich, A. (1976) *Proc. Nat. Acad. Sci. (USA)* 73, 804-808.
- Seeman, N.C., Rosenberg, J.M., Suddath, F.L., Kim, J.J.P. and Rich, A. (1976) *J. Mol. Biol.* 104, 109-144.
- Selsing, E., Arnott, S. and Ratliff, R.L. (1975) *ibid* 98, 243-248.
- Shapiro, R., Cohen, B.I., Shivey, S.J. and Maurer, H. (1969) *Biochem.* 8, 238-245.
- Shapiro, R. and Hachman, J. (1966) *ibid* 5, 2799-2807.
- Singer, B. (1975) in *Prog. Nucl. Acid Res. Mol. Biol.* 15, 219-284.
- Skoog, D.A. and West, D.M. (1969) *Fundamentals of Analytical Chemistry*, 2nd Edition, Holt, Rinehart and Winston, Inc., New York.
- Smith, M. and Khorana, H.G. (1963) in *Methods In Enzymology VI*, 645-669.
- Smith, M.G. (1967) *ibid* XII A, 545-550.
- Sobell, H.M. (1973) in *Prog. Nucl. Acid Res. Mol. Biol.* 13, 153-190.
- Stanley, W.M. (1967) in *Methods In Enzymology XII A*, 404-407.
- Stevens, C.L. and Felsenfeld, G. (1974) *Biopolymers* 12, 293-314.
- Stollar, B.D. and Raso, V. (1974) *Nature* 250, 231-234.
- Studier, R.W. (1965) *J. Mol. Biol.* 11, 373-390.
- Sugimoto, K., Sugisaki, H., Okamoto, T. and Tukanami, M. (1975) *Nucl. Acid Res.* 2, 2091-2100.
- Suwalsky, M., Traub, W., Schmuelli, U. and Subirana, J.A. (1969) *J. Mol. Biol.* 42, 363-373.
- Summers, W.C. and Szybalski, W. (1968) *Virology* 34, 9-16.
- Szybalski, W., Bovre, K., Fianndt, M., Guha, A., Hcadečna, Z., Kumar, S., Lozeron, H.A., Maher, V.M., Nijkamp, H.J.J., Summers, W.C. and Taylor, K. (1969) *J. Cell Physiol.* 74, Supplement 1, 33-70.

- Szybalski, W., Kubinski, H. and Sheldrick, P. (1966) Cold Spr. Harb. Symp. Quant. Biol. 31, 123-127.
- Teitelbaum, H. and Englander, S.W. (1975a) J. Mol. Biol. 92, 55-78.
- Teitelbaum, H. and Englander, S.W. (1975b) *ibid* 92, 79-92.
- Theille, D. and Guschlbauer, W. (1971) Biopolymers 10, 143-157.
- Tomasz, M., Mercado, C.M., Olson, J. and Chatterjie, N. (1974) Biochem. 13, 4878-4887.
- Torrence, P.F., DeClercq, E. and Witkop, B. (1976) *ibid* 15, 724-734.
- Tuniš-Schneider, M.J.B. and Maestre, M. (1970) J. Mol. Biol. 52, 521-541.
- Uhlenhopp, E.L. and Krasna, A. I. (1971) Biochem. 10, 3290-3295.
- Vinograd, J. (1963) in Methods In Enzymology VI, 854-870.
- Vogt, D. and Rich, A. (1970) in Prog. Nucl. Acid Res. Mol. Biol. 10, 183-265.
- Walz, A. and Pirotta, V. (1975) Nature 254, 118-121.
- Wang, J.C. (1974a) J. Mol. Biol. 87, 797-816.
- Wang, J.C. (1974b) *ibid* 89, 783-801.
- Waring, M.J. (1974) Biochem. J. 143, 483-486.
- Wartell, R.M., Larsen, J.E. and Wells, R.D. (1974) J. Biol. Chem. 249, 6719-6731.
- Weber, K. and Osborn, M. (1969) *ibid* 244, 4406-4412.
- Wells, R.D. and Larsen, J.E. (1970) J. Mol. Biol. 49, 319-342.
- Wells, R.D., Larsen, J.E., Grant, R.C., Shortle, B.E. and Cantor, C.R. (1970) *ibid* 54, 465-497.

APPENDIX 1

This section describes the application of ethidium bromide fluorescence techniques to studies of agents which alkylate and cross-link DNA, projects done in collaboration with Dr. J.W. Lown of the Department of Chemistry, University of Alberta.

The first reprint describes the development of these techniques and their usefulness in studying the mechanism of action of the antineoplastic agent mitomycin C. This compound alkylates and cross-links DNA in reactions that are pH dependent implicating the azeridine moiety as the primary alkylation site. Accompanying these reactions is a free radical cleavage of DNA but no depurination. Although reduction by NADH is thought essential for in vivo action, we have shown that at low pH cross-linking can occur in the absence of a reducing agent.

These studies have been extended in the second reprint to a series of chemically synthesized model bisazeridinopyrrolidinoquinones which also alkylate and cross-link DNA in pH dependent reactions. There seems a correlation between the extent and rate of cross-linking and the in vivo antineoplastic activity of some of these analogues which may prove useful as a preliminary screening step for these types of agents.

The third paper discusses the use of the fluorescence assay to measure DNA alkylation. The observation of a pH dependent recovery of fluorescence with alkylation by dimethyl sulfate has been compared to alkylation by mitomycin C (which does not show this behaviour) and supports the hypothesis that mitomycin C does not alkylate the 7-position of guanine.

(Reprinted from Canadian Journal of Biochemistry (1976) 54, 110-119.)

Studies related to antitumor antibiotics. Part V. Reactions
of mitomycin C with DNA examined by ethidium fluorescence assay

J. WILLIAM LOWN AND ASHER BEGLEITER¹
Department of Chemistry, University of Alberta,
Edmonton, Alberta T6G 2E1

and

DOUGLAS JOHNSON² AND A. RICHARD MORGAN
Department of Biochemistry, University of Alberta,
Edmonton, Alberta T6G 2E1

The cytotoxic action of the antitumor antibiotic mitomycin C occurs primarily at the level of DNA. Using highly sensitive fluorescence assays which depend on the enhancement of ethidium fluorescence only when it intercalates duplex regions of DNA, three aspects of mitomycin C action on DNA have been studied: (a) cross-linking events, (b) alkylation without necessarily cross-linking, and (c) strand breakage. Cross-linking of DNA is determined by the return of fluorescence after a heat denaturation step at alkaline pH's. Under these conditions denatured DNA gives no fluorescence. The cross-linking was independently confirmed by S₁ endonuclease (EC 3.1.4.-) digestion. At relatively high concentrations of mitomycin the suppression of ethidium fluorescence enhancement was shown not to be due to depurination but rather to alkylation, as a result of losses in potential intercalation sites. A linear relationship exists between binding ratio for mitomycin and loss of fluorescence. The proportional decrease in fluorescence with pH strongly suggests that the alkylation is due to the aziridine moiety of the antibiotic under these conditions. A parallel increase in the rate and overall efficiency of covalent cross-linking of DNA with lower pH suggests that the cross-linking event, to which the primary cytotoxic action has been linked, occurs sequentially with alkylation by aziridine and then by carbamate. Mitomycin C, reduced chemically, was shown to induce single strand cleavage as well as monoalkylation and covalent cross-linking in PM2 covalently closed circular DNA. The inhibition of this cleavage by superoxide dismutase (EC 1.15.1.1) and catalase (EC 1.11.1.6) and by free radical scavengers suggests that the degradation of DNA observed to accompany the cytotoxic action of mitomycin C is largely due to the free radical O₂⁻. In contrast to the behavior of the antibiotic streptonigrin, mitomycin C does not inactivate the protective enzymes superoxide dismutase or catalase. Lastly, mitomycin C is able to cross-link DNA in the absence of reduction at pH 4. This is consistent with the postulated cross-linking mechanisms.

¹NRCC Studentship holder 1970-1974.

²MRCC Studentship holder 1971-1975.

Introduction

There is much evidence that indicates DNA as the cell component most sensitive to the attack of alkylating agents (1-4). Although bifunctionality is not a prerequisite for antineoplastic activity, the most active agents are bifunctional. With respect to cytotoxicity, the greater effectiveness of antitumor agents of the bifunctional alkylating class, including the clinically important mitomycin C (5-7), has been attributed to their ability to cross-link complementary strands of DNA (8). Hitherto, cross-linking of DNA has been demonstrated by techniques such as cesium chloride density gradient centrifugation studies (7, 9) and by the hyperchromicity of cross-linked denatured DNA (10). Using these methods, cross-links introduced by nitrogen mustards (11) and mitomycin C (12, 13) have been reported. We wished to apply the ethidium fluorescence technique (14) to study the interactions of antitumor agents with nucleic acids. The fluorescence procedures complement existing techniques but also have the distinct advantages of sensitivity (typically 0.5 μ g of DNA may be employed), simplicity, rapidity, and adaptability, and lend themselves to an investigation of various aspects of interaction of antibiotics with DNA (14-18). We report here the exploitation of this method to estimate (a) cross-linked DNA, also called CLC-DNA³, (b) alkylation of DNA, and (c) cleavage of CCC-DNA. The assay for detecting CLC-DNA is based upon the enhanced fluorescence observed for ethidium bromide, which is bound to bihelical nucleic acids (14, 15, 19). We describe the application of this technique to a study of various aspects of the mechanism of cytotoxic action of mitomycin C.

It is considered that mitomycin C is subjected *in vivo* to an initial NADH mediated reduction with a cellular reductase to the hydroquinone with concomitant elimination of the 9a-methoxy grouping to form the reactive and unstable compound 2 (Scheme 1). This has led to the postulate that the lethal action of the mitomycin group of antibiotics can be accounted for by the introduction of covalent cross-links between complementary strands of DNA, thus preventing strand separation during the semiconservative replication process (20-22). Weissbach has demonstrated alkylation of nucleic acids with radioactively labelled mitomycin C (20). The existing evidence implicates the carbamate and aziridine functions, so that the covalently linked complex is envisaged as compound 3 (Scheme 1). The precise sites of binding on the DNA are still under active investigation (23-26).

Experimental

Materials

Ethidium bromide, calf thymus DNA, and α -amylase⁴ powder were purchased from Sigma Chemical Co., mitomycin C was from Calbiochem,

³CLC-DNA, covalently linked complementary-DNA; CCC-DNA, covalently closed circular-DNA; SDS, sodium dodecyl sulfate; OC, open circular; epr, electron paramagnetic resonance.

⁴ α -Amylase, EC 3.2.1.1; superoxide dismutase, EC 1.15.1.1; catalase, EC 1.11.1.6.

Sephadex G-100 superfine from Pharmacia, and DEAE Cellulose from Whatman. The λ and PM2 DNAs were prepared as before (15). Superoxide dismutase was the gift of Dr. Alan Davison, and catalase was from Sigma Chemical Co.

Fluorescence Assay for Detecting CLC³ Sequences

All measurements were performed on a G.K. Turner and Associates model 430 spectrofluorometer equipped with a cooling fan to reduce fluctuations in the xenon lamp source. Wavelength calibration was performed as described in the manual for the instrument. One centimeter round cuvettes were used. The excitation wavelength was 525 nm and the emission wavelength 600 nm. Medium sensitivity ($\times 100$ scale) was generally used and water was circulated between the cell compartment and a thermally regulated bath at 22°C. Small samples (5 - 20 μ l) from reaction mixtures were added to 2 ml of the assay mixture, which was 20 mM potassium phosphate, pH 11.7, and 0.4 mM EDTA, with 0.5 μ g of ethidium bromide per millilitre. The instrument was blanked with the assay mixture.

The cross-linking assay was carried out as follows. A 10 μ l aliquot of the cross-linking reaction mixture was diluted in 2 ml of the assay solution. The fluorescence of the diluted solution was measured. The solution was then heat denatured at 96°C for 2 min and equilibrated in a water bath at 22°C for 5 min. The fluorescence of the solution was again measured. The ratio of the fluorescence after heating to the fluorescence before heating gave the extent of covalent cross-linking.

General Procedure for Determination of Cross-linking of DNAs with Reduced Mitomycin C

Reaction mixtures were buffered to the appropriate pH with acetate at pH 4.5 or 5.0 or with potassium phosphate at pH 6.0, 7.2, 8.7, or 10.3. Mitomycin C was reduced in the cross-linking solutions by an aqueous solution of sodium borohydride. Cross-linking reactions were carried out on a scale of 40 - 100 μ l. Reaction solutions contained approximately 1.2 A₂₆₀ equivalents of DNA, 0.05 M buffer, 0.6×10^{-4} , 1.2×10^{-4} , 2.0×10^{-4} , and 4.0×10^{-4} M mitomycin C, and 1.3×10^{-3} , 2.2×10^{-3} , 3.1×10^{-3} , and 5.3×10^{-3} M sodium borohydride. Ten microlitre samples were removed at timed intervals and analyzed for extent of cross-linking by the fluorometric assay described above. A control reaction mixture prepared as above but containing no mitomycin was run with each experiment. Assay of the control reaction showed that there was no cross-linking in each case and that none of the components of the reaction mixture interfered with the ethidium fluorescence.

Purification and Fluorometric Assay of S₁ Endonuclease⁵

The S₁ endonuclease was purified by the method of Vogt (27) with the omission of the SP-Sephadex C-50 chromatography, the final step being Sephadex G-100 superfine chromatography in a buffer containing 30 mM sodium acetate, pH 4.5, 10 mM sodium chloride, 30 mM zinc sulfate, and 10% aqueous glycerol. The G-100 fraction on SDS polyacrylamide gel electrophoresis (28) gave one major protein band and one minor band and

⁵Aspergillus nuclease S₁ (EC 3.1.4.-).

was essentially inactive on duplex DNA (see Results). The standard S_1 endonuclease reaction mixture contained 30 mM sodium acetate, pH 4.5, 50 mM NaCl, 1 mM $ZnSO_4$, and 2 A_{260} equivalents of heat denatured calf thymus DNA, and was incubated at 45°C. A 20 μ l sample of the reaction mixture was added to 2 ml of ethidium bromide assay solution at pH 8 (5 mM Tris HCl, pH 8, 0.5 mM EDTA, and 0.5 μ g of ethidium bromide per millilitre). Under these conditions, denatured DNA exists with about 50% of its structure in short intramolecular duplex regions (14). On a nucleotide residue basis, the fluorescence enhancement is 50% that of native DNA, and this is lost on degradation with S_1 endonuclease. Therefore in calculations on the extent of cross-linked DNA by the S_1 assay, the DNA resistant to S_1 is taken to have twice the fluorescence enhancement per nucleotide residue of that which is degraded. Due to the slight activity of the S_1 endonuclease preparation on duplex DNA, the kinetics of degradation were always followed. After the initial very rapid degradation of denatured DNA, the duplex cross-linked DNA was very slowly degraded.

Escherichia coli DNA which had been covalently cross-linked with reduced mitomycin C was dialyzed overnight at 4°C in 10 mM potassium phosphate at pH 11.5 and 0.1 mM EDTA, neutralized with 1.0 M Tris HCl, pH 8 (final concentration, 25 mM), and heat denatured (5 min at 95°C). To 80 μ l were added 20 μ l $5 \times S_1$ buffer, pH 4.3 (final pH, about 4.6). After removal of the first 10 μ l sample, 1.5 U of purified S_1 endonuclease were added and the mixture was incubated at 45°C. Samples (10 μ l) were added to the pH 8 ethidium bromide solution (2 ml) and read as described previously. Heat denatured and native E. coli DNAs were incubated as controls.

Correlation of Loss of Fluorescence with Binding Ratio

Reactions were carried out on a 600 μ l scale. Reaction solutions contained of 0.520 A_{260} equivalent of λ DNA, 0.05 M buffer, 0, 1.2×10^{-4} , 1.8×10^{-4} , 2.4×10^{-4} , 3.0×10^{-4} , and 4.2×10^{-4} M mitomycin C, and 2.6×10^{-3} , 2.6×10^{-3} , 4.0×10^{-3} , 5.3×10^{-3} , 6.6×10^{-3} , and 9.2×10^{-3} M sodium borohydride. After 30 min the solutions were assayed for loss of before-heat fluorescence by the fluorometric assay described above. Samples taken for radioactive counting in Aquasol were corrected for mitomycin C quenching.

Unbound mitomycin C was removed by dialysis vs. a mixture of 10 mM potassium phosphate, pH 11.7, and 0.1 mM EDTA. Binding ratios were determined by the procedure of Tomasz (26) except that nucleotide concentrations were determined by radioactive counting. The extinction coefficient of the DNA at 314 nm was calculated from the control (mitomycin C concentration = 0) as 232. Extinction coefficients of 7000 for DNA at 260 nm and of 11,000 for bound mitomycin at 314 nm were used.

Initial monoalkylated mitomycin C concentration x 10 ⁻⁴ (M)	Loss of fluorescence (%)	DNA concentration after dialysis x 10 ⁻⁵ (M)	Absorbance of complex at 314 nm	Bound monoalkylated mitomycin C concentration x 10 ⁻⁶ (M)	Binding ratio
0	0	7.33	0.017	0	-
1.2	19	7.07	0.032	1.42	50
1.8	37	6.63	0.037	1.97	34
2.4	58	7.03	0.048	2.88	24
3.0	67	6.23	0.048	3.05	20
4.2	85	5.66	0.087	6.72	8

Binding of Ethidium Bromide to DNA Covalently Cross-Linked and Mono-alkylated with Mitomycin C

DNA samples which had been treated with reduced mitomycin C were dialyzed against a mixture of 10 mM potassium phosphate, pH 11.7, and 0.1 mM EDTA. The percentage of CLC-DNA was determined by ethidium fluorescence before and after dialysis. The absorbance of the dialyzed DNA was measured at 260 nm on a Gilford 2400 spectrophotometer. Increasing amounts of DNA were added to an ethidium bromide solution, pH 8.0, and the fluorescence per unit increment in OD₂₆₀ was calculated vs. a known amount of DNA as standard.

General Procedure for the Determination of Cleavage of PM2 CCC-DNA with Mitomycin C

Reaction mixtures contained 100 µg of mitomycin C per millilitre (0.3 mM), 200 µg of sodium borohydride per millilitre (5.3 mM), PM2 DNA at 1.12 A₂₆₀ equivalents, and 50 mM potassium phosphate, pH 7.2. Fifteen microlitre samples were analyzed by ethidium fluorescence at pH 11.7, as above. Control experiments without mitomycin C showed a 75% return of fluorescence after heating (identical for DNA alone), indicating that the PM2 DNA was nicked to the extent of about 20% (14) (CCC-DNA gives a 30% increase in fluorescence on nicking).

General Procedure for Determining Covalent Cross-linking of DNAs of Different G + C Content by Activated Mitomycin C

The DNAs used were *E. coli* (mol. wt., 14.8 x 10⁶, G + C content, 50%), calf thymus (mol. wt., 10 x 10⁶, G + C content, 40%), *Clostridium perfringens* (mol. wt., 11.4 x 10⁶, G + C content, 30%). The composition of the final reaction mixture was DNA at 1.20 A₂₆₀ equivalents, 50 mM potassium phosphate, pH 7.2, mitomycin C, 0.6 x 10⁻⁴ or 3.0 x 10⁻⁴ M, and sodium borohydride, 1.3 x 10⁻⁴ or 6.6 x 10⁻³ M, respectively. Reactions were run at ambient temperature and aliquots were removed at timed intervals and analyzed for the extent of covalent cross-linking by the pH 11.8 ethidium assay described above.

Control Experiments for Possible Inactivation of Catalase and Superoxide Dismutase by Mitomycin C

A solution containing mitomycin C at 0.3×10^{-4} M and sodium borohydride at 0.5×10^{-3} M in pH 7 phosphate buffer was incubated with catalase at 4×10^{-8} M at 0°C for 1 h. Two millilitres of this solution were added to H_2O_2 to obtain a final volume of 10 ml, 20 mM in H_2O_2 . The decomposition of H_2O_2 at 0°C was determined by analysis of 1-ml samples which were made up to 50 ml containing 1% sulfuric acid. To 0.5 ml of this solution was added successively 1 M potassium iodide (0.5 ml), 1 mM acidified ammonium molybdate solution (0.5 ml), and 2% starch solution (0.25 ml), in a total volume of 10 ml. The absorbance at 580 nm of the resulting blue solution is shown in Fig. 6.

The effect of mitomycin C on superoxide dismutase was tested by incubating 1.5×10^{-7} M superoxide dismutase with 0.3×10^{-4} M mitomycin C and 0.5×10^{-3} M sodium borohydride in phosphate buffer at pH 7.8 at room temperature for 1 h. Then 0.5 ml of this solution was added to a solution containing finally, in 5 ml, 0.1 mM xanthine, 0.1 mM EDTA, and 2×10^{-5} M cytochrome c. The absorbance at 550 nm on addition of xanthine oxidase (final concentration, 5 ng/ml) was followed.

Results

Detection of Covalent Cross-linking of DNA by Mitomycin C by the Ethidium Fluorescence Assay

Covalent cross-linking of λ -phage DNA occurred on incubating the DNA with reduced mitomycin C in a phosphate buffer at pH 7.2 at 22°C in the presence of sodium borohydride. Aliquots were withdrawn at intervals and the extent and progress of covalent cross-linking determined by the ethidium fluorescence assay. To measure cross-linking, λ DNA was heat denatured and cooled in the presence of ethidium. Under these conditions separable strands do not reanneal, and only CLC³ sequences can anneal to give ethidium fluorescence enhancement, the induced cross-link serving as a nucleation point for rapid renaturation. Temperature jump studies have shown that once such a nucleation point is present, the propagation of the helix proceeds at 10^7 - 10^8 base pairs per second (29). The high pH of the assay is to prevent spontaneous formation of short intrastrand bihelical structures after heating and cooling of the individual separated strands of DNA. Such structures are thermally unstable when compared to those formed with CLC-DNA and are due to a certain degree of self-complementarity within strands of naturally occurring DNAs (14, 15). The results of the new technique of fluorescence enhancement are therefore in accord with the demonstration of the cross-linking of DNA by mitomycin C by Iyer and Szybalski (21) and by others (2, 13, 25, 30). This correspondence was deemed desirable before the more sophisticated application of the technique to strand cleavage described below.

Confirmation of Covalent Cross-linking of DNA by Mitomycin C Employing an S₁ Endonuclease Assay

To confirm that the fluorescence enhancement assay procedure

detects the formation of CLC-DNA formed as a result of a chemical cross-linking event, experiments were performed with the enzyme S_1 endonuclease. This specifically cleaves single stranded DNA (23) and is essentially inactive on duplex DNA (24). Since the time for the S_1 endonuclease digestion is long enough to allow renaturation of denatured λ DNA, Escherichia coli DNA was used, which has a suitable C_0t value. The DNA treated with mitomycin C and sodium borohydride was dialyzed to remove excess inorganic salts and decomposed mitomycin C before treatment with the enzyme. The results, summarized in Table 1, confirm the formation of covalent cross-links with the antitumor agent. The incomplete cross-linking with E. coli DNA as compared with T7 (14) or λ DNA is probably a result of the much lower molecular weight of the E. coli DNA. There is good correlation between the fluorescence assay and the endonuclease assay. The fluorescence assay is normally carried out directly on the reaction solution. During dialysis there is no strand scission due to alkylation since the percentage of CLC-DNA is unaffected.

Table 1. Comparison of the cross-linking of E. coli DNA assayed by ethidium fluorescence and S_1 endonuclease sensitivity

Assay	Run No. ^a		
	1	2	3
	Cross-linked, %		
Ethidium fluorescence			
Before dialysis	34	48	61
After dialysis	39	51	60
S_1 endonuclease			
After dialysis	32	51	44

^aRuns 1, 2 and 3 contained 0.06, 0.15 and 0.2 mM mitomycin C respectively, with a constant molar ratio of sodium borohydride to mitomycin of 96:1.

Detection of Monoalkylation without Concomitant Depurination during the Treatment of DNA with Activated Mitomycin C

At low levels of mitomycin C the fluorescence enhancement before heating to detect CLC-DNA was unaffected since the amount of DNA chemically modified was insignificant compared with the number of ethidium intercalation sites. However, as the level of mitomycin was increased, a progressive decrease in the fluorescence was observed. Figure 1 and Table 2 indicate the extent of fluorescence loss with increasing mitomycin concentration. Three explanations seemed plausible: (a) alkylation of the DNA bases reducing the number of permitted ethidium intercalation sites either by steric hindrance or charge repulsion due to the positive charge on ethidium and on alkylated guanines; (b) alkylation followed by depurination or depyrimidation destroying intercalation sites; (c) cleavage and degradation of the DNA by reactive free radicals paralleling the action of the antitumor quinone-containing drug streptonigrin (31). There is evidence in the literature that mitomycin C degrades DNA as well as inducing cross-links (32, 33). The following

Table 2. Radioactivity assay for alkylation of $(d[^{14}\text{C}]\text{G})_n \cdot (d[^3\text{H}]\text{C})_n$ by mitomycin C^a

Mitomycin C, $\mu\text{g/ml}$	^3H , cpm	^{14}C , cpm	$^3\text{H}/^{14}\text{C}$, ratio	Decrease in fluorescence with <i>E. coli</i> , %
20	1292	1785	0.724	16.1
40	1225	1682	0.728	43.5
60	1265	1733	0.730	61.7
80	1149	1418	0.810	72.2
100	1187	1528	0.776	79.6

^aThe molar ratio of mitomycin C to sodium borohydride was 1:96 in all experiments.

experiments enabled us to distinguish between these various possibilities. Points b and c were tested simply by using a labelled synthetic DNA, poly(dG-dC) with ^{14}C -labelled G and ^3H -labelled C. The labelled polynucleotide was incubated with progressively increasing concentrations of mitomycin C in parallel with *E. coli* DNA. There was a progressive decrease in the ethidium fluorescence. Using an acid insolubility assay, the results in Table 2 show that there is no loss of soluble radioactivity and that the ratio of ^3H to ^{14}C counts is essentially constant under conditions in which increasing concentrations of mitomycin produce 16.1 - 79.6% reduction in ethidium fluorescence. This confirms that there has been no detectable loss of either purine or pyrimidine bases as a result of monoalkylation and excludes c.

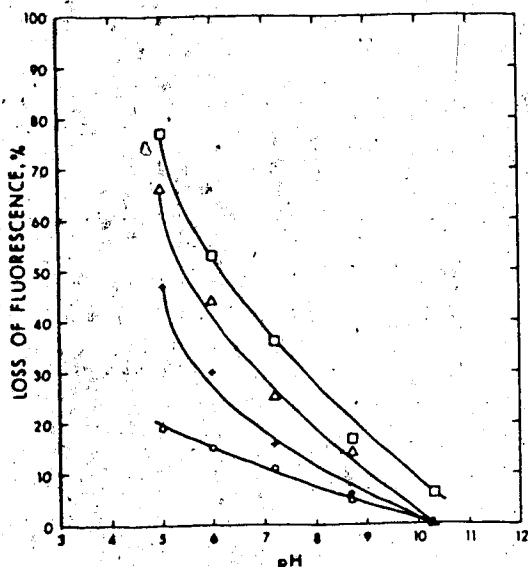


Fig. 1. The pH dependence of alkylation of DNA by reduced mitomycin C. The reactions were at 22°C in 50 mM phosphate at the appropriate pH and with λ DNA at 1.2 A₂₆₀ equivalents. The mitomycin C concentrations were 0.6×10^{-4} , 1.2×10^{-4} , 2.0×10^{-4} , and 4.0×10^{-4} M and the sodium borohydride 1.3×10^{-3} , 2.2×10^{-3} , 3.1×10^{-3} , and 5.3×10^{-3} M for the symbols o, +, Δ , and \square , respectively.

The extent of binding for progressively increasing amounts of mitomycin was determined by a modification of the procedure of Tomasz (26) by UV absorbance of the drug-DNA complex at 314 nm. The concentrations of the ^3H -labelled DNA before and after dialysis were determined by counting. It may be seen from Fig. 2 that there is a linear relationship between loss of fluorescence and mitomycin binding ratios over an extensive range.

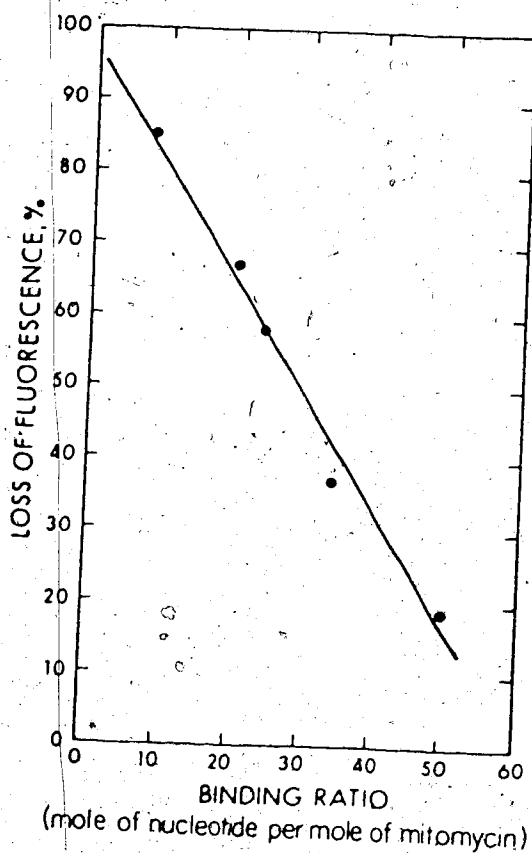


Fig. 2. Dependence of binding ratio between mitomycin C and DNA on loss of before-heat fluorescence.

To further confirm that the drop in fluorescence with time was due to alkylation and not some product of the reaction mixture interfering with the fluorescence assay, the DNA was treated with reduced mitomycin C to varying extents such that the fluorescence drop varied between 0 and 75%. The DNA was then dialyzed as described in Methods and the fluorescence per absorbance unit was determined. It was shown that the fluorescence enhancement was linearly related to the amount of absorbance added for a given dialyzed sample, and that the ratio of fluorescence to A_{260} units varied from an arbitrary value of 1 for DNA showing no fluorescence drop to 0.18 for DNA showing a 75% fluorescence drop. For intermediate values there was almost a linear relationship. It is evident that the loss of fluorescence in the reaction mixture is not due to fragmentation of the DNA but rather to loss of intercalation sites by alkylation the only major modification mitomycin is known to confer on DNA. Iyer and Szybalski (21) found that only about one in five to ten antibiotic bound molecules formed cross-links, the others being attached to one strand mostly by monoalkylation (cf. also Ref. 34). Therefore using the fluorescence procedure, the decrease in the before-heating

fluorescence value may now be employed as a measure predominantly of monoalkylation, which prevents ethidium binding by the mechanism detailed in a above.

It may be seen from Fig. 1 that for a given pH value there is progressive loss of fluorescence with increasing concentration of activated mitomycin C, confirming the detection of increasing proportions of alkylation accompanying covalent cross-linking of DNA.

pH Dependence of Cross-linking and Monoalkylation of DNA by Mitomycin C and the Sequence of Covalent Cross-linking

It is significant that the decrease in fluorescence due to mitomycin C is strongly pH dependent with lower pH favoring more rapid alkylation. This strongly suggests that under these conditions the aziridine function alkylate the bases of DNA first. This conclusion is in agreement with previous results in which the product after treatment of mitomycin C with a reducing agent followed by secondary rearrangement and then subjected to reoxidation corresponded to the structure in which the aziridine ring was opened (4, Scheme 1). The preparation and properties of compound 4 have been described (35 - 38). The dependence of the rate of induced covalent cross-linking on pH was determined, as shown in Fig. 3. The trend toward more efficient covalent cross-linking with lower pH is clear. The results, which parallel those obtained for monoalkylation, again suggest that the first event in cross-linking is due to attack by the acid sensitive aziridine moiety under these conditions. Since tumor cells tend to have a lower pH as well as a more reducing environment, these factors could lead to selectivity of action (39).

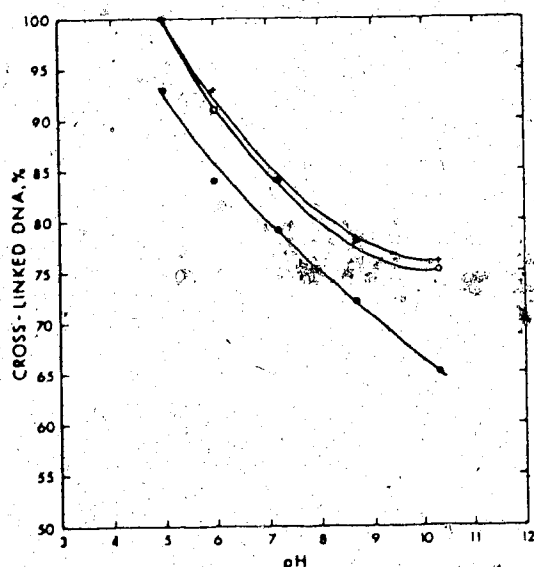


Fig. 3. The pH dependence of cross-linking DNA by reduced mitomycin C. The conditions were as described under Fig. 1 but the fluorescence values were obtained after heating the DNA-ethidium mixture (Methods). The mitomycin C concentrations were 0.6×10^{-4} , 1.2×10^{-4} , and 2.0×10^{-4} M, and the sodium borohydride 1.3×10^{-3} , 2.2×10^{-3} , and 3.1×10^{-3} M for the symbols ●, ○ and +, respectively.

Dependence of Efficiency of Covalent Cross-linking of DNA by Mitomycin C on G + C Content of DNA

We applied the ethidium fluorescence assay to detect covalent cross-links and monoalkylation in three natural DNAs of different G + C content, *Clostridium perfringens* (30%), calf thymus (40%), and *E. coli* (50%). The cross-linking efficiencies are not strictly comparable because of slight differences in average molecular weights as determined by sedimentation velocities. Since only one cross-link per DNA is sufficient to produce rapid renaturation after cooling regardless of the length of the polynucleotide, DNAs of lower molecular weight require more cross-linking events on a nucleotide residue basis to obtain the same percentage of cross-linked DNA. Assuming a Poisson's distribution of the links, and further, that one link is sufficient to permit the spontaneous renaturation of the molecule, the average number of cross-links per molecule was estimated ($\bar{m} = \ln(1/P_0)$, in which P_0 is the proportion of the molecules unlinked) to be 0.54, 0.92 and 1.27 for the three DNAs at a mitomycin concentration of 3.0×10^{-4} M, and 0.08, 0.29 and 0.46 at a mitomycin concentration of 0.6×10^{-4} M. These values are closely comparable with similar estimates made by Iyer and Szybalski for mitomycin cross-linking (5).

The Mechanism of DNA Degradation by Mitomycin C

Mitomycin C has been observed to cause DNA degradation (32, 33), which accompanies covalent cross-linking; hitherto this had been considered to be due largely to the activation of intracellular deoxyribonucleases (40, 41). To determine if mitomycin C also induces single strand cleavage of DNA, in common with streptonigrin (42 and references therein), in the course of its cytotoxic action, experiments were performed with CCC-DNA derived from PM2 bacteriophage. The amount of ethidium taken up by CCC-DNA is restricted because of topological constraints. If one or more single strand nicks are induced by chemical means, this results in a release of topological constraints and the OC form permits the intercalation of more ethidium with an increase in the observed fluorescence for PM2 DNA of about 30% (14). Upon heating and cooling, the OC-DNA is denatured (in contrast to CCC-DNA) into one circular single strand and one linear single strand which do not bind ethidium at pH's >11.5, and the fluorescence falls to zero. The results of various treatments on CCC- and OC-DNA are shown in Fig. 4. Assay for strand scission in DNA using CCC-DNA is complicated by concomitant cross-linking and also alkylation. However, neither of these latter reactions can give rise to an increase in fluorescence, which can be accounted for only by nicking CCC-DNA. However, the loss of fluorescence normally observed on heating the nicked DNA is not observed due to cross-linking. Indeed, the OC-DNA originally contaminating the CCC-DNA (75% return of fluorescence after heat treatment) appears as CLC-DNA since at early times there is 100% return of fluorescence after heating. It was shown in a control experiment that sodium borohydride is without effect on PM2 CCC-DNA. The results, which are summarized in Fig. 5, confirm that mitomycin C when reductively activated does induce single strand cleavage of DNA, as shown by the rise in fluorescence. This was independently confirmed by sedimentation velocity studies in which the compact CCC-DNA ($s_{20,w} = 30$) was converted to material with a

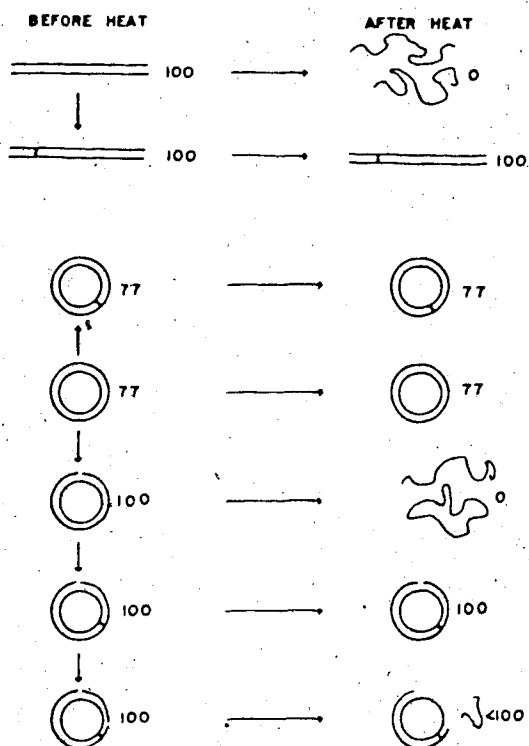


Fig. 4. A diagrammatic representation of the various forms of DNA and the effects of heat treatment, with the relative fluorescence values on a per nucleotide bases. The PM2 CCC-DNA is negatively supercoiled as isolated, but positively supertwisted in the assay mixture due to unwinding by ethidium. The supertwists are not therefore indicated.

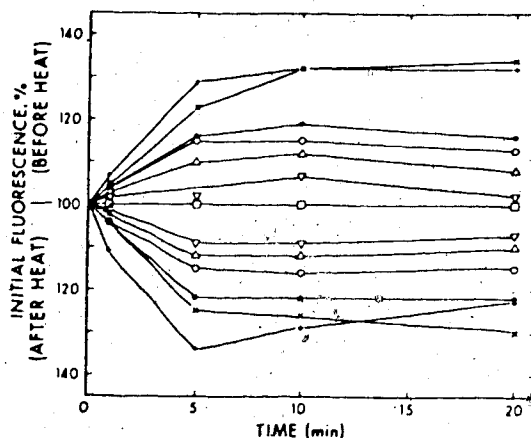
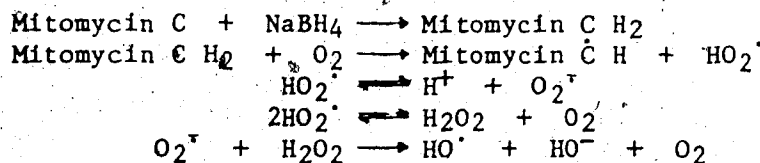


Fig. 5. Single strand scission of PM2 CCC-DNA by mitomycin C. Reactions were carried out at ambient temperature in phosphate buffer, pH 7.2, containing 1.13 A₂₆₀ equivalents of PM2 DNA. Additional components: (∇) mitomycin C 3.0×10^{-4} M, sodium borohydride 5.3×10^{-3} M, isopropyl alcohol 2.5×10^{-1} M; (Δ) mitomycin C 3.0×10^{-4} M, sodium borohydride 5.3×10^{-3} M, sodium benzoate 5.0×10^{-2} M; (o) mitomycin C 3.0×10^{-4} M, sodium borohydride 5.3×10^{-3} M, catalase 4.1×10^{-6} M; (●) mitomycin C 3.0×10^{-4} M, sodium borohydride 5.3×10^{-3} M, catalase 4.1×10^{-6} M, superoxide dismutase 6.1×10^{-5} M; (⊕) mitomycin C 3.0×10^{-4} M, sodium borohydride 5.3×10^{-3} M, superoxide dismutase 3.0×10^{-5} M; (x) mitomycin C 3.0×10^{-4} M, sodium borohydride 5.3×10^{-3} M; (□) control.

sedimentation rate of OC-DNA ($s_{20,w} = 23$). The induction of single strand cleavage may be retarded by catalase or by a combination of catalase and superoxide dismutase or by free radical scavengers such as isopropyl alcohol or sodium benzoate (see Fig. 5). This suggests a mechanism of cleavage similar to that operating for reduced streptonigrin, in which cleavage of the PM2 CCC-DNA is induced by hydroxyl radicals as follows (31):



This scheme requires the intermediacy of the semiquinone of mitomycin C which in contrast to that of streptonigrin must have a very short lifetime since, unlike the latter, it has not been detected by epr *in vivo* or *in vitro* (42). Recent electroanalytical data give an estimated lifetime of mitomycin C semiquinone of ~ 10 s (43). In contrast to streptonigrin (44), mitomycin C did not inactivate the action of the enzymes catalase (see Fig. 6), nor superoxide dismutase (see Fig. 7).

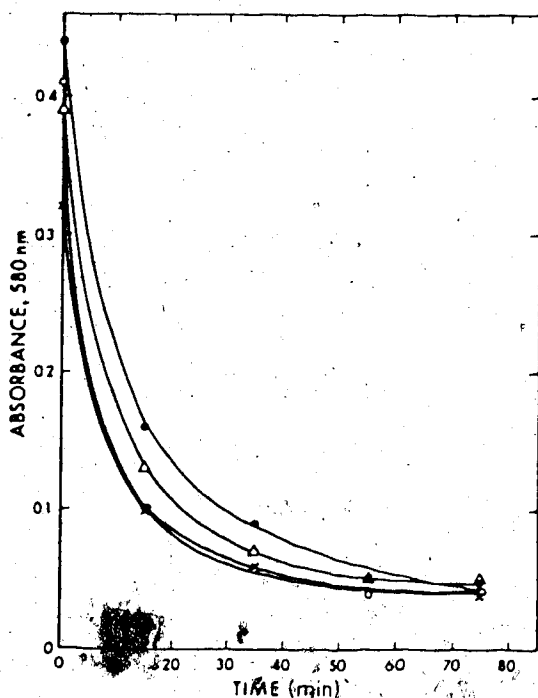


Fig. 6. Control experiments for inactivation of catalase decomposition of H_2O_2 . Reactions were carried out at $0^\circ C$ in a total volume of 10 ml, buffered at pH 7.0 by 0.06 M potassium phosphate, and containing 0.02 M H_2O_2 and 8×10^{-9} M catalase. Additional components: (x) mitomycin C 6.0×10^{-6} M, (Δ) sodium borohydride 1.1×10^{-4} M, (\bullet) mitomycin C 6.0×10^{-6} M and sodium borohydride 1.1×10^{-4} M.

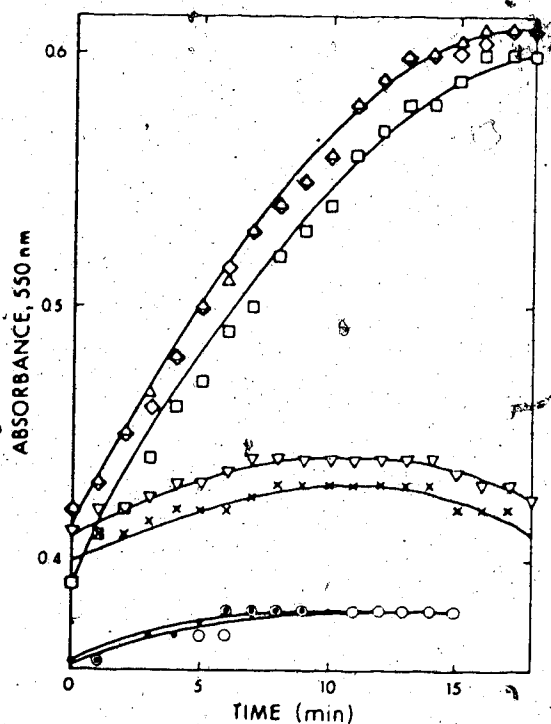
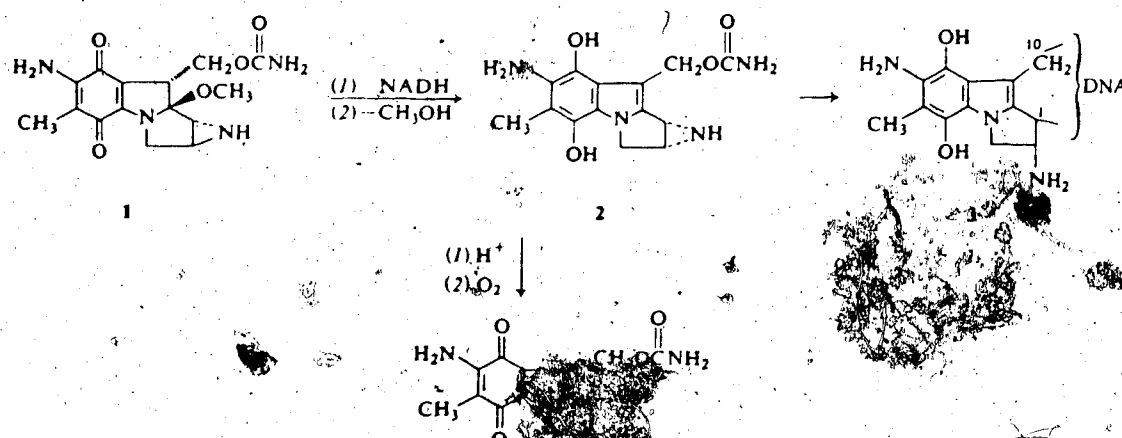


Fig. 7. Control experiments for inactivation of superoxide dismutase action on the reduction of cytochrome c. Reactions were carried out at $25^\circ C$ in a total volume of 3.5 ml, buffered at pH 7.8 by 0.05 M potassium phosphate and containing 10^{-4} M EDTA, 10^{-4} M xanthine, and 2×10^{-5} M cytochrome c, and initiated by the addition of 100 μ l of a solution of xanthine oxidase (0.18 μ g/ml). Additional components: (\bullet) superoxide dismutase 1.5×10^{-8} M; (\circ) mitomycin C 3.0×10^{-6} M, superoxide dismutase 1.5×10^{-8} M; (x) mitomycin C 3.0×10^{-6} M, sodium borohydride 5.3×10^{-5} M, superoxide dismutase 1.5×10^{-8} M; (∇) sodium borohydride 5.3×10^{-5} M, superoxide dismutase 1.5×10^{-8} M; (Δ) mitomycin C 3.0×10^{-6} M, sodium borohydride 5.3×10^{-5} M; (\diamond) mitomycin C 3.0×10^{-6} M.

Cross-linking by Mitomycin C without Reduction

As shown in Scheme 1, the reduction of mitomycin C is thought to activate the aziridine ring by promoting the elimination of methanol (5). The aziridine ring is then more readily attacked by nucleophiles on the DNA. However, lowering the pH alone was found to be sufficient to promote alkylation by the aziridine ring followed by cross-linking via the carbamate. Freese and Cashel have demonstrated that treatment of DNA with low pH conditions can induce covalent cross-links (45); however, careful controls showed that under the conditions of the present experiment no acid-promoted cross-linking was significant. Figure 8 shows the kinetics of cross-linking in the absence of borohydride. Cross-linking is considerably slower than in the presence of reducing agent but it does not have to be reduced even within the cell for cross-linking to occur. A curve obtained for T7 DNA was almost identical with that for λ DNA.



SCHEME 1. The chemical transformations of mitomycin C involved in enzymatic reduction and covalent attachment to DNA.

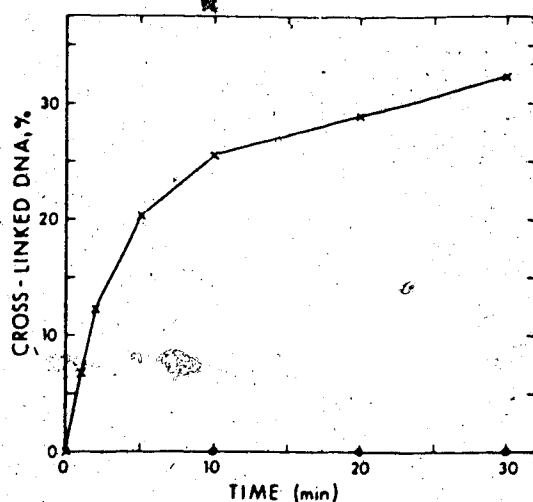


Fig. 8. The cross-linking of λ DNA by mitomycin C without reduction. The reaction mixture contained λ DNA at 0.7 A₂₆₀ equivalents, 5 mM sodium acetate, pH 4, and 3.0×10^{-4} M mitomycin C, at 22°C. Samples of 15 μ l were added to the alkaline ethidium assay mixtures and the percentage of cross-linked DNA was equated with the percentage of fluorescence remaining after the heat step. Under these conditions the fluorescence remained constant after heating. (●) Control experiment at pH 4 with no mitomycin.

Conclusion

The fluorescence techniques we describe can be used with suitable DNA substrates to investigate the cross-linking, alkylation, and strand breakage of DNA conveniently and rapidly. There are many possibilities for the study of antibiotics which interact with DNA. So far, because of the high sensitivity of fluorescence, the large dilution into the assay mixture has not yet resulted in any reaction component interfering with the fluorescence. The only precaution is that ethidium itself will cleave DNA slowly (data of Morgan), requiring both light and oxygen. Therefore it is recommended that the samples assayed be read immediately or be kept in the dark. Applications of this technique in studying the action of other clinically useful synthetic and natural antitumor agents will be reported.

Acknowledgement

This research was supported by grants to J.W.L. from the National Cancer Institute of Canada, the National Research Council of Canada and by the Department of Chemistry, University of Alberta.

1. Ross, W.C.J. (1962) Biological Alkylating Agents, Butterworth & Co. (Publishers) Ltd., London
2. Wheeler, G.P. (1962) Cancer Res. **22**, 651-688
3. Montgomery, J.A., Johnson, T.P. & Shealy, Y.F. (1970) Drugs for Neoplastic Diseases in Medicinal Chemistry (Berger, A., ed.), part I, pp. 680-783, Wiley-Interscience, New York
4. Gale, E.F., Cundliffe, E., Reynolds, P.E., Richmond, M.H. & Waring, M. (1972) The Molecular Basis of Antibiotic Action, pp. 246-252, John Wiley & Sons Inc., New York
5. Szybalski, W. & Iyer, V.N. (1967) Antibiotics. I. Mechanism of Action (Gottlieb, D. & Shaw, P.D., eds), pp. 211-245, Springer-Verlag, Inc., New York
6. Kirsch, E.J. (1967) Antibiotics. II. Biosynthesis (Gottlieb, D. & Shaw, P.D., eds.), pp. 66-76, Springer-Verlag, Inc., New York
7. Iyer, V.N. & Szybalski, W. (1963) Proc. Natl. Acad. Sci. U.S.A. **50**, 355-361
8. Brookes, P. & Lawley, P.D. (1961) Biochem. J. **80**, 496-503
9. Brookes, P. (1966) Cancer Res. **26**, 1994-2003
10. Hamaguchi, K. & Geldushek, E.P. (1961) J. Am. Chem. Soc. **84**, 1329-1338
11. Kohn, K.W., Spears, C.L. & Doty, P. (1966) J. Mol. Biol. **19**, 266-288
12. Cohen, R.J. & Crothers, D.M. (1970) Biochemistry **9**, 2533-2539
13. Pritchard, A.E. & Eichinger, B.E. (1974) Biochemistry **13**, 4455-4460
14. Morgan, A.R. & Paetkau, V. (1972) Can. J. Biochem. **50**, 210-216
15. Morgan, A.R. & Pulleyblank, D.E. (1974) Biochem. Biophys. Res. Commun. **61**, 346-353
16. Burnotte, J. & Verley, W.G. (1972) Biochim. Biophys. Acta **269**, 370-375
17. Russell, A.D. (1969) Prog. Med. Chem. **6**, 186-199

18. Coulter, M., Flintoff, W., Paetkau, V., Pulleyblank, D. & Morgan, A.R. (1974) Biochemistry **13**, 1603-1609
19. LePecq, J.B. & Paoletti, C. (1967) J. Mol. Biol. **27**, 87-106
20. Lipsett, M.N. & Weissbach, A. (1965) Biochemistry **4**, 206-211
21. Iyer, V.N. & Szybalski, W. (1963) Proc. Natl. Acad. Sci. U.S.A. **50**, 355-361
22. Schwartz, H.S., Sodergren, J.E. & Philips, F.S. (1966) Science **142**, 1181-1183
23. Sutton, W.D. (1971) Biochim. Biophys. Acta **240**, 522-531
24. Beard, P., Morrow, J.F. & Berg, P. (1973) J. Virol. **12**, 1303-1313
25. Tomasz, M. (1970) Biochim. Biophys. Acta **213**, 288-295
26. Tomasz, M., Mercado, C.M., Olson, J. & Chatterjie, N. (1974) Biochemistry **13**, 4878-4887
27. Vogt, V.M. (1973) Eur. J. Biochem. **33**, 192-200
28. Shapiro, A.L., Vinuela, E. & Maizel, J.V. (1967) Biochem. Biophys. Res. Commun. **28**, 815-820
29. Eigen, M. & Porschke, D. (1970) J. Mol. Biol. **53**, 123-141
30. Wilson, D.A. & Thomas, C.A. (1974) J. Mol. Biol. **84**, 115-144
31. Cone, R., Hasan, S.K., Lown, J.W. & Morgan, A.R. (1975) Can. J. Biochem. (1976) Can. J. Biochem. **54**, 219-223
32. Reich, E., Shatkin, A.J. & Tatum, E.L. (1960) Biochim. Biophys. Acta **45**, 608-610
33. Wakaki, S. (1961) Cancer Chemother. Rep. **13**, 79-86
34. Weissbach, A. & Lisio, A. (1965) Biochemistry **4**, 196-200
35. Garratt, E.R. (1963) J. Med. Chem. **6**, 488-501
36. Garratt, E.R. & Schroeder, W. (1964) J. Pharm. Sci. **53**, 917-923
37. Kirsch, E.J. & Korshalla, J.D. (1964) J. Bacteriol. **87**, 247-255
38. Webb, J.D. (1962) J. Am. Chem. Soc. **84**, 3185-3187
39. Dermer, O.C. & Ham, G.E. (1969) Ethylenimine and Other Aziridines, pp. 425-441, Academic Press Inc., New York
40. Kersten, W. (1962) Biochim. Biophys. Acta **55**, 558-560
41. Nakato, Y., Nakato, K. & Sakamoto, Y. (1961) Biochem. Biophys. Res. Commun. **6**, 339-343
42. Ishizu, K., Dearman, H.H., Huang, M.T. & White, J.R. (1968) Biochim. Biophys. Acta **165**, 283-285
43. Begleiter, A., Lown, J.W., Plambeck, J.A. & Rao, G.M. (1975) Can. J. Biochem., submitted for publication
44. Akhtar, M.H., Hasan, S.K., Lown, J.W., Plambeck, J.A. & Sim, S.K. (1975) Can. J. Biochem., submitted for publication
45. Freese, E. & Cashel, M. (1964) Biochim. Biophys. Acta **91**, 67-77

(Reprinted from Canadian Journal of Chemistry (1975) 53, 2891-2905.)

Studies Related to Antitumor Antibiotics. Part VI. Correlation
of Covalent Cross-linking of DNA by Bifunctional Aziridinoquinones
with their Antineoplastic Activity

M. HUMAYOUN AKHTAR,¹ ASHER BEGLEITER,² DOUGLAS JOHNSON,³
 J. WILLIAM LOWN, LARRY McLAUGHLIN,⁴ AND SOO-KHOON SIM⁵

Departments of Chemistry and Biochemistry, University of Alberta,
 Edmonton, Alberta T6G 2G2

Certain bisaziridinopyrrolidinoquinone analogs, which contain the structural moieties essential for physiological activity in the parent antitumor agent mitomycin C, have been synthesized. These compounds efficiently induce covalent cross-links in DNA as shown by the ethidium fluorescence assay which was confirmed by an independent S₁ endonuclease assay. The interaction of clinically active and structurally related antitumor aziridinoquinones with DNA have been examined similarly. The aziridinoquinones cross-link DNA efficiently with a marked pH dependence. Parallel dependence is observed on pH and concentration of alkylating species in the concomitant alkylation which does not result in cross-linking as measured by the suppression of the before heat fluorescence. The latter phenomenon was shown by the application of radiolabelled polynucleates not to be accompanied by depurination. A direct correlation exists between the extent of covalent cross-linking and (G + C) content of various DNA's of comparable molecular weight as in the case of mitomycin C. Estimates of the average number of cross-links per DNA molecule range from 0.61 to 1.71 depending on (G + C) content. The rate of acid assisted opening of a model aziridinoquinone measured spectrophotometrically at different pH values parallels the observed rate of covalent cross-linking and alkylation. It was shown independently that the intermediate 2,5 bis(2-acetoxyethylamino)-3,6-dimethoxy-1,4-benzoquinone does not cross-link DNA. A correlation is made of antineoplastic activity against a variety of tumors with covalent cross-linking ability using λ -DNA.

Introduction

In the alkylating class of antitumor antibiotics the most effective

¹National Cancer Institute of Canada Postdoctoral Fellow 1973-1975.

²NRCC Studentship holder 1971-1972. Province of Alberta Graduate Fellowship holder 1974-present.

³MRC Studentship holder 1972-present.

⁴NRCC Studentship holder 1975-present.

⁵NRCC Postdoctorate Fellow 1974-present.

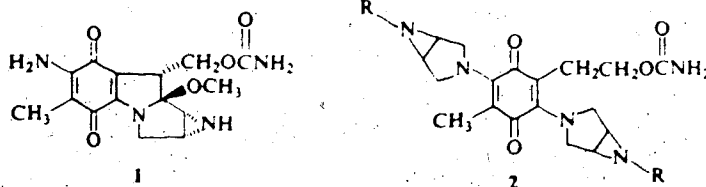
are bifunctional including many chemically important agents such as mitomycin C and synthetic agents e.g. Trenimon (1a). There is much evidence to indicate that DNA is the cell component most sensitive to the attack of such agents (2). As we described in Part V of this series the method of fluorescence enhancement employing the intercalative trypanocidal dye ethidium bromide which specifically detects double stranded DNA is a convenient procedure for investigating many aspects of the interaction of alkylating agents with the cell's genetic material (3). We describe the application of this technique to a study of the rate, extent, geometrical, substituent, and purine base specificity requirements for the covalent cross-linking of polynucleates, and attempt to correlate such factors with their antineoplastic properties.

Results and Discussion

Synthesis of Analogs of Mitomycin C which Covalently Cross-link DNA

In their studies on the mode of action of mitomycin C, 1, Szybalski and Iyer (4) showed that the rate of cell death correlated well with the degree of DNA cross-linking and have calculated that one cross-link per genome is sufficient to cause cell death. An examination of the literature of cancer chemotherapy reveals that many effective bifunctional agents have quite widely different geometries (1a). To examine further the characteristics of cross-linking of DNA with a view ultimately of establishing a rapid and convenient screen for potential antitumor agents, we sought initially a group of analogs of mitomycin C. Despite intensive and ongoing efforts by several groups of workers, mitomycin C has not as yet yielded to a total synthesis (5). There is also interest in chemically modified forms of mitomycin C (5h). We have prepared a group of analogs which possess what are regarded as the essential structural moieties for physiological activity, i.e. the bisaziridinopyrrolidinoquinones, 2.

The rationale is that compounds 2 retain the reactive aziridine and carbamate functions which separately have been shown to alkylate DNA (1b, 6). The distance between the two potential aziridine alkylating centers in 2 is comparable with that of the clinically useful 2,5-diaziridinoquinones (1). In addition, the greater conformational flexibility between the alkylating centers of 2 with the concomitant increase in the number of possible alkylating sites on DNA may compensate for the reduction in reactivity resulting from the loss of conjugative enhancement afforded by the indole nucleus in 1. It has not been demonstrated that the rate of alkylation is significant in determining antitumor activity. The quinone function is retained for two reasons (i) so that

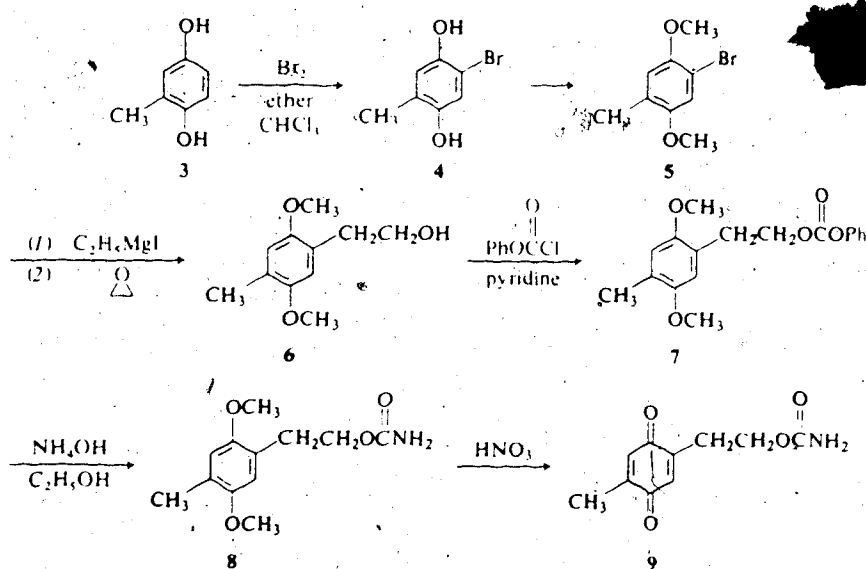


the structure of analogs 2 should resemble 1 for possible intercalative properties (7) and (11) we have established that mitomycin (3) in common with the structurally related antibiotic streptonigrin (8) degrades DNA employing its oxidative capacity which contributes significantly to their cytotoxic properties. In this connection there is much accumulated evidence that quinone containing substances display marked antibacterial and antitumor activity (5h, 9). In the event, analogs of type 2 proved to be quite efficient cross-linking agents which are useful in delineating the geometrical and conformational constraints in cross-linking of DNA.

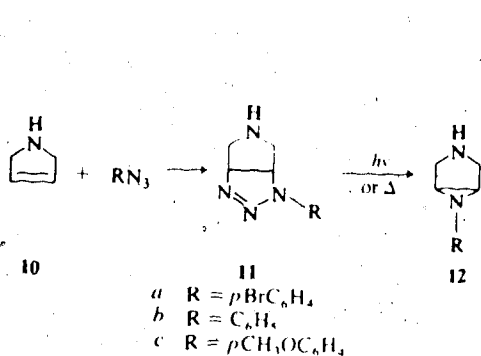
Functionalized quinones bearing the required carbamate side chain were prepared by the route illustrated in Scheme 1. The required bicyclic aziridines were prepared via 1,3-dipolar azide addition to 3-pyrroline and subsequent photolysis of the triazolines (10) (Scheme 2). The bicyclic aziridines were then coupled to the functionalized quinones using copper acetate as catalyst (11) (Scheme 3).

Detection of Covalent Cross-linking of DNA by Bicycloaziridinoquinones and Confirmation by S₁ Endonuclease

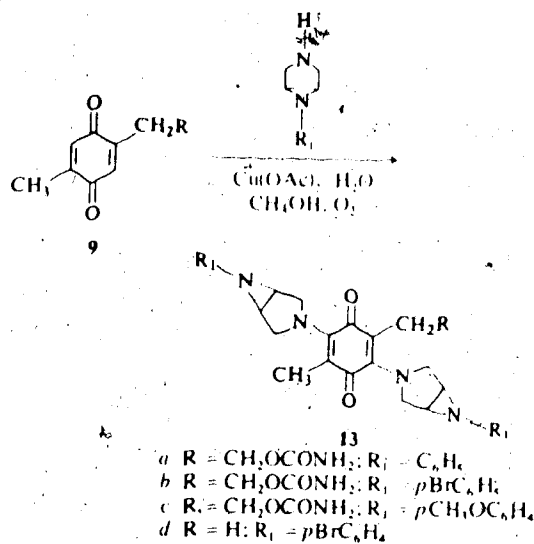
When the synthetic analogs 13 were incubated in 20% aqueous pyridine with λ -phage DNA (mol. wt. = 31×10^6) in an acetate buffer the induction of covalent cross-links was detected as summarized in Table 1. It is evident from the results that covalent cross-linking to the DNA is occurring quite efficiently across the two aziridine positions (compare 13d with 13b). The span between C₁ and C₁₀ of the activated form of mitomycin is ca. 4.3 Å compared with the span between the alkylating centers of 13d of 10.1 - 10.8 Å indicating bifunctional agents of quite different dimensions may be accommodated by cross-linked DNA. Secondly, an electron-withdrawing group in R₁ enhances the efficiency of covalent cross-linking.



SCHEME 1



SCHEME 2



SCHEME 3

TABLE 1. Induction of covalent cross-links in λ-DNA by mitomycin C analogs

Compound	Concentration (μg/μl)	Max in cross-linking (%)	Time to max in cross-linking (min)
13d	2.5	78	240
13b	2.5	61	180
13a	2.5	38	90
13c	2.5	34	240

The induction of CLC sequences with compounds 13d received independent confirmation by the use of the S₁ endonuclease assay described previously employing *Escherichia coli* DNA (3) (see Table 2).

TABLE 2. Confirmation of covalent cross linking of DNA by mitomycin analogs with S₁ endonuclease assay

	Time (min)			
	10	90	195	270
% cross-linking by CLC assay	16	20	27	25
% cross-linking by S ₁ endonuclease assay	9	15	19	16

The substantially lower values for the induction of covalent cross-linking reflects the use of *E. coli* DNA of much lower molecular weight (14.8×10^6) than that of λ -DNA (31×10^6). Since only one cross-link is required per molecule to be detected by the CLC assay, a given concentration of alkylating agent will induce proportionately fewer cross-links in the *E. coli* DNA. The S_1 endonuclease assay gives different values because the time required for digestion permits a small amount of spontaneous renaturation of the *E. coli* DNA at the pH used to be compatible with the enzyme. In addition the temperature used in the enzyme digestion probably permits some slow degradation of double stranded DNA presumably via the natural "breathing" mechanism which produces transient single strand regions (12). There was no evidence of radical induced single strand cleavage of PM2 circular DNA by 13d as has been found for mitomycin C and streptonigrin (3).

Mode of Cytotoxic Action of Structurally Related Aziridinoquinones

Many aziridine containing compounds of quite different structures have useful antitumor properties (1b). Thus TEM (14, 2,4,6-tris(1-aziridinyl)-s-triazine) was the first alkylating agent found suitable for oral administration and is still in clinical use (13). Also included are tetramin (15) active against leukemia L1210 (14), TEPA (16a), phosphoramides like tris(1-aziridinyl)phosphine oxide triethylene phosphoramidate and thio-TEPA the sulfur analog 16b which effect complete regression of Flexner-Jobling rat carcinoma (15), and *N,N'*-octamethylenebis-1-aziridine-acetamide (17) which is active against Ehrlich ascites carcinoma in mammals (16). Interest in the antitumor properties of the above compounds led to the synthesis and evaluation of many aziridinoquinones from which many effective agents were found including the clinically active benzoquinones 2,5-bis(1-aziridinyl)-3,6-dipropoxy-p-benzoquinone (18a), 2,5-bis(1-aziridinyl)-3,6-bis(2-methoxyethoxy)-p-benzoquinone (18b) (17), and tris(1-aziridinyl)-p-benzoquinone, Trenimon (19)(18). In common with other alkylating agents, they exhibit greatest effectiveness against leukemias and other lymphomas such as Hodgkin's disease. The mechanisms by which aziridine containing agents exert their antitumor activity cannot as yet be stated with confidence. Among the suggestions that have been made include (i) their alkylating ability (2a), (ii) their covalent cross-linking of DNA (1, 2), and (iii) that hydrogen peroxide or other oxidizing species formed by intracellular redox reactions of quinones are the real cytostatic agent (19). Efforts have been made, without notable success, to correlate antitumor activity with magnetic susceptibility and electron delocalization (20), and with partition coefficients between benzene and aqueous phosphate buffer solutions (21).

The convenience of the ethidium fluorescence assay described above offers a means for investigating many of the suggestions that have been made with respect to the modes of action. Three general types of aziridinoquinones were synthesized, 20, 21 and 22. The induction of CLC sequences in λ -DNA was established for compounds of the type 20 and 21 in the concentration range 0.05 - 1.00 $\mu\text{g}/\mu\text{l}$ using the ethidium assay (3, 22) as illustrated in Fig. 2 and Tables 6 and 7 where agents are listed in order of cross-linking ability. Independent confirmation that this assay detects CLC sequenced DNA for this group of bifunctional alkylating agents was obtained by the S_1 endonuclease assay (3) as summarized in Table 3.

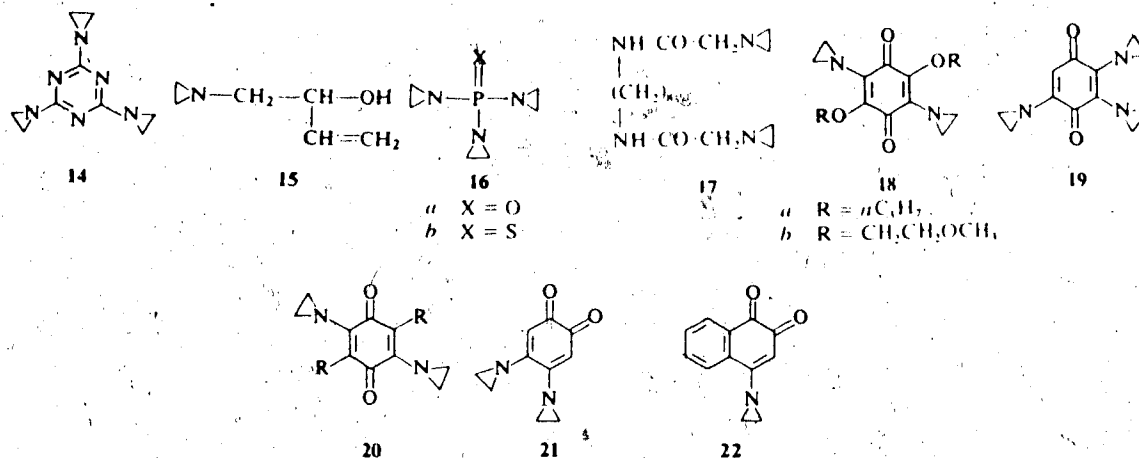


TABLE 3. Confirmation of covalent cross-linking of DNA by aziridinoquinone (20) with S₁ endonuclease assay

	Time (min)		20 R = CH ₃	
	0	45	135	270
% cross-linking by CLC assay	3.4	42.5	65.3	36.8
% cross-linking by S ₁ endonuclease*	9.7	26.7	42.0	30.6

*Corrected for double strand digestion and the fact that FU/A260 for single stranded DNA \approx 1/2 FU/A260 for double stranded DNA.

A correspondence is again noted for these independent assays bearing in mind the remarks about the S₁ assay made earlier. It may be seen that for 1,4-benzoquinones alkoxy substituents enhance both antineoplastic activity and cross-linking efficiency whereas chloro substituents suppress both these phenomena. A carbamate side chain, unless activated as in the mitomycin C structure does not contribute to increased DNA cross-linking. Ortho substituted bifunctional agents are particularly effective in cross-linking and in vivo antitumor data are awaited with interest. The monofunctional aziridine ortho and para substituted naphthoquinones are included as controls and, as expected, do not exhibit cross-linking.

pH Dependence of Covalent Cross-Linking and Alkylation without Depurination of DNA by Aziridinoquinones

As has been observed with the antitumor antibiotic mitomycin (3), the detection of CLC sequenced DNA is accompanied by a suppression of the before heat denaturation fluorescence reading. A synthetic polynucleotide containing selective radioactive labels in the purine and pyrimidine bases was treated with an aziridinoquinone to the stage where in a control

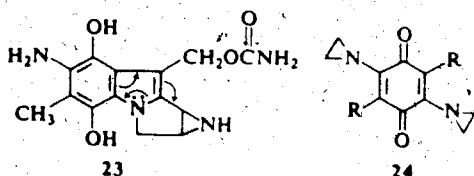
experiment an appreciable decrease in before-heat fluorescence value was observed. The alkylated DNA's were washed with trichloroacetic acid and counted. The results summarized in Table 4 show that no depurination accompanies alkylation or covalent cross-linking as was found for the antibiotic mitomycin C. This evidence together with the close parallel between cross-linking and suppression of before-heat fluorescence (see Figs. 1 and 2) strongly suggest that the latter phenomenon is due to alkylation of DNA which does not lead to cross-links and is manifest by a destruction of potential ethidium intercalation sites. Several physical explanations are possible for the latter phenomenon, for example steric hindrance to approach of the ethidium or a referee has suggested quenching of the ethidium fluorescence by nearby bound drug or by drug modified bases. We are currently examining the physical cause by employing a range of ethidium analogs but meanwhile the decrease in before-heat fluorescence is used as a measure of single covalent attachment of drugs to DNA.

TABLE 4. Radioactivity assay for monoalkylation of polynucleates with aziridinoquinones with no depurination

Time (h)	^3H (FP/TCA channel) counts $\times 10^{-3}$	^{14}C (FP/TCA channel) counts $\times 10^{-3}$	$^3\text{H}/^{14}\text{C}$
0	11.4	16.0	0.713
2	11.3	17.5	0.646
18	12.6	20.4	0.618
46	14.3	22.4	0.638
65	16.7	23.6	0.708

Freese and Cashel (23) have reported a small amount of induced cross-links in DNA by low pH alone. For example at pH 4.2 and at 25°C their sample was cross-linked to the extent of 11% over a 2 h period. In our studies of pH dependence (Figs. 1 and 2) strict controls were run with λ DNA at the corresponding pH but in the absence of the substrate. Over the time scale of our experiments no acid induced cross-linking was detected by the CLC assay.

The extent of alkylation as measured by the decrease in before-heat fluorescence showed a much more pronounced pH dependence than was found with mitomycin C (see Fig. 1). Similarly the concomitant covalent cross-linking of DNA by the aziridinoquinones shows a much more marked pH dependence than reduced mitomycin C (see Fig. 2). This reflects the structural differences; while the aziridine moiety of the activated mitosene 23 received assistance to opening by conjugative interaction of the indole nitrogen lone pair at any pH value (4), the aziridine groups in 24 require protonation to assist alkylation.



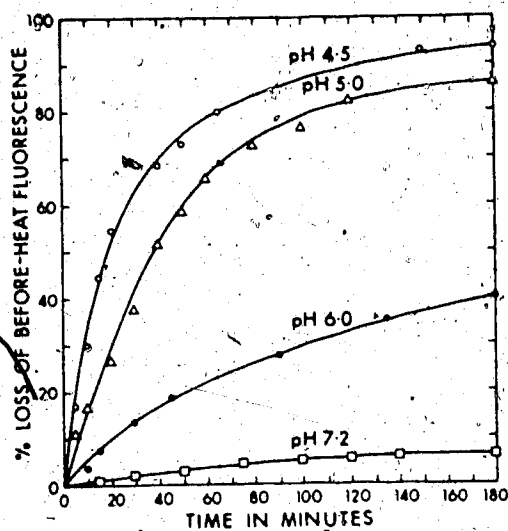


FIG. 1. The pH dependence of alkylation of λ DNA by 2,5-bis(aziridinyl)-3,6-dimethoxy-1,4-benzoquinone at a final concentration of 0.8 $\mu\text{g}/\mu\text{l}$. Reactions were performed in 1.0 M buffered aqueous solutions at 37°C, with a final DNA concentration of 1.40 O.D. 260 units.

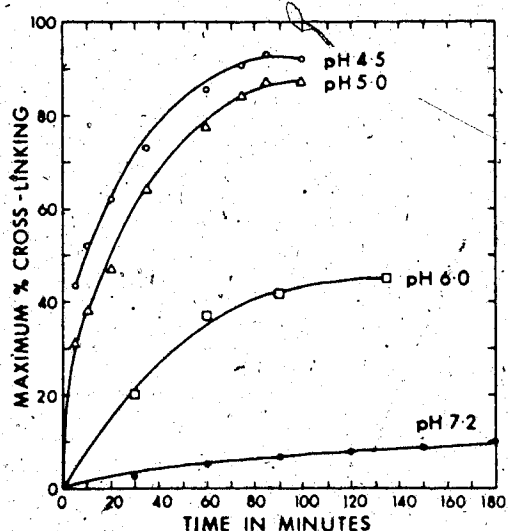


FIG. 2. The pH dependence of covalent cross-linking of λ DNA by 2,5-bis(aziridinyl)-3,6-dimethoxy-1,5-benzoquinone at a final concentration of 0.05 $\mu\text{g}/\mu\text{l}$. Reactions were carried out in ca. 1.0 M buffered aqueous solutions at 37°C with a final DNA concentration of 1.40 O.D. 260 units.

Dependence of Extent of Covalent Cross-linking of DNA's by Aziridinoquinones on (G + C) Content of DNA

No evidence has as yet been presented for any base preference in the alkylation of DNA by aziridinoquinones. Therefore we examined the interaction of 20' (R = OCH₃) with three different natural DNA's of different (G + C) content: *Clostridium perfringens*, 30%; calf thymus, 40%; and *E. coli* 50%. These three DNA's had comparable molecular weights as determined by sedimentation velocity studies and therefore their reactivity towards the aziridinoquinone could be compared directly. It may be seen from Fig. 3 that a direct correlation obtains between maximum extent of covalent cross-linking with higher (G + C) content for a given concentration of the cross-linking agents. Assuming a Poisson's distribution of the links and further that one link is sufficient to permit the spontaneous renaturation of the molecule an estimate of the average number

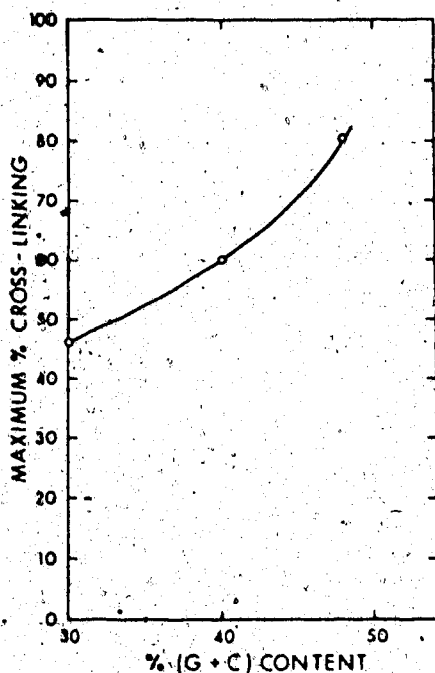


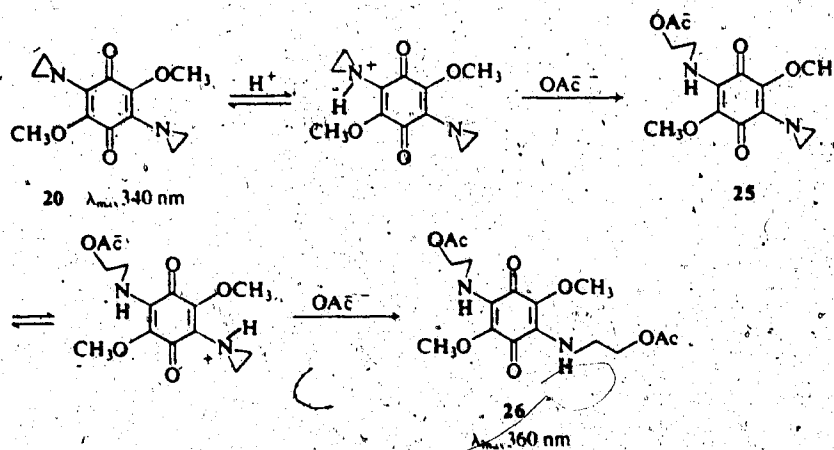
FIG. 3. The dependence of maximum percentage covalent cross-linking of DNA's by 2,5-bis(aziridinyl)-3,6-dimethoxy-1,4-benzoquinone (0.05 $\mu\text{g}/\mu\text{l}$) on the percentage (G + C) content of the DNA. The DNA's used were *Clostridium perfringens* (30% G + C), mol. wt. 11.4×10^6 ; calf thymus (40% G + C), mol. wt. 10.8×10^6 ; *E. coli* (50% G + C) 14.8×10^6 , with final concentrations respectively of 1:40, 1:145, and 1:03 O.D.₂₆₀ units.

of cross-links per molecule was made, $m = \ln(1/P_0)$, where P_0 is the proportion of the molecules unlinked as 0.62, 0.93, and 1.71 for the three DNA's. These are closely comparable with similar estimates made by Iyer and Szybalski (24) for mitomycin cross-linking. Recent work by Tomasz (25) rules out direct alkylation of the N-7 position of guanine by mitomycin C but does not exclude reaction at O-6 as originally suggested by Szybalski and Iyer (4). This may then apply to the aziridinoquinones.

Kinetics of Acid Assisted Ring Opening of Aziridinoquinones

The rate of acid assisted opening of 20 in 1 M sodium acetate buffers in the range pH 4.0 to 6.0 in 25% tetrahydrofuran - 75% water was determined spectrophotometrically employing concentrations comparable with those used for DNA cross linking, by measuring the rate of appearance of the ring opened species 26 at 380 nm. Since attempts at product isolation at intermediate stages afforded only 20 or 26 it was concluded that the lifetime of 25 was very short under the solvolysis conditions and therefore its equilibrium contribution to the absorbance at 380 nm could be neglected to a first approximation (Scheme 4).

The pseudo unimolecular rate constants at different pH values are listed in Table 5. It may be seen that the pH dependence of the aziridine opening parallels the rate of covalent cross-linking (Table 5 and Fig. 2) and of alkylation of DNA (Fig. 1). It was shown in an independent experiment that the diacetate 26 in which the aziridine rings were opened did not cross-link DNA. Therefore the strong pH dependence of the cross-linking suggests, as expected, that the active species involved directly in covalent bonding to DNA is the intermediate aziridinium ion.



SCHEME 4

TABLE 5. Pseudo unimolecular rate constants for the acid catalyzed ring opening of 2,5-diaziridino-3,6-benzoquinone

pH	Rate constant $k \times 10^{-5} \text{ (s}^{-1}\text{)}$
4.5	9.04
5.0	8.35
6.0	2.14
7.2	Too slow to measure
8.7	Too slow to measure

Correlation of Covalent Cross-Linking with Antineoplastic Activity

Having established a convenient procedure for detecting alkylation and covalent cross-linking of various DNA's by aziridinoquinones and other alkylating agents it is encouraging to observe that a fairly good correlation exists between the extent and rate of covalent cross-linking of DNA and antineoplastic activity against leukemia L1210 and several solid tumors (see Table 6). This parameter may prove useful for prescreening antitumor agents for clinical trials. It is recognized that other biological and pharmacological parameters, in addition to DNA covalent cross-linking (i.e. drug uptake, partition, metabolism, and toxicity) contribute to the ultimate effectiveness of cancer inhibitory properties. Table 7 lists covalent cross-linking results for additional aziridinoquinones for which, as yet, no *in vivo* antitumor data is available.

Experimental

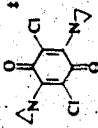
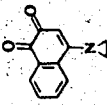
Melting points were determined on a Fisher-Johns apparatus and are uncorrected. The i.r. spectra were recorded on a Perkin-Elmer model 421

TABLE 6. Correlation of covalent cross-linking of λ DNA by bifunctional alkylating agents with antitumor activity against various tumors*

Structure	λ DNA cross-linking											
	L1210†		W-256		CA-755		S-180		KB	Concen- tration	Maxi- mum	Time to reach maximum
	OD	ILS	OD	ILS	OD	TWI	OD	TWI	ED50	($\mu\text{g}/\mu\text{l}$)	(%)	(min)
	1.5	60	1.0	95	1.0	90	3.0	75	0.04	0.04	100	5
	0.1	47	0.1	96	0.04	70	0.13	49	<0.01	0.4	100	2
	0.5	26	-	-	0.25	60	1.25	39	<1.0	0.01	92	10
	2.0	36	2.0	95	-	-	-	-	-	0.4	92	60
	0.01	39	-	-	0.05	80	0.13	65	4.9	0.04	82	120
	50	1.0	1.0	95	3.0	78	5.0	5.0	0.07	0.4	85.5	30
	2.0	7.0	0.98	84	2.0	80	3.0	63	-	0.04	79	60
										0.4	55	255

continued

TABLE 6 continued

Structure	λ DNA cross-linking														
	OD	ILS	OD	ILS	OD	ILS	OD	TWI	OD	TWL	KB	ED50	Concentration (µg/µl)	Maxim. num. (%)	Time to reach maximum (min)
	11.22	0	-	-	11	50	25	35	-	-	-	-	0.4	18	120
	100	Toxic	-	-	-	-	-	-	-	-	-	-	0.4	0	-

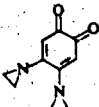
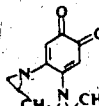
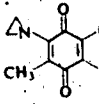
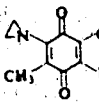
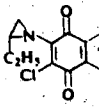
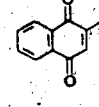
*Abbreviations used: OD optimal dose, ILS increased life span of test animals; TWI percentage tumor weight inhibition; ED50 effective dose for 50% survival.

†L1210, Leukemia 1210; W-256, Walker carcinoma 256; CA-755, carcinoma 755; S-180, Erlich ascites (9).

‡Shows antibacterial activity against Staphylococcus aureus, E. coli, and Streptococcus faecalis.

§Shows marked carcinostatic activity against Jensen sarcoma.

TABLE 7. Covalent cross-linking of λ DNA by aziridinoquinones

Structure	Concentration ($\mu\text{g}/\mu\text{l}$)	λ DNA cross-linking	
		Maximum (%)	Time to reach maximum
	0.4 0.04	85.5 80	30 105
	0.4 0.04	78.4 32.3	120 45
		59	60
	0.4	38	30
	0.24	24	270
	0.4	0	-

*Shows substantial monoalkylation.

spectrophotometer and only the principal, sharply defined peaks are reported. The n.m.r. spectra were recorded on Varian A-60 and A-100 analytical spectrometers. The spectra were measured on approximately 10-15% (w/v) solutions usually in CDCl_3 , with tetramethylsilane as a standard. Line positions are reported in p.p.m. from the reference. Mass spectra were determined on an Associated Electrical Industries MS-9 double focusing high resolution mass spectrometer. The ionization energy, in general, was 70 eV. Peak measurements were made by comparison with perfluorotriethylamine at a resolving power of 15000. Kieselgel DF-5 (Camag, Switzerland) and Eastman Kodak precoated sheets were used for thin-layer chromatography. Microanalyses were carried out by Mrs. D. Mahlow of this department. First derivative e.p.r. spectra were measured on a Varian V-2503 spectrometer fitted with a V-4532 dual cavity operating at a nominal frequency of 9.5 GHz. The microwave power incident on the cavity was attenuated to 10 dB below maximum. Hyperfine couplings were measured

by comparison with a peroxyamine disulfonate solution in the audio cavity. The triplet spacing of the standard was taken to be 13.0 Oe.

Materials

Ethidium bromide, calf thymus DNA, and α -amylase powder were purchased from Sigma Chemical Co., Sephadex G-100 superfine was from Pharmacia and DEAE cellulose was obtained from Whatman and washed before use.

4-Phenyl-2,3,4,7-tetraazobicyclo[3.3.0]oct-1-ene

A mixture of 6.14 g (60 mmol) of phenylazide and 5.60 g (60 mmol) of 3-pyrroline (75% pure) was set aside in the dark at ambient temperature for 3 weeks. The resulting precipitate was collected, washed with light petroleum, and recrystallized from ethyl acetate-petroleum ether to give 11b 6.75 g (57% yield) as a tan solid m.p. 111-112°C.

Anal. Calcd. for $C_{10}H_{12}N_4$ (mol. wt. 188.1062): C, 63.81; H, 6.43; N, 29.76. Found 188.1072 (mass spectrum): C, 63.80; H, 6.19; N, 29.45.

The i.r. spectrum ν_{max} ($CHCl_3$): 3323 (NH); 1590 cm^{-1} (N=N). The n.m.r. spectrum δ_{TMS} ($CDCl_3$): 1.43 (s, 1H, NH); 2.68-3.60 (m, 4H, CH_2); 4.32 (dd, 1H, H_1 , $J_{15} = 10$ Hz, $J_{18'} = 4$ Hz); 5.15 (dd, 1H, H_5 , $J_{56'} = 6$ Hz); 6.80 - 7.60 (m, 5H, ArH).

4-(p-Methoxyphenyl)-2,3,4,7-tetraazabicyclo[3.3.0]oct-1-ene (11c)

This compound was prepared in a similar fashion from 2.2 g (15 mmol) of p-methoxyphenylazide and 1.4 g (15 mmol) of 3-pyrroline (75% pure) in 30% yield as a white crystalline solid m.p. 108.5-109°C.

Anal. Calcd. for $C_{11}H_{14}N_4O$ (M - N_2 190.1106): C, 60.53; H, 6.47; N, 25.67. Found 190.1107 (mass spectrum): C, 60.52; H, 6.42; N, 25.19.

The i.r. spectrum ν_{max} ($CHCl_3$): 3305 (NH), 1580 cm^{-1} (N=N). The n.m.r. spectrum δ_{TMS} ($CDCl_3$): 1.46 (broad 1H, NH); 2.69-3.62 (m, 4H, CH_2); 3.79 (s, 3H, OCH₃); 4.35 (dd, 1H, H_1 , $J_{15} = 10$ Hz, $J_{18'} = 4$ Hz); 5.15 (dd, 1H, H_5 , $J_{56'} = 6.5$ Hz); 6.80-7.33 (m, 4H, ArH).

6-Phenyl-3,6-diazabicyclo[3.1.0]hexane

A solution of 2.60 g (14 mmol) of 4-phenyl-2,3,4,7-tetraazabicyclo[3.3.0]oct-1-ene in 280 ml of tetrahydrofuran under nitrogen was irradiated with a Hanovia high pressure mercury lamp (200 W) fitted with a Pyrex filter with stirring and cooling for 6 h. The solvent was removed in vacuo and the residue extracted with hot ether (6 x 100 ml). The ether extracts were concentrated giving 12b as a red brown oil, 1.95 g (87% yield).

Mol. Wt. Calcd. for $C_{10}H_{12}N_2$: 160.1001. Found (mass spectrum): 160.1007.

The n.m.r. spectrum δ_{TMS} ($CDCl_3$): 1.65-2.07 (broad 1H, NH), 2.66 (s, 2H, methine); 2.75 (AB quartet, 4H, CH_2 , $J = 12.5$ Hz); 6.65-7.34 (m,

5H, ArH). The absorption spectrum: 239 (log ϵ 4.75), 277 nm (log ϵ 3.90).

6-(p-Methoxyphenyl)-3,6-diazabicyclo[3.1.0]hexane

A solution of 0.906 g (4 mmol) of 4-(p-methoxyphenyl)-2,3,4,7-tetraazabicyclo[3.3.0]oct-1-ene in 120 ml of tetrahydrofuran under nitrogen was irradiated as described in the above procedure. The solvent was evaporated and the residue treated with 100 ml of ether. The resulting precipitate was filtered. The filtrate was evaporated and the residue crystallized from benzene - light petroleum affording 12c 0.742 g (98% yield) as an off-white solid, m.p. 36-38°C.

Anal. Calcd. for $C_{11}H_{14}N_2O$ (mol. wt. 190.1106); C, 69.45; H, 7.42; N, 14.72. Found 190.1105 (mass spectrum): C, 68.90; H, 7.57, N, 14.67.

The n.m.r. spectrum δ_{TMS} ($(CD_3)_2CO$): 2.79 (s, 2H, methine); 3.70 (s, 3H, OCH_3); 2.82 (AB quartet, 4H, methylenes, $J = 12.5$ Hz); 6.41-7.08 (m, 4H, ArH). The absorption spectrum (CH_3CN): 238 (log ϵ 4.21), 295 nm (log ϵ 3.30).

2,5-Bis-3'[-6'-p-bromophenyl-3',6'-diazabicyclo[3.1.0]-hexane]3-(β -carbamoyloxyethyl)-6-methyl-1,4-benzoquinone

A solution of 0.400 g (2.0 mmol) of freshly crushed cupric acetate monohydrate and 1.800 g (7.5 mmol) of 6-(p-bromophenyl)-3,6-diazabicyclo[3.1.0]hexane (23) in 40 ml of methanol was purged with oxygen. While bubbling oxygen through the stirred solution, a solution of 0.313 g (1.5 mmol) of 2-(β -carbamoyloxyethyl)-5-methyl-1,4-benzoquinone (24) in 75 ml of methanol was added. The reaction mixture was stirred at room temperature for 2 days, then was concentrated to ca. 5 ml and subjected to chromatography on a neutral alumina (Woelm) column eluting with methanol. The dark red band was collected and concentrated and the residue was crystallized from ethyl acetate-light petroleum to afford 13b as a purple solid, m.p. 111-113°C, which slowly turned brown on exposure to light and air.

Anal. Calcd. for $C_{30}H_{29}Br_2N_5O_4$ (mol. wt. 683): N, 10.25; Br, 23.39. Found (683, ebullioscopic): N, 9.89; Br, 23.05.

The i.r. spectrum ν_{max} ($CHCl_3$): 3544, 3434 (NH_2), 1720 (carbamate C=O), 1585 cm^{-1} (quinone C=O). The absorption spectrum (CH_3CH): 248 (log ϵ 4.26), 282 (log ϵ 3.67), 396 (log ϵ 3.09), 503 nm (log ϵ 2.57). The e.p.r. spectrum (generated by treating a 1.2×10^{-2} M methanolic solution of 13b with sodium methoxide in air), developed a signal of maximum intensity in 30 min which persisted for 2 1/2 h consisting of 10 lines h.f.s. 1.4-1.8 Oe of spectrum width 12.3 Oe.

2,5-Bis-3'[-6'-p-bromophenyl-3',6'-diazabicyclo[3.1.0]-hexane]-3,6'-dimethyl-1,4-benzoquinone

A similar reaction between 0.300 g (1.5 mmol) of freshly crushed cupric acetate monohydrate and 1.800 g (7.5 mmol) of 6-(p-bromophenyl)-

3,6-diazabicyclo[3.1.0]-hexane (26) with 0.204 g (1.5 mmol) of 2,5-dimethyl-1,4-benzoquinone in methanol afforded 13d 0.511 g (56% yield) as a brownish purple solid, m.p. 107-110°C, which slowly changed to a brown solid on exposure to light and air.

Anal. Calcd. for $C_{28}H_{24}Br_2N_4O_2$: N, 9.18, Br, 26.18. Found: N, 9.06; Br, 27.89.

The i.r. spectrum ν_{max} ($CHCl_3$): 1588 cm^{-1} (C=O). The absorption spectrum (CH_3CN): 250 (log ϵ 4.70), 285 (log ϵ 3.88), 328 (log ϵ 3.63), 395 (log ϵ 3.33), 501 nm (log ϵ 2.76). The e.p.r. spectrum (generated by treating a 1.2×10^{-2} M methanolic solution of 13d with sodium methoxide in air), developed a signal of maximum intensity within 30 min which persisted for 2 1/2 h and consisted of 11 lines, h.f.s. 1.4-1.7 Oe of total spectrum width 14.2 Oe.

2,5-Bis-3'-[6'-phenyl-3',6'-diazabicyclo[3.2.0]hexane]-3-(β -carbamoyloxyethyl)-6-methyl-1,4-benzoquinone

A similar reaction between 0.400 g (2.0 mmol) of cupric acetate and 1.60 g (10.0 mmol) of 6-phenyl-3,6-diazabicyclo[3.1.0]hexane with 0.418 g (2.0 mmol) of 2-(β -carbamoyloxyethyl)-5-methyl-1,4-benzoquinone (24) in methanol afforded 13a as a red-brown solid from ethyl acetate-light petroleum, 0.892 g (85% yield), m.p. 80-83°C, which slowly turned brown on exposure to air and owing to its instability was characterized spectroscopically.

The i.r. spectrum ν_{max} ($CHCl_3$): 3546, 3426 (NH_2); 1725 (carbamate C=O); 1595 cm^{-1} (quinone C=O). The absorption spectrum (CH_3CN): 241 (log ϵ 4.58), 282 (log ϵ 3.92), 394 (log ϵ 3.22), 503 nm (log ϵ 2.72). The e.p.r. spectrum (generated from 13a as described above) developed a signal due to the semiquinone of maximum intensity in 30 min which persisted for 2 1/2 h and consisted of 10 lines h.f.s. 1.5-1.8 Oe of total spectrum width 12.5 Oe.

2,5-Bis-3'-[6'-p-methoxyphenyl-3',6'-diazabicyclo[3.1.0]-hexane]-3-(β -carbamoyloxyethyl)-6-methyl-1,4-benzoquinone

A similar reaction of 0.400 (2.0 mmol) of cupric acetate and 1.900 g (10 mmol) of 6-p-methoxyphenyl-3,6-diazabicyclo[3.1.0]hexane in 50 ml of methanol with 0.418 g (2.0 mmol) of 2-(β -carbamoyloxyethyl)-5-methyl-1,4-benzoquinone (27) afforded 13c 0.199 g (17% yield) as a purple solid from ethyl acetate, m.p. 98-103°C which slowly turned brown on exposure to light and air.

Anal. Calcd. for $C_{32}H_{35}N_5O_6$: C, 65.63; H, 6.02; N, 11.96. Found: C, 65.11; H, 6.41; N, 9.99.

The i.r. spectrum ν_{max} ($CHCl_3$): 3520 and 3418 (NH_2); 2826 (OCH_3); 1723 (carbamate C=O); 1568 cm^{-1} (quinone C=O). The absorption spectrum (CH_3CN): 242 (log ϵ 4.52), 290 (log ϵ 3.97), 397 (log ϵ 3.47), 506 nm (log ϵ 2.94). The e.p.r. spectrum (generated from 13c as described above) developed a signal of the semi quinone within 30 min which persisted for over 2 h and consisted of an unresolved singlet of spectrum width 5.8 Oe.

Synthesis of Aziridinoquinones

Most of the aziridinoquinones studied were prepared by published procedures (17). The general method is illustrated by the following example.

Preparation of Tetramethoxy-1,4-benzoquinone

A slurry of 24.5 g (0.1 mol) of chloranil in 75 ml of methanol was added to a solution of 9.8 g (0.42 mol) of sodium in 250 ml of methanol. During addition the temperature of the reaction mixture was kept at 15-25°C by means of external cooling. The reaction mixture was then heated on a steam bath for 6 h. The cooled reaction mixture deposited bright orange crystals which were collected, washed with cold water, and taken up in dichloromethane. The solution was decolorized with charcoal, filtered and the solvent removed in vacuo to give bright orange crystals of the product, 16.7 g (73.2% yield), m.p. 133-134°C (lit. (28) m.p. 135-136°C).

Reaction of Tetramethoxy-1,4-benzoquinone with Aziridine

To a suspension of 1.05 g (5 mmol) of tetramethoxy-1,4-benzoquinone in 30 ml of methanol was added a solution of 0.280 g (65 mmol) of aziridine in 10 ml of methanol. The reaction mixture was stirred at room temperature for 2 days. The resulting reddish-brown 2,5-bis(aziridinyl)-3,6-dimethoxy-1,4-benzoquinone was collected by filtration, 0.875 g (75% yield), m.p. 189-190°C (lit. (17a) m.p. 193-194.5°C). The n.m.r. spectrum: δ_{TMS} (CDCl₃): 2.28 (s, 8H, aziridinyl protons) and 3.92 (s, 6H, OCH₃).

New compounds prepared using these procedures include:

(i) 2,5-Bis(2-methylaziridinyl)-3,6-dimethyl-1,4-benzoquinone in 63% yield, m.p. 147-150°C.

Anal. Calcd. for C₁₄H₁₈N₂O₂: C, 68.29; H, 7.31; N, 11.38. Found: C, 68.21; H, 7.61; N, 11.72.

(ii) 2,5-Bis(2-ethylaziridinyl)-3,6-dimethyl-1,4-benzoquinone in 50% yield, m.p. 125-126°C.

Anal. Calcd. for C₁₆H₂₂N₂O₂: C, 70.44; H, 8.03; N, 10.08. Found: C, 70.04; H, 8.54; N, 10.38.

(iii) 4,5-Bis(2-methylaziridinyl)-1,2-benzoquinone in 47% yield, m.p. 135-138°C.

Anal. Calcd. for C₁₂H₁₄N₂O₂: C, 66.05; H, 6.42; N, 12.85. Found: C, 65.85; H, 6.51; N, 13.01.

Fluorescence Assay for Detecting CLC Sequences and Monpalkylation

The general procedure employing a G.K. Turner and Associates model 430 spectrofluorometer has been described previously. The assay mixture was prepared by mixing 2 ml of a 1 M K₂HPO₄-KOH buffer (at pH 12.0) with 0.2 ml of a 0.2 M solution of EDTA disodium salt (buffered at pH 8 with

2 M K_3PO_4) and with 0.05 ml of a 1 mg/ml solution of ethidium bromide in water. The resulting mixture was made up to 100 ml with distilled water and was covered with aluminum foil to protect it from the light. The instrument was blanked using 2 ml of the above solution. The cross-linking assays were carried out as follows.

Bicycloaziridinobenzoquinones

The cross-linking agents were added as 5 $\mu\text{g}/\mu\text{l}$ solutions in 40% pyridine - 60% water. DNA was added as an aqueous solution. Reactions were buffered to pH 4.5 with 1 M sodium acetate - acetic acid buffer. Cross-linking reactions were carried out on a 60 μl scale. The reaction solutions were incubated at 37°C and had concentrations of 1.06 O.D. 260 units of λ DNA, 0.05 M of buffer, 2.5 $\mu\text{g}/\mu\text{l}$ of cross-linking agent and 20% pyridine; 10 μl aliquots were removed at timed intervals and analyzed for the extent of cross-linking by CLC assay described previously (3). A control reaction mixture prepared exactly as above but containing no cross-linking agent was run with each experiment. In no case was there evidence for acid induced covalent cross-linking.

Bisaziridinoquinones

A 10 μl aliquot of the cross-linking reaction mixture (ca. 5 $\mu\text{g}/\mu\text{l}$ of alkylating agent in 25% tetrahydrofuran - 75% water, 1 M sodium acetate buffer and DNA) was diluted in 2 ml of the solution. Similarly a 10 μl aliquot was withdrawn from a reaction mixture containing no alkylating agent (control) and was diluted in 2 ml of the assay solution. The solutions were analyzed by the CLC assay described previously (3). A typical run is given in complete form for 2,5-bis(aziridino)-3,6-dimethoxy-1,4-benzoquinone at pH 5.0 with a concentration of 0.8 $\mu\text{g}/\mu\text{l}$.

Time (min)	Before-heat fluorescence*	After-heat fluorescence	% Cross-linking
0	70	3.5	0
5	64	12.5	19.5
10	60	17	28.3
20	52	23	44.2
30	45	24	53
40	35	20	57
50	30	18	63
60	25	17	67
80	20	15	75
100	15	12	80
120	13	11	82
150	10	8	80
180	9	6	67

*Control fluorescence = 70 constant throughout experiment.

Covalent Cross-Linking of DNA's with Different (G + C) Content with 2,5-Bis(aziridino)-3,6-dimethoxy-1,4-benzoquinone

The CLC assays were performed at pH 4.5 and 37°C as described

above using the following solutions of natural DNA's.

Clostridium perfringens DNA (30% G + C)

The assay mixture was prepared using 7 μ l of the DNA stock solution (O.D.₂₆₀ = 20), 5 μ l of 1 M sodium acetate buffer pH 4.5, 8 μ l of water, and 80 μ l of a solution of 20 (R = OCH₃) in 25% aqueous tetrahydrofuran (final concentration of agent 0.05 μ g/ μ l and final concentration of DNA was 1.40 O.D.₂₆₀). The control was similar but lacked 20 (R = OCH₃).

Calf Thymus DNA (40% G + C)

The assay mixture was prepared using 30 μ l of the DNA stock solution (O.D.₂₆₀ = 4.58), 5 μ l of 1 M sodium acetate buffer pH 4.5, 5 μ l of water, and 80 μ l of the solution of agent 20 (R = OCH₃) (final concentration of agent was 0.05 μ g/ μ l and of DNA 1.145 O.D.₂₆₀). Control as above.

E. coli DNA (50% G + C)

The assay mixture was prepared using 25 μ l of the DNA stock solution (O.D.₂₆₀, 1.03), 5 μ l of 1 M sodium acetate pH 4.5, 5 μ l of water, and 40 μ l of a 25% aqueous solution of 20 (R = OCH₃) (final concentration of agent 0.05 μ g/ μ l, and final concentration of DNA was 1.03 O.D.₂₆₀). Control as above.

Assay for Covalent Cross-Linking of E. coli DNA using S₁ Endonuclease

E. coli DNA which had been covalently cross-linked with the bifunctional alkylating agent was dialyzed overnight at 4 °C vs. 10 mM potassium phosphate at pH 11.5, 0.1 mM EDTA, neutralized with 0.5 M tris hydrochloride pH 7.5 (~25 mM), and heat denatured (5 min at 95°C then ice treatment). To 80 μ l were added 20 μ l 5 x S₁ buffer pH 4.5 (final pH about 4.6). After removal of the first aliquot, 2 μ l of purified S₁ endonuclease (610 U/mg, 1.28 mg/ml) was added and the mixture incubated at 45°C. Aliquots were removed and examined with ethidium bromide solution pH 8.0 and read as described previously. Heat denatured and native E. coli DNA's were incubated as controls.

Assay for Depurination of Radioactively Labeled Polynucleates Treated with 2,5-Bis(aziridino)-3,6-dimethoxy-1,4-benzoquinone

Poly dG.dC(¹⁴CG).d(³HC) 0.339 A₂₆₀/ml was incubated at 37°C in 50 mM sodium buffer pH 5.0 with 260 μ g/ml of 2,5-bis(aziridino)-3,6-dimethoxy-1,4-benzoquinone in 18% aqueous tetrahydrofuran. At intervals duplicate samples were removed, placed on Whatman filter discs, washed with 5% trichloroacetic acid, then twice with ethanol, dried, and counted. The results summarized in Table 4 show no loss of purine or pyrimidine bases accompany treatment of the DNA by the aziridinoquinone.

Kinetic Studies of the Rate of Acid Catalyzed Ring Opening of Aziridinoquinones

A 1.04 x 10⁻³ M solution of the 2,5-bis(aziridinyl)-3,6-dimethoxy-

1,4-benzoquinone was prepared in 25% THF - 75% H₂O at room temperature and transferred in 160 μ l aliquots to reaction tubes and then 10 μ l of water, 20 μ l of λ DNA, and 10 μ l of 1 M sodium acetate buffer (of the appropriate pH) were added. The tubes were sealed with Parafilm and placed in a constant temperature bath. Several reaction tubes were withdrawn at convenient intervals, diluted with 25% THF - 75% H₂O to 5 ml and the concentration of 2,5-bis(2-acetoxyethylamino)-3,6-dimethoxy-1,4-benzoquinone was established by its absorbance at 380 nm. It was demonstrated that both the aziridinoquinone and the 2-acetoxyethylaminoquinone obeyed the Beer-Lambert Law in the optical density range of 0.02 - 0.4. Allowance was made for residual absorption at 380 nm due to the aziridine (see Table 8).

The reaction followed good first-order (pseudo unimolecular) kinetics for the formation of the diacetate the time dependence of which is shown in full for the run at pH 4.5 (see Table 9).

TABLE 8. Absorption spectra

Wavelength (nm)	Absorbance <u>20</u>	Absorbance <u>26</u>
330	0.29	0.20
340	0.31	0.29
250	0.275	0.375
360	0.20	0.43
370	0.135	0.39
380	0.08	0.270
400	0.03	0.055

TABLE 9. Rate of acid assisted ring opening of 2,5-bis(1-aziridinyl)-3,6-dimethoxy-1,4-benzoquinone

Time (min)	Optical density	$k \times 10^5$ (s ⁻¹)
0	0.08	-
30	0.11	9.15
60	0.135	9.04
90	0.154	8.97
120	0.169	9.08
150	0.185	9.03
210	0.211	8.75
270	0.225	9.04
330	0.240	9.14
420	0.251	9.13

This research was supported by grants to J.W.L. from the National Cancer Institute of Canada, the National Research Council of Canada, and

by the Department of Chemistry, University of Alberta. We thank Dr. A. Hogg and Mr. R. Swindlehurst for the mass and n.m.r. spectra, and Mrs. Talat Akhtar for the preparation of many intermediates.

1. J.A. MONTGOMERY, T.P. JOHNSTON, and Y.F. SHEALY. In Drugs for neoplastic diseases. In Medicinal Chemistry. Pt. 1. Edited by A. Burger. Wiley-Interscience, New York. 1970. (a) p. 680; (b) p. 695.
2. (a) W.C.J. ROSS. Biological alkylating agents. Butterworths, London. 1962; (b) G.P. WHEELER. Cancer Res. 22, 651 (1962).
3. W.J. LOWN, A. BEGLEITER, A.R. MORGAN, and D. JOHNSON. Can. J. Biochem. 54, 110 (1976).
4. (a) W. SZYBALSKI and V.N. IYER. Fed. Proc. 23, 946 (1964). (b) W. SZYBALSKI and V.N. IYER. In Antibiotics I - mechanism of action. Edited by D. Gottlieb and P.D. Shaw. Springer-Verlag, New York. 1967. p. 211.
5. (a) W.A. REMERS and M.J. WEISS. J. Med. Chem. 11, 737 (1968) and papers cited therein. (b) R.W. FRANCK et al. J. Org. Chem. 38, 3487 (1973); 39, 3739 (1974) and references therein. (c) T. HIRATA, Y. YAMADA, and M. MATSUI. Tetrahedron Lett. 4107 (1969). (d) T. TAKADA and S. OHKI. Chem. Pharm. Bull. (Jpn.), 19, 977 (1971). (e) T. TAKADA, S. KUNUGI, and S. OHKI. Chem. Pharm. Bull. (Jpn.), 19, 982 (1971). (f) P. GERMERAAD and H.W. MOORE. J. Org. Chem. 39, 774 (1974). (g) T. TAKADA and M. AKIBA. Chem. Pharm. Bull. (Jpn.), 20, 1785 (1972). (h) S. KINOSHITA, K. UAU, K. NAKANO, M. SHIMIZU, T. TAKAHASHI, and M. MATSUI. J. Med. Chem. 14, 103 (1971); 14, 109 (1971).
6. (a) S.V. BHIDE, Chem. Biol. Interactions, 8, 19 (1974). (b) G. PRODI, P. ROCCHI, and S. GRILLI. Cancer Res. 30, 2887 (1970). (c) T.A. LAWSON and A.W. POUND. Pathology, 3, 223 (1971). (d) T.A. LAWSON and A.W. POUND. Chem. Biol. Interactions, 4, 329 (1970).
7. (a) E.F. GALE, E. CUNDLIFFE, P.E. REYNOLDS, M.H. RICHMOND, and M.J. WARING. The molecular basis of antibiotic action. J. Wiley, New York. 1972. p. 214. (b) L.S. LERMAN, J. Mol. Biol. 3, 18 (1961).
8. (a) P. HOCHSTEIN, J. LASZLO, and D. MILLER. Biochem. Biophys. Res. Commun. 19, 289 (1965). (b) J.R. WHITE and H.L. WHITE. Mol. Pharm. 4, 579 (1968). (c) R. CONE, S.K. HASAN, J.W. LOWN, and A.R. MORGAN, Can. J. Biochem. 54, 219 (1976).
9. (a) Proc. Symp. Quinones as Anticancer Agents. Cancer Chemother. Rep. 4, (1974). (b) E.F. ELSLAGER. In Medicinal Chemistry. 2nd ed. Edited by A. Burger. Interscience Publishers, New York. 1960. pp. 851-876. (c) P. TRUITT, F. MAHON, O. PLATAS, R.L. HALL, and T. ELERIS. J. Org. Chem. 25, 962 (1960).
10. (a) S. OIDA, H. KAWANO, Y. OHASHI, and E. OHKI. Chem. Pharm. Bull. (Jpn.), 18, 2478 (1970). (b) P. SCHIENER. Tetrahedron, 24, 2757 (1968).
11. A.H. CROSBY and R.E. LUTZ. J. Am. Chem. Soc. 78, 1233 (1956).
12. B. McCONNELL and P.H. VON HIPPEL. J. Mol. Biol. 50, 297 (1970).
13. (a) S.M. BUCKLEY, C.C. STOCK, M.L. CROSSLEY, and C.P. RHOADS. Cancer Res. 10, 207 (1950). (b) J. H. BURCHENAL, M.L. CROSSLEY, C.C. STOCK and C.P. RHOADS. Arch. Biochem. Biophys. 26, 321 (1950).
14. (a) H. OETTEL. Angew. Chem. 71, 222 (1959). (b) J.M. VENDETTI, A. GOLDEN, and I. KLINE. Cancer Chemother. Rep. 4, 73 (1961). (c) W. SCHULZE. Deut. Med. Wochschr. 82, 1465 (1957); (d) F.R. WHITE.

- Cancer Chemother. Rep. 4, 52 (1959).
15. C. HEIDELBURGER and M.E. BAUMANN. Cancer Res. 17, 277 (1957).
 16. W.A. SKINNER and J. SCHOLLER. Cancer Chemother. Rep. 51, 205 (1967).
 17. (a) S. PEDERSEN, W. GAUSS, and E. URBSCHAT. Angew. Chem. 67, 217 (1955). (b) W. GAUSS and S. PEDERSEN. Angew. Chem. 69, 252 (1957). (c) G. DOMAGK. Ann. N.Y. Acad. Sci. 68, 1197 (1958).
 18. W. GAUSS and G. DOMAGK. German Patent 1,044,816 (1958). Chem. Abstr. 55, 11435f (1961).
 19. (a) H. BERG and G. HORN. Naturwissenschaften, 50, 356 (1963). (b) G. HORN. Chem. Zvesti, 18, 363 (1964); Chem. Abstr. 61, 15947.
 20. (a) G. MAYR and G.C. RABOTTI. Experientia, 13, 252 (1957). (b) E.M. McCRAY and H.F. SCHOOF. J. Econ. Entomol. 60, 60 (1967).
 21. A.H. SOLOWAY et al. J. Med. Pharm. Chem. 5, 1371 (1962).
 22. (a) A.R. MORGAN and V. PAETKAU, Can. J. Biochem. 50, 210 (1972). (b) A.R. MORGAN and D.E. PULLEYBLANK. Biochem. Biophys. Res. Commun. 61, 346 (1974). (c) M. COULTER, W. FLINTOFF, V. PAETKAU, D. PULLEYBLANK, and A.R. MORGAN. Biochemistry 13, 1603 (1974).
 23. E. FREESE and M. CASHEL. Biochim. Biophys. Acta, 91, 67 (1964).
 24. V.N. IYER and W. SZYBALSKI. Proc. Natl. Acad. Sci. 50, 355 (1963).
 25. M. TOMASZ, Biochim. Biophys. Acta 213, 288 (1970).
 26. J.W. LOWN and A. BEGLEITER. Can. J. Chem. 52, 2331 (1974).
 27. H. NAKAO, M. ARAKAWA, T. NAKAMURA and M. FUKASHIMA. Chem. Pharm. Bull. (Jpn.), 20, 1962, 1968 (1972).
 28. B. EISTERT and G. BOCK. Ber. 92, 1239 (1959).

(Submitted for publication to Canadian Journal of Biochemistry, 1976)

Effects of Alkylation by Dimethyl Sulfate, Nitrogen Mustard
and Mitomycin C on DNA Structure as Studied by the
Ethidium Binding Assay

Hansen Hsiung¹, J. William Lown

Department of Chemistry
University of Alberta
Edmonton, Alberta
T6G 2G2

Douglas Johnson

Department of Biochemistry
University of Alberta
Edmonton, Alberta
T6G 2G2

¹National Cancer Institute of Canada Postdoctoral Fellow 1975-76.

ABSTRACT:

The extent of alkylation of DNA by dimethyl sulfate, nitrogen mustard and the antibiotic mitomycin C is related to the resulting decrease in the fluorescence of intercalated ethidium. The fluorescence losses due to the first two types of reagents show a marked pH dependence with greater losses of fluorescence being observed at alkaline pH's. At pH 11.6 the fluorescence shows a slow recovery so that with low levels of methylation (~4% deoxyguanosine residues modified) one observes complete return of fluorescence. We postulate that these phenomena are due to conversion of 7-methyldeoxyguanosine to the zwitterionic form and partial denaturation of the DNA duplex with loss of ethidium binding sites. Hydroxide ion catalyzed imidazole ring opening, and the removal of the positive charge permits reannealing with concomitant return of the ethidium intercalation sites. This conclusion is substantiated by enzymatic hydrolysis of [¹⁴C] methylated DNA and identification of the two types of deoxyguanosine residues formed under the different conditions of the ethidium assay. The distinctly different behavior of mitomycin C confirms previous conclusions that its alkylation, preferentially on guanine, does not take place at the N-7 position.

INTRODUCTION:

Many effective antitumor agents as well as carcinogens and mutagens belong to the class of alkylating agents (1). There is much evidence

(inactivation of viruses, antimitotic, cytological and mutagenic effects) from in vitro and in vivo reactions and physico-chemical alterations that indicates nucleic acids are often the principal target site for such agents (1-3). While alkylation of DNA bases may be detected by using radioactive labels, a more convenient assay which can discriminate between different sites of covalent attachment would clearly be useful.

We describe how the fluorescence properties of the trypanocidal drug ethidium bromide, may be useful in this regard. It was observed by Le Pecq and Paoletti (4) that ethidium bromide, which is widely used as a histological stain for nucleic acid containing structures in cells, intercalates into duplex nucleic acids. The intercalation process shows little or no base preference and the primary sites are saturated when one drug molecule is bound for every 4 or 5 nucleotides. Binding is also independent of pH within the range where the double helix is stable (3). During this primary binding the fluorescence shows a fifty-fold enhancement. This phenomenon has been attributed to the removal of quenching by the polar solvent as the dye is absorbed into the hydrophobic region of the duplex (3,4). This property has been made use of by Morgan in the development of elegant and convenient assays for detecting covalent cross-linking and strand scission of DNA by a variety of agents (5,6). Recently, these techniques have been used to examine the interaction of certain antitumor antibiotics with nucleic acids (7-9). During these studies it was noted that the loss in ethidium fluorescence which accompanies alkylation of DNA by mitomycin C (with concomitant loss of potential intercalation sites) is linearly related to the extent of alkylation. In this paper the alkylation of DNA by dimethyl sulfate, nitrogen mustard and mitomycin C is studied in more detail. The effects of alkylation on ethidium binding to DNA are examined and the alkylation induced structural changes on DNA at different pH's are also studied by the fluorescence technique.

METHODS:

Materials. Reagent grade dimethyl sulfate and deoxyguanosine were obtained from Aldrich. [^{14}C]-Dimethyl sulfate was from New England Nuclear with a specific activity of 13 mCi/nmole. Ethidium bromide and calf thymus DNA were obtained from Sigma, the 2'-deoxynucleosides from ICN and mitomycin C from Calbiochem. λ -DNA and [^3H]- λ -DNA were prepared as before (6). The mitomycin C stock solution (10^{-3} M in distilled water) was kept at 4° in the dark. Nitrogen mustard (methyl bis-(8-chloroethyl)amine hydrochloride) was prepared from 2-methylamino-ethanol (10). 7-Methylguanosine was prepared from guanosine following a procedure due to Jones and Robins (11). The chromatographically pure product was dried under vacuum m.p. $158-160^\circ$ (lit (11) m.p. $159-160^\circ$). 7-Methyl-2'-deoxyguanosine 1b was prepared from deoxyguanosine by the procedure of Jones and Robins (11). The white crystalline product was washed with ether and dried, 81% yield m.p. 135° (lit (11) m.p. 135°). 2-Amino-5-(n-methylformamido)-6-(D-2'-deoxyribofuranosylamine)-4-pyrimidinal 4b was prepared from 7-methyldeoxyguanosine by the procedure of Townsend and Robins in 55% yield (12).

Fluorescence assays. The techniques employed in the assay for alkylation were similar to those used in the assay for CLC (covalently linked complementary) sequences in DNA which have been described (5,6). The standard fluorescence solutions which were 20 mmolar potassium phosphate (pH 7 or 11.6), 0.4 mmolar EDTA, 0.5 $\mu\text{g/ml}$ of ethidium bromide were stored in the dark. Aliquots of the treated DNA solutions (5-20 μl) from reaction mixtures were added to 2 ml of the solution. The fluorescence values were read on a Turner Spectrofluorometer model 430 with excitation at 525 nm and emission at 600 nm using the ethidium solution as blank. Cuvettes (1 cm, round borosilicate glass) were used and the cell compartment was thermostatted at 23°.

Methylation of DNA by dimethyl sulfate. Unlabelled and [^{14}C]-dimethyl sulfate (specific activity of 13 mCi/mole) were prepared as 1 M stock solutions in acetonitrile previously dried over calcium hydride. Aqueous DNA solutions, either λ or calf thymus (5-10 A_{260}) in cacodylate buffer, were methylated by the addition of 20 mmolar dimethyl sulfate in solution (15). The acid released by the aqueous hydrolysis of the methylating agent was neutralized by addition of 0.3 M cacodylate buffer pH 8.0 so that the pH did not fall below 6. The reaction was allowed to proceed for 1 hr at 37° by which time most of the dimethyl sulfate was consumed either by reaction with DNA or hydrolysis. After the methylation was completed, a 75 μl aliquot was removed and dialyzed at 0-4° against three changes of 400 ml of 0.02 M phosphate pH 7 buffer at intervals of 6 hr. After dialysis, the methylated DNA solution was assayed for ^{14}C by adding 10 ml of scintillation fluid (Scinti-Verse, Fisher) and counting on a Searle Analytic Inc. Mark III 6880 Liquid Scintillation System. Counting efficiency normally at 60-70% was determined either by channels ratio or the external standard method. The DNA concentration was determined by uv absorption at 260 nm and the extinction coefficient (ϵ) at this wavelength was taken as 7000. A 5 μl aliquot of the reaction mixture was also added to both pH 7 and 11.6 ethidium stock solutions to measure the fluorescence values at timed intervals 0, 10, 20, 30, 60, 90 and 120 min after the addition of DNA samples to the ethidium test solutions. Greater extents of methylation were achieved by using proportionally greater concentrations of dimethyl sulfate.

$d(\text{C})_n \cdot d(\text{G})_n$ (Miles Laboratories) at a concentration of 1 A_{260} was alkylated by similar procedures with increasing concentrations of dimethyl sulfate. At pH 11.6 the fluorescence showed a complete return to the control value (no dimethyl sulfate present) when $d(\text{C})_n \cdot d(\text{G})_n$ was incubated with 20 mmolar dimethyl sulfate. Since about 90% of methylation of DNA occurs on G-7 (15,16,21) and because 3-methylated A shows no base catalyzed opening, the assumption is made that methylation at sites other than G may be ignored for the interpretation of the fluorescence data (see discussion).

Alkylation of calf thymus DNA by nitrogen mustard (methyl bis-(8-chloroethyl)amine). Calf thymus DNA was alkylated by incubation with the nitrogen mustard for 1 hr at pH 8.0 at 37° in 0.25 M cacodylate buffer. The final concentration of DNA in the reaction mixture was 7.5 A_{260} , and that of the nitrogen mustard 10-50 mmolar. A 5 μl

aliquot of the nitrogen mustard alkylated DNA was also added to the ethidium solutions at pH 7 and 11.6 for the fluorescence assays. Time dependent studies on the fluorescence behavior were also carried out as described above for methylated DNAs.

Alkylation of [³H]-λ-DNA by mitomycin C. The reaction of reductively activated mitomycin C with [³H] DNA (specific activity 40,000 cpm/A₂₆₀ unit) was carried out following the procedure described previously (7). Unbound mitomycin C was removed by dialysis against a solution of 10 mmolar potassium phosphate and 0.1 mmolar EDTA at pH 11.6. The extent of alkylation was determined by absorption spectroscopy (13) and the nucleotide concentration by radioactive counting of ³H. Extinction coefficients of 7000 at 260 nm for DNA and 11,000 for covalently bound mitomycin C at 314 nm were used (see Figure 3).

Enzymatic hydrolysis of methylated DNA. Calf thymus DNA (concentration 7.5 A₂₆₀) was methylated by [¹⁴C]-dimethyl sulfate (100 mmolar) and the extent of methylation was monitored by the loss of fluorescence as described above. The methylated DNA was then subjected to dialysis against either pH 7 or pH 11.6 20 mmolar potassium phosphate buffer for 16 hr. The potassium phosphate was removed by dialysis prior to the enzyme treatment. A 100 μl aliquot of each dialyzed methylated DNA sample was taken and treated sequentially with the three hydrolyzing enzymes. The methylated DNA was first incubated with pancreatic DNase (50 μg/ml) for 1 hr at 37° in 10 mmolar MgCl₂, 50 mmolar tris-HCl pH 7.5 buffer. Snake venom phosphodiesterase (final concentration 50 μg/ml) was then added and the incubation period was continued for another hour. Finally the DNA hydrolyzate was treated with bacterial alkaline 5'-phosphomonoesterase (E. C. 3.1.3.1) (72 μg/ml) at 37° for 1 hr. The hydrolyzate was concentrated by gentle blowing of nitrogen and saved for the paper and thin layer chromatography studies.

Sedimentation studies on methylated DNA. Methylated λ-DNA or calf thymus DNA as well as native DNAs were dialyzed against 20 mmolar potassium phosphate buffers at pH 7 and pH 11.6. The molecular weights of the DNAs after dialysis were determined from sedimentation velocity measurements using a Beckman Model E analytical ultracentrifuge equipped with a scanner (18).

Paper Chromatography. No. 1 Whatman paper was used in descending paper chromatography. The developing solution was taken from the upper layer of a (1:1) 2-butanol-water mixture (14). Radiolabelled deoxyribonucleosides from the enzyme hydrolysis of the ¹⁴C-methylated calf thymus DNA were spotted together with authentic deoxyribonucleosides and methylated deoxyribonucleosides. The chromatogram was developed for 30 hr, dried and cut into 2 cm wide strips. The radioactivity was counted in a scintillation counter. The locations of the bands and the authentic unlabelled standards were visualized under uv light (see Figure 5).

Thin layer chromatography. Compounds 1b and 4b (see Scheme) are well separated on silica gel S11G-25 precoated plates (Macherey-Nagel Co., Doren, Germany) using ethanol:water (7:3) as eluant. The deoxyribo-

nucleosides from the enzyme hydrolyzed [^{14}C]-methylated DNA were accordingly separated by silica gel thin layer chromatography. The cpm were plotted as before along with the locations of authentic unlabelled standards visualized under uv light.

UV Absorption spectra. 7-methyldeoxyguanosine 1b was prepared as a 10^{-3} M solution in distilled water. A 50 μl aliquot of this solution was diluted to 1 ml with potassium phosphate buffers (0.05 M) of different pH values. The final concentration of 1b was 5×10^{-5} M in buffer. The uv spectra were determined at timed intervals, 0, 0.5 and 2 hrs.

RESULTS:

pH Dependence of Fluorescence Loss Due to Reaction of DNA with Dimethyl Sulfate. Methylation of λ -DNA causes a progressive loss of fluorescence as measured in the ethidium assay (Figure 1) and the fluorescence loss is also strongly pH dependent. In the pH 7 ethidium solution, the loss of fluorescence shows a linear dependence with the extent of methylation. However, at pH 11.6 the loss of fluorescence is no longer linear. λ -DNA with relatively low degrees of methylation (~4% modified dG) shows similar fluorescence values at pH 11.6 to those at pH 7, but as the extent of methylation increases, the fluorescence loss is more pronounced at the higher pH values. Native DNA shows the same ethidium fluorescence values independent of pH.

The results of equilibrium dialysis of ethidium against methylated λ -DNA show less ethidium is bound to the alkylated DNA than to the native DNA (see Table 1). This rules out the possibility that the observed loss of fluorescence is due to quenching by the methylated residues in the DNA. In parallel experiments a sedimentation study showed that a reduction in the molecular weight of the DNA was not itself responsible for the losses of fluorescence noted earlier.

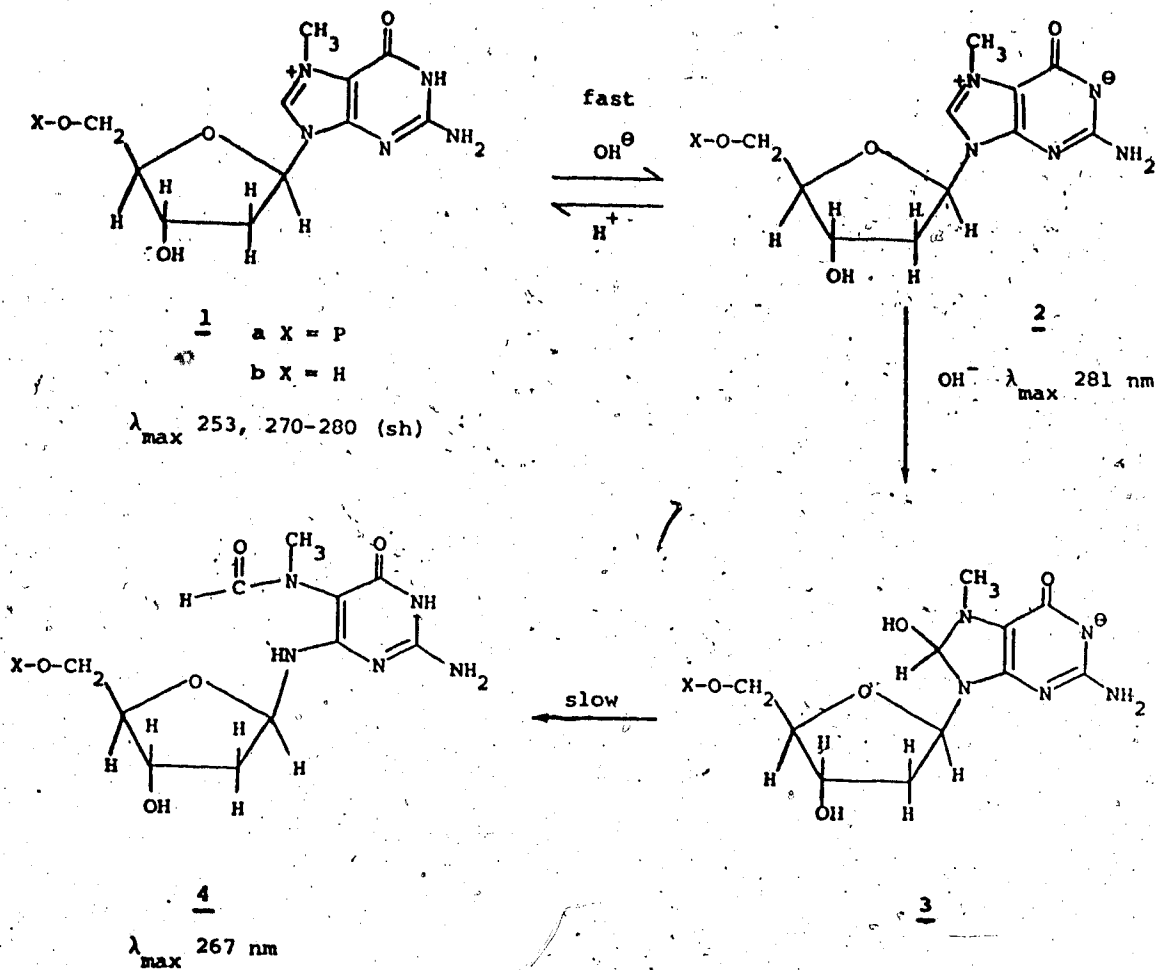
Binding of ethidium to alkylated DNAs. The binding constants of ethidium to the dialyzed methylated DNAs were determined in 20 mmolar potassium phosphate buffer at pH 7. Both primary (intercalative) and secondary binding were observed from the Scatchard plots, the mathematical treatment of which followed that of Le Pecq and Paoletti (4). Binding constants and total binding sites for the primary binding are given in Table 2. The results clearly indicate that the binding constant of ethidium was not altered by methylation; however, the total number of binding sites is decreased in proportion to the extent of methylation. Therefore, the fall in fluorescence correlates well with the loss of binding sites. One per cent of methylation of the DNA bases causes a six to eight per cent loss of fluorescence. This implies that for each methylation event, 3-4 nucleotide base pairs were eliminated as potential intercalation sites for the ethidium dye. By contrast, the larger molecule mitomycin C causes a proportionately greater destruction of intercalation sites (7). (One per cent alkylation by mitomycin C causes a nine to twelve per cent loss of fluorescence).

Time-dependent fluorescence change of methylated DNA. The fluorescence of ethidium bound to methylated DNA showed not only a pH dependent decrease but also a marked time dependence in the assay at 11.6. As shown in Figure 2, when the methylated DNAs were added to pH 11.6 ethidium buffer, a marked initial decrease in fluorescence as compared to native DNA was observed. The fluorescence of methylated DNA gradually returned to a higher value with time, although the control native DNA showed a consistent unchanged value. In the first ten minutes or so the fluorescence intensity of the former increased rapidly, then the increase slowed and reached a plateau in about two hours. For DNAs with lower degrees of methylation (<4% deoxyguanosine residues methylated) the fluorescence returned to the value of native DNA. However, for greater extents of alkylation (>6% dG modified) the recovery in the fluorescence was much slower and the fluorescence did not return to that of native DNA. The permanent fluorescence loss of highly alkylated DNA was shown to be partially due to an increase in the proportion of single-stranded DNA after dialysis vs pH 11.6 buffer as measured by the hydroxyapatite method (17).

In contrast to methylation, alkylation of DNA by mitomycin C showed distinctly different behavior where the fluorescence loss for a given extent of alkylation was independent of both pH and remained constant in the ethidium buffer at pH 11.6 (see Figure 3 and 4).

It has been demonstrated by Lawley (21), Uhlenhopp and Krasna (15) and by Singer (16) that the principal methylation sites on DNA are the 7-position of guanine and the 3-position of adenine in a 6:1 ratio when dimethyl sulfate is used. Dimethyl sulfate was selected in the present work because of the S_N2 character of its reactions to minimize phosphate esterification (19). Since no change of the uv spectrum of 3-methyladenosine upon alkaline titration has been reported and in view of the known chemistry of 7-methylguanosine, we consider that the return of fluorescence with time is best explained on the basis of the following model (see Scheme) although we emphasize that the scheme is hypothetical and other mechanisms may be possible.

Normally on amidic proton at N-1 on deoxyguanosine has a high pKa value. However, quaternization at N-7 results in a considerable lowering of the pKa so the transformation to the zwitterion 2 occurs readily (see Scheme). The structure 2 would be expected to be unstable at high pH (~ 10) and this results in a slow opening of the imidazole ring via 3 to give 4. Removal of the positive charge at N-7 in this process restores the amidic N-1 proton to its normal pKa value. If exclusion of ethidium from potential binding sites is primarily due to charge repulsion for low levels of methylation, then the high pH conversion of 1 to 4 with the concomitant removal of positive charge would permit a slow recovery of the ethidium fluorescence. For higher levels of methylation partial denaturation as well as charge repulsion may be responsible for fluorescence loss, so that renaturation by restoration of hydrogen bonding in the ring-opened product may be the major cause of the return of fluorescence. When >6% dG residue are modified, some irreversible denaturation occurs and the fluorescence no longer returns to the control values.



SCHEME

Enzymatic hydrolysis of [^{14}C] methylated DNA. To test this hypothesis, [^{14}C] methylated calf thymus DNA was dialyzed against both pH 7 and pH 11.6 potassium phosphate buffers and then subjected to enzymatic hydrolysis to identify the primary products of alkylation. The DNA was treated sequentially with (i) pancreatic deoxyribonuclease, (ii) snake venom phosphodiesterase and (iii) bacterial alkaline 5'-phosphomonoesterase. The hydrolyzate was then subjected to paper chromatography and the results are shown in Figure 5. On the paper chromatogram the methylated DNA, after dialysis against pH 7 buffer and enzymatic hydrolysis, showed a radioactivity peak which correspond to 7-methyldeoxyguanosine. In contrast, when the DNA was dialyzed against pH 11.6 buffer, the radioactive peak corresponded to the ring-opened product from 4. In both

instances there were significant counts at the origin and this presumably arises from some polar material (e.g. nucleotides) from the incomplete hydrolysis of DNA. The thin layer chromatography substantiates these results confirming that the ring-opened material predominates at the high pH. 7-Methyldeoxyguanosine residues in DNA are readily depurinated by acid and it was observed that even on the silica gel plate, compound 1b decomposed partially to 7-methylguanine.

UV spectra of 7-methyldeoxyguanosine and its pH dependence. Independent evidence for the transformations of scheme 1 and estimates of their rates were obtained by examining the effects of pH on the uv absorption spectrum of 7-methyldeoxyguanosine (Figure 6) which has been examined by Brookes and Lawley (22) and others (23-24). At pH 2.4 1b showed an absorption maximum at 253 nm and a shoulder between 270-280nm. As the pH of the solution was increased, the absorption at 253 nm immediately decreased and a new maximum appeared at 281 nm so that at pH > 10, the 281 nm peak was the only one observed and is ascribed to the zwitterion 2b. The latter was unstable at pH > 10 and was slowly transformed into a new species which exhibited a maximum at 267 nm and which was identified as the imidazole ring-opened species 4b (Figure 7). (The half life of 2b at pH 11.6 is approximately 30 min.) The latter process, unlike the essentially instantaneous ionization of 1b, occurred over a period of 1 hr, closely comparable with the rate of the time dependent fluorescence recovery noted earlier.

DISCUSSION:

The pH dependence of the ethidium assay is evidently quite different on the one hand for methylation and on the other hand for reaction with mitomycin C. Quite similar fluorescence behavior as was observed for methylation was exhibited for reaction of nitrogen mustard with DNA. This produced results closely similar to those shown in Figures 1 and 2. Nitrogen mustard has also been shown to alkylate predominantly at the N-7 position of deoxyguanosine (20). The strong pH and time dependence of the ethidium fluorescence of methylated DNA is tentatively ascribed to a slow base catalyzed imidazole ring opening characteristic of 7-alkylation of deoxyguanosine residues at high pH. The N-1 proton of deoxyguanosine in DNA will have a higher pKa than that of free 7-methyldeoxyguanosine (6.7) since this proton is involved in hydrogen bonding with a deoxycytidine residue of the complementary strand of the double helix. At pH 7 the methylated DNA bihelical structure is relatively stable since the Watson-Crick hydrogen bonded base pairing is still intact. Therefore at neutral pH the loss of fluorescence which is linear with the extent of methylation, may be attributed largely to the charge repulsion between the quaternized bases and the positively charged ethidium. At high pHs (>10) dissociation of the N-1 proton of the 7-methylguanosine residues occurs resulting in disruption of the G-C base pairing. This breakage of the hydrogen bonding does not irreversibly disrupt the bihelical structure until greater extents of methylation were reached (>6% dG). This results in more extensive disruption of the duplex as more hydrogen bonds are broken and eventually effects separation of the strands.

The loss of fluorescence of the methylated DNA becomes more pronounced at pH 11.6 than at pH 7 and is progressive with greater extents of methylation. The model studies as well as evidence in the literature (16,21,22) confirm that at high pH there is a slow base catalyzed imidazole ring opening of only the 7-alkylated bases. After the ring opens and the positive charge is removed, the N-1 proton of the guanosine is less acidic. The return of the N-1 proton restores the cooperative hydrogen bonding between the G-C pairs and consequently one observes the gradual return of fluorescence. With low extents of 7-alkylation the original DNA duplex structure is completely restored whereas with higher degrees of 7-alkylation the resulting duplex destabilization permits only partial restoration. The distinctly different behavior with mitomycin C is consistent with this interpretation. Mitomycin C is known to alkylate predominantly the guanine residues of DNA and recent work by Tomasz has ruled out the N-7 position (13). In addition for a given extent of alkylation, mitomycin C results in a greater fluorescence loss. This suggests that whereas charge repulsion may be the primary cause of loss of fluorescence by methylation, in the case of alkylation by mitomycin C, both charge repulsion and steric hindrance may also be factors in fluorescence loss.

Regardless of the precise interpretation of the fluorescence recovery, the loss of ethidium fluorescence is a useful parameter for measuring the extent of alkylation of DNA.

The authors wish to thank Dr. A.R. Morgan for helpful discussions in connection with this work. This research was supported by grants to J.W.L. from the National Cancer Institute of Canada, The National Research Council of Canada and by the Department of Chemistry, University of Alberta.

REFERENCES:

1. Montgomery, J.A., Johnston, T.P., and Shealy, Y.F. (1970) in *Medicinal Chemistry* Ed. Burger, A. Wiley-Interscience New York pp. 680-783.
2. Ross, W.C.J. (1962) *Biological Alkylating Agents*, Butterworths, London.
3. Gale, E.F., Cundliffe, E., Reynolds, D.E., Richmond, M.H., and Waring, M.J. (1972) "Biochemical Targets for Drug Action" Chapter in the *Molecular Basis of Antibiotic Action*, Wiley-Interscience, New York, pp. 24-48.
4. LePecq, J.B. and Paoletti, C. (1967) *J. Mol. Biol.*, 27, 87-106.
5. Morgan, A.R., and Paetkau, V. (1972) *Can. J. Biochem.* 50, 210-216.
6. Morgan, A.R., and Pulleyblank, D.E. (1974) *Biochem. Biophys. Res. Commun.*, 61, 396-403.
7. Lown, J.W., Begleiter, A., Johnson, D., and Morgan, A.R. (1976) *Can. J. Biochem.*, 54, 110-119.
8. Akhtar, M.H., Begleiter, A., Johnson, D., Lown, J.W., McLaughlin,

- L., and Sim, S.K. (1975) *Can. J. Chem.*, 53, 2891-2905.
9. Cone, R., Hasan, S.K., Lown, J.W., and Morgan, A.R. (1976) *Can. J. Biochem.*, 54, 219-223.
 10. Hanby, W.E., and Rydon, H.N. (1947) *J. Chem. Soc.*, 513-519.
 11. Jones, J.W., and Robins, R.K. (1963) *J. Amer. Chem. Soc.*, 85, 193-201.
 12. Townsend, L.B., and Robins, R.K. (1968) in *Synthetic Procedures in Nucleic Acid Chemistry*, Ed. by Zorbach, W.W. and Tipson, R.S., Vol. 1, pp. 315-316.
 13. Tomasz, M., Mercado, C.M., Olson, J., and Chatterjee, N. (1974) *Biochemistry*, 13, 4878-4887.
 14. Fink, K. and Adams, W.S. (1966) *J. Chromatography*, 22, 118-129.
 15. Uhlenhopp, E.L. and Krasna, A.I. (1971) *Biochemistry*, 10, 3290-3295.
 16. Singer, B. (1975) in *Progress of Nucleic Acid Research and Molecular Biology*, Ed. by Cohn, W.E., Academic Press, New York, Vol. 15, pp. 219-284.
 17. Paetkau, V. and Langman, L. (1975) *Anal. Biochem.*, 65, 525-532.
 18. Studier, F.W. (1965) *J. Mol. Biol.*, 11, 373-385.
 19. Reference 16, p. 330.
 20. Reference 16, p. 271.
 21. Lawley, P.D. (1966) in *Progress of Nucleic Acid Research and Molecular Biology*, Ed. by Cohn, W.E., Academic Press, New York, Vol. 5, pp. 89-162.
 22. Brookes, P. and Lawley, P.D. (1961) *J. Chem. Soc.*, 3923-3928.
 23. Bredereck, H., Kupsch, G. and Wieland, H. (1959) *Chem. Ber.*, 92, 583-587.
 24. Townsend, L.B., and Robins, R.K. (1963) *J. Amer. Chem. Soc.*, 85, 242-243.

TABLE 1

Equilibrium Dialysis of Ethidium versus Methylated and Native DNAs

	[Ethidium] _{free} (M)	[Ethidium] _{Bound} (M)
Native ¹ λDNA	5.2 x 10 ⁻⁷	9.0 x 10 ⁻⁶
Methylated ² DNA (at pH 7)	12.9 x 10 ⁻⁷	7.4 x 10 ⁻⁶

¹S_{20,w} 29.6

²S_{20,w} 28.5, This sample corresponds to 3.05% methylation in DNA nucleotides.

TABLE 2
Binding Studies of Ethidium on the Various Methylated λ -DNA's

DMS concentration used in methylation	% methylation in DNA nucleotides	K_a (x10 ⁷) Association Constants	B_T (relative) Total Binding Sites	Relative Fluorescence at pH 7.0 (from Fig.1)
0	0	2.9	100	100
20	1.23	2.8	92.4	92
30	1.56	2.9	87.4	88
40	2.25	2.7	85.7	83
50	3.05	2.9	78.1	77

LEGENDS TO FIGURES

- FIGURE 1 Decrease in relative ethidium fluorescence produced by progressive [^{14}C] methylation with 0, 10, 20, 30 etc. mmolar dimethyl sulfate at 37° for 1 hour as a function of pH. The extent of methylation was determined by radioactive counting.
- FIGURE 2 Time dependence of fluorescence at pH 11.6 of ethidium bound to λ -DNA treated with dimethyl sulfate (DMS):
 ◇ native DNA; ● 20 mmolar DMS; ▽ 40 mmolar DMS;
 △ 60 mmolar DMS; □ 70 mmolar DMS.
- FIGURE 3 Binding of ethidium at pH 7 and pH 11.6 to λ -DNA alkylated with mitomycin C: ○ pH 7 ethidium buffer; ▽ pH 11.6 ethidium buffer.
- FIGURE 4 Time dependence of fluorescence at pH 11.6 of ethidium bound to λ -DNA treated with mitomycin C (MMC) and NaBH_4 : ○ native DNA; × 0.25 mmolar MMC and NaBH_4 ; ◇ 0.36 mmolar MMC and NaBH_4 ; * 0.48 mmolar MMC and NaBH_4 .
- FIGURE 5 [^{14}C] radioactivity scan of paper chromatograms of enzyme hydrolyzates from [^{14}C] methylated calf thymus DNA dialyzed against pH 7 and pH 11.6 buffers. Strip 4 corresponds to 7-methyldeoxyguanosine, strip 5 to the ring opened nucleoside 4b and strip 7 to deoxyguanosine.
- FIGURE 6 pH dependence of the uv absorption spectrum of 7-methyl-2'-deoxyguanosine as 5×10^{-5} M in 0.05 molar phosphate buffers.
- FIGURE 7 Time dependence of the uv absorption spectrum of 7-methyl-2'-deoxyguanosine 5×10^{-5} M at pH 11.6, 0.05 molar phosphate buffer.

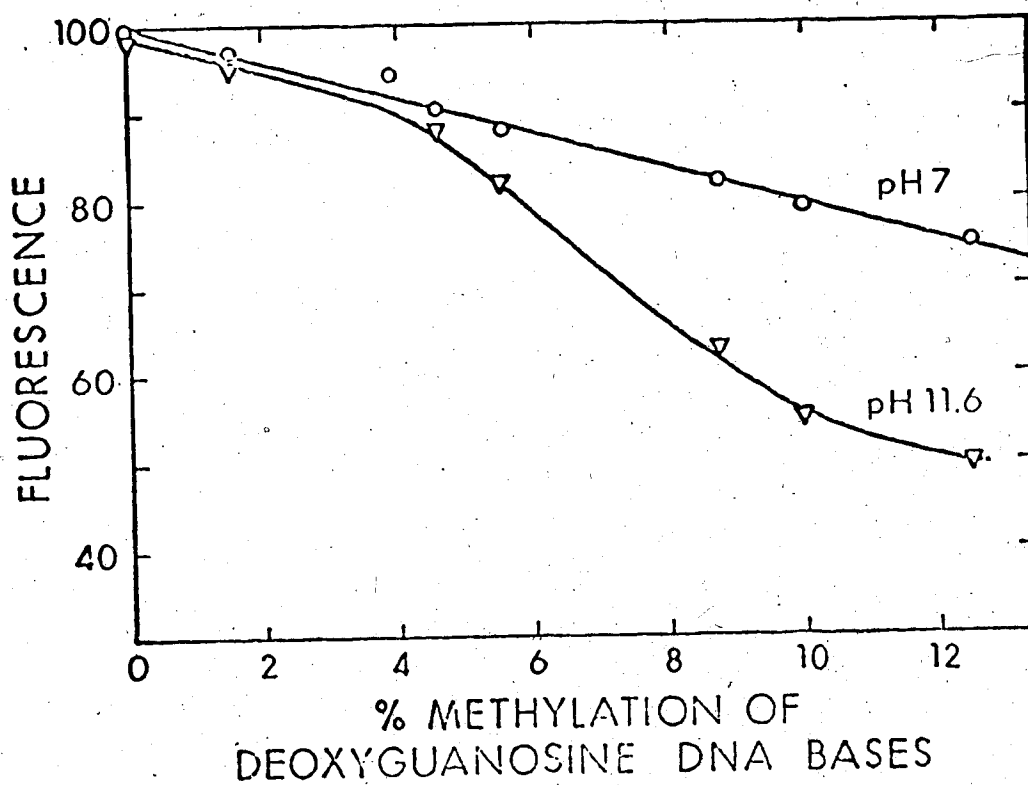


Figure 1.

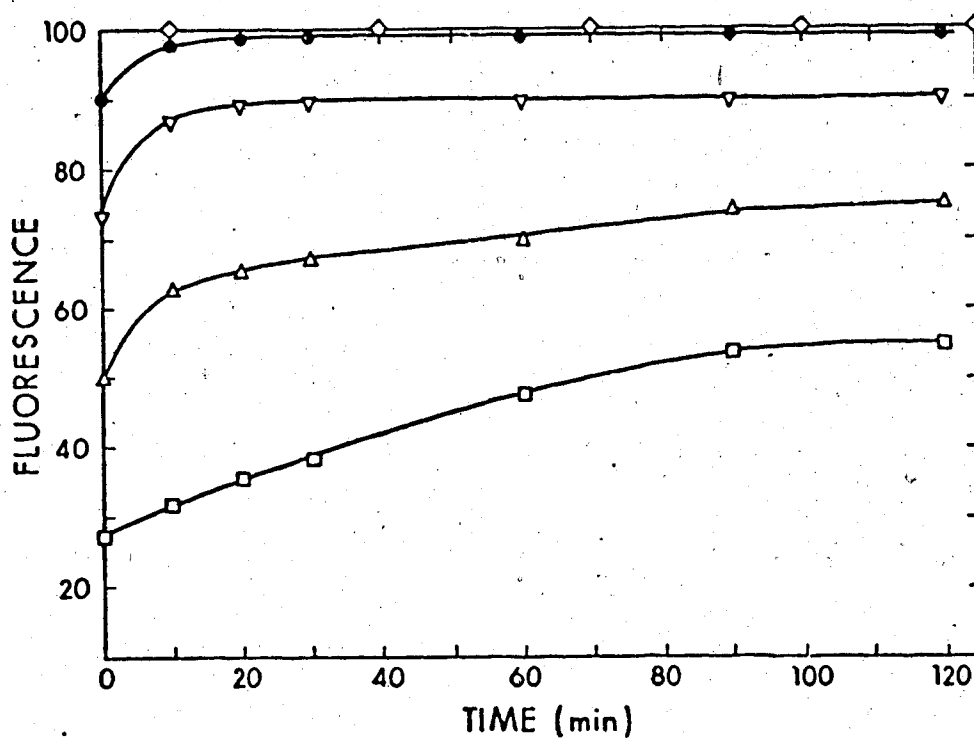


Figure 2.

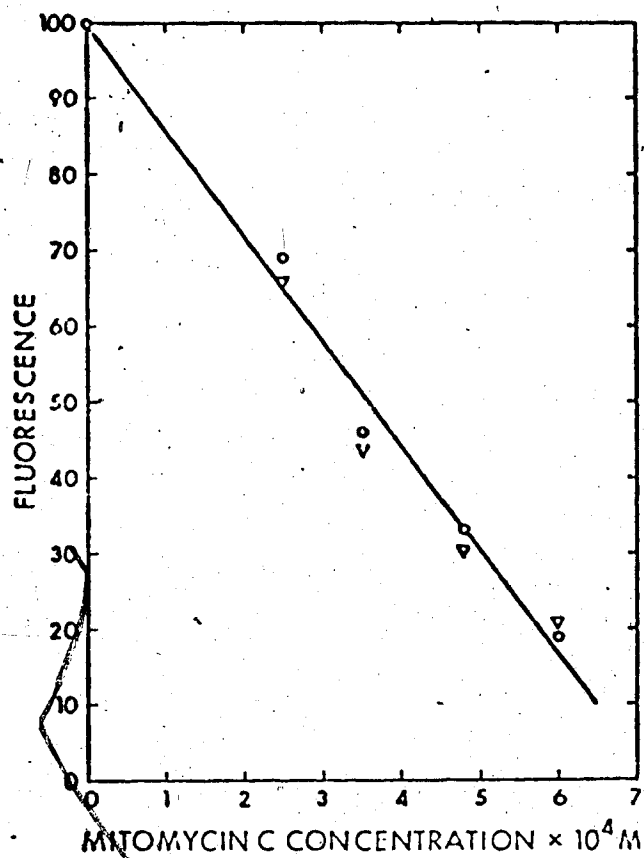


Figure 3.

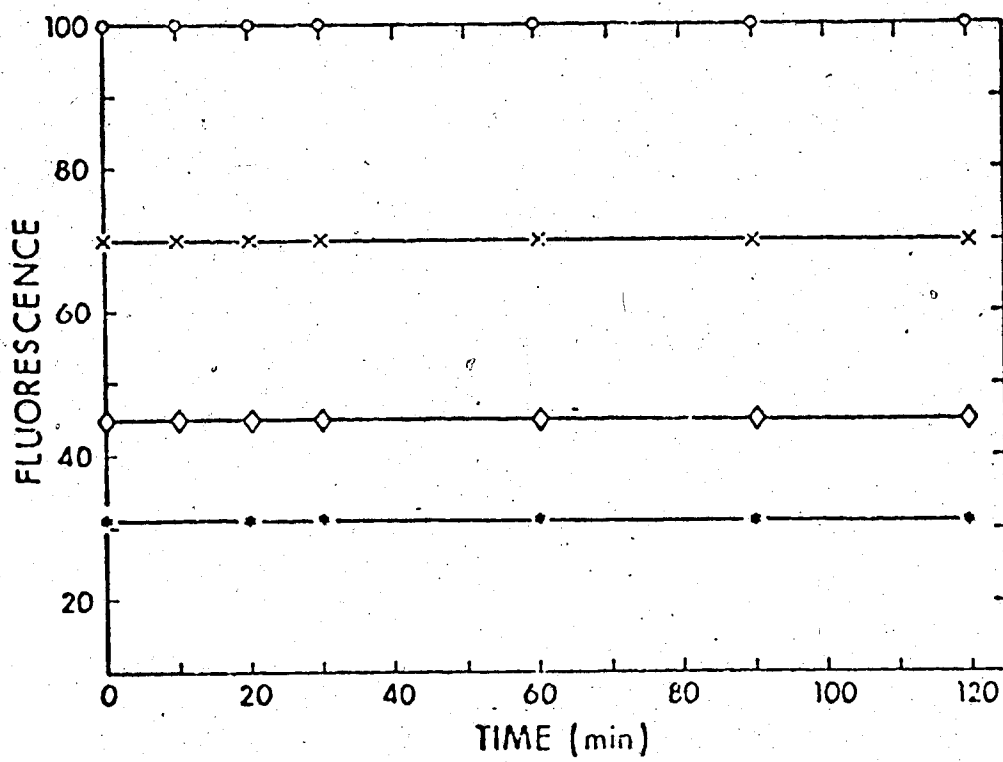


Figure 4.

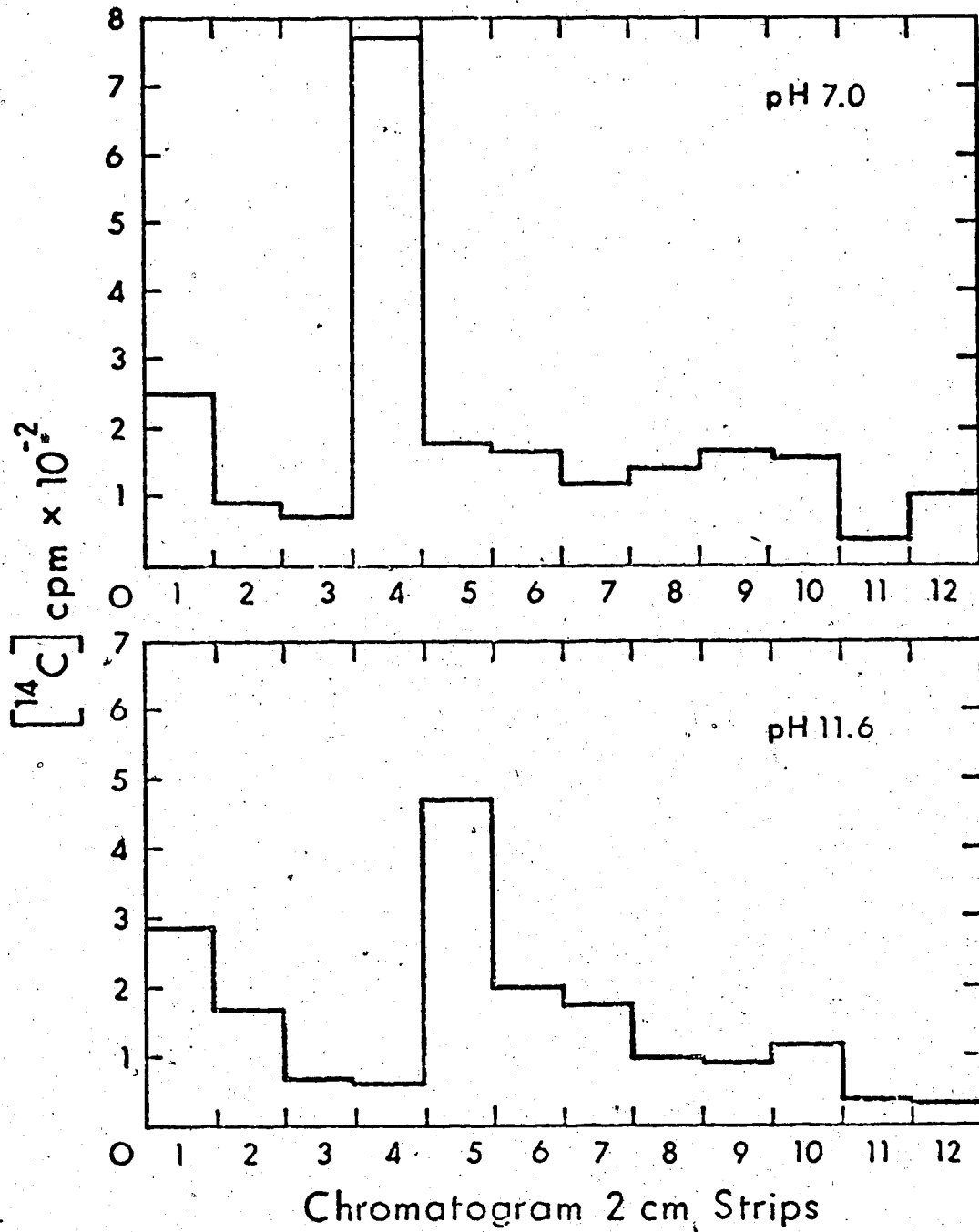


Figure 5.

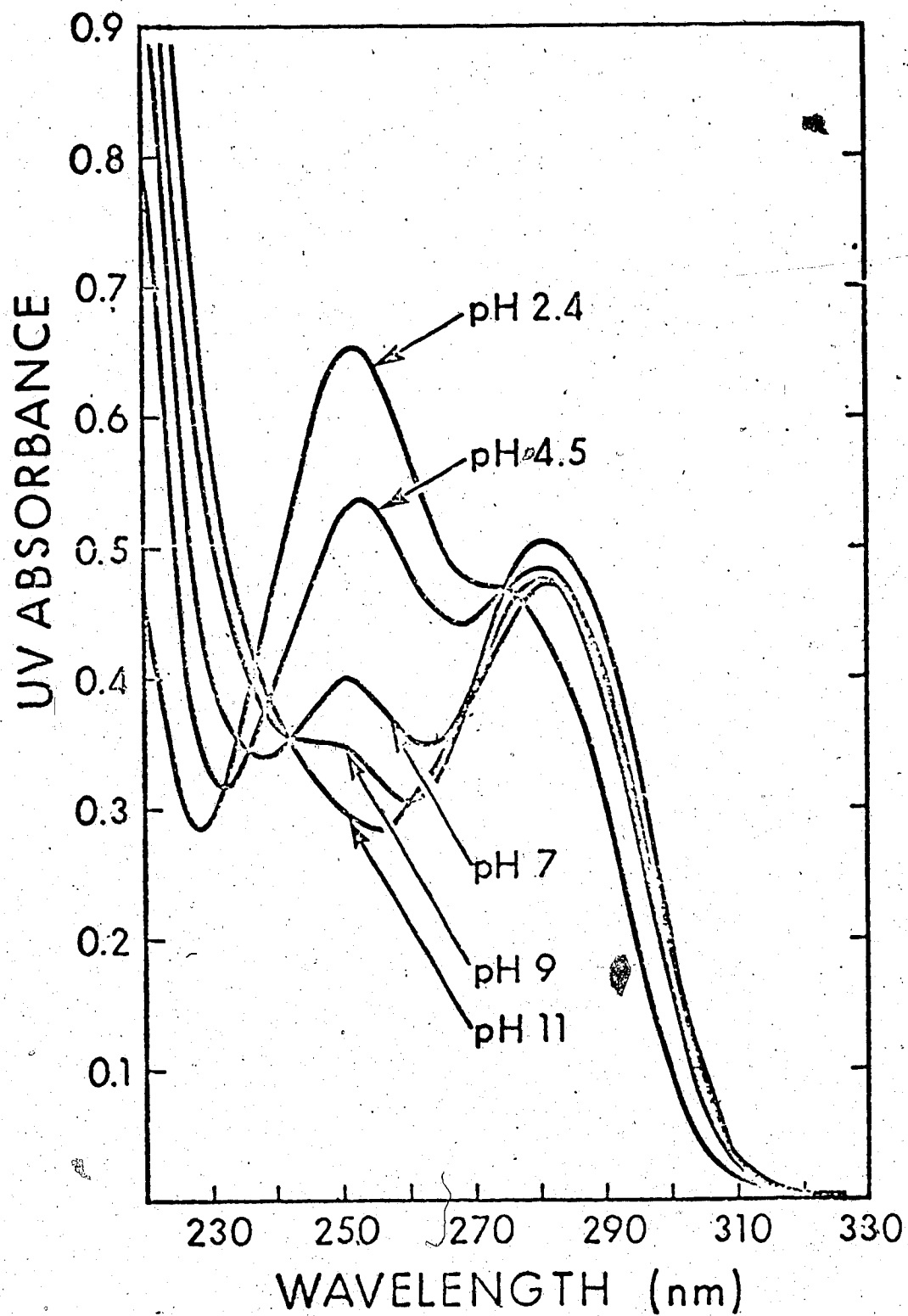


Figure 6.

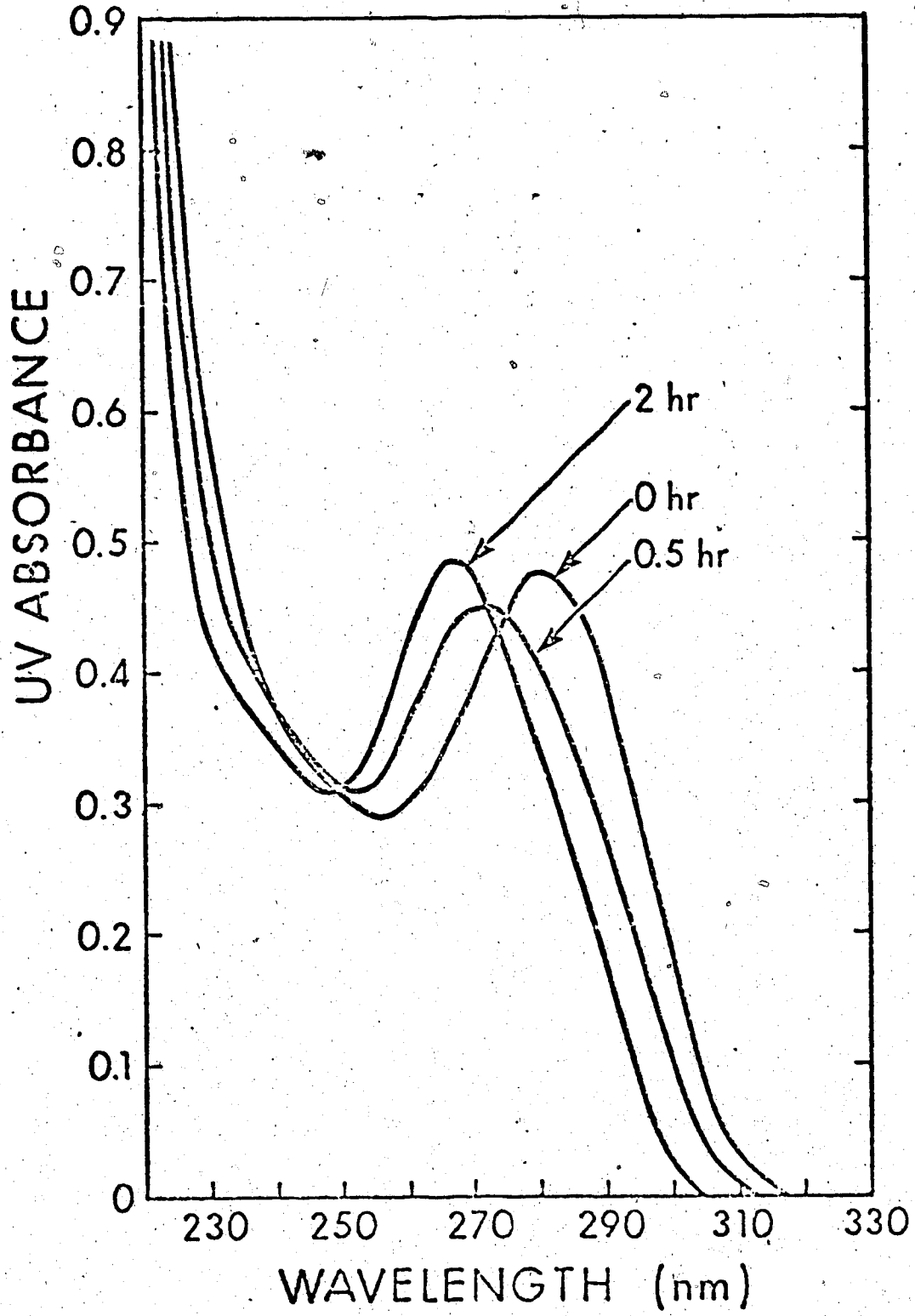


Figure 7.

APPENDIX 2

During attempts to incorporate deoxynucleoside analogues into $d(TC)_n \cdot d(GA)_n$ in order to ascertain which sites could be involved in stabilizing the multiplex structure via hydrogen bond formation, a method that was useful for a small scale reaction was developed to convert the appropriate deoxynucleoside 5'-monophosphate to the corresponding 5'-triphosphate. The enzyme, phosphoenolpyruvate synthetase, isolated and studied in this department by Suree Narindrasorasak, proved immensely helpful. In collaboration with Dr. Malcom MacCoss of the Chemistry Department, who supplied most of the adenosine 5'-monophosphate analogues we have determined the specificity of this enzyme. Recently, we have also been able to show that deoxytubercidin 5'-monophosphate and 6-Me deoxyadenosine 5'-monophosphate are substrates as would be expected since the corresponding ribo analogues are substrates.

(Accepted for publication in Biochemical and Biophysical Research Communications (1976).)

THE ENZYMIC SYNTHESIS OF ATP ANALOGUES

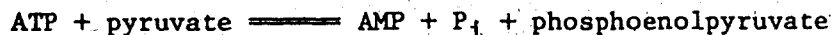
Doug Johnson*, Malcolm MacCoss**, and Suree Narindrasorasak*

Department of Biochemistry* and Chemistry**
University of Alberta, Edmonton, Alberta, Canada T6G 2H7

ABSTRACT: The enzymatic synthesis of selected adenosine 5'-triphosphate analogues from their respective 5'-monophosphates has been achieved using phosphoenolpyruvate synthetase. Adenosine 5'-monophosphate analogues altered at positions 1, 6, 7, 8 or 9 of the purine ring, or at the ribose 2'- or 3'-positions are substrates with 30% conversion to the nucleoside 5'-triphosphate.

INTRODUCTION:

Phosphoenolpyruvate synthetase catalyzes the phosphorylation of pyruvate from the β -phosphate of ATP¹ via an enzyme-phosphate intermediate (Cooper and Kornberg, 1965 and 1967).



We have used the reverse reaction to synthesize a variety of ATP analogues modified in the sugar or purine ring moieties without any need for the protection of reactive groups. Also radiolabelling of the β - or γ -phosphate positions of these analogues is possible.

From the variety of analogues tested we can infer which positions on AMP are involved in substrate recognition.

MATERIALS AND METHODS:

Nucleosides and nucleotides were purchased from the following suppliers: Calbiochem (rAMP, rCMP, rCTP, rGTP); P.L. Biochemicals (rATP, dATP, 1-MeAMP, 6-MeAMP, rGTP, rTu); Pfanstiehl, Germany (araA); Raylo, Canada (dAMP); Sigma (rIMP, rITP). Nucleosides were chemically phosphorylated to their 5'-monophosphates by the method of Yoshikawa *et al* (1969) and purified by chromatography on Dowex 1x2 (formate) developed

¹NMP refers to any nucleoside 5'-monophosphate, NTP to the 5'-triphosphate. rTu and araA are abbreviations for tubercidin and 9- β -D-arabinofuranosyladenine (structures of respective 5'-monophosphates given in Fig. 1). Abbreviations for methylated adenosines are taken from the Handbook of Biochemistry, Chemical Rubber Co..

with a linear gradient of formic acid (M.J. Robins and M. MacCoss, to be published). Adenosine derivatives methylated at the 2'- or 3'-positions were prepared by methods described by Robins *et al* (1974). 6,6-Me₂-adenosine was prepared from the 6-chloropurine riboside with anhydrous dimethylamine (see Robins *et al* (1976) for analogous preparation). AMPOX-RED was prepared by the method of Smrt *et al* (1975) with minor modifications.

Phosphoenolpyruvate synthetase, purified from lactate-grown *Escherichia coli* by the method of Berman and Cohn (1970) was judged 90% pure by polyacrylamide gel electrophoresis. The assay conditions for the forward reaction were 0.1 M Tris HCl pH 8.0, 10 mM MgCl₂, 2 mM pyruvate, 1 mM nucleoside 5'-triphosphate and 15 µg/ml enzyme (specific activity 19 U/mg in forward direction) and for the reverse reaction 0.1 M KP_i pH 6.8, 20 mM MgCl₂, 10 mM phosphoenolpyruvate (Sigma), 10 mM nucleoside 5'-monophosphate and 130 µg/ml enzyme. Both reactions were incubated at 30°C. Synthesis of NTP was monitored for up to 16 hours by thin layer chromatography on cellulose sheets (Eastman #13255) with isobutyric acid/ammonium hydroxide/H₂O (60/1/40 by volume) as solvent and on P.E.I. cellulose sheets (Baker) with 1.6 M LiCl as solvent (K. Randerath and E. Randerath, 1967).

Reaction products were separated by DEAE Cellulose chromatography with a linear gradient 0 - 0.6 M in triethylammonium bicarbonate pH 7.5 (Smith and Khorana, 1963) and concentrated by lyophilization.

RNA polymerase reactions were performed with *E. coli* RNA polymerase (Burgess, 1969) in a reaction mixture containing 50 mM Tris HCl pH 8.0, 10 mM MgCl₂, 50 µg/ml dTC·dGA, 0.25 mM ¹⁴C-GTP (9,200 cpm/nmole), 0.25 mM rATP analogue, 200 µg/ml RNA polymerase. This polyribopurine synthesis can be distinguished from contaminating poly rG synthesis by observation of the kinetics of synthesis.

RESULTS AND DISCUSSION:

Figure 1 gives the structures of the less common AMP analogues, and the ability of various analogues to act as phosphoenolpyruvate synthetase substrates for both the forward and reverse reactions is summarized in Table 1. As expected, at no time was ribonucleoside 5'-diphosphate synthesis observed.

In the reverse direction dAMP, araAMP, 3'-MeAMP, 6-MeAMP, TuMP, FMP and AMP can be phosphorylated with ≈30% recovery of the NTP from a DEAE Cellulose column. 2'-MeAMP is converted to the triphosphate with about 15% recovery and 1-MeAMP is phosphorylated with 5 - 17% recovery. This variability is probably due to the insolubility of this analogue under the reaction conditions. 6,6-Me₂AMP, AMPOX-RED and αAMP (the 1'-epimer of 5'-AMP) are not substrates and 6,2'-Me₂AMP is phosphorylated to a very low extent. The 6-keto nucleotides IMP and GMP and the 4-amino pyrimidine nucleotide CMP cannot substitute for AMP in the reverse reaction nor can the corresponding 5'-triphosphates substitute for ATP in the forward direction.

TABLE 1. Substrate Recognition by Phosphoenolpyruvate Synthetase

COMPOUND	REVERSE REACTION: Isolation of NTP by DEAE Cellulose Chromatography ^{1,2}	FORWARD REACTION: Initial Reaction Rate of Analogue Compared to ATP ¹
AMP/ATP	34	1.00
dAMP/dATP	33	0.33
2'-MeAMP	15	ND ⁴
3'-MeAMP	24	ND
1-MeAMP	5-17 ³	ND
6-MeAMP/6-MeATP	34	0.23
6,6-Me ₂ -AMP	0	ND
6,2'-Me ₂ AMP	1	ND
araAMP/araATP	28	0.31
αAMP	0	ND
AMPOX-RED	0	ND
TuMP/TuTP	29	0.71
FMP/FTP	28	0.42
GMP/GTP	0	0
IMP/ITP	0	0
CMP/CTP	0	0

¹As described in Materials and Methods.

²Percent of ultraviolet absorbing material ($\lambda = 260$ nm) eluting as NTP.

³Variable, see text.

⁴ND, not determined.

Although dATP, 6-MeATP, araATP, TuTP and FTP are ultimately synthesized to the same extent as ATP, their initial rates for the forward reaction are very different. Compared to ATP these range from 0.23 for 6-MeATP to 0.71 for TuTP. These NTPs were also checked as substrates for *E. coli* RNA polymerase and each was incorporated into polyribopurine (data not shown). As expected araATP showed less than 3% synthesis compared to ATP (Cohen 1966).

Several conclusions can be drawn from an evaluation of the substrate specificity. Firstly, the 2'- or 3'-positions appear unimportant for recognition since AMP, dAMP, araAMP, 2'-MeAMP and 3'-MeAMP are all substrates. The lower yield of 2'-MeATP may reflect a steric problem and this would preclude the phosphorylation of AMP analogues by this method if the 2' substituent is even bulkier. Removal of the structural rigidity of the ribose ring as in AMPOX-RED results in a loss of substrate recognition. As expected, the configuration at the anomeric centre is also important since αAMP is not a substrate. With regard to the heterocyclic base, variations in the imidazole ring are tolerated since both TuMP and FMP are substrates. Methylation of the 1-position does not result in a loss of recognition. If the 6-amino is monomethylated, recognition is not affected but dimethylation at the 6-position results in a complete lack of synthesis. Replacement of the 6-amino by oxygen, as in IMP or GMP, results in no synthesis of the corresponding triphosphate. These last results indicate that of the various positions tested only the 6-

amino is directly involved in substrate recognition, presumably forming a hydrogen bond to the enzyme. Since the 4-amino pyrimidine CMP is not phosphorylated the purine ring moiety is necessary.

In comparison to chemical methods of NTP synthesis (Smith and Khorana, 1963) this enzymatic synthesis is limited both by substrate recognition and reaction scale since it is not suitable for the routine synthesis of mmoles of NTP without a large enzyme supply (yield from 1 kilogram of cells is about 200 mg). However, it is convenient for the synthesis of 25 - 50 μ moles of a particular NTP without the need for blocking agents and requires no "seed" NTP as does a previously described enzymatic synthesis of FTP (Ward, Cerami and Reich, 1969). Since the β -phosphate is derived from phosphoenolpyruvate and the γ -phosphate from buffer, specific radiolabelling should also be possible.

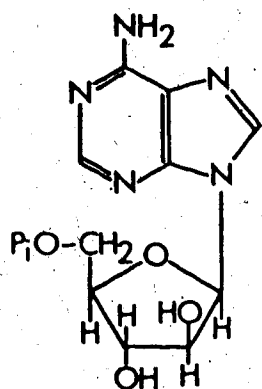
ACKNOWLEDGEMENTS:

The authors wish to thank Mr. G.G. Cross for the preparation of AMPOX-RED and Drs. W.A. Bridger, A.R. Morgan and M.J. Robins for discussions. This work was supported by Medical Research Council of Canada grants to W.A.B. and A.R.M. and grants from the National Cancer Institute of Canada and National Research Council (A5890) to M.J.R.

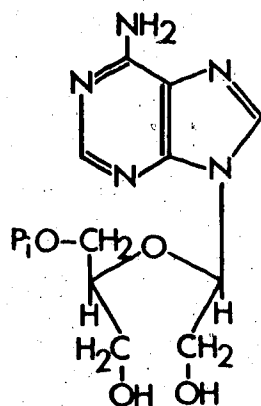
REFERENCES:

- Berman, K., and Cohn, M. (1970). *J. Biol. Chem.* 245, 5304 - 5318.
 Burgess, R.R. (1969). *J. Biol. Chem.* 244, 6160-6167.
 Cohen, S.S. (1966). *Progr. Nucleic Acid Res. Mol. Biol.* 5, 1-88.
 Cooper, R.A., and Kornberg, H.C. (1965). *Biochim. Biophys. Acta* 104 618-620.
 Cooper, R.A., and Kornberg, H.C. (1967). *Biochem. J.* 105, 49C-50C.
 Randerath, K., and Randerath, E. (1967). *Methods in Enzymology* XIIA, 323-347.
 Robins, M.J., Naik, S.R., and Lee, A.S.K. (1974). *J. Org. Chem.* 39 1891-1899.
 Robins, M.J., MacCoss, M., and Lee, A.S.K. (1976). *Biochem. Biophys. Res. Commun.* (in press).
 Smith, M., and Khorana, H.G. (1963). *Methods in Enzymology* VI, 645-669.
 Smrt, J., Mikhailov, S.N., Hynie, S., and Florent'ev, V.L. (1975). *Coll. Czech. Chem. Comm.* 40, 3399-3403.
 Ward, D.C., Cerami, A., and Reich, E. (1969). *J. Biol. Chem.* 244, 3243-3250.
 Yoshikawa, M., Kato, T., and Takenishi, T. (1969). *Bull. Chem. Soc. Japan*, 42, 3505-3508.

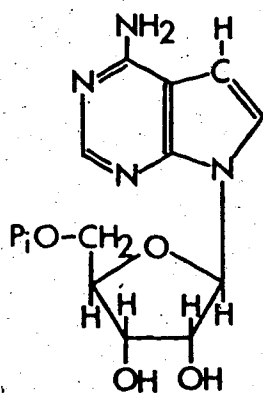
Figure 1. Structures of various AMP analogues.



araAMP

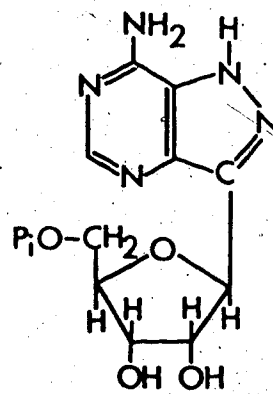


AMP OX-RED



TuMP

TUBERCIDIN 5'-MONOPHOSPHATE



FMP

FORMYCIN 5'-MONOPHOSPHATE

Terminal deoxynucleotidyl transferase (TDT) isolated from calf thymus was used to synthesize the random $d(\text{Py})_n \cdot d(\text{Pu})_n$ DNA that was used in the replication and multiplex studies. Initial attempts to isolate TDT by the modified procedure described in the text resulted in the isolation of a new TDT, designated TDT2, which has similar enzymatic properties as TDT1 but differs in molecular weight and has the ability to copy a DNA template. The data presented suggest that both TDT1 and TDT2 are derived from a DNA polymerase and make an in vivo role for TDT unlikely.

In addition to the discussion in this paper, several other comments can be made concerning this area of research.

The detection of TDT activity in partially purified extracts by the use of assay systems containing DNA (native, activated, denatured) as primer and a low (typically μ molar) concentration of one deoxynucleoside 5'-triphosphate of very high specific activity (typically 23 mCi/ μ mole) may lead to inaccurate results. This activity may be DNA polymerase since quantitation of the observed synthesis reveals ~ 1 residue incorporated per 10^6 - 10^7 daltons of DNA (Srivastava, 1974) a terminal addition that could be catalyzed by a DNA polymerase. A recent report of the isolation of "TDT" from germinating wheat embryo (Brodnievicz-Proba and Buchowicz, 1976) also could be criticized on these grounds. Hence, more thorough analysis of purified fractions is necessary before the presence of TDT can be confirmed, and quantitation of the extent of incorporation is important.

Both TDT1 and TDT2 are inhibited 20 fold by the substitution of

cacodylate with Tris buffers. This effect of Tris buffers has been noted before but does not appear reproducible by different experimenters (Kung et al, 1976). However, the use of Tris as a buffer for the measurement of TDT activity (Marcus et al, 1976; Srivastava, 1974; Sarin and Gallo, 1974) may lead to low estimates of TDT activity.

Also different authors have used various templates and dNTP substrates for their assay systems which makes direct comparisons impossible. In this respect the use of Mn^{++} may also be suspect since it is known to change the specificity of E. coli DNA polymerase I towards nucleoside 5'-triphosphates (Kornberg, 1974) and may be altering the activity and specificity of the observed TDT.

(Submitted for publication in Biochemical and Biophysical Research Communications (1976).)

THE ISOLATION OF A HIGH MOLECULAR WEIGHT TERMINAL DEOXYNUCLEOTIDYL
TRANSFERASE FROM CALF THYMUS*

Douglas Johnson** and A. Richard Morgan

Department of Biochemistry
University of Alberta
Edmonton, Alberta, Canada, T6G 2H7

SUMMARY: A new terminal deoxynucleotidyl transferase (TDT)¹ has been isolated from calf thymus of higher molecular weight than that originally isolated by Bollum (1962). The enzymes are probably metabolically related as one or the other is found depending on the purification procedure. However, a direct conversion from one to the other has not been achieved. Although most of the enzymatic properties are very similar in contrast the new TDT also has the ability to use a template. This suggests that TDT's may be proteolytic degradation products of template-requiring DNA polymerases. Thus the finding of TDT's in a variety of rapidly metabolizing cells could be due to the uncovering of proteolytic activity rather than the synthesis of a new class of template-independent polymerases.

INTRODUCTION:

Terminal deoxynucleotidyl transferase (TDT)¹ catalyses the primer-dependent but template independent polymerization of deoxynucleoside 5'-triphosphates. First detected in calf thymus extracts and purified by Bollum (Bollum, 1962), similar activities have recently been reported in various normal and malignant human cells grown in culture (Srivastava, 1974) and isolated from the whole blood cells of patients with acute lymphocytic leukemia (McCaffrey *et al*, 1973) or with chronic myelogenous leukemia in blast crisis (Sarin and Gallo, 1974) and from the peripheral blood leukocytes of a patient with chronic myeloblastic leukemia (Bhattacharyya, 1975). Although the *in vivo* function of TDT is unknown, speculation has centred on its apparent relation to the

¹In this paper TDT1 refers to the enzyme originally isolated by Bollum and TDT2 to the higher molecular weight enzyme described here. Other abbreviations used are: CCC DNA for covalently-closed circular DNA, OC DNA for open circular DNA, pOHMB for p-Hydroxymercuribenzoate, NEM for N-ethylmaleimide and SDS for sodium dodecyl sulfate. pT₄₋₅ refers to a mixture of pT₄ and pT₅, dNTP to the deoxynucleoside triphosphate.

*This work is supported by the Medical Research Council of Canada.

**Recipient of a Medical Research Council Studentship.

thymus, suggesting a function in the immune system (Baltimore, 1974). Its use as a diagnostic tool for certain leukemic states has also been proposed (Sarin and Gallo, 1974).

This communication describes the isolation and characterization of a second TDT from calf thymus, distinct from Bollum's enzyme, with a higher molecular weight. However, they may be related in that depending upon the experimental conditions used for purification either TDT1 or TDT2 (but not both) is found.

MATERIALS AND METHODS:

The isolation of TDT2 uses many of the purification steps described by Bollum (Bollum, 1968) with the order rearranged to facilitate the purification. At no stage was a low pH (i.e. <7.0) incubation as described by Bollum included. TDT activity was measured (Bollum, 1968) at 37°C with pT₄₋₅ as primer in reaction mixtures containing 40 mM Na cacodylate pH 7.0, 1 mM dithiothreitol, 1 mM dNTP and either 10 mM MgCl₂ or 1 mM CoCl₂. DNA polymerase (which copurifies with TDT during the early stages of purification and can be used as a marker for TDT) was detected by an ethidium fluorescence assay (Morgan and Pulleyblank, 1974). The reaction mixture contained 50 mM KP_i pH 7.5, 1 mM of each dNTP, 10 mM MgCl₂, and 1 A₂₆₀ of heat-denatured calf thymus DNA. 10 µl samples were added to 2 ml of the high pH ethidium assay mixture. The product is mostly covalently-linked complementary DNA as indicated by the return of fluorescence after a heating and cooling cycle.

The modified procedure is as follows: 450 g of calf thymus were suspended in 50 mM Tris HCl pH 7.5, 100 mM NaCl, 1 mM EDTA and disrupted using a Colloid Mill (Gifford-Wood, Hudson, New York). After filtration through cheesecloth and removal of chromatin by centrifugation (23,000 g, 20 minutes) polymerase activity was precipitated by the addition of solid (NH₄)₂SO₄ to .50% saturation and centrifuged at 8,000 x g for 15 minutes. The pellet was suspended in 0.2 M KP_i pH 7.5, 1 mM 2-mercaptoethanol (Buffer B) and the ionic strength lowered to that of Buffer B with the addition of 50 mM KP_i pH 7.5, 1 mM 2-mercaptoethanol. Nucleic acid was removed with DEAE cellulose equilibrated in Buffer B (Bollum, 1968) by a batchwise procedure. After the removal of adsorbant by filtration, the filtrate was diluted 1:4 with 1 mM 2-mercaptoethanol and protein adsorbed to phosphocellulose (500 ml packed volume) for chromatography (Bollum, 1968).

Fractions with DNA polymerase activity were concentrated, resuspended in 0.1 M KP_i pH 7.5, 1 mM 2-mercaptoethanol and after dialysis against the same buffer, chromatographed on Sephadex G-100 (Bollum, 1968). TDT activity was pooled and chromatographed over a single-stranded calf thymus DNA-agarose column (Schaller *et al*, 1972) and eluted with a linear KCl gradient in 25 mM KP_i pH 7.5, 1 mM EDTA, 1 mM 2-mercaptoethanol, 5% (v/v) glycerol (TDT2 activity eluted as a single peak at ~65 mM KCl). Subsequent purifications over Sephadex G-100 were with this same buffer at various KCl concentrations. For comparative purposes TDT1 was isolated by the normal procedure up to and including Sephadex G-100 chromatography (Bollum, 1968). One unit of TDT activity incorporates 1

nmole of dNTP per hour at 37°C.

Heat denaturation of TDT2 was performed at 50°C in 25 mM KP_i pH 7.5, 1 mM EDTA, 1 mM 2-mercaptoethanol, 50% (v/v) glycerol. Endonuclease activity was measured fluorometrically (Morgan and Pulleyblank, 1974) with PM2 CCC DNA as substrate in 30 mM KP_i pH 7.5, 10 mM $MgCl_2$, 1 A260 PM2 DNA at 37°C. Exonuclease activity was also measured fluorometrically with heat denatured calf thymus DNA as substrate in a reaction mixture containing 20 mM KP_i pH 7.5, 10 mM $MgCl_2$, 1 A260 DNA. One unit hydrolyses 1 nmole of DNA phosphate per hour at 37°C.

SDS polyacrylamide gel electrophoresis was performed as described by Weber and Osborn, 1969.

RESULTS:

During attempts to isolate TDT1 a second, distinct TDT activity was isolated when the purification procedure was modified as described in Materials and Methods. With this procedure all the TDT was of a higher molecular weight than TDT1 (32,360 daltons, Chang and Bollum, 1971).

Figure 1 shows the elution profile of this activity on Sephadex G-100. The excluded peak is DNA and the elution position of TDT1 is marked by the arrow. This new activity has a much higher molecular weight than TDT1 and its elution position is not changed by the addition of KCl to the eluting buffer up to 1.0 M or increasing the buffer concentration to 0.1 M KP_i . Calibration of the G-100 column shows the activity to be included to a slightly greater extent than *E. coli* DNA polymerase I (105,000 daltons) but eluting well before bovine serum albumin (68,000 daltons). SDS polyacrylamide gel electrophoresis of TDT2 (Figure 2) shows essentially one peak of 79,000 daltons with *E. coli* RNA polymerase subunits as markers. Contamination by TDT1 should give a band at 26,500 daltons (β subunit, Chang and Bollum, 1971); however, even when the gel was deliberately not completely destained, no discernable band at the expected position was detectable. These data suggest that TDT2 is a single polypeptide of 79,000 daltons distinct from TDT1.

We have been able to obtain fractions with a specific activity of 10,000 units/mg (with dATP as substrate in the presence of Mg^{++}) which also suggests that this activity is not due to a slight contamination with TDT1 (which is not visible in SDS gels and would have to chromatograph anomalously on G-100). Although this TDT2 activity can be repeatedly chromatographed on G-100, eluting at the same position as in Figure 1, it appears unstable, losing activity rapidly upon manipulation. The TDT2 used in the subsequent experiments was stable stored in 50% (v/v) glycerol at -20°C for 1 year.

Some properties of TDT2 are summarized in Tables 1 and 2. With respect to substrate specificity, TDT2 resembles TDT1 preferring purine dNTPs with Mg^{++} present and pyrimidine dNTPs with Co^{++} present. However,

unlike TDT1 there seems to be slightly better polymerization with Co^{++} even with purine dNTPs. Table 2 compares some properties of TDT2 with TDT1. Both activities depend on exogenously added primer and are inhibited by NEM, pOHMB and SDS to about the same extent when these are included in the reaction mixture. The presence of Triton X-100 has a similar effect on both activities (Chang and Bollum, 1971; Kato *et al.*, 1967). The use of Tris buffers at pH 7.5 drastically reduces the observed activity for both TDT1 and TDT2. The two enzymes have different pH optima (7.5 for TDT2 compared to 7.0 for TDT1) and consistent with the molecular weights TDT2 sediments at 4-5S, whereas TDT1 sediments at 3.65S.

In crude extracts of calf thymus after chromatin had been spun down, no TDT activity could be detected using over a 500 fold range in concentration whereas DNA polymerase activity was readily detected. For both enzymes two assay procedures were used, either the incorporation of radio-labelled dNTPs into TCA insoluble material or the ethidium fluorescence assay. The latter is particularly useful for confirming DNA polymerase in the presence of any possible TDT. Even in the presence of all 4 dNTPs, the product of TDT is a random polymer which shows about 5% the fluorescence of duplex DNA under the high pH ethidium fluorescence assay (Morgan and Pulleyblank, 1974). This small amount of fluorescence disappears after a heat denaturation step. Using denatured calf thymus DNA as template and primer for DNA polymerase the product is a hairpin duplex and the increase in fluorescence of samples with time as duplex is formed is paralleled by the increase in fluorescence with time after heat denaturation, (Coulter *et al.*, 1974). The possibility that TDT was not detected in crude extracts due to nucleases or inhibitors was tested by reconstruction experiments in which purified TDT1 or TDT2 were added back to crude extracts. The activity of TDT1 was reduced 50%, the activity of TDT2 was abolished. This suggests that although TDT2 cannot be detected in crude extracts, TDT1 should still be observable. However, it is possible that a small part of the large increase in TDT activity observed upon storage may be due to removal of an inhibitor. Also this extract (4 mg/ml) contained a high concentration of RNA which may interfere by binding these enzymes. Also depending on the purification procedure TDT activity was observed to appear over a period of weeks in certain fractions stored in ice. In a procedure closely resembling Bollum's (1974) except that the ammonium sulfate precipitation (0-45% saturation fraction) preceded the phosphocellulose adsorption (at pH 7.6 rather than 6.5) the hydroxylapatite column gave a peak of DNA polymerase lacking TDT. After two months of storage in the eluting buffer (~ 0.25 M KPi , pH 7.6, 1 mM 2-mercaptoethanol), it had developed a high level of TDT activity with a lower level of DNA polymerase activity. Attempts to accelerate the conversion of the remaining polymerase to TDT using widely varying levels of trypsin, chymotrypsin and pronase were unsuccessful. The lower pH of 6.5, conditions used in certain steps of Bollum's procedure, is known to favor the action of cathepsins (Fرتون, 1960), and could account for the production of TDT1 in one case and TDT2 in the other. TDT1 will not use activated DNA as a primer, requiring a 3'-OH end (Bollum, 1974) which is not hydrogen bonded to a complementary strand (Table 2). Although Berg has found terminal

addition to EcoRI-treated SV40 DNA which he attributes to the transient separation of the duplex at the ends, forming non-hydrogen bonded primers, this phenomenon is observed only for a small percentage of the molecules (Jackson *et al*, 1972) and could be also attributed to endonuclease in his TDT1 preparations. In contrast TDT2 uses activated DNA as primer.

TDT2 was also found to have template guided DNA polymerase activity (Table 2) which was not due to contaminating DNA polymerase α which is well separated from TDT2 on Sephadex G-100. The TDT2 was rerun on Sephadex G-100 and DNA polymerase activity still chromatographed with the TDT2 although there was now no DNA polymerase activity in the excluded portion of the column. The TDT polymerase was readily distinguished from TDT using the ethidium fluorescence assay as above. The TDT activity was sensitive to mercurials as is DNA polymerase α (Weissbach, 1975), and thus is probably not DNA polymerase β . Its molecular weight excludes DNA polymerase γ .

TDT2 is contaminated by trace amounts of endonuclease (as measured by the conversion of PM2 CCC DNA to OC DNA) and exonuclease (~ 13 U/mg) activity which were not separable from TDT2 upon chromatography over single-stranded DNA-agarose or Sephadex G-100. These did exhibit different heat inactivation profiles with TDT2 the most heat sensitive, being completely inactivated by heating 5 minutes at 50°C. The exonuclease activity was inactivated >90% by heating 30 minutes at 50°C while this treatment inactivated <10% of the endonuclease. These levels of nuclease would not interfere with the DNA polymerase assay.

DISCUSSION:

In contrast to the two TDT activities previously reported with identical molecular weights, (Marcus *et al*, 1976), TDT1 and TDT2 are distinctly different proteins as determined by their physical properties. Their TDT activity varies in a parallel fashion under a variety of conditions. The higher molecular weight of TDT2 and its ability to act as a DNA polymerase and TDT, which activity appears to arise on storage of semi-purified fractions of calf thymus DNA polymerase, is highly suggestive that TDTs are derived from DNA polymerase by proteolysis. It remains to be shown that a purified DNA polymerase can be converted to a TDT. Chang and Bollum (1972) reported that antibody directed against DNA polymerase α (6S-8S DNA polymerase) does not cross-react with TDT1 although inhibition of DNA polymerase activity from a variety of mammalian sources was observed. Kung *et al*, (1976) have recently demonstrated that anti-TDT1 antibody does not inhibit DNA polymerase α activity. However, no firm conclusions can be made from these studies as to the relatedness of the proteins since the polymerase antigenic determinants may have been modified or removed by proteolysis. Although we suggest that the presence of TDT may be artifactual, it still may be diagnostic for certain cell types as suggested by Sarin and Gallo, 1974. However, suggestions that TDT may have a physiological role such as generating antibody diversity (Baltimore, 1974) would seem unlikely.

REFERENCES:

- Aposhian, H.V. and Kornberg, A., (1962) *J. Biol. Chem.* 237, 519-525.
- Baltimore, D., (1974) *Nature* 248, 409-411.
- Bhattacharyya, J.R., (1975) *Biochem. Biophys. Res. Comm.* 62, 367-375.
- Bollum, F.J., (1962) *J. Biol. Chem.* 237, 1945-1949.
- Bollum, F.J., (1968) in *Methods in Enzymology XII B*, 591-611.
- Bollum, F.J., (1974) in *The Enzymes X* (Paul D. Boyer, editor), Academic Press, New York, pp. 145-171.
- Brodniewicz-Proba, T., and Buchowicz, J., (1976) *FEBS Letters* 65, 183-186.
- Chang, L.M.S. and Bollum, F.J., (1971) *J. Biol. Chem.* 246, 909-916.
- Chang, L.M.S. and Bollum, F.J., (1972) *Science* 175, 1116-1117.
- Coulter, M., Flintoff, W., Paetkau, C., Pulleyblank, D. and Morgan, A.R., (1974) *Biochemistry* 13, 1603-1609.
- Fruton, J.S., (1960) in *The Enzymes* (Boyer, Lardy and Myrback, editors), Academic Press, New York, pp. 233-241.
- Jackson, D.A., Symons, R.H. and Berg, P., (1972) *Proc. Nat. Acad. Sci. (USA)* 69, 2904-2909.
- Kato, K., Goncalves, J.M., Houts, G.E. and Bollum, F.J. (1967) *J. Biol. Chem.* 242, 2780-2789.
- Kornberg, A., (1974) in *DNA Synthesis*, W.H. Freeman and Company, San Francisco, pp. 107-108.
- Kung, P.C., Gottlieb, P.D. and Baltimore, D., (1967) *J. Biol. Chem.* 251, 2399-2404.
- Marcus, S.L., Smith, S.W., Jarowoski, C.I. and Modak, M.J., (1976) *Biochem. Biophys. Res. Comm.* 70, 37-44.
- McCaffrey, R., Smoler, D.F. and Baltimore, D., (1973) *Proc. Nat. Acad. Sci. (USA)* 70, 521-525.
- Morgan, A.R. and Pulleyblank, D.E., (1974) *Biochem. Biophys. Res. Comm.* 61, 396-403.
- Sarin, P.S. and Gallo, R.C., (1974) *J. Biol. Chem.* 249, 8051-8053.
- Schaller, H., Nusslein, C., Bonhoeffer, F.J., Kurz, C. and Nietzschmann, I., (1972) *Eur. J. Biochem.* 26, 474-481.
- Srivastava, B.I.S., (1974) *Cancer Res.* 34, 1015-1026.
- Weber, K. and Osborn, M., (1969) *J. Biol. Chem.* 244, 4406-4412.
- Weissbach, A., (1975) *Cell* 5, 101-108.

TABLE 2

COMPARISON OF THE PROPERTIES OF TDT1 AND TDT2

Conditions*	TDT2		TDT1	
	nmoles dNTP incorporated/ mg protein/hour	%	nmoles dNTP incorp- orated/ mg protein/hour	%
Complete reaction mixture	245	100	1,878	100
Primer omitted	0	0	0	0
Primer omitted + activated calf thymus DNA	329	134	90	5
Complete + 0.01% SDS	27	11	97	6
Complete + 0.1% Triton, X-100	188	77	1,407	75
Complete + 5mM NEM	20	8	428	23
Complete + 0.1mM pOHMB	189	77	1,214	65
DNA polymerase activity	43.3	-	0	-
pH optimum (cacodylate buffer)	7.5	-	7.0	-
Cacodylate replaced by Tris HCl or Tris Acetate pH 7.5	12	5	94	5
S Value	4-5		3.65	

* Assay conditions as outlined in Materials and Methods with Mg^{++} and dATP and 50 μM pT₄₋₅ as primer. Activated calf thymus DNA (Aposhian and Kornberg, 1962) was substituted for pT₄₋₅ as primer at 120 μM . Most values are the average of four determinations. Conditions for sedimentation and markers are given in Chang and Bollum (1971). DNA polymerase activity was assayed by the fluorescence assay described in Materials and Methods.

TABLE 1

Substrate Specificity of TDT2

dNTP	nmoles dNTP incorporated per mg protein per hour at 37°C	
	Mg ⁺⁺	Co ⁺⁺
dATP	245 (1.00)	276 (1.13)
dGTP	400 (1.63)	564 (2.30)
dCTP	32 (0.13)	3525 (14.39)
dTTP	25 (0.10)	4033 (16.46)

TDT activity was assayed as described in Materials and Methods with P^{T}_{4-5} (50 μ M final concentration) as primer. Incorporation relative to Mg⁺⁺ dATP (1.00) given in brackets. All values are the average of four determinations.

Figure 1. Chromatography of TDT2 activity over Sephadex G-100 in 25 mM KP_1 pH 7.5, 1 mM EDTA, 1 mM 2-mercaptoethanol, 5% glycerol, 0.5 M KCl. The heavy arrow indicates the elution position of TDT1. Both activities were assayed as described in Materials and Methods with Mg^{++} dATP as substrate.

Figure 2. A. Tracing of a SDS polyacrylamide gel of the TDT2 activity isolated by Sephadex G-100 chromatography in Figure 1² deliberately incompletely destained (see Results). B. Determination of the molecular weight of the main protein band of A (indicated by the arrow) with E. coli RNA polymerase subunits as internal standards.

